

Genetic Markers In The Differential Diagnosis In A Family Setting Of Episodic Loss Of Consciousness

March 2000

Thesis presented in partial fulfillment for the requirements of the
degree MASTER OF SCIENCE in MEDICAL SCIENCES
at the Faculty of Medicine,
UNIVERSITY OF STELLENBOSCH



STUDY LEADER: Dr. Valerie Corfield

Saralene Iona Thomas

DECLARATION

I, the undersigned, hereby declare that the work contained in this thesis is my own original work and has not previously in its entirety, or in part, been submitted at any university for a degree.

Signature:.....

Date:.....

SUMMARY

This thesis focuses on the molecular causes of two inherited diseases, identified in South African families, namely the long QT syndrome (LQTS) and a familial form of myoclonic epilepsy (FME).

The long QT syndrome is a cardiac repolarization disorder characterized by the occurrence of life threatening cardiac arrhythmias that can present as fainting attacks, and the occurrence of sudden cardiac death in young otherwise healthy individuals. Linkage analysis demonstrated genetic heterogeneity in LQTS, and mutations in four cardiac ion channels, namely those encoding a voltage-gated potassium channel (*KVLQT1*), the gene encoding human minimal potassium (hminK), also known as (*KCNE*), human ether-a-go-go gene (*HERG*) and a cardiac sodium channel (*SCN5A*), as well as an as yet unidentified gene on chromosome 4, were shown to result in the phenotypic expression of this disease. Five South African families of Afrikaner descent were shown to harbour an Ala212Val mutation in *KVLQT1*, these families also shared the same haplotype at this locus, suggesting the presence of a founder effect.

The epilepsies are a clinically variable and genetically heterogeneous group of neurologic disorders characterized by the transient disturbances of neuronal synchrony. Linkage analysis has established the chromosomal location in well over hundred rare epilepsy syndromes, which show a simple inheritance pattern. Some of the first epilepsy genes identified were also voltage-gated or ligand-gated ion channels.

An important mutual characteristic of LQTS and epilepsy is episodic loss of consciousness; the latter is a common reason for misdiagnoses of LQTS as epilepsy. In the present study, both these disorders were investigated with the aim of employing genetic markers to determine the chromosomal locus in both diseases, as an adjunct to clinical diagnosis.

In the LQTS study, all probands referred with the clinical diagnosis of LQTS were first screened for the Ala212Val mutation in *KVLQT1* by allele specific restriction enzyme analysis (ASREA). Using the probands, pedigrees were constructed where possible, and linkage analysis was performed at four of the known LQTS loci, if the Ala212Val mutation was absent. Mutation screening employing ASREA and polymerase chain reaction (PCR)-based single strand conformational polymorphism (SSCP) analysis was used to search for known and novel mutations after linkage analysis had implicated the disease-causing gene or locus.

Four of a panel of 12 LQTS probands carried the *KVLQT1* Ala212Val mutation. Three pedigrees of different South African population groups, namely Afrikaner, Mixed ancestry and Indian descent were constructed from the panel. The *KVLQT1* Ala212Val mutation was present in the family of Afrikaner descent; however, in the other two families, this mutation was absent, subsequently, linkage analysis was performed in these pedigrees. In the family of Mixed ancestry, significant negative LOD scores (-3.12, -5.01 and -3.23) were generated at the *HERG*, *SCN5A* and chromosome 4 loci, respectively; however at the *KVLQT1* locus an equivocal lod score of 0.92 was generated. Mutation screening of *KVLQT1* by ASREA and PCR-SSCP analysis identified an intronic polymorphism, but no disease-causing sequence variation in this family. In the Indian family, significant negative LOD scores (-2.78, -2.62 and -2.78) were found at the *SCN5A*, *KVLQT1* and chromosome 4 loci, respectively, and an equivocal LOD score of 0.20 was generated at the *HERG* locus.

In the epilepsy study, one family with a form of familial myoclonic epilepsy (FME) was identified, and the responsible disease-causing locus or genes of three plausible candidate forms of epilepsy were investigated for their involvement in this disease. These epilepsy syndromes included progressive myoclonus type one (EPM1), dentato-rubro-pallidoluysian-atrophy (DRPLA) and a chromosome 8p disease-associated locus. Linkage analysis was used to test linkage of FME to these three plausible candidate loci. Significant negative LOD scores were generated at all three loci at $\theta = 0.00$, at the *EPM1* locus LOD scores of -14.29, -12.83 and -6.82 were found at the marker loci *D21S2040*, *D21S1912* and *D21S1959*, respectively. At the *DRPLA* locus a LOD score of -14.50 was found at $\theta = 0.00$ and at the chromosome 8p locus, the LOD scores generated were 0.69, -4.46 and 0.68 at the marker loci *D8S504*, *D8S264* and *D8S1781*, respectively, at $\theta = 0.00$.

The application of genetic markers was useful in solving the differential diagnosis in the LQTS affected families. The *KVLQT1* Ala212Val mutation was identified as cause of LQTS in the family of Afrikaner descent, a different *KVLQT1* mutation was implicated as cause of the disease in a family of Mixed ancestry and *HERG* was implicated as causative gene in a family of Indian descent. This is the first report of genetic heterogeneity in South African LQTS families. In the epilepsy study, three highly plausible candidate epilepsy syndromes were excluded as cause of FME.

The results obtained in the LQTS study have important implications. The precipitating factors, incidence and lethality of cardiac events, and consequently choices concerning patient management and treatment, vary according to the disease-causing gene involved. The results obtained in the epilepsy study provided evidence to support the hypothesis that FME is a new clinical and genetic entity.

OPSOMMING

Hierdie tesis konsentreer op die molekulêre oorsake van twee oorerflike siektes, geïdentifiseer in Suid Afrikaanse families, naamlik lang QT sindroom (LQTS) en familêre myokloniese epilepsie (FME).

Die lang QT sindroom is a kardio-repolarisasie siekte wat gekenmerk word deur die voorkoms van lewens gevaarlike ritme stoornisse, wat kan presenteer as floute aanvalle en skielike kardiaale dood in jong, andersins gesonde individue. Genetiese heterogeniteit was met behulp van koppeling analise in LQTS gedemonstreer. Mutasies in vier kardio-ioon kanale naamlik 'n stroom beheerde kalium kanaal (*KVLQT1*), die geen wat koddeer vir die menslike minimale kalium protein (hminK), *KCNE*, menslike eter-a-go-go geen (*HERG*) en 'n kardio natrium kanaal (*SCN5A*) sowel as 'n tot nou toe ongeïdentifiseerde geen op chromosoom 4 was bewys om verantwoordelik te wees in meeste gevalle van die fenotipiese uitdrukking van die siekte. In vorige studies, is bewys dat vyf Suid Afrikaanse families van Afrikaner afkoms die Ala212Val mutation in *KVLQT1* dra, en geaffekteerde lede van hierdie familie dieselfde haplotipe by hierdie lokus deel, dit dui op 'n stigtings effek in hierdie subpopulasie groep.

Die epilepsies is 'n kliniese differse en geneties heterogeniese groep van neurologiese siektes, gekenmerk deur 'n kortstondige versteuring van neuronale synchronisasie. Koppelings analise het die chromosomale posisies van meer as honderd skaars epilepsie syndrome met eenvoudige oorerfings patrone geïdentifiseer. Van die eerste epilepsie gene wat geïdentifiseer is, was stroom-beheerde of ligand-beheerde ion kanale.

'n Belangrike gemeenskaplike eienskap van LQTS en epilepsie is die episodiese verlies van bewussyn, 'n algemene rede vir die misdiagnose van LQTS as epilepsie. In die huidige studie was albei hierdie siekte toestande ondersoek met die doel om genetiese merkers te gebruik om die chromosomale posisies van beide siektes te bepaal en sodoende 'n bydrae te lewer in die kliniese diagnose.

In die LQTS studie was die indeks gevalle wat verwys was met die kliniese diagnose van LQTS eers getoets vir die Ala212Val mutasie in *KVLQT1* met behulp van alleel-spesifieke restriksie ensiem analise (ASREA). Waar moontlik was stambome saamgestel vanaf die indeks gevalle en koppeling analise was uitgevoer by vier van die bekende LQTS lokusse indien die Ala212Val mutasie afwesig was in die indeks geval. Mutasie analise met behulp van ASREA

en polimerase ketting reaksie (PKR) gebasseerde enkel string konformasie polimorfisme analise was gebruik om te soek vir bekende en nuwe mutasies in die geen geïmpliseer deur koppelings analise as die siekte-veroorsakende geen.

Die Ala212Val mutasie was teenwoordig in vier uit die paneel van twaalf LQTS indeks gevalle. Drie stambome, van verskillende Suid Afrikaanse subpopulasie groepe, naamlik Afrikaner, gemengde herkoms en Indieër oorsprong was saamgestel vanaf die paneel. Die Ala212Val mutasie was teenwoordig in die familie van Afrikaner afkoms, maar nie in die ander twee families nie. gevolglik was koppelings analise in hierdie families uitgevoer. In die familie van gemengde herkoms was betekenisvolle negatiewe LOD waardes (-3.12, -5.01 en -3.23) gegenereer by *HERG*, *SCN5A* en die chromosome 4 lokus onderskeidelik. By die *KVLQTI* lokus was 'n swak positiewe LOD waarde van 0.92 bereik. In die Indieër familie was weereens betekenisvolle negatiewe LOD waardes (-3.78, -2.62 en -2.78) gegenereer by onderskeidelik *SCN5A*, *KVLQTI* en die chromosome 4 lokus terwyl 'n swak positiewe LOD waarde van 0.20 by *HERG* behaal is.

Een familie met FME was geïdentifiseer en die kliniese eienskappe van hierdie vorm van epilepsie was vergelyk met ander bekende epilepsies en sodoende was drie hoogs waarskynlike kandidaat vorms van epilepsie syndrome geïdentifiseer. Hierdie drie epilepsie syndrome was verder ondersoek en sluit in progressiewe myokloniese epilepsie tipe I (EPM1), dentato-rubro-pallidoluisian-atrofie (DRPLA) en 'n vorm van epilepsie wat geposisioneer is op chromosoom 8p. Koppeling analise was toegepas tussen FME en die drie kandidaat epilepsie syndrome. Betekenisvolle negatiewe LOD waardes was bereik by by al drie lokusse by $\theta = 0.000$, by die *EPM1* lokus was LOD waardes van -14.29, 12.53 en 6.52 gevind by merkers *D21S2040*, *D21S1912* en *D21S1959*, onderskeidelik. By die DRPLA lokus was 'n LOD waarde van -14.80 gevind en LOD waardes van 0.69, -4.46 en 0.68 by die chromosoom 8 lokus by merkers *D8S504*, *D8S264* en *D8S1781* onderskeidelik.

Die gebruik van genetiese merkers was waardevol in die uitlê van die differensieële diagnose in die LQTS families. Die Ala212Val mutasie was bevestig in 'n familie van Afrikaner afkoms, 'n ander *KVLQTI* mutasie was geïmpliseer as oorsaak van die siekte in die familie van gemengde herkoms en *HERG* was geïmpliseer as siekte-veroorsakende geen in die Indieër LQTS familie. Dit is die eerste verslag van genetiese heterogeniteit in Suid Afrikaanse LQTS

families. In die epilepsie studie was drie hoogs aanneemlike kandidaat epilepsie syndrome uitgesluit as oorsaak van die siekte in FME.

Die resultate verkry in die LQTS studie het belangrike implikasies, aangesien die presipitasie faktore, behandeling en medikasie verskil, afhangende van die spesifieke siekte-veroorsakende geen betrokke. Die resultate verkry in die epilepsie studie verskaf bewyse in guns van die hipotese dat FME 'n nuwe kliniese en genetiese entiteit is.

ACKNOWLEDGEMENTS

This study was performed in the US/MRC Centre for Molecular and Cellular Biology in the Department of Medical Physiology and Biochemistry, University of Stellenbosch. I would like to acknowledge the MRC for their financial support.

To my study leader, Valerie Corfield, thank you for all your help, patience and sacrificing lots of your free time to assist in the preparation of this thesis.

To Hanlie, thank you for reading sections of this thesis, your much appreciated comments and sharing your expertise throughout this project

To Drs Paul Brink, Jonathan Carr and Clive Corbett, thank you for providing the blood samples that were required for this research project, and to all the families who took part I express my gratitude.

To my colleagues Donita, Alan, Suzanne, Zola, Kholiswa, Juanita, Craig, Pedro and Toy, thank you for your encouragement and providing a pleasant working environment.

To my family, Mom, Dad, Fannie, Melony, Gavin and Pearl thanks for your love, support and patience throughout this project.

To Marlin, for believing in me, for supporting me, but most of all for loving me.

To the Lord, who gave me the strength and the wisdom to complete this thesis.

TABLE OF CONTENTS

Contents	Page
Declaration	ii
Summary	iii
Opsomming	vi
Acknowledgements	ix
List of abbreviations	xi
One letter and three letter amino acid abbreviations	xiv
List of figures	xv
List of tables	xix
Chapter 1: Literature review	1
Chapter 2: Materials and Methods	69
Chapter 3: Results	88
Chapter 4: Discussion	160
Appendix I	175
Appendix II	185
References	187

LIST OF ABBREVIATIONS

α	alpha
AgNO ₃	silver nitrate
APS	ammonium persulphate
ASREA	Allele-specific restriction enzyme analysis
ATP	adenosine triphosphate
bp	base pair
β	Beta
^o C	degree celsius
Ca ⁺	calcium ion
cDNA	complementary deoxyribonucleic acid
Cl ⁻	chloride ion
cm	centimeter
cM	centimorgan
CSTB	cystatin B
dATP	deoxyadenosine triphosphate
dCTP	deoxycytosine triphosphate
dGTP	deoxyguanine triphosphate
dNTP	deoxynucleotide triphosphate
dTTP	deoxythymidine triphosphate
DNA	deoxyribonucleic acid
DRPLA	Dentato-rubro-pallido-luysian atrophy
ECG	electrocardiogram
<i>E.coli</i>	<i>Escherschia coli</i>
EDTA	(ethylenedinitrilo) tetraacetic acid
EEG	electroencephalogram
EPM1	Progressive myoclonus epilepsy type I
FME	Familial myoclonic epilepsy
g	gram
HD	Huntington's disease
<i>HERG</i>	human-ether-a-go-go gene
<i>hminK</i>	human minimal potassium

H ₂ O	water
<i>H-ras-1</i>	Harvey ras-1
I _{Kr}	rapidly activating current
I _{Ks}	slowly activating current
ILAE	International League Against Epilepsy
JLNS	Jervell Lange-Nielsen syndrome
K ⁺	potassium ion
kb	kilobase
<i>KCNE1</i>	gene encoding the human minimal potassium protein
<i>KVLQT1</i>	voltage-gated potassium channel gene
LOD score	logarithm of the odds score
LQTS	Long QT syndrome
mg	milligram
M	molar
MgCl ₂	magnesium chloride
mM	millimolar
ml	millilitre
mRNA	messenger ribonucleic acid
Na ⁺	sodium ion
NaOH	sodium hydroxide
NaBH ₄	sodium borohydride
ng	nanogram
nm	nanometre
P1	Bacteriophage P1
PCR	polymerase chain reaction
PCR-SSCP	PCR-based single strand conformational polymorphism
PME	Progressive myoclonus epilepsy
QTc	QT interval corrected for heart rate
RFLP(s)	restriction fragment length polymorphism(s)
r.p.m.	revolutions per minute
RWS	Romano Ward syndrome
s	seconds
<i>SCN5A</i>	cardiac sodium channel gene

SDS	sodium dodecyl sulphate
STRP(s)	short tandem repeat polymorphism(s)
TBE	tris, boric acid and EDTA buffer
TE	tris, EDTA buffer
μg	microgram
μl	microlitre
μM	micromolar
uv	ultraviolet
V	volts
W	watts
YAC(s)	yeast artificial chromosomes

ONE LETTER AND THREE LETTER AMINO ACID ABBREVIATIONS

Alanine	Ala	A
Arginine	Arg	R
Asparagine	Asn	N
Aspartic acid	Asp	D
Glutamic acid	Glu	E
Glutamine	Glu	Q
Glycine	Gly	G
Histidine	His	H
Isoleucine	Ile	I
Leucine	Leu	L
Lysine	Lys	K
Methionine	Met	M
Phenylalanine	Phe	F
Proline	Pro	P
Serine	Ser	S
Threonine	Thr	T
Tryptophan	Trp	W
Valine	Valine	V

LIST OF FIGURES

	PAGE
Chapter 1	
Figure 1.1 QT prolongation	12
Figure 1.2 Genetic recombination	20
Figure 1.3 Heterozygous and homozygous allelic forms of a genetic marker	21
Figure 1.4 Ideogram and genetic map of chromosome 21	29
Figure 1.5 Ideogram and genetic map of chromosome 7	41
Figure 1.6 Ideogram and genetic map of chromosome 3	41
Figure 1.7 Ideogram and genetic map of chromosome 4	44
Figure 1.8 Schematic illustration of the five phases of the repolarization depolarization cycle.	46
Figure 1.9 Example of an ion channel residing in the cell membrane	48
Figure 1.10 Example of an ion channel pore.	48
Figure 1.11 Schematic presentation of the predicted topology of the protein encoded by <i>HERG</i> and the location of LQTS associated mutations	51
Figure 1.12 Schematic presentation of the predicted topology of the protein encoded by <i>SCN5A</i> and the location of LQTS associated mutations	54
Figure 1.13 Ideogram and genetic map of chromosome 11	56
Figure 1.14 Schematic presentation of the predicted topology of the protein encoded by <i>KVLQT1</i> and the location of LQTS associated mutations	59
 Chapter 3	
Figure 3.1a The original pedigree 201 showing the family in which FME segregate	92
Figure 3.1b Pedigree 201 structure altered for LOD score analysis	
Figure 3.2.1 Autoradiograph showing alleles at the DNA marker <i>D21S2040</i> in pedigree 201 in which FME segregates	93
Figure 3.2.2 Autoradiograph showing alleles at the DNA marker <i>D21S1259</i> in pedigree 201 in which FME segregates	94
Figure 3.2.3 Autoradiograph showing alleles at the DNA marker <i>D21S1912</i> in pedigree 201 in which FME segregates	95

Figure 3.3.1	Autoradiograph showing alleles at the DNA marker <i>D8S504</i> in pedigree 201 in which FME segregates	96
Figure 3.3.2	Autoradiograph showing alleles at the DNA marker <i>D8S264</i> in pedigree 201 in which FME segregates	97
Figure 3.3.3	Autoradiograph showing alleles at the DNA marker <i>D8S1781</i> in pedigree 201 in which FME segregates	98
Figure 3.4.1	Autoradiograph showing alleles of the expanded triplet repeat in atrophin in pedigree 201 in which FME segregates	99
Figure 3.4.2	Pedigree 201 showing the allelic distribution at the triplet repeat marker in the atrophin gene in those individuals who participated in the linkage study	100
Figure 3.5	Pedigree 201 showing the haplotypes inherited at the <i>EPMI</i> locus	103
Figure 3.6	Pedigree 201 showing the haplotypes inherited at the chromosome 8 locus	104
Figure 3.7	Pedigree 202, the new family identified in which FME segregates	106
Figure 3.8	Extended pedigree 201 in which FME segregates	107
Figure 3.9a-b	Founder mutation screening by ASREA in a panel of unrelated affected individuals	109
Figure 3.10.1	Pedigree 167 of Mixed ancestry descent in which the autosomal dominant form of LQTS segregates	112
Figure 3.10.2	Pedigree 168 of Afrikaner descent in which the autosomal dominant form of LQTS segregates	113
Figure 3.10.3	Pedigree 169 of Indian descent in which the autosomal dominant form of LQTS segregates	114
Figure 3.11.1	Founder mutation screening by ASREA in pedigree 167	115
Figure 3.11.2	Founder mutation screening by ASREA in pedigree 168	116
Figure 3.12.1	Autoradiograph showing alleles at the DNA marker <i>TH</i> in pedigree 167	119
Figure 3.12.2	Autoradiograph showing alleles at the DNA marker <i>DIIS1318</i> in pedigree 167	120
Figure 3.12.3	Autoradiograph showing alleles at the DNA marker <i>DIIS860</i> in pedigree 167	121
Figure 3.12.4	Autoradiograph showing alleles at the DNA marker <i>DIIS1323</i> in pedigree 167	122

Figure 3.12.5 Autoradiograph showing alleles at the DNA marker <i>D11S1331</i> in pedigree 167	123
Figure 3.13.1 Autoradiograph showing alleles at the DNA marker <i>TH</i> in pedigree 169	124
Figure 3.13.2 Autoradiograph showing alleles at the DNA marker <i>D11S1318</i> in pedigree 169	125
Figure 3.13.3 Autoradiograph showing alleles at the DNA marker <i>D11S860</i> in pedigree 169	126
Figure 3.13.4 Autoradiograph showing alleles at the DNA marker <i>D11S1323</i> in pedigree 169	127
Figure 3.13.5 Autoradiograph showing alleles at the DNA marker <i>D11S1331</i> in pedigree 169	128
Figure 3.14.1 Autoradiograph showing alleles at the DNA marker <i>D7S636</i> in pedigree 167	130
Figure 3.14.2 Pedigree 167 showing the allelic distribution at the DNA marker <i>D7S636</i> in the individuals who participated in the linkage analysis Study	131
Figure 3.15.1 Autoradiograph showing alleles at the DNA marker <i>D7S636</i> in pedigree 169	132
Figure 3.15.2 Pedigree 169 showing the allelic distribution at the DNA marker <i>D7S636</i> in the individuals who participated in the linkage analysis study	133
Figure 3.16.1 Autoradiograph showing alleles at the DNA marker <i>D3S1298</i> in pedigree 167	135
Figure 3.16.2 Pedigree 167 showing the allelic distribution at the DNA marker <i>D3S1298</i> in the individuals who participated in the linkage analysis study	136
Figure 3.17.1 Autoradiograph showing alleles at the DNA marker <i>D3S1298</i> in pedigree 169	137
Figure 3.17.2 Pedigree 169 showing the allelic distribution at the DNA marker <i>D3S1298</i> in the individuals who participated in the linkage analysis study	138
Figure 3.18.1 Autoradiograph showing alleles at the DNA marker <i>D4S402</i> in pedigree 167	139
Figure 3.18.2 Pedigree 167 showing the allelic distribution at the DNA marker <i>D4S402</i> in the individuals who participated in the linkage analysis study	140

Figure 3.19.1	Autoradiograph showing alleles at the DNA marker <i>D4S402</i> in pedigree 169	141
Figure 3.19.2	Pedigree 169 showing the allelic distribution at the DNA marker <i>D4S402</i> in the individuals who participated in the linkage analysis study	142
Figure 3.20	Haplotypes across the <i>KVLQT1</i> locus in pedigree 167	144
Figure 3.21	Haplotypes across the <i>KVLQT1</i> locus in pedigree 169	145
Figure 3.22.1	PCR-SSCP analysis of the S2-S6 regions of <i>KVLQT1</i> in pedigree 167 on a 10% polyacrylamide gel with glycerol	149
Figure 3.22.2	PCR-SSCP analysis of the S2-S6 regions of <i>KVLQT1</i> in pedigree 167 on a 10% polyacrylamide gel without glycerol	150
Figure 3.22.3	PCR-SSCP analysis of the S2-S6 regions of <i>KVLQT1</i> in pedigree 167 on a 5% polyacrylamide gel with glycerol	151
Figure 3.22.4	PCR-SSCP analysis of the S2-S6 regions of <i>KVLQT1</i> in pedigree 167 on a 5% polyacrylamide gel without glycerol	152
Figure 3.23	Sequence variation identified in the S2-S3 region of an affected individual of pedigree 167, compared with the sequence of an unaffected individual and the normal published sequence	153
Figure 3.24.1	Allele specific restriction enzyme analysis (ASREA) of the reported Ala49Pro mutation in the S2-S3 region of <i>KVLQT1</i>	157
Figure 3.24.2	Allele specific restriction enzyme analysis (ASREA) of the reported Arg61Glu mutation in the S2-S3 region of <i>KVLQT1</i>	158
Figure 3.24.3	Allele specific restriction enzyme analysis (ASREA) of the reported Val125Met mutation in the S3-S4 region of <i>KVLQT1</i>	159

LIST OF TABLES

		Page
Chapter 1		
Table 1.1	The genetic localization and disease causing genes of known forms of epileptic syndromes	7
Table 1.2	Identified LQTS genes and their chromosomal positions	61
 Chapter 2		
Table 2.1	DNA sequences of the eight regions of the <i>KVLQT1</i> gene analyzed	74
Table 2.2	Thermocycling parameters used for the STRPs markers analyzed with radioactive PCR	76
Table 2.3	The first ten <i>KVLQT1</i> mutations described by Wang et al., (1996) and restriction enzyme sites that they affect	78
Table 2.4	Electrophoreses and gel drying conditions of SSCP gels	80
Table 2.5	STRPs markers analyzed by radioactive PCR	84
Table 2.6	Details on the alleles of the polymorphic markers analyzed by radioactive PCR	85
 Chapter 3		
Table 3.1	Pairwise two point LOD scores between FME and the causitive loci of the three candidate forms of epilepsy, namely EPM1, DRPLA and the chromosome 8 locus	105
Table 3.2	Pairwise two point LOD scores between LQTS and the polymorphic markers at the <i>KVLQT1</i> , <i>HERG</i> , <i>SCN5A</i> and the chromosome 4 locus in pedigree 167	146
Table 3.3	Pairwise two point LOD scores between LQTS and the polymorphic markers at the <i>KVLQT1</i> , <i>HERG</i> , <i>SCN5A</i> and the chromosome 4 locus in pedigree 169	147

CHAPTER 1

LITERATURE REVIEW

Contents	Page
INTRODUCTION	3
1.1 BACKGROUND ON EPILEPSY	3
1.1.1 History of Epilepsy	3
1.1.2 Classification of Epilepsy	4
1.1.3 The Role of Genetics in Epilepsy	5
1.1.3.1 Progressive myoclonus epilepsy	8
1.1.3.2 Dentato-rubro-pallido-luysian-atrophy	9
1.1.4 Treatment of Epilepsy	10
1.2 BACKGROUND ON LQTS	11
1.2.1 Jervell Lange Nielsen Syndrome	11
1.2.2 Romano Ward Syndrome	13
1.2.3 Acquired forms of LQTS	15
1.2.4 Treatment of LQTS	15
1.3 CONFUSION IN DIAGNOSIS	16
1.4 MOLECULAR GENETIC TECHNIQUES	18
1.4.1 Identification of Disease-Causing Loci with Linkage Analysis	18
1.4.2 Linkage Disequilibrium	22
1.4.3 Genetic Fine Mapping and Physical Mapping	23
1.4.4 Identification of Candidate Genes	24
1.4.5 Identification of the Disease-Causing Gene	25
1.4.5.1 PCR-SSCP analysis	26

1.5 APPLICATION OF MOLECULAR GENETICS IN TWO FAMILIAL FORMS OF EPILEPSY	27
1.5.1 Progressive Myoclonus Epilepsy	27
1.5.1.1 Linkage analysis in EPM1	27
1.5.1.2 Identification of the EPM1 disease-causing gene	30
1.5.2 DRPLA	33
1.5.2.1 Linkage analysis in DRPLA	33
1.5.2.2 Identification of DRPLA disease-causing gene	34
1.5.3 Chromosome 8 p linked form of epilepsy	37
1.6 IMPORTANCE OF MAPPING EPILEPSY SUSCEPTIBILITY GENES	37
1.7 APPLICATION OF MOLECULAR GENETICS IN LQTS	38
1.7.1 Linkage Analysis	38
1.7.1.1 Linkage of LQTS to chromosome 11p15.5	38
1.7.1.2 Genetic heterogeneity in LQTS	39
1.7.1.3 Linkage of LQTS to chromosome 7q35-36	40
1.7.1.4 Linkage of LQTS to chromosome 3p21	40
1.7.1.5 Linkage of LQTS to chromosome 4p25-27	43
1.7.2 Identification and Characterization of LQTS Disease-causing Genes	45
1.7.2.1 LQTS candidate genes	45
1.7.2.1.1 Identification of the LQT2 causative gene, <i>HERG</i>	49
1.7.2.1.2 Identification of the LQT3 causative gene, <i>SCN5A</i>	52
1.7.2.1.3 Identification of the LQT1 causative gene, <i>KVLQT1</i>	55
1.7.2.1.4 Identification of a fifth disease-causing locus, <i>KCNE1</i>	60
1.7.2.1.5 Summary of identified LQTS disease-causing genes	60
1.7.3 Hypothesis to Explain LQTS	61
1.8 THE IMPORTANCE OF MAPPING LQTS DISEASE-CAUSING GENES	64
1.9 PRESENT STUDY	66

INTRODUCTION

It is sometimes difficult to make an unequivocal clinical diagnosis in the case of episodic loss of consciousness, because of the complexity of possible underlying causes. It may be difficult to determine if the patient is displaying syncope, as in the case with Long QT Syndrome (LQTS), or if he is having an epileptic seizure (Schott et al., 1977; Ballardie et al., 1983; O'Callaghan and Trump 1993; Singh et al., 1993; Paci et al., 1994). The diagnostic confusion between LQTS and various epileptic conditions as a result of their clinical presentation provided the rationale, and the availability of three affected South African families in which LQTS segregates, as well as a family in which a type of genetic epilepsy segregates, provided an opportunity to investigate the molecular causes of both these disorders. In the first two sections of this report, the development of scientific knowledge regarding aspects of these two conditions, since they were first observed or described, will be summarized. This will be followed by a section which describes the basis for the diagnostic confusion between these two disorders. Thereafter, relevant molecular genetic techniques will be discussed and a section on the application of these techniques in studies of LQTS and two genetic forms of epilepsy will succeed this.

1.1 BACKGROUND ON EPILEPSY

1.1.1 History of Epilepsy

Epilepsy is as old as mankind and the first written description of a secondarily generalized convulsion was found in the oldest written language, Akkadian, in Mesopotamia (now Iraq) dating back to about 3,000 years ago (reviewed by Goldensohn et al., 1997). At that time, people believed that supernatural forces controlled all events and individual behavior, and the presence of the seizures was attributed to the god of the moon. About 2,000 years ago, cases of epilepsy were also described in Egypt, China, India, and Babylonia (reviewed by Goldensohn et al., 1997).

The first known attempt at a scientific explanation of epilepsy was made about 400 B.C. in a book entitled "On the Sacred Disease" (reviewed by Engel, 1989). This book was written by a Greek physician of the school of Hippocrates and he dedicated this book to Hippocrates, who considered epilepsy to be a disease of the brain caused by superfluity of the phlegm that led to abnormal brain consistency. In this book, the author rejected the belief that individual Greek gods caused epilepsy and that superstitions and magic could prevent or cure epilepsy and he pointed out that epilepsy is hereditary and attributed it to a dysfunction of the brain (reviewed

by Engel, 1989). Although Hippocrates (460-357 B.C) and physicians of his school considered epilepsy as a disease of the brain, Charles le Pois (1563-1636) was the first one to clearly state that all epilepsies were of brain origin (reviewed by Schmidt and Wilder, 1968).

The European physicians were unaware of “On the Sacred Disease” because generally they did not read Greek, and the book was not translated into Latin. Thus, they still attributed epilepsy to supernatural forces, through the 15th century until the 16th century, when Da Vinci’s drawings of anatomic dissections, and those by Vesalius, provided new insight to the possible physiological cause of epilepsy (reviewed by Goldensohn et al., 1997). Despite these interventions, people suffering from epilepsy were still considered to be possessed by evil spirits, unclean and contagious, because most natural therapies suggested for epilepsy were ineffective and some supernatural therapies appeared to be more beneficial (Engel, 1989).

Much progress in the field of epilepsy research has been made since the first description of the disease, but to discuss all this information is beyond the scope of this review. However, the age-old stigma and myths associated with epilepsy began to lift, as more insight relevant to the understanding of epilepsy became available.

1.1.2 Classification of the Epilepsies

“ The epilepsies have been classified and reclassified upon the basis of each of their attributes - seizure pattern, temporal occurrence, aetiology and accompaniments. There are quite clearly as many classifications as there are needs to classify “ (Williams, 1988).

Due to the confusion created by the different classification systems, the Commission of Classification and Terminology of the International League Against Epilepsy (ILAE) saw the need for a standard classification. The first International Classification of Epileptic Seizures was made in 1970 (reviewed by Goldensohn, 1997), this system was revised in 1981 leading to the detailed classification of seizure types (Commission on Classification and Terminology of the ILAE, 1981). The classification of the seizure types primarily distinguishes between generalized onset seizures, which are presumed to involve the entire brain from the onset and partial onset seizures, in which seizures begin in a localized brain region (Commission on Classification and Terminology of the ILAE, 1981).

Certain forms of epileptic seizure disorders have special clinical and electroencephalogram (EEG) characteristics regardless of their polyaetiological background. These forms have important differences in course and prognosis, and based on this, could be divided into epileptological entities or epileptic syndromes (Duchownny and Harvey, 1996). In 1985, the ILAE presented a classification of epilepsies into epileptic syndromes, which was revised in 1989 (Commission on Classification and Terminology of the ILAE, 1989). This classification system combines information on seizure type, age at onset, aetiology, clinical course and EEG findings.

The syndrome classification primarily distinguishes between generalized and partial epilepsies and can further be subclassified according to their aetiology into the idiopathic, cryptogenic and symptomatic groups (Commission on Classification and Terminology of the ILAE, 1989). The set of syndromes presumed to be genetic in origin are referred to as “idiopathic”, whereas the epilepsies with unknown aetiological factors that are not included in the idiopathic syndromes are referred to as “cryptogenic”. The remainder with identified aetiological factors are called “symptomatic” (reviewed by Jain, 1997).

The observation of familial aggregation of either the epilepsy, or the associated EEG abnormality, and the higher concordance rates in monozygotic than dizygotic twins have led to the interpretation that most idiopathic generalized epileptic syndromes are genetic in origin (Jain, 1997). Partial epilepsies have long been considered as too complex to justify them as candidates for genetic studies, because they occur in strong association with a variety of cerebral lesions. However, clinical observations have suggested that genetic factors also may play some role in the pathogenesis of partial epilepsies (Jain, 1997).

1.1.3 The Role of Genetics in Epilepsy

As is clear from their classification, the epilepsies comprise a heterogeneous group of disorders in which there is a predisposition to recurrent seizures or fits. Seizures in turn represent an “occasional excessive and disorderly discharge of neurons” (Ryan, 1995). Thus, epileptic behavior is modulated by mechanisms that alter both neuronal excitability and neuronal synchronization (Engel, 1989). Regulation of the cortical excitability in the normal brain depends upon ionic fluxes across membranes, neuronal morphology, transmitter and receptor interaction, neuronal circuitry and extracerebral systems that influence cerebral function. All

these biochemical features represent the expression of genetic information, suggesting the contribution of genetics in epilepsy. However, when a single phenotype has many causes, it becomes difficult to determine patterns of genetic transmission (Engel, 1989).

In the past, epileptic disorders were considered to be either genetically or environmentally induced, but today it is recognized that a variety of genetic, environmental and physiological factors influence the appearance of the more common forms of epilepsy (Ottman et al., 1996). However, an epidemiological study performed by Ottman in 1997 identified a substantial genetic contribution to epilepsy and showed that genetic, and not environmental, factors account for most of the familial aggregation seen in seizure disorders (Ottman, 1997). There are well over 100 rare single gene mendelian disorders in which epileptic seizures appear as part of the phenotype (Ryan, 1999). The susceptibility loci and genes in most of these disorders have been identified, as linkage analysis in clinically homogeneous disorders with simple inheritance is relatively straight forward and is often achieved with a single large family or multiple small families. Table 1.1 shows some of these epilepsy syndromes in which the susceptibility loci and genes have been identified. However, epilepsy attributable to these disorders comprises only a small portion of all epilepsies, the remainder are thought to be mainly multifactorial diseases with oligogenic or polygenic backgrounds (Berkovic, 1997). In most of the epilepsies, especially the more common forms, the mode of inheritance is unknown and molecular approaches have been unsuccessful and controversial (Berkovic, 1998). The more complex inheritance pattern seen in many common epilepsies could result from low penetrance, genetic heterogeneity or both (Ryan, 1999).

Some of the first genes identified in human epilepsy syndromes were voltage-gated or ligand-gated ion channels (Steinlein et al., 1995; Singh et al., 1998; Charlier et al., 1998; Ryan, 1999) (Table 1.1). Ion channel defects was also found in a number of diseases known to occur intermittently in otherwise healthy individuals. These discoveries suggested that subtle, prevalent genetic variations in ion channel genes could also be involved in the aetiology of the common forms of idiopathic epilepsies with complex modes of inheritance (Ryan, 1999). However, to date, no ion channel variants have been implicated convincingly in susceptibility to common epilepsies (Ryan, 1999).

TABLE 1. The genetic localization and disease-causing genes associated with some known forms of epileptic syndromes

Epileptic Syndrome	Genetic Locus	Causative Gene
Idiopathic Generalised Epilepsies		
Juvenile myoclonic epilepsy	Chr. 6p	
Benign familial neonatal convulsions	Chr. 20q Chr. 8 q	<i>KCNQ2</i> <i>KCNQ3</i>
Benign familial infantile convulsions	Chr. 19q	
Progressive epilepsy with mental retardation	Chr. 8p	
Benign adult familial myoclonic epilepsy	Chr. 8q	
Generalized epilepsy with febrile seizures	Chr. 19q	<i>SCN1B</i>
Progressive Myoclonus Epilepsy		
EPM1	Chr.21q	<i>CSTB</i>
Neuronal ceroid lipofuscinoses, infantile	Chr. 1	
Neuronal ceroid-lipofuscinoses, juvenile	Chr. 16p	
Gaucher's disease	Chr. 1	
Sialidosis type I	Chr. 10	
MERRF	mtDNA	tRNA ^{Lys}
Idiopathic Partial Epilepsy		
Autosomal dominant nocturnal frontal lobe epilepsy	Chr. 20	<i>CHRNA4</i>
Partial epilepsy with auditory features	Chr.10q	
Autosomal dominant febrile seizures	Chr. 8q	
Neurodegenerative disorders		
DRPLA	Chr.12p	Atrophin

(Compiled from Delgado-Escueta et al., 1994; Johns, 1995; Duchowny and Harvey, 1996; Berkovic, 1997; Ottman, 1997; Plaster et al., 1999; Ryan, 1999)

Chr = chromosome, *CHRNA4* = Nicotinic acetylcholine receptor α_4 -subunit, *CSTB* = Cystatin B, DRPLA= Dentato-rubro-pallido-luysian-atrophy, EPM1= Progressive myoclonic epilepsy type I, mtDNA= Mitochondrial DNA, MERRF= Myoclonus epilepsy and ragged-red fibres, *KCNQ2* = Voltage sensitive K⁺-channel, *KCNQ3* = Voltage sensitive K⁺-channel and *SCN1B* = Voltage sensitive Na⁺-channel β -subunit.

As is clear from the discussion above, the epilepsies comprise a clinically and genetically heterogeneous group of disorders and a detailed discussion of all of the different types of epilepsies are beyond the scope of the present review. In this study, the focus will be on three specific types of epilepsy syndromes, namely Progressive myoclonus epilepsy type I (EPM1), Dentato-rubro-pallido-luysian-atrophy (DRPLA) and form of epilepsy that showed linkage to chromosome 8p, because of their relevance as plausible candidates for FME, the type of epilepsy that forms the basis of this part of the study.

1.1.3.1 Progressive myoclonus epilepsy

Familial myoclonic epilepsy (FME) is a form of progressive myoclonus epilepsy (PME). The PMEs are a clinically and aetiologically heterogeneous group of rare genetic disorders characterized by myoclonus, tonic-clonic seizures and progressive neurological dysfunction, particular ataxia and dementia (Berkovic et al., 1986). At least five diseases, or disease groups, account for most cases of PME worldwide. These are PME of Unverricht-Lundborg type, also known as EPM1, Lafora's disease, neuronal ceroid lipofuscinoses, mitochondrial disorders and the sialidoses (Marseille Consensus Group, 1990). Based on characteristic clinical features four of these disease groups could definitively be excluded as candidates for FME; however, the fifth one, EPM1 was considered as plausible candidate as will be discussed in section 4.3.

Unverricht described in 1891 the first clinical picture of familial myoclonus, which is nowadays known as EPM1 (Koskiniemi et al., 1974). The first symptom he observed were grand mal seizures at the age of 6 to 13 years, while muscle jerking, i.e. myoclonus, appeared later. In the period between 1903 and 1912, Lundborg described 17 patients from nine families in Sweden who apparently had the same disease. He found in addition to the muscle jerks and grand mal seizures, a later onset, dementia and various neurological symptoms. This syndrome was subsequently named the Unverricht-Lundborg's disease (Koskiniemi et al., 1974). Although it is now known that the PMEs are a heterogeneous group of disorders and a specific diagnosis can be made on the specific type of PME, in the past, PME was often regarded as a final clinical diagnosis (Berkovic, 1986).

Progressive myoclonus epilepsy type 1, or Unverricht-Lundborg disease, is now defined as an autosomal recessive inherited disease that is characterized by myoclonus that can be precipitated by movement, stress, or sensory stimuli and progressively increases in severity and frequency, often becoming incapacitating (reviewed by Berkovic et al., 1993). The mean

age of onset is 10.8 years (range 8-13 years) and myoclonic and tonic-clonic seizures occur in all cases with absences and drop attacks in a minority of cases. At the onset of the disease, neurological signs are absent or minimal, but dysarthria, ataxia and intention tremor is eventually seen in all cases. Intellectual decline is very gradual, the progression of the disease is at a variable rate, and periods of stabilization may occur (reviewed by Berkovic et al., 1986).

The diagnosis of EPM1 is clinical; the key features are: (i) the patient's age at onset, (ii) the severity and continuous nature of the myoclonus, (iii) the absence of severe or early dementia, (iv) a clinical history of EPM1, (v) typical EEG abnormalities, and (vi) clinical exclusion of the other four subtypes of PME (Berkovic et al., 1986; Lafreniere et al., 1995). On histopathological examination, widespread degenerative changes are seen in the brain, with no evidence of storage material, which is observed in the other four subtypes of PME (Koskiniemi et al., 1974).

1.1.3.2 Dentato-rubro-pallido-luysian-atrophy

The first report of DRPLA was from Smith et al., (1958) who described a middle-aged patient of Yugoslavin origin with ataxia and choreoathetotic movements and combined dentato-rubral and pallido luysian degeneration, by post-mortem examination. Smith proposed the term "dentato-rubro-pallido-luysian-atrophy" based on his neuropathologic findings in sporadic cases. Since its first description, DRPLA has been extensively characterized in the Japanese population, where its prevalence is estimated at approximately one case per million people, while it is thought to be exceeding rare in both Northern American and European kindreds. (Miwa, 1994).

Consequently, DRPLA was defined as a rare neurodegenerative disorder characterized by combined degeneration of the dentafugal and pallidofugal systems (Naito and Oyanagi 1982; Takahashi et al., 1988). Although this disease may occur sporadically, it is more commonly inherited as an autosomal dominant trait. The clinical features of the disease are diverse, with varying combinations of myoclonus and other movement disorders, epilepsy, cerebellar ataxia and cognitive impairment (Takahata et al., 1978). This is a progressive disorder, with the age of onset ranging from the first to the seventh decade, with a mean age of onset of 30 years (reviewed by Koide et al., 1994).

There seems to be a close correlation between age of onset and clinical features, patients presenting under the age 20 years (juvenile onset) show a form of PME characterized by

myoclonus, epileptic seizures, dementia and ataxia (reviewed by Komure et al., 1994). However, patients presenting after the age of 40 years (late adult onset) have cerebellar ataxia, choreoathetosis and dementia, while patients whose ages at onset range from 20-40 years show transitional forms between the juvenile and late adult onset (reviewed by Komure et al., 1994). There is an accelerated age at onset and enhanced severity of the disease in successive generations that is more prominent in paternal than in maternal transmission (Sano et al., 1994).

The identification of the clinical features associated with DRPLA paved the way to the identification of the disease-causing gene. It was hypothesized that genes with trinucleotide repeats, which are expressed in human brain, may be plausible candidates for DRPLA, the basis of this hypothesis will be discussed in section 1.5.2.2 (Koide et al., 1994; Nagafuchi et al., 1994). Through screening databases containing previously described genes containing triplet repeats, a gene, *CTG-B37* later named atrophin, was identified as the disease-causing gene (Koide et al., 1994; Nagafuchi et al., 1994).

1.1.4 Treatment of epilepsy

Epilepsy is a chronic disorder, or group of disorders, characterized by seizures that usually recur unpredictably in the absence of consistent provoking factors (Scheuer and Pedley, 1990). Accurate classification of epileptic syndromes, and specifically type of seizure, is essential to all aspects of managing seizures, from the initial diagnostic evaluation to the decision about whether to treat, with what drug and for how long. The first level of treatment for epilepsy is the administration of antiepileptic drugs, when seizures fail to respond to epileptic drugs, brain surgery is a therapeutic alternative (Scheuer and Pedley, 1990).

1.2 BACKGROUND ON LQTS

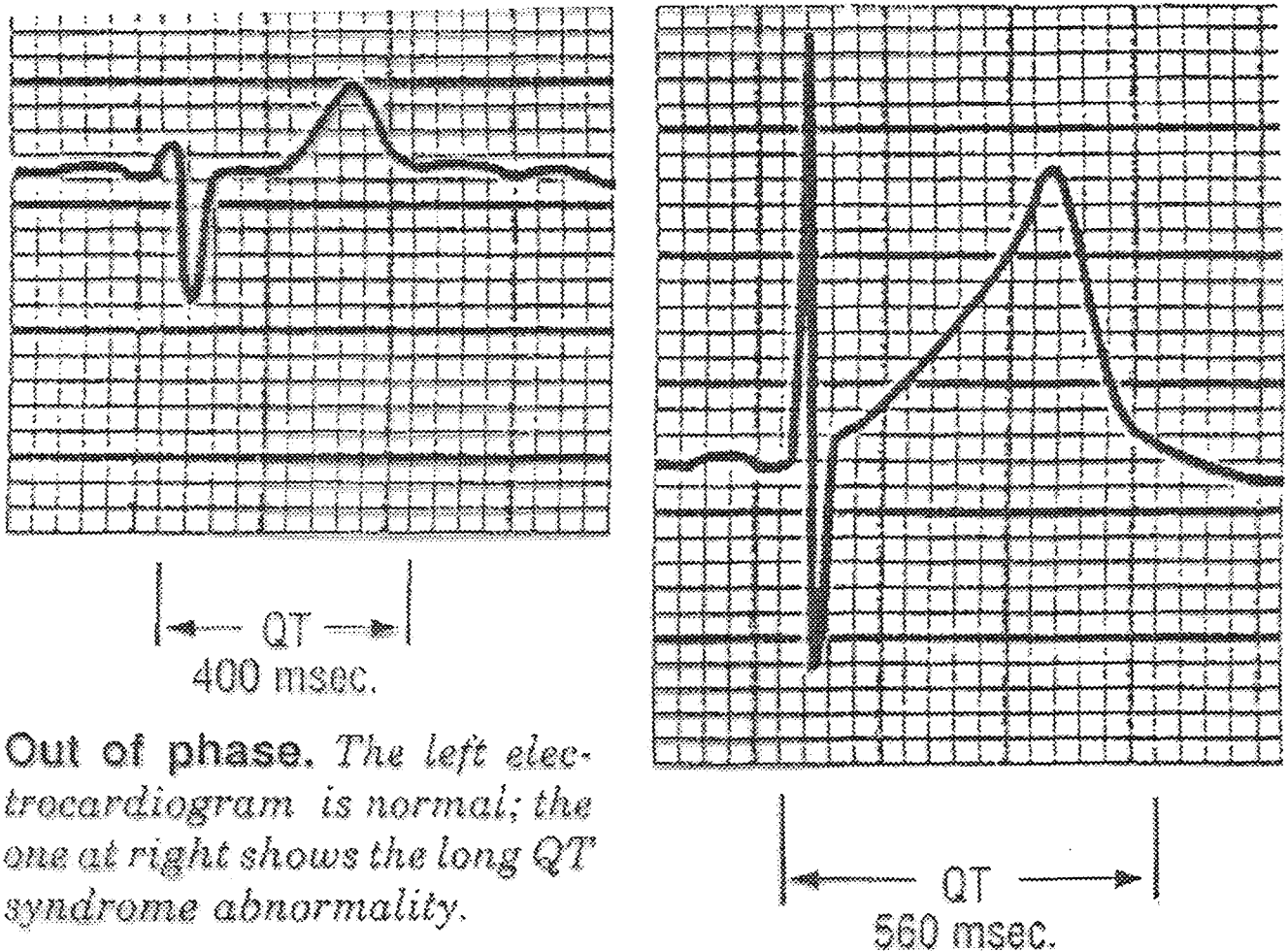
The Long QT Syndrome is a cardiovascular repolarization disorder that is characterized by the occurrence of life threatening arrhythmias, such as torsade de pointes and ventricular fibrillations. These arrhythmias can present as seizures, syncope and sudden cardiac death in young otherwise healthy individuals (Keating et al., 1996).

This disorder was named the LQTS because of the prolonged QT interval on the electrocardiogram (ECG) that is present in affected individuals (figure 1.1) (Marx, 1991). The QT interval represents the time in the heartbeat when the heart muscle is recovering from one contraction, before it can be triggered to contract again (Barinaga, 1998). Thus, the prolongation of the QT interval lengthens the recovery time of the heart and makes it more variable from cell to cell. This can cause the electrical impulse that allows the heart to contract to sweep through the heart muscle in an irregular fashion. The latter can interfere with the heart rhythm and can send the heart into fibrillation and sudden death (Barinaga, 1998).

The LQTSs can be inherited or acquired; hereditary LQTS is rare and affects 1 in 10 000 people but for those people the risk of death can be 50% over 10 years (Barinaga, 1998). The LQTSs are genetically heterogeneous disorders and two distinct genetic forms of this disease, an autosomal recessive form, the Jervell Lange-Nielsen Syndrome (JLNS) (Jervell and Lange-Nielsen, 1957), and a autosomal dominant form the Romano-Ward Syndrome (RWS) (Ward, 1964; Romano et al., 1963) have been described to date. Families affected by RWS were investigated in the present study.

1.2.1 Jervell Lange-Nielsen Syndrome

In 1957, Jervell and Lange-Nielsen reported the first case of LQTS in a family of six, where four of the children had a combination of deaf-mutism and a peculiar heart disease (Jervell and Lange-Nielsen, 1957). The deaf mute children suffered from “fainting attacks” occurring from the age of three to five years, but otherwise seemed quite healthy. No signs of heart disease could be discovered in the clinical examination. The ECGs, however, revealed a pronounced prolongation of the QT-interval in all cases, and three of the deaf-mute children died suddenly at the ages of four, five and nine years, respectively (Jervell and Lange-Nielsen, 1957).



Out of phase. The left electrocardiogram is normal; the one at right shows the long QT syndrome abnormality.

Fig.1.1 QT prolongation. The electrocardiograms show that the QT interval in a patient with LQTS is longer (560ms) compared to an individual in which this condition is absent (400ms). Thus the heart of a patient with LQTS takes longer to recover from an action potential than a normal heart (figure taken from Marx, 1991).

1.2.2 Romano Ward Syndrome

In 1964, Ward observed a syndrome in an Irish family with the following features: (i) prolonged, but variable, QT interval on the ECG at rest, (ii) attacks of ventricular flutter or fibrillation following exertion or emotional disturbance, (iii) normal interval between heart sounds, (iv) absence of valvular or gross myocardial disease and (v) familial incidence (Ward, 1964). At the same time, Romano et al., (1963) described a three-month old female infant with similar clinical features. In the families described by Romano and his associates, (Romano et al., 1963) and by Ward (1964), a prolonged QT interval was observed and sudden death also occurred, as in the condition described by Jervell and Lange-Nielsen. However, in Romano and Ward's families the hearing was normal, and direct familial transmission was consistent with an autosomal dominant mode of inheritance (Romano et al., 1963 and Ward, 1964), in contrast to the autosomal recessive mode of inheritance described in the Jervell Lange-Nielsen Syndrome (Fraser, 1964).

To assist in a better understanding of the natural history of this disease, its clinical features and the long-term efficiency of different therapeutic approaches, the group of Schwartz and Moss established a worldwide prospective study in 1979. In 1985, a preliminary report of the first 196 patients with LQTS in this program was published (Moss et al., 1985). The precipitating factor of syncope in 58% of the cases was intense emotion (fright or anger), vigorous exercise in 45% and a loud noise often producing a startling awakening in 9% of cases (Moss et al., 1985). During the past 20 years, 728 families with clinically identified LQTS have been enrolled in this International Long-QT Syndrome Registry (Zareba et al., 1998). The clinical findings of this study identified a broad spectrum of clinical manifestations among LQTS patients. Affected persons had a prolonged QT interval, relative sinus bradycardia and a propensity to recurrent syncope, malignant ventricular tachyarrhythmias of the torsades de pointes type and sudden death (Moss and Robinson, 1992). Brief episodes of alternation of the T-wave could also develop in LQTS patients, following the same stimuli which usually trigger synocopal attacks. Abnormal U-waves or T-U-waves were also seen in some patients (Schwartz, 1975).

Molecular genetic techniques have been employed to determine the molecular cause of the disease. The progress to date on the molecular genetic studies will be summarized in the following paragraph; however, it will be discussed in detail in section 1.7.

In 1991, Keating's group demonstrated linkage between the autosomal dominant form of LQTS and the *Harvey ras-1* gene (*H-ras-1*) on the short arm of chromosome 11 (Keating et al., 1991). Benhorin et al., (1993) provided evidence for genetic heterogeneity in LQTS in a large Israeli family. Later that same year, Keating's group confirmed this finding in two of their families which did not link to the chromosome 11 locus (Curran et al., 1993). This finding was followed by Keating's group's report of two LQTS loci that mapped to chromosome 3 and 7, and evidence for further heterogeneity (Jiang et al., 1994). In 1995, a fourth LQTS-causing locus was mapped to chromosome 4 (Schott et al., 1995). The same year, Keating's group identified the genes for both the chromosome 3 and 7 type of LQTS as a cardiac sodium channel gene (*SCN5A*) (Wang et al., 1995a) and a cardiac potassium channel gene, the human ether-a-go-go gene (*HERG*), respectively (Curran et al., 1995). In 1996, Keating's group also identified the gene causing the chromosome 11 form of LQTS as that encoding a voltage-gated potassium channel (*KVLQT1*) (Wang et al., 1996a). In 1996, the groups of Sanguinetti et al., (1996) and Barhanin et al., (1996) independently showed that *KVLQT1* associated with hminK to form the channel underlying the I_{Ks} cardiac current. The group of Splawski et al., (1997) identified a fifth disease-causing locus, as *KCNE1*, the gene encoding hmin K.

Fraser et al., (1964) speculated on the possibility that a factor common to both the heart and the ear electrolyte disequilibrium could explain the pathogenesis of LQTS. They considered the fact that the extra-cellular concentrations of, for example, the potassium ion (K^+) are important in cardiac conduction, and some of the ECG features in LQTS could result from K^+ imbalance. Furthermore, the endolymph of the inner ear is unusual in that the K^+ concentration is similar to that normally found in intra-cellular fluids and this might be of importance to normal conduction in the auditory nerve. However, Fraser could not demonstrate abnormalities in the level of any intra- or extra-cellular electrolyte in the blood of LQTS-affected persons he studied (Fraser et al., 1964).

Early in 1997, Neyroud et al., (1997) showed at a molecular level that JLNS and RWS can be caused by mutations in the same gene, *KVLQT1*. However Jeffrey et al., (1992) failed to find linkage in another JLNS family between the disease and *H-ras-1*, a polymorphic marker located 2 centimorgan (cM) distal to the *KVLQT1* locus. This result could be explained by either a recombination event that had occurred in this family between *H-ras-1* and the disease locus, or genetic heterogeneity in JLNS (Neyroud et al., 1997). Genetic heterogeneity was established in JLNS by Tyson et al., (1997) through exclusion of the *KVLQT1* locus with

linkage analysis in a single small consanguineous family. The group subsequently showed that a homozygous mutation in *KCNE1* was responsible for the disease in this family. In the study of Duggal et al., (1998), four JLNS families were investigated for mutations in *KVLQT1* and *KCNE1*, in one of these families, *KCNE1* was implicated as the causative gene and *KVLQT1* in the second family. However, in the two remaining families no mutations were detected in either of these genes, suggesting the possibility of additional genetic heterogeneity in this disorder.

1.2.3 Acquired forms of LQTS

Although much research has been done on the inherited forms of LQTS, acquired and sporadic forms of this disease have also been reported (Schwartz et al., 1985). Acquired forms of LQTS are most frequently the result of medications, often antiarrhythmic or psychoactive drugs such as quinidine and thloridazum. However, the condition can also be caused by neurologic, metabolic or other cardiac abnormalities (Keating, 1996).

1.2.4 Treatment of LQTS

The availability of effective therapy for this often lethal disease emphasizes the importance of early and accurate diagnosis. At present, there are three modalities of treatment for patients with LQTS: (i) β -blockers (Moss, 1986), (ii) pacemakers (Eldar et al., 1987; Moss et al., 1991) and (iii) left-cervicothoracic sympathetic ganglionectomy (Moss and McDonald, 1971; Bhandari et al., 1984; Schwartz, et al., 1991a). The primary goal of therapy is to prevent life-threatening arrhythmogenic syncope and sudden cardiac death. The therapy has to be individualized for each patient, as will be discussed below.

The role of sympathetic tone, in the setting of overactivity of the left and/or underactivity of the right stellate ganglion, in precipitating adrenergic-dependant torsade de pointes, has led to the use of β -adrenergic agents as primary therapy and left cervicothoracic sympathectomy as secondary therapy (Moss and Robinson, 1992). β -Blockers have proven to be effective in preventing syncope in 75-80% of LQTS cases (Schwartz et al., 1985; Jackman et al., 1988). Despite full dose β -blockade, 20-25% of patients continue to have syncopal episodes and remain at high risk for sudden cardiac death (Schwartz et al., 1985; Jackman et al., 1988). It is for these patients that left cervicothoracic sympathectomy should be considered (Moss and McDonald, 1971). Implantation of an automatic defibrillator could provide additional protection in those patients unresponsive to the latter therapy (Moss et al., 1991). Permanent

pacing has been reported to prevent torsade de pointes in a small number of patients with LQTS. Pacing appears to be most beneficial in those patients developing profound bradycardia with pharmacological therapy, or in those where pauses or slow ventricular rates precede the initiation of torsade de pointes (Moss et al., 1991).

The recent advances in the molecular genetics of LQTS have opened a new avenue for the application of gene specific therapies, but this will be discussed in detail in the section 1.8.

1.3 CONFUSION IN DIAGNOSIS

In their report in 1964, Fraser et al., (1964) described the syncope attacks displayed by LQTS-affected individuals in detail. They observed a resemblance of the syncope attacks displayed by LQTS patients to epilepsy or hysterical or behavioral episodes. In 1991, Schwartz et al., gave further insight into why LQTS patients were first seen by a neurologist or a psychiatrist (Schwartz et al., 1991b). The syncope attacks displayed by LQTS patients were due to a precipitous decrease in cardiac output that caused patients to lose consciousness, as a result of the rapid rate of the ventricular tachycardia or torsades de pointes. If the hypofusion was of sufficient duration, ensuing cerebral hypoxia might lead to convulsions. These events usually occurred after situations with high emotional content, which is why these episodes were frequently thought to represent a hysterical reaction; the presence of the convulsions often leads to the erroneous diagnosis of a seizure disorder (Schwartz et al., 1991b).

The fact that LQTS is a rare disorder is also one of the reasons that it is not often included in the primary differential diagnosis of syncope, thus misinterpretation as epilepsy may occur. If siblings are also affected, genetic epilepsy may even be diagnosed (Schwartz et al., 1991b). The misdiagnosis of LQTS as an idiopathic seizure disorder has led to inappropriate treatment of patients, at the risk of their lives. The diagnosis of LQTS is difficult and even if an ECG is performed and a family history of the disease is present, there are still a number of factors that could influence the diagnosis. Firstly, the family history may be unremarkable, because many LQTS gene carriers have relatively normal QT intervals. This realization was made in 1979, already, with an extraordinary family studied by Coumel and Slama that included 11 children affected by LQTS; among them were six sudden deaths including siblings with normal QT intervals (reviewed by Schwartz, 1985).

Diagnosis can further be hampered by the overlapping of QT intervals between affected and unaffected individuals (Vincent et al., 1992). This was demonstrated in a retrospective study of

three chromosome 11-linked kindreds in which gene carriers could unequivocally be identified, by using molecular genetic techniques, 83 individuals were classified as affected and 116 as unaffected. This study demonstrated that the QT interval corrected for heart rate (QTc) in gene carriers varied from 0.41s to 0.59s (mean = 0.49s), and in non-carriers ranged from 0.38s to 0.47s (mean = 0.42s). Diagnosis of LQTS based on a QTc of >0.44s led to the misclassification of five gene carriers (6%) and 17 noncarriers (15%) (Vincent et al., 1992).

The QT interval is inherently variable, changing in a given person in relation to heart rate, autonomic tone, age, sex, usage of medication and the presence of other disorders. Furthermore, diagnosis could be missed because ECG is not routinely performed in young, otherwise healthy, individuals (Vincent et al., 1992).

Correct diagnosis is of fundamental importance, to clearly distinguish between LQTS and genetic forms of epilepsy that display similar clinical symptoms, because effective treatment for both disorders is available. In the case of LQTS, the mortality among untreated symptomatic patients is high, 20% in the first year after the initial syncope and approximately 50% within 10 years (Keating, 1992). The current diagnostic criteria have led to misdiagnosis and missed diagnosis of affected LQTS patients; thus, there was a need to develop new methods of diagnosis that can support the present one. Molecular genetic techniques could provide a very accurate means of diagnosis. However, this technique requires the identification and characterization of causative genes of the disease.

One strategy to identify the gene that is responsible for an inherited disorder is the application of linkage analysis to firstly identifies the chromosomal localization of the gene. After the disease locus has been positioned, a battery of molecular genetic techniques can be employed, to ultimately identify and characterize the specific gene and mutations in the gene, that are causing the defect leading to the clinical manifestation of the disease (reviewed by Keating, 1992).

In the next section, the basis of the molecular genetic techniques employed in previous studies performed on LQTS and the three types of familial epilepsy that are examined in this report will be discussed briefly. This will be followed by a section where the applications of these techniques in the above-mentioned disorders will be highlighted.

1. 4 MOLECULAR GENETIC TECHNIQUES

1.4.1 Identification of Disease-causing Loci with Linkage Analysis

The molecular genetic approach to familial diseases is to identify the gene(s) and the associated mutation(s) that are causing the specific disease, in order to find explanations for the basic mechanisms that result in the clinical expression of the disease.

Before the era of genetic linkage analysis, the search for the causative gene started with the identification of proteins that might be important in the specific disorder under investigation. These proteins were then studied and, if biochemical or physiological abnormalities were found, it was possible to work back to the gene that encoded the protein and then to identify disease-causing mutation(s) in the gene (reviewed by Keating, 1992). However, it is now possible to start by closing in on the defective gene itself. This strategy begins with the chromosomal localization of the gene that is responsible for a particular inherited disorder (White and Lalouel, 1988).

The way genes are inherited is exploited by the linkage analysis strategy; in the late nineteenth century, Mendel demonstrated that traits were inherited as independent units; and that the inheritance of one trait did not influence the likelihood of the inheritance of a second (reviewed by Keating, 1992). This fundamental rule of inheritance is known as Mendel's law of independent assortment. Morgan and his co-workers proposed in the early 1900's the existence of an exception to this rule. These investigators noted, in their breeding experiments with *Drosophila*, that certain traits, or genes, were inherited together more frequently than would be predicted by chance, thus these genes were coinherited or linked. These genes were coinherited or linked because they were physically located close to each other on the same chromosome (reviewed by Keating, 1992).

Linkage analysis is a technique that can be used, in multigenerational families affected by a disease showing a mendelian inheritance pattern, to identify the chromosome on which the disease-causing gene is located. Polymorphic chromosomal markers positioned close to the disease gene are employed in linkage analysis (figure 1.2) (reviewed by Keating, 1992). However, it is the phenomenon of recombination that makes it possible to find linkage between a marker and a disease (figure 1.2). If there were no recombination, only 22 markers, that is one per autosome, would be required to determine on which chromosome a genetic locus was located; however, it would not be possible to narrow the region of the chromosome

on which the gene actually lies (White and Lalouel, 1988). Parental chromosomes are not transmitted to offspring in their original form; during the generation of germ cells, recombination, or crossing over, occurs between loci on homologous chromosomes (figure 1.2) (Keating, 1992). The closer together two loci lie on the same parental chromosome, the less often their alleles are separated as deoxyribonucleic acid (DNA) is exchanged between homologous chromosomes during meiosis (figure 1.2) (White and Lalouel, 1988). Thus, two genetic loci that are separated by a few thousand base pairs would rarely recombine, conversely two loci on the same chromosome that are separated by 20 million base pairs would recombine, in approximately 20% of meiosis (Keating, 1992). Statistical analysis can be used to calculate the odds that an allele of the DNA marker and the disease gene are inherited more often than would be expected by chance and are therefore linked. The odds are expressed in logarithmic form called the logarithm of the odds score (LOD score). Once linkage between a polymorphic marker and a disease locus has been identified, the detection of recombination events between the disease locus and additional markers in the target search area can be used to refine the location of the disease locus (Keating, 1992).

Two allelic forms of a genetic marker (one of maternal and the other of paternal origin) are present in each individual. An individual is heterozygous (figure 1.3) for a marker if he has two different alleles of a marker, conversely he is homozygous (figure 1.3) if the alleles are identical (Keating, 1992). The genotype of each marker tested for each family member is defined. The haplotype, the particular combination of alleles at linked loci in a defined region of a chromosome, can be determined and, if all the affected individuals share the same haplotype, there will be a high degree of probability that the marker is cosegregating with the disease and linkage can be proven (Keating, 1992).

As the Human Genome Project (Collins and Galas, 1993), the cooperative effort to map and sequence the entire human genome, progresses, the human gene map has become saturated with polymorphic markers. This is the consequence of one of the main goals of the Human Genome Project, namely to develop a 2-5 centimorgan (cM) spaced high-resolution human genetic map of highly informative markers. Another important implication of the Human Genome project is the advances in genotyping technology that lead to the development of new types of genetic markers, such as short tandem repeat polymorphisms (STRPs) also referred to as microsatellite markers (Collins and Galas, 1993). These types of genetic markers replaced

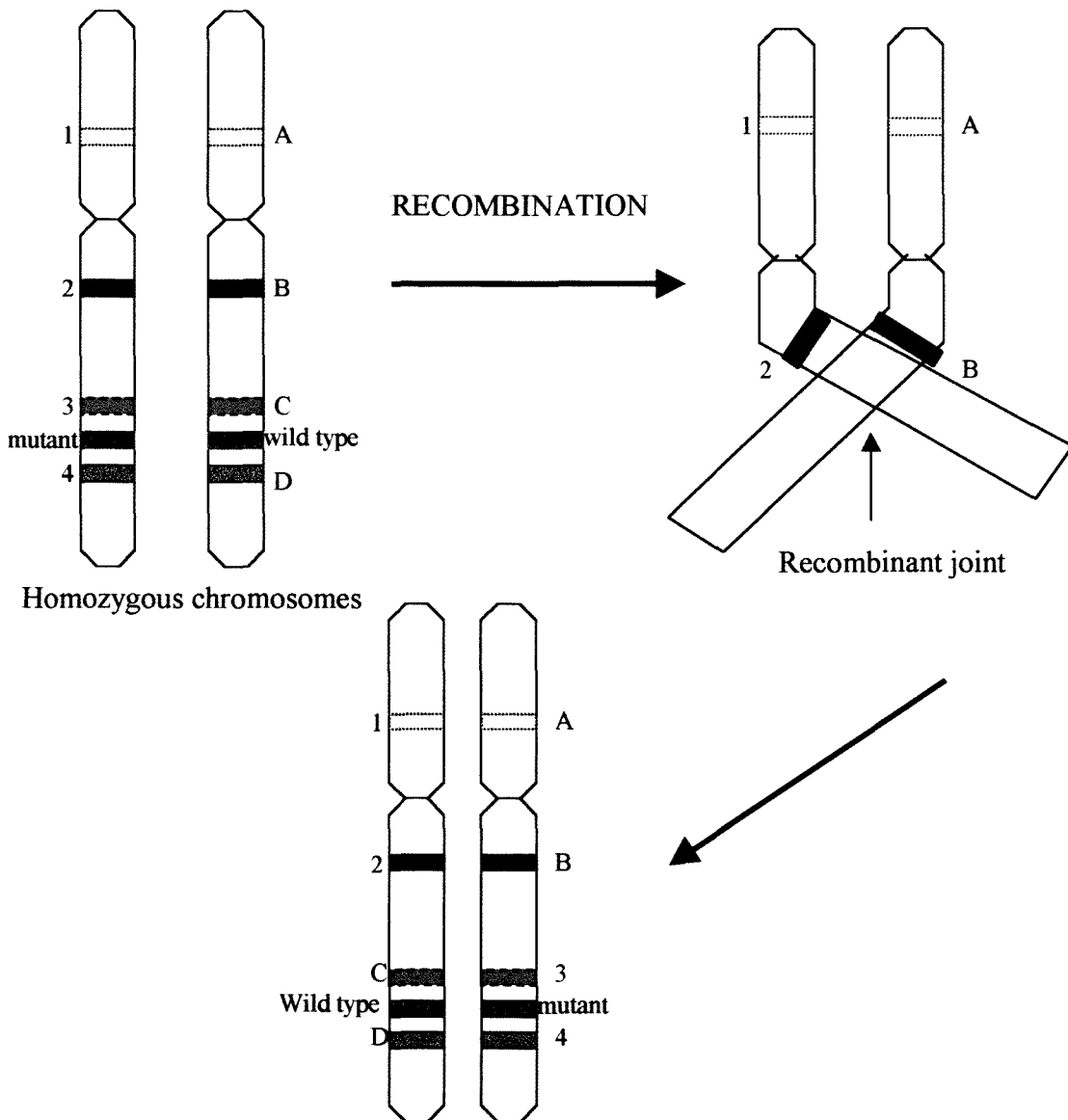


Fig. 1.2 Genetic recombination. The closer together two genetic loci lie on the same parental chromosome the less often their alleles are separated during meiotic recombination between homozygous chromosomes and these loci are said to be linked. The alleles of two genetic loci that are situated far apart on the same chromosome have a higher chance of being separated during recombination events. The numbers 1, 2, 3 and 4, represent the alleles of different marker loci positioned on the homologous chromosome on which the mutant allele is located. The letters A, B, C and D, represent the alleles of these marker loci positioned on the homologous chromosome on which the wild type allele of a disease-causing locus is located. The alleles 3 and 4 are linked to the mutant allele, as these alleles are not separated during recombination, while alleles 1 and 2 are unlinked, alleles C and D are linked to the wild type allele and alleles A and B are not linked to the wild type.

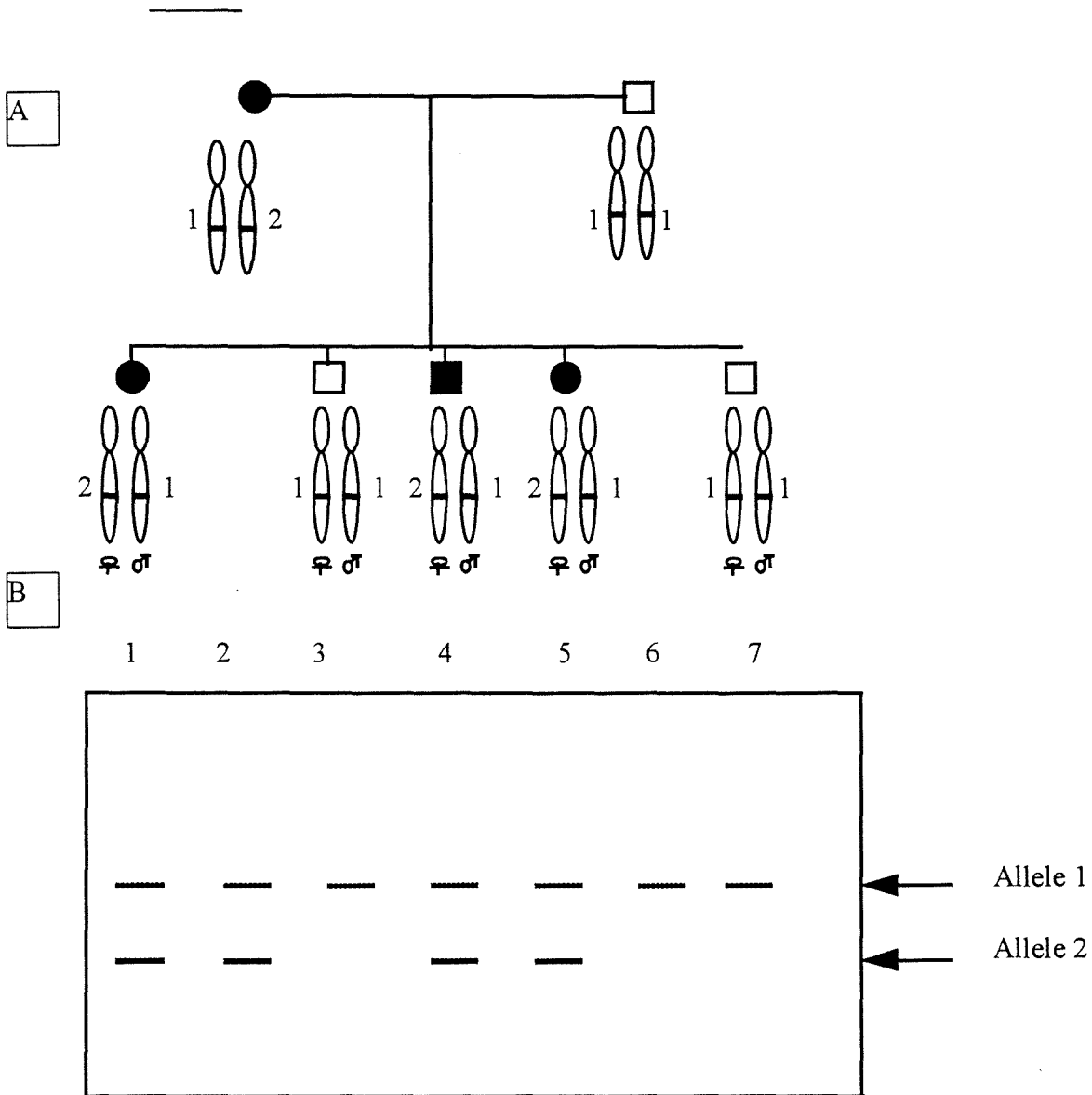


Fig. 1.3 Heterozygous and homozygous allelic forms of a genetic marker. (A) Family in which a genetic marker was genotyped. Where it can be deduced, the alleles inherited from the mother and father are indicated. (B) Lanes 1, 2, 4 and 5 represent the heterozygous allelic form of a genetic marker showing two different alleles of the marker, lanes 3, 6 and 7 show the homozygous form of the genetic marker where the two alleles are identical. Allele two segregates with the disease as it is present in all affected individuals. (□= allele inherited from the father; □= allele inherited from the mother; □ = unaffected male; ○= unaffected female ■= affected male; ●=affected female).

the earlier forms of DNA markers such as restriction fragment length polymorphisms (RFLPs) that required standard Southern blot and hybridization techniques (Weber and May, 1989).

The abundant interspersed repetitive units, that were identified in the human genome formed the basis for the development of the STRP type of genetic marker (Weber, 1990). These repetitive DNA sequences units can consist of di- tri- or tetra-nucleotide repeats, however, in the present study, mostly dinucleotide repeats such as, $(dC-dA)_n$ and $(dG-dT)_n$, hereafter designated $(CA)_n$, were used and, therefore, will be discussed in the next paragraph.

In the human genome, there are between 50,000 - 100,000 interspersed $(CA)_n$ blocks, with the range of n being roughly 15-30. Uniform spacing of the $(CA)_n$ blocks throughout the genome would place them every 30-60 kb (Weber, 1990). The function of these $(CA)_n$ blocks is unknown, but it has been proposed that they serve as hot spots for recombination (Slighton et al., 1980) or participate in gene regulation (Hamada et al., 1984).

Linkage analysis allows mapping of the causative gene to within a distance of 5-10 cM between flanking markers; however, a distance of 2.2 cM is thought to contain about 100 gene transcripts (Collins, 1992). Therefore, it is necessary to reduce the search area further, after linkage analysis has indicated the approximate chromosomal position of the gene. One approach is the usage of genetic fine mapping and physical mapping techniques (Wicking and Williamson, 1991).

1.4.2 Linkage disequilibrium mapping

The presence of recombinants aids in the narrowing of the critical search area of a disease-causing gene (Keating, 1992). Methods that would allow for increasing the number of recombinants could contribute to the narrowing of the critical search region. One way to achieve this is through increasing the number of families under study, however, this is not always practical due to limited numbers of informative families. An alternative method of obtaining additional recombinants, and thus mapping at a higher resolution, is through linkage disequilibrium mapping, that is the non-random association of alleles at linked loci (Hästbacka et al., 1992; Jorde, 1995).

When a disease mutation is introduced into a population for the first time, either by a new mutation or the immigration of a mutation carrier, the mutant allele would necessarily reside on a single chromosome with a unique set of marker alleles, thus displaying a unique haplotype (Jorde, 1995). Consequently, there would be a complete disequilibrium between these markers and the disease mutation: that is, the disease mutation would only be found in the presence of a specific set of marker alleles. Genetic markers nearest to the disease gene will recombine least often and should show the highest degree of allelic association with the disease. The disequilibrium would gradually decrease as recombinations between the disease mutation and the marker polymorphisms occur through subsequent generations leading subsequently to a decrease in the length of the characteristic haplotype (Jorde, 1995). Thus, disequilibrium analysis increases the number of recombinants that can be detected, because the number of recombinants that occur through many generations is far greater than that observed from any pedigree based linkage study (Xiong and Guo, 1997).

By employing linkage disequilibrium mapping, it is possible to map genes at a scale finer than 1cM. The first step in this process is to determine the haplotypes of disease-bearing chromosomes for an extremely dense collection of genetic markers, the linkage disequilibrium is then measured by applying a statistical association test to haplotype data. However the methodological development of linkage disequilibrium mapping requires profound knowledge of population genetics of the population analyzed (Hästbacka et al., 1994).

1.4.3 Genetic Fine Mapping and Physical Mapping

To move from the linked marker to the disease-causing gene, a physical map of the area where the marker is situated must be generated and new polymorphic markers covering the target area must often be identified (Wicking and Williamson, 1991). Flanking markers, that are tightly linked to, but are recombinant with, the disease phenotype, must be identified, which will allow the gene to be approached from either direction and also define the interval in which the gene resides. Recombination breakpoints, occurring in certain individuals in certain families, can help to narrow the area of interest to an area flanked by very tightly linked markers, this area can further be refined by physical mapping (Wicking and Williamson, 1991). The latter includes the cloning and subcloning of the contiguous stretch of DNA between the two genetic markers flanking the region containing the disease gene (Keating, 1992).

Cloning vectors that can be used include the P1 bacteriophage cloning system (Sternberg, 1990), yeast artificial chromosomes (YACs) (Green and Maynard, 1990), bacterial artificial chromosomes (BAC) (Willems and Skurray, 1987) and cosmid cloning vectors (Sternberg, 1990). The bacteriophage P1 cloning vector contains P1 components included in a circular plasmid that can incorporate 70-90 kb of foreign DNA (Sternberg, 1990). The YAC cloning system is based on the introduction of exogenous linear DNA molecules into a yeast host. The YACs are capable of harbouring several hundred kilobase fragments of linear DNA and these long stretches of DNA can then be analyzed in detail (Green and Maynard, 1990). The BAC cloning system is based on the *Escherichia coli* (*E.coli*) fertility F¹ plasmid. The F¹ plasmid copy number is 1-2 per *E.coli* cell, thus reducing the potential for recombination between cloned DNA fragments that it carries (Willems and Skurray, 1987). The cosmid cloning system permits cloning, isolation and recovering of DNA inserts as large as 45kb which can be packaged efficiently into phage lambda particles (Sternberg, 1990).

Polymorphic DNA markers can then be developed from the cloned segments and subsequently used to determine the orientation of the overlapping clones to construct the physical map. Integration of these markers into the genetic map can be used in genetic fine mapping to narrow the search area further (Keating, 1992).

1.4.4 The Identification of Candidate Genes

Once the minimal critical search area has been identified, the genes that reside in the physically mapped, refined target area must be identified. Genes in this area can become candidates by position and their candidacy is strengthened if their physiological or biochemical function might play a role in the development of the disease, for example ion channel genes that are candidates for LQTS (Moss, 1986, Keating, 1996). Sometimes, the search for the disease-causing gene is accelerated by a cytogenetically detectable anomaly in a patient, as was the case in the Duchenne muscular dystrophy search (Monaco et al., 1986). In a few cases, such as in Huntington's disease (The Huntington's Disease Collaborative Research Group, 1993) and DRPLA (Koide, et al., 1994; Nagafuchi, et al., 1994), the presence of an expanded trinucleotide repeat has provided clues to the identification of the disease-causing gene. However, it is unrealistic to expect these fortuitous aids in most mapping endeavors, that is why novel coding sequences within these refined search areas must often be identified. Methods to identify these coding sequences include the detection of CpG islands (Bird, 1987) as potential sign-posts for the 5' ends of some transcription units and direct selection of cDNA,

the hybridization of radiolabelled cDNAs to arrayed genomic clones (Hochgeschwender et al., 1989). Exon trapping, the capturing of expressed sequences from fairly large genomic sequences (Duyck et al., 1990), and software trapping, the analyses of DNA databases (Kamb et al., 1995), are also methods that can be used to identify coding sequences.

1.4.5 The Identification of the Disease-causing Gene

When a transcription unit is identified in the target region, it becomes a candidate for a given disease gene based on its chromosomal location (Wicking and Williamson, 1991). Candidates identified in this manner, as well as candidates identified by virtue of their physiological or biochemical function, require several forms of analysis to confirm that they are the genes which, when mutated, cause the disease.

In order to show that a candidate gene is the disease-causing gene, it must be possible to prove that this gene is expressed in the tissues most commonly affected in the diseased individual (Wicking and Williamson, 1991). It is also desirable to show that sequence homology exists between the candidate gene sequence and already characterized gene sequences encoding proteins that could be involved in the aetiology of the disease. If DNA from the affected families is analyzed with probes from the candidate gene sequence, and no recombination events between the closest flanking markers and the candidate gene are detected, the candidate gene could also be considered as the disease-causing gene (Wicking and Williamson, 1991).

Additional strong evidence that the correct gene has been isolated will be provided by the detection of mutations in DNA from patients and obligate carriers (Keating, 1992). Methods to identify disease-associated mutations in the candidate genes include polymerase chain reaction (PCR)- based single strand conformational (SSCP) analysis (Orita et al., 1989 a, b), PCR-based differential gradient gel electrophoresis (PCR-DGGE) (Gejman and Gelernter, 1993), direct sequencing and allele specific restriction enzyme analysis (ASREA). In the present study PCR-SSCP analysis and ASREA were employed, PCR-SSCP analysis will be discussed in section 1.4.5.1.

Evidence that a candidate gene is the disease gene includes the cosegregation of a mutation with the disease in one family, and the identification of unrelated affected families with identical or other mutations in the same gene and the identification of germ line mutations in sporadic cases of the disease and absence of these mutation in unrelated unaffected control

individuals. Once the gene has been identified, the structure and function of the protein product of the gene can be examined by use of biochemical and physiological techniques (Keating, 1992). The ultimate proof that a candidate gene is indeed the disease-causing gene is correlation of structural and functional data. An example of the latter is the ability of an unmutated copy of the gene to complement the underlying biochemical or physiological phenotype when introduced into the mutated gene sequence or related sequences (Wicking and Williamson, 1991).

1.4.5.1 PCR-SSCP Analysis

The PCR-SSCP analysis is the most widely used mutation screening technique to detect single base pair changes in PCR-amplified DNA fragments from selected regions of candidate genes (Gejman and Gelernter, 1993). This technique is based on the fact that single base pair substitutions or sequence variations affect the mobility of single stranded DNA through polyacrylamide gels (Orita et al., 1989 a, b). The analysis is carried out by denaturing the PCR amplified selected DNA region at 95⁰C and then electrophoretically separating the alleles on a non-denaturing polyacrylamide gel. Under these conditions, the single strands fold back on themselves in a sequence dependent manner and sequence variations can frequently induce differential electrophoretic mobility, presumably due to alternative geometrical conformations. The mobility shift of DNA fragments bearing these single point substitutions can be markedly affected by temperature changes and variations in the gel composition, and, therefore a variety of different conditions are normally used to improve the resolving power (Gejman and Gelernter, 1993). Screening is typically performed under one or more of four different gel conditions: room temperature or 4⁰C in the presence or absence of 10% glycerol. However, although this technique is widely utilized, a 100% success rate is not always achieved (Orita et al., 1989b).

Mutation screening employing PCR-SSCP analysis is usually performed in two stages; the first stage includes identification of the gene containing the mutation, while stage two concerns the identification of the nature of the mutation by sequencing.

1.5 APPLICATION OF MOLECULAR GENETICS TECHNIQUES IN TWO FAMILIAL FORMS OF EPILEPSY

1.5.1 Progressive Myoclonus Epilepsy Type 1 (EPM1)

1.5.1.1 Linkage analysis in EPM1

As the pathogenesis of EPM1 is unknown, one way of approaching the pathogenetic mechanisms underlying the disorder is characterizing of the genes that cause the disease. To this end, Lehesjoki et al., undertook a systematic genome search to find the causative gene by employing linkage with polymorphic DNA markers in EPM1-affected families (Lehesjoki et al., 1991; Lehesjoki et al., 1992; Lehesjoki et al., 1993).

Linkage analysis was performed in twelve Finnish families who were clinically diagnosed with EPM1; these families included 68 individuals, of whom 26 were affected (Lehesjoki et al., 1991). A total genome search was performed and linkage was detected after 25% of the genome was excluded by the testing of 64 markers. Linkage was detected with marker *D21S112* and confirmed with the markers *BCEI* and *D21S154*, which had been localized by physical methods to chromosome 21q22.3. The maximum LOD score for *D21S112* was 6.91 at $\theta = 0.034$ and for *BCEI* and *D21S154*, maximum LOD scores of 5.49 and 4.25 respectively were derived at $\theta = 0.00$ (Lehesjoki et al., 1991).

In 1992, Lehesjoki et al., (1992), in an effort to refine the search area of the *EPM1* locus, performed a linkage study in thirteen Finnish families, twelve of these families were employed in the earlier study of this group, that initially localized the *EPM1* gene to chromosome 21q22.3. The study included 73 individuals, of whom 28 were affected, the diagnostic criteria used were: (i) age at onset between 6 and 15 years; (ii) tonic-clonic seizures, often presenting as first symptom; (iii) stimulus-sensitive myoclonus; (iv) characteristic EEG findings with generalized spike-wave and polyspike-wave paroxysms and sensitivity to photic stimulation; (v) progressive course. In their second study, Lehesjoki and co-workers found that the two markers that showed recombination with EPM1 were *MX1* and *CD18* (figure 1.4). The maximum LOD score for linkage between EPM1 and *MX1* was 2.80 at $\theta = 0.036$ and for *CD18* it was 4.82 at $\theta = 0.029$. No recombinations was detected between the disease phenotype and marker loci *BCEI*, *D21S19*, *D21S42*, *D21S113*, *D21S154* and *PFKL* (figure 1.4) and the maximum LOD scores for linkage at these six loci at $\theta = 0.00$ were 5.98, 1.60, 3.28, 5.42, 4.25 and 6.30 respectively. Thus, *MX1* and *CD18* flank the region in which *EPM1*

resides, this region encompasses 20.3cM on the genetic map (figure 1.4) (Lehesjoki et al., 1992).

In the following year, the same group (Lehesjoki et al., 1993) found a new flanking marker, *D21S212*, that showed recombination with the disease locus, with a maximum LOD score of 7.78 at $\theta = 0.02$. The *EPM1* locus was now positioned in the 7 cM region flanked by *D21S212* and *CD18* (figure 1.4) (Lehesjoki et al., 1993).

To further refine the position of the causative gene, linkage disequilibrium mapping was applied (Lehesjoki et al., 1993). Using this technique, twelve multiplex families were analyzed at the linked marker loci on the *EPM1*-bearing chromosome. No significant evidence for linkage disequilibrium was seen for any alleles at loci *D21S212*, *BCE1*, *D21S19*, *D21S42*, *D21S113* and *CBS* (figure 1.4); however, significant evidence of linkage disequilibrium was found for loci *D21S25*, *D21S141*, *PFKL* (CA repeat), *PFKL* (*KpnI*), *D21S154*, *D21S171* and *CD18* (figure 1.4) indicating that the *EPM1* locus was likely to lie in this area.

The study was then extended to include an additional 26 families and the seven loci that showed significant linkage disequilibrium were analyzed further (Lehesjoki et al., 1993). Linkage disequilibrium can only be performed in populations that fulfill certain criteria, namely, populations that have a high proportion of disease-causing alleles originating from a single ancestral mutation sufficiently long ago for recombination to have significantly reduced the region of strongest linkage disequilibrium. The Finnish population fulfills these criteria, since the present day population of 5 million is believed to have expanded from a small number of founders some 2 000 years ago (Lehesjoki et al., 1993). Linkage disequilibrium mapping used this information, together with the degree of linkage disequilibrium observed at the tested markers in a mathematical equation, to determine the distance between the *EPM1* locus and these markers. Using this technique, *EPM1* was mapped to a genetic distance of within about 0.13-0.30 cM encompassed by *D21S25*, *PFKL* and *D21S154* (Lehesjoki et al., 1993).

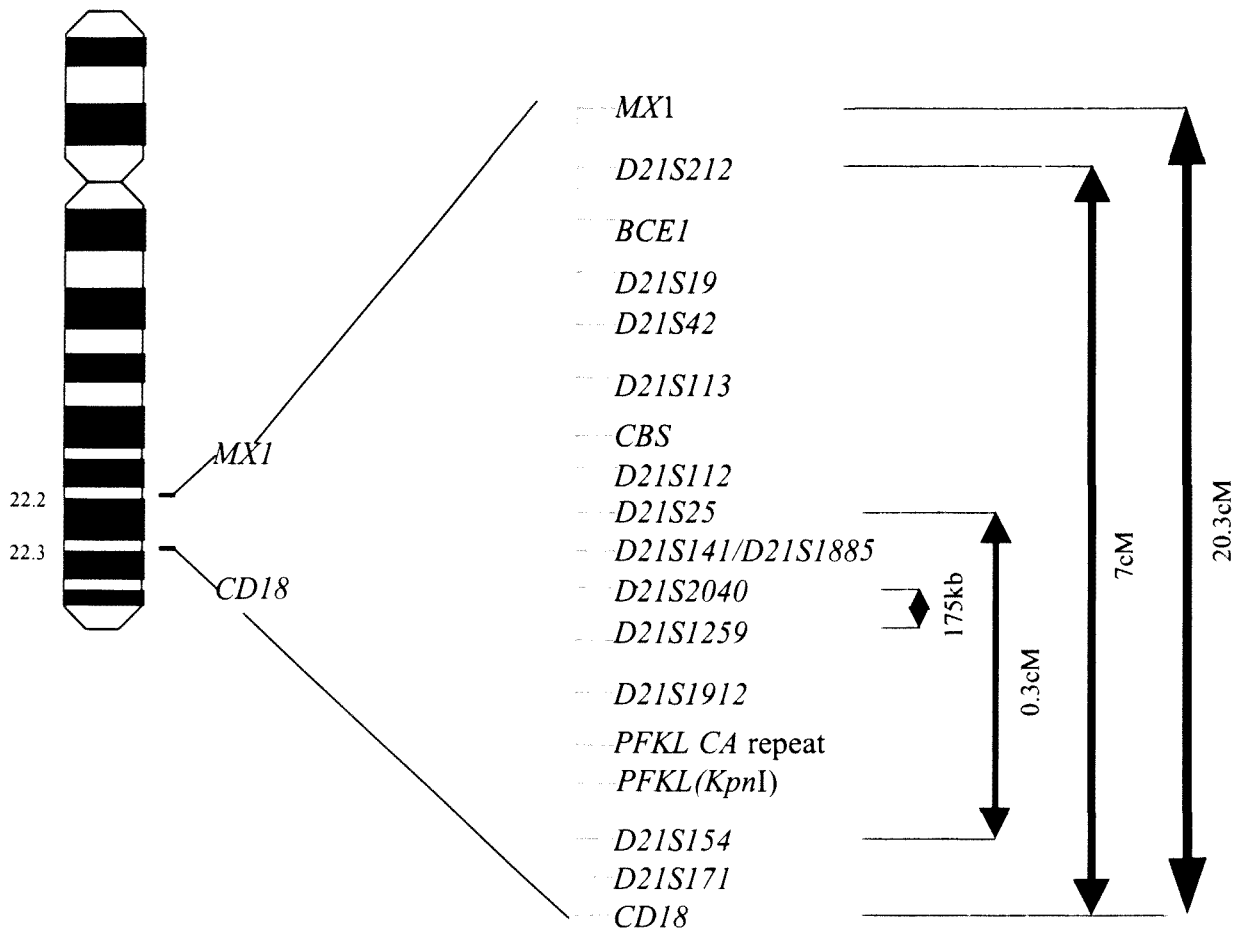


Fig. 1.4 Ideogram and genetic map of chromosome 21 showing how the critical search area for EPM1 was narrowed from 20.3 cM to 175 kb (Compiled from Rouyer et al., 1990; Lehesjoki et al, 1991; 1992; 1993; Virtaneva et al., 1996).

In an effort to further narrow the region in which the gene must reside, Virtaneva and his group used a contiguous array of cosmid, BAC and P1 clones covering the critical region to search for, and to map, new, suitably-spaced highly polymorphic genetic markers (Virtaneva et al., 1996).

Linkage disequilibrium mapping and haplotype analysis were employed to analyze five new markers, *D21S1885*, *D21S2040*, *D21S1259*, *D21S1912* and *PFKL* (figure 1.4) in 53 unrelated Finnish families. In each family, only one affected individual and both parents, if available, were considered. To determine if there was a single allele with a significantly higher frequency on the disease-bearing chromosome than on normal chromosomes, the haplotypes of these 53 patients were compared with alleles on the normal chromosomes of 73 parents. Significant linkage disequilibrium was detected for all markers studied. The frequency of the most common allele on the *EPM1*-bearing chromosome versus the normal chromosomes were 93%/73% (*D21S1885*), 96%/58% (*D21S2040*), 96%/40% (*D21S1259*), 93%/21% (*D21S1912*) and 79%/14% (*PFKL*) (Virtaneva et al., 1996).

Haplotype construction of the markers in the *EPM1*-critical region was performed in 88 *EPM1* and 62 normal chromosomes (Virtaneva et al., 1996). An ancestral haplotype of 3-2-4-4-2 at the loci listed in the preceding paragraph was seen in 65 *EPM1* and in only 7 normal chromosomes, historical recombination events had occurred in haplotypes in 22 *EPM1*-chromosomes. As a result of the putative historical recombinations, the critical region of the *EPM1* gene could be predicted to lie between the markers *D21S2040* and *D21S1259* (figure 1.4) (Virtaneva et al., 1996). This region was entirely encompassed in a 750 kilobase (kb) bacterial clone contig generated by sequence tagged site content mapping and walking. A detailed restriction map of the contig was used to determine the distance between these DNA markers, defining the boundaries of *EPM1* to about 175kb (Virtaneva et al., 1996).

1.5.1.2 Identification of disease-causing genes in *EPM1*

Positional cloning techniques were employed to find the disease-causing gene in the absence of obvious candidate genes for *EPM1* in the critical region. Direct cDNA selection was used to isolate segments of expressed DNA from the 175 kb region (Virtaneva et al., 1996) and a previously described protein, cystatin B (*CSTB*), a cysteine protease inhibitor, was identified with cDNAs from BAC clone 52C10. The gene encoding *CSTB* had not previously been mapped to a human chromosome; however, these data indicated that it resided in this segment

of human chromosome 21, and based on its location it became a strong candidate for the *EPM1*-causative gene (Pennacchio et al., 1996). Previous reports that the gene encoding *CSTB* was widely expressed were confirmed by demonstrating that a probe made from the cDNA clone detected a messenger ribonucleic acid (mRNA) approximately 0.8kb in length in eight human tissues, including heart, brain, placenta, lung, liver, skeletal muscle, kidney, and pancreas (Pennacchio et al., 1996).

On northern blots, lymphoblastoid cells from affected individuals from four different families had reduced levels of *CSTB* mRNA, compared to those in unaffected, noncarrier individuals and carrier parents of affected individuals (Pennacchio et al., 1996). In order to explain these findings, the gene encoding *CSTB* from affected individuals was sequenced. The entire nucleotide sequence of the human gene from an unaffected chromosome was first determined, this sequence revealed that the gene is 2500 base pair (bp) in length and contains three small exons encoding a 98-amino acid protein. Using the nucleotide sequences, primers were designed to amplify the gene encoding *CSTB*, and the amplified PCR product sequence was determined in an affected individual from each of four *EPM1* families. Two different mutations were identified in the *CSTB* gene on sequence comparison between DNA from a control individual and *EPM1* patients. One was a G→C transversion at the last nucleotide of intron 1, altering the sequence of the highly conserved 3' splice site AG dinucleotide. The second mutation, which was found in the alleles of the *CSTB* gene from two of the four families, changed CGA to TGA, generating a translation stop codon at amino acid position 68 (Pennacchio et al., 1996).

The recognition site for the restriction enzyme *Bfal* is destroyed by the 3' splice site mutation and a simple test to screen for this mutation could be developed, no mutant alleles were found after screening for this change in 95 unrelated, unaffected individuals (Pennacchio et al., 1996). The stop codon mutation was screened for by direct sequencing of PCR products of 70 alleles from unaffected control individuals, no mutant alleles were found in these samples. Pennacchio et al., succeeded in identifying the disease-causing gene in three of the four families under study. However, in the remaining family, which had the characteristic common Finnish haplotype, no sequence differences in the gene encoding *CSTB* were detected (Pennacchio et al., 1996).

In an effort to identify additional *EPMI* mutations, Lafreniere et al., (1997) performed PCR-SSCP analysis in 20 unrelated patients and 20 controls of different ethnic groups. Three SSCP variants were detected, however two of these conformers were the result of the two mutations previously described by Pennacchio et al., (1996). The third SSCP variant was identified as a novel 2bp deletion at bp 313-314, predicted to cause a frame shift, resulting in premature termination of the nascent protein three codons down stream of the deletion. However, the majority of the tested *EPM1* patients did not show any SSCP variants compared to controls in each of the three exons of the *CSTB* gene that were examined (Lafreniere et al 1997).

Southern blot analysis was performed using a 2.5 kb *HindIII/PstI* fragment isolated from cosmid Q37H6, which contains most of the *CSTB* gene, as probe for *EPM1* patients' DNA digested with *Hind III*, *Eco RI* or *Sac I* (Lafreniere et al., 1997). A 600 to 900 bp larger band was consistently found in *EPMI* patients' chromosomes, but not in normal chromosomes. This larger fragment segregated with the disease and was found in all the *EPMI* chromosomes for which no SSCP variants were detected, the size of the enlarged fragments were clearly variable among patients, suggesting an unstable expansion (Lafreniere et al., 1997).

At the same time, the group of Virtaneva et al., (1997) also found Southern blots of *PstI*-digested genomic DNA from *EPM1* patients to show abnormally enlarged fragments, compared to control individuals. Sequencing of the coding region, introns and the 3' end of the gene revealed nothing abnormal; however, both the groups of Lafreniere and Virtaneva had some difficulties in amplifying the 5' region from exon 1 to the *PstI* site in *EPM1* patients (Lafreniere et al., 1997; Virtaneva et al., 1997). In the controls, PCR amplification yielded fragments of the expected size. In order to characterize the expansion, Virtaneva's group sequenced the insert of a λ clone containing the 5' region and the additional DNA material recovered from a λ vector genomic DNA library made from an *EPM1* patient (Virtaneva et al., 1997). Lafrenieres' group first determined the localization of the insertion in the larger *PstI* fragment by amplifying the entire *CSTB*-genomic DNA in several overlapping fragments (Lafreniere et al., 1997). Primers flanking and partially overlapping this polymorphic repeat region upstream and downstream were used to amplify DNA fragments of *EPM1* patients. Sequencing of this expansion revealed a minisatellite with an 18 bp unit that was repeated several times at the 5' region of the expansion and a repeated 15-mer unit at the 3' end of the expansion (Lafreniere et al., 1997; Virtaneva et al., 1997). Sequencing across the entire expansion was unsuccessful, as it was impossible to overcome compressions in the long repeat

arrays. The expansion lengths ranged from 0.5 to 1.5 kb and no correlation between expansion size and clinical disease severity was found (Virtaneva et al., 1997).

The groups of Lafreniere and Virtaneva found that the unstable minisatellite expansion accounted for the majority of EPM1 patients worldwide (Lafreniere et al., 1997; Virtaneva et al., 1997). Seventy-eight percent of the unrelated EPM1 chromosomes studied by Lafreniere et al., harboured this DNA insertion mutation in the 5' flanking region of the *CSTB* gene (Lafreniere et al., 1997). In Finland, this expansion was detected in 102/106 (96%) *EPM1* chromosomes and it accounted for 33/34 (97%) *EPM1* chromosomes in the Mediterranean region (Virtaneva et al., 1997).

Thus, in summary, the *CSTB* gene has been identified as the *EPM1*-causative gene and it is apparent from the studies performed that the main molecular defect in *EPM1* is absence or reduced levels of functional CSTB protein most probably due to reduced transcription of the *CSTB* gene (Lafreniere et al., 1997; Virtaneva et al., 1997). This is most probably the result of either truncation of the protein due to the stop codon mutation (Pennacchio et al., 1996) or the 3' splice site deletion at bp 313-314 which causes a frame shift introducing a stop codon (Lafreniere et al., 1997). In addition, inappropriate splicing of the transcript due to the 3' splice site mutation (Pennacchio et al., 1996) or diminished levels of mRNA due to an unstable insertion in the 5' flanking region of the *CSTB* gene (Lafreniere et al., 1997; Virtaneva et al., 1997) could also lead to a reduced transcription of the *CSTB* gene.

1.5.2 DRPLA

1.5.2.1 Linkage Analysis in DRPLA

Several cases of DRPLA had originally been reported under the diagnosis of Huntington's disease (HD), although it was possible to differentiate DRPLA from HD through differences in their pathological features (Kondo et al., 1990; Nørremølle et al., 1995). This misdiagnosis could be attributed to the fact that the clinical features of patients with late adult onset of DRPLA are sometimes indistinguishable from the clinical features of HD. Both these diseases are inherited in an autosomal dominant fashion, further contributing to the difficulty in differentiation between them (Kondo et al., 1990).

In 1990, the group of Kondo et al., (1990) initiated a linkage analysis study to determine if DRPLA is a distinct neurodegenerative disorder or an allelic variant of HD. The DNA

polymorphic marker *D4S10*, which was proven to be linked to HD in a previous study (Gusella et al., 1983), was used to perform linkage analysis, in four DRPLA families in affected and unaffected subjects of age 40 years and older (Kondo et al., 1990). The locus for hereditary DRPLA was excluded from the vicinity of *D4S10* at $\theta = 0.0125$ LOD score -2.281, thus indicating that hereditary DRPLA and HD are distinct. Although the Huntingtons locus was excluded as a cause of DRPLA, it was still sometimes difficult to distinguish patients showing choreoathetosis and dementia with mild cerebellar ataxia from Huntington's patients, in the absence of pathological examination of the brain (Nagafuchi, 1994). If the locus for DRPLA could be assigned to a specific chromosome, or the gene causing the disease was identified, it would be easier to differentiate this disease from HD and other similar diseases (Kondo, 1990).

Two independent research groups, Koide et al., (1994) and Nagafuchi et al., (1994), continued the search for the causative gene for DRPLA and in 1994 both of them reported that patients suffering from DRPLA had a CAG repeat expansion in a gene termed *CTG-B37* localized on chromosome 12. The two groups used different strategies to arrive at the same conclusion. Nagafuchi's group initiated a linkage analysis study in fourteen families with a total of 45 affected individuals using polymorphic markers mapped throughout the genome (Nagafuchi et al., 1994). They identified the short arm of chromosome 12 as the most plausible region containing the gene responsible for DRPLA. The disease-causing gene for DRPLA was found to segregate with *CD4*, LOD score of 3.61 at $\theta = 0.00$, and with *F8VWF*, LOD score = 3.32 at $\theta = 0.06$, on chromosome 12p12. After the disease-causing locus was found, several genes on chromosome 12p, potentially involved in neuronal processes, were examined as candidate genes, including neurotrophin 3 and proline-rich protein family genes (Nagafuchi et al., 1994). However, the group of Koide et al., did not perform linkage analysis and they started their study by directly closing in on the causative gene by searching genes with unusual triplet repeat expansions (Koide et al., 1994). The rationale for their approach will be discussed in the next section.

1.5.2.2 The Identification of the DRPLA Disease-Causing gene

Koide's group's approach, to directly close in on the causative gene by searching genes with unusual triplet repeat expansions, was based on the hypothesis that DRPLA is the result of a unstable triplet repeat expansion (Koide et al., 1994). The disease shares genetic and clinical features with a group of disorders in which unstable expansions of triplet repeats was

identified. These diseases include fragile X syndrome (Fu et al., 1991), spinal and bulbar muscular atrophy (La Spada et al., 1991), myotonic dystrophy (Brook et al., 1992; Buxton et al., 1992; Fu et al., 1992; Harley et al., 1992), HD (The Huntington's Disease Collaborative Research Group, 1993) and spinocerebellar ataxia type 1 (Orr et al., 1993). The common features of these disorders are: (i) considerable heterogeneity in clinical presentations and ages at onset, even in a single pedigree, (ii) an increase in the severity of symptoms with accelerated ages of onset in successive generations and (iii) paternal bias in the transmission of the most severe forms (Koide et al., 1994). Given this background, Koide et al., (1994) hypothesized that genes with trinucleotide repeats, which are expressed in human brain, may be highly plausible candidates for DRPLA. The group of Nagafuchi et al., (1994) also changed direction given this knowledge, and considered genes containing triplet repeats located on chromosome 12p as candidates for DRPLA.

The studies performed on the disorders in which triplet repeat expansions had been found previously led to compilation of a catalogue of genes containing repeats of simple sequences, by scanning databases and experimental screening of various libraries (Li et al., 1993). The groups of Koide and Nagafuchi searched for previously published genes containing trinucleotide repeats, through screening these databases and experimental libraries (Koide et al., 1994; Nagafuchi et al., 1994).

Nagafuchi's group examined the *CTG-B37* repeat described in such a catalogue, because it was linked to a marker on chromosome 12 and their linkage analysis results had implicated chromosome 12p as the candidate region (Nagafuchi et al., 1994). PCR amplification was employed to determine whether the *CTG-B37* repeat varied in DRPLA patients compared to control individuals. PCR products from most normal individuals were in the size range of 116-161bp and two alleles were clearly identified. However, when DRPLA patients' DNA was analyzed, multiple indistinct DNA bands appeared in the region of 240-320bp, in addition to DNA bands derived from the other allele that was in the normal range. The enlarged DNA fragments were observed in all patients diagnosed with DRPLA (Nagafuchi et al., 1994).

The group of Koide et al., (1994), in their search for previously published genes containing trinucleotide repeats, identified the same gene, *B37*. This CAG repeat was analyzed using the genomic DNA from patients with various forms of hereditary ataxia. The study subjects of Koide et al., (1994) included 22 DRPLA patients, 28 patients showing ataxia or extrapyramidal

signs, other than DRPLA, and 61 control individuals. An enlarged PCR product was observed in only the 22 DRPLA patients.

Both these research groups subcloned the PCR products corresponding to normal alleles and expanded alleles from DRPLA patients (Koide et al., 1994; Nagafuchi et al., 1994). The CAG repeat was found to be highly polymorphic and fifteen normal alleles, ranging from 8-25 repeats, were identified (Koide et al., 1994). DRPLA patients were all heterozygous, with one allele in the normal range and a second expanded allele within the range of 54-68 repeat units (Koide et al., 1994).

Koide et al., (1994) demonstrated that there was a good correlation between the degree of expansion and age of onset and DRPLA patients with juvenile onset (onset before 20 years) had a tendency to contain large expansions of the CAG repeat. In the pedigrees studied by Nagafuchi, it was evident that the size of the expanded allele increased from generation to generation when the disease was transmitted from the father. However, enlarged fragments were almost the same, or even decreased, when the disease was transmitted from the mother (Nagafuchi et al., 1994). Although Koide's group only analyzed five cases of paternal transmission and two cases of maternal transmission, they came to the same conclusion as Nagafuchi's group (Koide et al., 1994).

In 1995, Onodera et al., (1995) undertook to isolate the full-length cDNA clone of the DRPLA gene, because of the discrepancies in the sequence reported by Nagafuchi in 1994 (Nagafuchi et al., 1994). The nucleotide sequence described by Onodera et al., (1995) essentially agreed with that of Nagafuchi et al., (1994), but there were dissimilarities in 15 regions. In addition to the 15 regions, the 49 bp sequence at the 3' noncoding region was absent in Nagafuchi's sequence and, in particular, there were gaps at nucleotide (nt) 2352, 2401, and 2449 in the latter's sequence, which led to different deduced amino acid residues at 785-817. Onodera et al., (1995) predicted the DRPLA cDNA to encode a 1185 amino acid protein with a predicted molecular mass of 125 kD, named DRPLA protein (DRPLAP).

In summary, the DRPLA disease-causing locus was localized to the short arm of chromosome 12 (Nagafuchi et al., 1994). It was hypothesized that genes expressed in the brain with a triplet repeat in their coding regions would be highly plausible candidates for DRPLA. This hypothesis was made based on the similarities between DRPLA and other neurodegenerative disorders, where triplet repeat expansions have been identified as the causative mutation,

(Nagafuchi et al., 1994; Koide et al., 1994). By screening databases and experimental screening of various libraries, a gene with a CAG repeat was picked up that was expanded in DRPLA patients. The nucleotide sequence of this gene was determined and the CAG repeat was analyzed in DRPLA patients and unaffected subjects; it was found that the CAG repeat ranged from 8-25 repeats in normal individuals and from 54-68 repeats in DRPLA patients (Nagafuchi et al., 1994; Koide et al., 1994).

1.5.3 Chromosome 8p linked form of epilepsy

A Japanese group investigated a form of epilepsy with similar clinical features to those seen in FME and in their study linkage was found to the DNA marker *D8S264* (personal communication, Berkovic).

1.6 IMPORTANCE OF MAPPING EPILEPSY GENES

The advances in molecular genetics and the identification of families affected by well-defined epilepsy syndromes have led to the localization of several disease-causing genes and even the identification of these genes in some cases. The identification of genes influencing susceptibility to epilepsy could facilitate early identification of at risk individuals, early

treatment and perhaps prevention of the disorder in some individuals (Ottman, 1997). Once the mutated gene has been identified, the mechanism by which such inheritance leads to a specific epilepsy syndrome could be investigated on a molecular, cellular and systematic level (Delgado-Escueta et al., 1994). This can lead to a better understanding of the pathogenesis of the disease and development of new strategies for treatment and prevention targeted at the specific cellular or molecular defects believed to be important in seizure generation. (Dichter, 1997).

Some of the first genes identified in human epilepsy syndromes were voltage-gated or ligand-gated ion channels (Steinlein et al., 1995; Singh et al., 1998; Charlier et al., 1998; Ryan, 1999). Ion channel defects were also found in a number of diseases known to occur intermittently in otherwise healthy individuals. These discoveries suggested that subtle, prevalent genetic variations in ion channel genes could also be involved in the aetiology of the common forms of idiopathic epilepsies with complex modes of inheritance (Ryan, 1999). However, to date, no

ion channel variants have been implicated convincingly in susceptibility to common epilepsies (Ryan, 1999).

A mayor stumbling block in clarification of the aetiology of the epilepsies has been a lack of an adequate and systematic classification (Steinlein, 1998). Characterizing the genetic contribution to human epilepsy could play an important role in the development of a more clinically useful classification of seizure disorders (Ryan, 1999). The increasing knowledge from the fields of molecular genetics, in parallel with developments at a clinical level could change the approach, from the present classification based on subdivisions into idiopathic, cryptogenic and symptomatic categories, to more aetiologically oriented and disease specific categories (Duchowny and Harvey, 1996). Improving the classification of epilepsy genotypes will improve calculations of sibling risk for seizures and abnormal EEG patterns. This should, in turn, improve the accuracy of risk assessments and facilitate genetic counseling, providing an accurate and balanced picture of possible family burden (Delgado-Escuera et al., 1994).

Although not all epilepsies are genetic in origin, insights derived from the study of genetic epilepsies may increase the understanding of these disorders and may help to elucidate mechanisms and improve therapy for genetic as well as acquired forms of epilepsy.

1.7 APPLICATION OF MOLECULAR GENETICS TECHNIQUES IN LQTS

1.7.1 Linkage Analysis

1.7.1.1 Linkage of LQTS to chromosome 11p15.5

In 1991, Keating's group performed a genome wide search, in a large Utah family, in an effort to find the disease-causing gene for the autosomal dominant form of LQTS (Keating et al., 1991). To avoid misclassification of individuals, a conservative approach to phenotypic assignment was used, in which the diagnosis of LQTS was made on the basis of a QTc \geq 0.45s in an individual with symptoms, or a QTc \geq 0.47s in the absence of symptoms. An individual with a QTc $<$ 0.42s was classified as unaffected and when the QTc was between 0.42 and 0.46s, in an asymptomatic individual, the disease status was classified as unknown (Keating et al., 1991). Linkage was performed using the LINKAGE program (Lathrop and Lalouel, 1984), with the penetrance set at 0.90, the disease frequency assumed to be 0.001 and the female and male recombination frequency equivalent. Keating and co-workers tested 245 markers in the family, excluding 60% of the human genome, before a linked marker was found (Keating et

al., 1991). This was a DNA marker termed *pTBB-2*, defining a restriction site polymorphism at the *H-ras-1* locus, which was found to be tightly linked to the *LQT* locus, with a maximum LOD score of 16.44 at a $\theta=0$. Linkage was confirmed with a second DNA probe at *H-ras-1*, *pUC EJ6.6*, which gave identical results (LOD score of 16.44 at $\theta = 0.00$) (Keating et al., 1991). The *H-ras-1* locus had previously been mapped to chromosome 11p by linkage with other known loci and by physical mapping with somatic cell hybrids (Kidd et al., 1989). *In situ* hybridization had previously confirmed this chromosomal assignment and provided independent subregional localization of the *H-ras-1* locus to the short arm of chromosome 11p15.5 (Jhanwar et al., 1983; de Martinville et al., 1983).

1.7.1.2 Genetic heterogeneity in LQTS

In June 1993, Benhorin and associates reported a large Israeli family, comprising 131 individuals, of whom 28 were affected, in which there was an absence of linkage between LQTS and *H-ras-1* (Benhorin et al., 1993). They performed genetic analyses with 74 individuals using two different methods. The first method they used was a complex segregation analysis that resulted in evidence for a single completely dominant allele. The major LQTS locus and the *H-ras-1* marker were used in a combined linkage and segregation analysis, which showed that the major LQTS locus was not tightly linked to *H-ras-1* for this specific family. The best recombination fraction estimate was 0.494, which was close to the value of 0.50 that corresponds to no linkage (Benhorin et al., 1993). The second analysis was conventional linkage analysis using the same criteria as in the study by Keating et al., (1991), these results also excluded linkage to *H-ras-1*. Taken together, these data and that of Keating et al., (1991) implicated genetic heterogeneity in LQTS (Benhorin et al., 1993).

In August of that same year, Curran and his colleagues confirmed linkage of the disease to the short arm of chromosome 11p15.5 in seven LQTS families and also characterized two families that were not linked to *H-ras-1* (Curran et al., 1993). Linkage analysis was performed in two multigenerational families with autosomal dominant LQTS, one of Italian descent including 16 family members (kindred 1756), and one of Polish descent comprising 15 family members (kindred 1977). Highly polymorphic markers at the *H-ras-1* locus were used, as well as genetic markers from different regions of 11p15.5. Significant negative LOD scores were obtained at all these loci suggesting that the gene responsible for LQTS in both these families was not linked to *H-ras-1*. This data implicated locus heterogeneity for autosomal dominant LQTS and confirmed Benhorin's findings (Curran et al., 1993).

1.7.1.3 Linkage of LQTS to chromosomes 7q35-36

After heterogeneity had been identified in LQTS in 1993 (Benhorin et al., 1993; Curran et al., 1993), Keating's group initiated a study to identify new *LQTS* loci in 15 multigenerational families with autosomal dominant LQTS (Jiang et al., 1994). These families were not related and were of varying North American descent, including Polish, Italian, English, German, Swiss, Finnish, Norwegian and Russian origin. To avoid misclassifying individuals, the same conservative approach to phenotypic assignment was used as described in the study by Keating et al., (1991).

The linkage analysis studies were initiated in two kindreds (1756, 1977) that were not linked to chromosome 11p15.5 (Curran et al., 1993). In this study, 110 STRP markers spanning the genome, also including markers mapping near genes that were candidates for the disease based on a physiological rationale, were used to perform genotypic analysis (Jiang et al., 1994). Linkage was identified after 35% of the genome was excluded employing 70 markers. Linkage was detected with DNA marker *D7S483* on the long arm of chromosome 7, at $\theta = 0.001$ LOD score 2.71, in kindred 1977 and 1.54 in kindred 1756 (figure 1.5). The combined LOD score for both families was 4.25, suggesting that the gene responsible for LQTS was located near *D7S483* (Jiang et al., 1994).

Linkage analysis was performed on 13 other families to test the hypothesis that a gene for LQTS mapped to the long arm of chromosome 7, seven of these families showed positive LOD scores at *D7S483* (Jiang et al., 1994) (figure 1.5). A LOD score of greater than 3 was detected in two families and the maximum combined LOD score for the nine chromosome 7-linked families was 19.41, corresponding to odds in favour of linkage of greater than 10^{19} to 1. Taken together, these data indicated tight linkage between *D7S483* (figure 1.5) and a LQTS disease locus, which was, designated *LQT2* (Jiang et al., 1994).

1.7.1.3 Linkage of LQTS to chromosome 3p21

Six of the fifteen families included in the study of Jiang et al., (1994) generated significantly negative LOD scores at the genetic marker *D7S483*, thus indicating that these families were not linked to the chromosome 7 locus. To confirm this result, genotypic analysis with a neighbouring polymorphic marker, *D7S505* (figure 1.5), was performed and a negative LOD score was obtained employing this marker in all six families (Jiang et al., 1994). None of the 15 families studied by Jiang et al., demonstrated linkage to markers on chromosome 11p15.5,

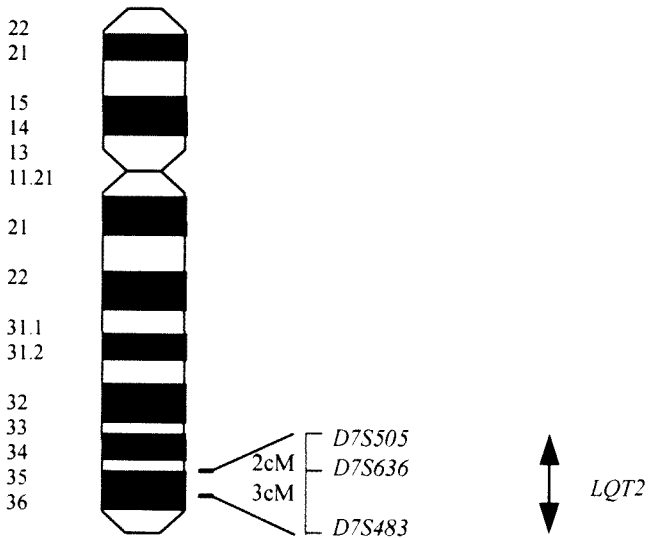


Fig. 1.5 Ideogram and genetic map of chromosome 7 showing the location of LQT2. Brackets indicate the positions of the markers *D7S505*, *D7S636*, *D7S642* and *D7S483*, which showed significant LOD scores with the *LQT2* locus. The distances between the markers are indicated in cM (figure taken from Jiang et al., 1994).

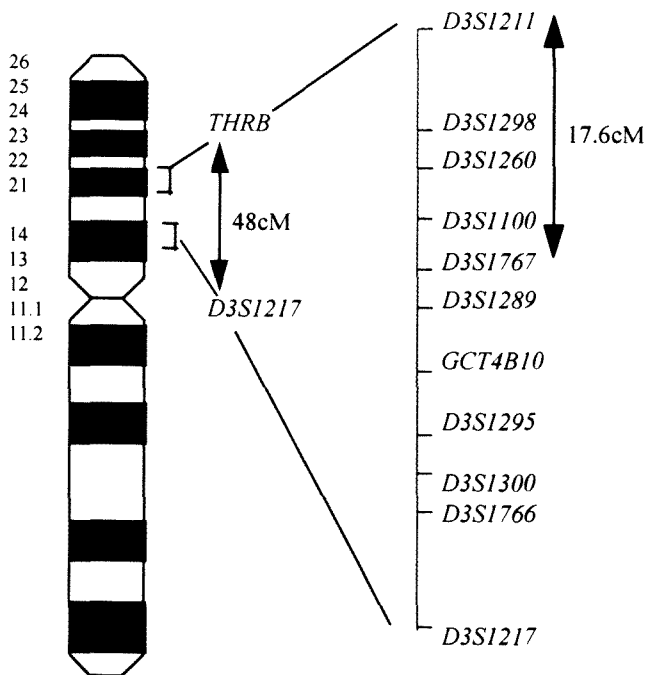


Fig. 1.6 Ideogram and genetic map of chromosome 3 showing the location of LQT3. Brackets show physical locations of *THR8* and *D3S1217*. LQT3 is genetically linked to the region between *D3S1211* and *D3S1767* (figure taken from Jiang et al., 1994).

thus excluding the *LQT1* locus. Thus, in these six families, the *LQT1* and *LQT2* loci were excluded indicating that another *LQTS* locus must exist (Jiang et al., 1994).

A random genome search was performed in one of these six families, in an effort to localize a third *LQTS* gene and strong suggestive evidence of linkage was obtained with a microsatellite marker at *THRB* on chromosome 3 (LOD score 2.75 at $\theta = 0.05$) (Jiang et al., 1994). The genetic marker *D3S1217* that maps approximately 48 cM centromeric to *THRB*, also showed distant positive linkage. Consequently, seven markers (*D3S1211*, *D3S1298*, *D3S1260*, *D3S1100*, *D3S1767*, *D3S1289* and *GCT4B10*) (figure 1.6), mapping to the interval between *THRB* and *D3S1217*, were employed in linkage analysis to confirm linkage to chromosome 3 in this specific family. The markers at *D3S1100* and *D3S1298* were completely linked to the LQTS phenotype, with LOD scores of 5.35 and 3.61, respectively, at $\theta = 0.001$ (Jiang et al., 1994).

Linkage analysis was then performed in the other five families with the markers *D3S1100* and *D3S1298*. Two families were completely linked to these markers and the combined pairwise LOD scores in the three linked families at *D3S1100* and *D3S1298* were 6.72 and 6.39, respectively (Jiang et al., 1994). Haplotype analysis was performed in these three families to refine the position of the locus. The identification of obligate recombinants at *D3S1211* and *D3S1767* allowed the disease-causing gene to be mapped to an estimated 17.6 cM interval between the centromeric and telomeric flanking markers (figure 1.6). The disease-causing locus identified in these three families was designated *LQT3*. However, significantly negative LOD scores were obtained at *D3S1100* and *D3S1298* in the three other families, suggesting the existence of further locus heterogeneity for autosomal dominant LQTS. (Jiang et al., 1994).

In summary, in a study performed by Jiang et al., (1994), not one of the fifteen multigenerational families in whom autosomal dominant LQTS segregated who were investigated, demonstrated linkage to the *LQT1* locus. Nine of the fifteen families showed positive LOD scores with the marker *D7S483*, the remaining six families generated significant negative LOD scores at this locus. Three of the remaining 6 unlinked families were linked to a 17.6 cM interval on the short arm of chromosome 3, flanked by the markers *D3S1211* and *D3S1767* telomeric and centromeric, respectively. The chromosome 7 disease-causing locus was designated *LQT2* and the chromosome 3 locus *LQT3* (Jiang et al., 1994). The remaining three unlinked families suggested the presence of further heterogeneity in LQTS.

1.7.1.4 Linkage to Chromosome 4q25-27

The fact that there were still families that did not link to any of the previously identified loci suggested the presence of another LQTS disease-causing locus. This led to the subsequent linkage studies performed by Schott et al., (1995) in a four-generation family, which included 65 members, 56 of whom were still alive. The conservative approach of phenotypic analysis was again followed (Keating et al., 1991) and the family was examined with the *H-ras-1* clone *pEJ6.6* (Keating et al., 1991), and anonymous markers *D11S899*, *D11S1338*, *D11S907* and *CEB41* (located on chromosome 11p15.5), as well as *D7S483* (located on chromosome 7) and *D3S1766* and *D3S1768* (located on chromosome 3) (Jiang et al., 1994). Negative LOD scores were derived at all these markers, clearly excluding linkage of the disease to *LQT1*, *LQT2*, and *LQT3* (Schott et al., 1995).

Consequently, a genome-wide genotypic analysis was performed with 208 selected microsatellite markers located every 20cM and having a reported high heterozygosity rate (Schott et al., 1995). No significant linkage was obtained for 139 markers, leading to exclusion of 67% of the genome before positive results were obtained for markers located on chromosome 4q25-27. Maximum LOD scores obtained for markers *D4S193*, *D4S406*, *D4S402*, *D4S430* and *D4S1615* (figure 1.7) at $\theta = 0$ were 6.67, 6.60, 7.05, 4.89 and 4.32, respectively. Haplotype analysis showed a recombination event at *D4S430* and *D4S1570*, thus positioning the candidate area between *D4S1570*, on the centromeric side, and *D4S430* on the telomeric side, covering 18cM (figure 1.7). This disease-causing locus was designated *LQT4* (Schott et al., 1995).

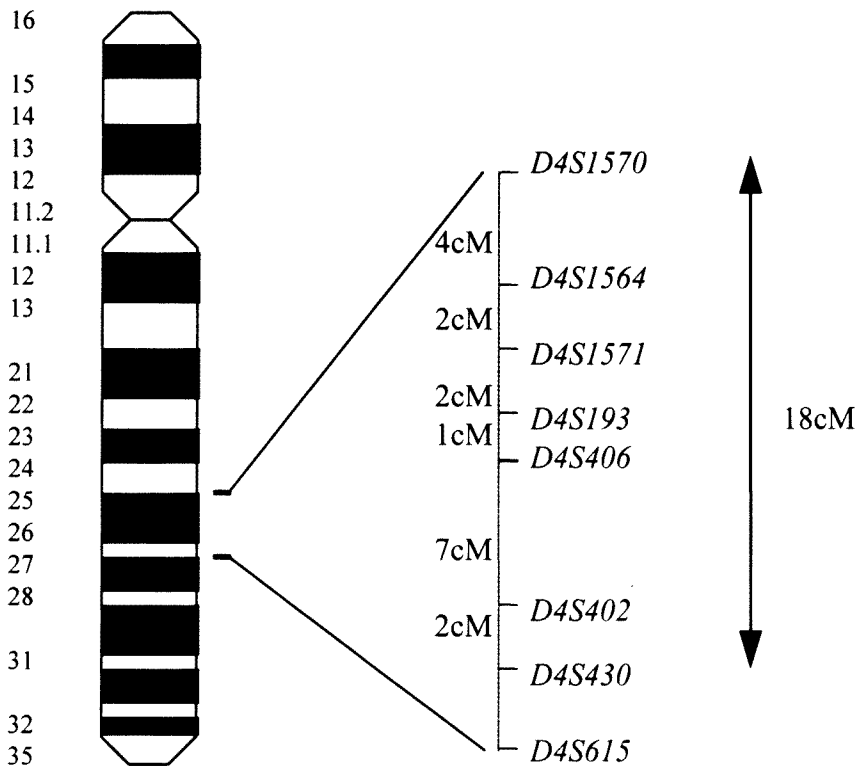


Fig. 1.7 Ideogram and genetic map of chromosome 4 showing the DNA markers in the area of the disease gene. The *LQT4* locus was located in an area of 18cM between *D4S1570* and *D4S430* (Taken from Schott et. al., 1995).

1.7.2 Identification and characterization of LQTS-causing genes

1.7.2.1 LQTS candidate genes

Although little was known about the physiology of LQTS, the disorder was most oftenly associated with prolongation of the QT interval on ECG, which reflects a delayed repolarization of the cardiac action potential (Welsh and Hoshi, 1995). The cardiac action potential is composed of a depolarization phase that results from activation of voltage-dependent sodium ion (Na^+) channels, and a repolarization phase when these channels are inactivated and voltage-dependent K^+ -channels are activated (Welsh and Hoshi 1995).

The repolarization-depolarization cycle consists of 5 phases (figure 1.8) (Dorney et al., 1990). The resting membrane potential of cardiac muscle cells is about -90mV (interior negative to exterior). Changes in the external K^+ concentration affect the resting membrane potential whereas changes in the internal Na^+ concentration affect the magnitude of the action potential. When the cell has an electrical transmembrane charge of -90mV , a stimulus from a neighbouring cell results in rapid depolarization (phase 0) of the cell. During this process, the Na^+ and calcium ion (Ca^{2+}) channels open and Na^+ and Ca^{2+} enter the cell until the electrical transmembrane charge is $+30\text{mV}$. The cell is now depolarized and is therefore positively charged on the inside. It is during this phase that muscle contraction occurs, with the influx of Ca^{2+} from the sarcomere, which allows the binding of actin and myosin. The myocardial cell now enters phases 1 and 2, during which the Na^+ channels close (phase 1) and the Ca^{2+} influx is equal to K^+ efflux, resulting in no net change in the transmembrane potential (phase 2). Rapid repolarization (phase 3) of myocardial cells follows, with the closing of the Ca^{2+} channels preventing Ca^{2+} from entering the cell. Large amounts of K^+ leave the cell with the opening of the K^+ channels, restoring the resting potential of the cell (Dorney et al., 1990).

Hydrolysis of adenosine triphosphate (ATP) provides energy to the Na^+/K^+ pump, which actively pumps K^+ into the cell and Na^+ out of the cell. The transmembrane potential returns to -50mV and the cell cycle goes into the resting phase ready for the next cycle.

It is clear from the cardiac action potential and the repolarization-depolarization cycle of which it is composed that abnormal behaviour of ion channels could delay repolarization.

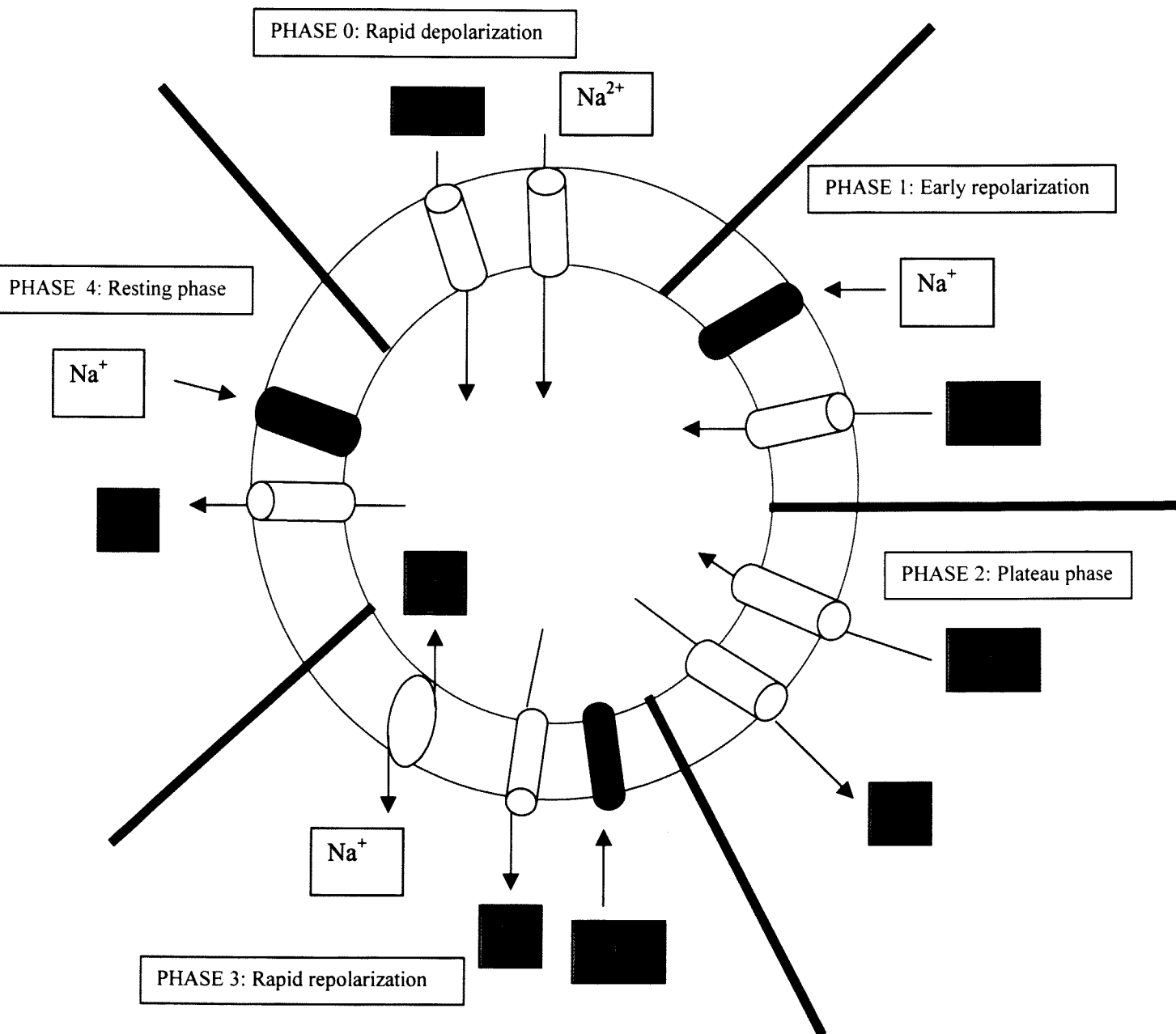


Fig. 1.8 Schematic illustration of the five phases of the repolarization depolarization cycle. The inner and the outer circles represent the inner and outer cell membranes respectively (IN = intracellular region). The arrows indicate the direction of the flow of the ions across the cell membrane, the black cylinders indicate ion channels that are blocked and the clear cylinders indicate open ion channels. During phase 3 the $\text{Na}^{+}/\text{K}^{+}$ pump is activated to actively pump K^{+} into the cell and Na^{+} out of the cell against a concentration gradient.

Consequently, genes encoding cardiac channels, or their modulators, were considered plausible candidate genes for LQTS (Welsh and Hoshi, 1995). Ion channels are individual proteins, or complexes of proteins, that reside in the cell membrane (figure 1.9). The distinguishing characteristic of ion channel proteins is that, in response to such exogenous signals as a change in voltage across the cell membrane, they can form pores (figure 1.10) for entry or egress of specific ions, Na^+ , K^+ , Ca^{2+} , etc. A key feature of the cardiac cell membrane during repolarization is that even very small changes in individual ion currents can markedly alter the delicate balance between inward and outward current flow during repolarization, thereby prolonging or shortening the action potential. This fundamental concept provides the basis for understanding how subtle abnormalities in individual ion channel genes can cause LQTS (Attali, 1996).

Cardiac K^+ -channels and Na^+ -channels became even stronger candidates, based on experimental models in which blockades of K^+ -currents and potentiation of late Na^+ -currents lengthened the QT interval and enhanced early afterdepolarization (Dumaine et al., 1996). Although voltage-gated Na^{2+} -channels are responsible for the rapid influx of Na^+ -ions, accounting for the initial upstroke of the action potential, a persistent late component of inward Na^+ current could have the effect of delaying the myocardial repolarization (Dumaine et al., 1996). Cardiac K^+ -channels regulate the resting membrane potential and action potential duration (Brown, 1997). The K^+ current that passes through the cardiac channels corresponds to the sum of two distinct currents: a rapidly activating current, I_{Kr} and a slowly activating current I_{Ks} (Attali, 1996).

Based on their strong plausibility, K^+ - and Na^+ -channels present in the critical search region of LQTS were tested to determine if they were the disease-causing genes. Four LQTS disease-causing genes each encoding an ion channel protein, have been identified namely; *HERG* (Curran et al., 1995), *SCN5A* (Wang et al., 1995a), *KVLQT1* (Wang et al., 1996a) and *KCNE1* (Splawski et al., 1997) located on chromosome 7, 3, 11 and 21, respectively. The gene at the chromosome 4 locus (LQT4) has not been identified.

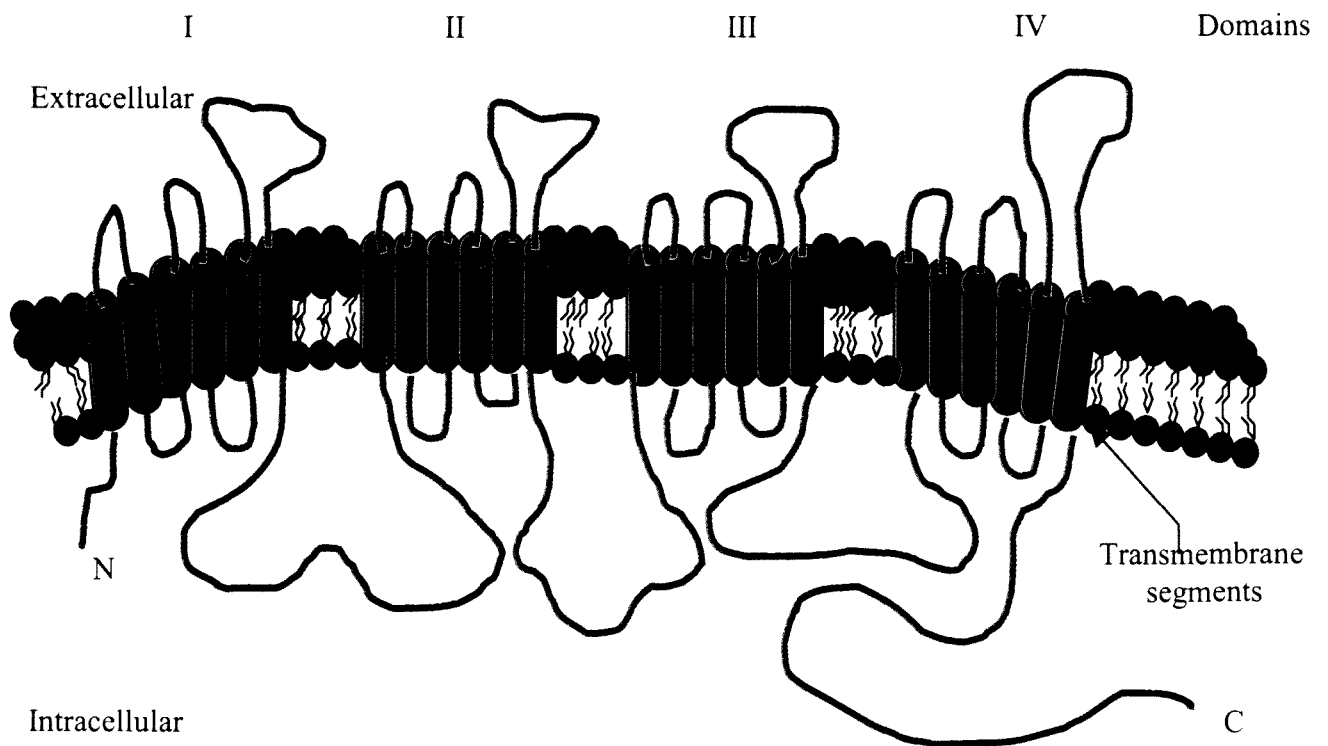


Fig. 1.9 Example of an ion channel residing in the cell membrane. Ion channels are composed of domains (I, II, III, IV) each containing six transmembrane segments, all of which have important functions (figure taken from Towbin, 1995).

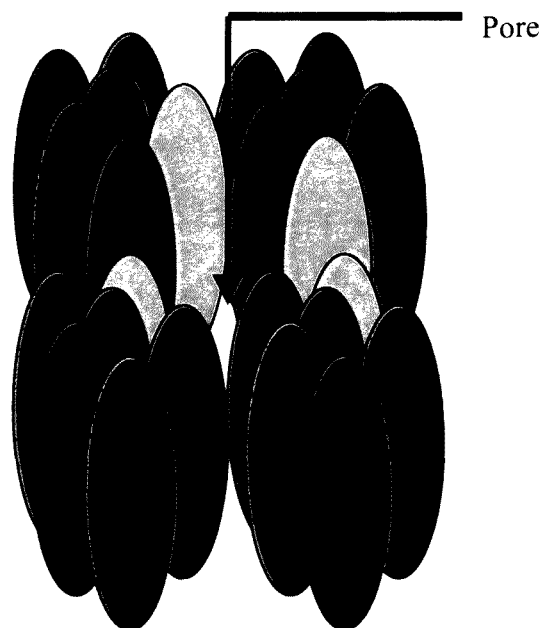


Fig. 1.10 Example of an ion channel pore. The domains of the ion channel assemble to form a pore (figure taken from Roden et al., 1996).

1.7.2.1.1 Identification of the LQT2-causing gene, *HERG*

As mentioned in the previous section, genes that encode ion channels, or their modulators, became highly plausible candidates for LQTS. Based on this hypothesis and their chromosomal location, a skeletal muscle chloride channel (*CLCN1*) (Koch et al., 1992) and a cardiac muscarinic-acetylcholine receptor (*CHRM2*) (Bonner et al., 1987) became candidates for *LQT2*, but subsequent linkage analyses excluded these genes (Curran et al., 1995).

Warmke and Ganetsky (1994) identified the human-ether-a-go-go gene (*HERG*) (figure 1.11) and subsequently mapped it to chromosome 7 and in the study performed by Curran et al., (1995) the candidacy of *HERG* as causative gene for *LQT2* was pursued. The ether-a-go-go (*eag*) gene was originally identified in *Drosophila* on the basis of its leg-shaking mutant phenotype that could be attributed to an increase in neuronal excitability and transmitter release at the neuromuscular junction (Trudeau et al., 1995). The *Drosophila eag* gene encodes a Ca^{2+} -modulated K^{+} -channel (Bruggeman et al., 1993); however this *eag* locus defines an extended gene family in which subfamilies are divided based on sequence similarities. These subfamilies are named:- *Eag* for the original isolate from *Drosophila*, *Elk* for eag-like K^{+} -channels and *Erg* for eag-related genes (Warmke and Ganetsky, 1994).

The *HERG* gene belongs to the *Erg* subfamily isolated from human hippocampus, encoding a K^{+} -channel with inward rectifying properties (Trudeau et al., 1995). These inward rectifiers belong to a large group of K^{+} -selective ion channels that preferentially conduct inward K^{+} -currents at voltages negative to the K^{+} -equilibrium potential. In the heart, these K^{+} -channels regulate the resting potential and contribute to the terminal phase of repolarization through their small outward conductances (Warmke and Ganetsky, 1994). At positive voltages they close, thus helping to maintain the plateau of the action potential. The K^{+} current that passes through the cardiac delayed-rectifier channels corresponds to the sum of two distinct currents; a rapidly activating current, I_{Kr} , and a slowly activating current, I_{Ks} (Attali, 1996)

To test the candidacy of *HERG*, Keating's group initiated genotype analyses with polymorphic markers linked to the known LQTS loci in five new unrelated LQTS families of varying descent, including Mexican (Spanish), German, English and Danish descent (Curran et al., 1995). The disease phenotype in these families was linked to the polymorphic markers on chromosome 7q35-36. Previous studies performed by this group had identified nine other chromosome 7-linked families (Jiang et al., 1994) and the maximum combined two-point LOD

score for these fourteen families was 26.14. Previous studies placing *LQT2* between *D7S505* and *D7S483* were confirmed. Given the position of *LQT2*, the localization of *HERG* was refined, by employing two physical mapping techniques, to determine if it also maps to this area on chromosome 7 (Curran et al., 1995). Firstly, *HERG* was mapped on a set of YAC contigs constructed for chromosome 7 (Green et al., 1994), which localized the gene to the same YAC as *D7S505*, a polymorphic marker that was tightly linked to *LQT2*. Secondly, *HERG* was mapped to chromosome 7q35-36 using fluorescent in situ hybridization (FISH) with a P1 genomic clone containing *HERG* (Curran et al., 1995).

To determine if *HERG* was the *LQT2* locus, PCR-SSCP analysis was used to identify mobility shifts within this gene in the chromosome 7-linked families (Curran et al., 1995). Two aberrant SSCP conformers were identified in DNA from patients and controls; these conformers were cloned and sequenced. However, both mobility shifts resulted from sequence changes in which the substitution did not affect the predicted amino acid sequence of *HERG*. These *HERG* polymorphisms were used for genotypic analysis in the chromosome 7-linked families. No recombination events between *HERG* and LQTS were identified in any of these families, and the maximum LOD score for 14 families was 9.64 ($\theta = 0.0$). These data indicated that *HERG* was completely linked to *LQT2* (Curran et al., 1995).

To test the hypothesis that *HERG* is *LQT2*, further PCR-SSCP analyses were used to screen for mutations in affected individuals of linked kindreds (Curran et al., 1995). This approach identified two intragenic deletions in the *HERG* gene that were associated with LQTS in two families and three additional aberrant SSCP conformers were identified in affected members of three more kindreds. An aberrant conformer was also identified in a sporadic affected individual, which was not detected in either parent. None of the aberrant conformers were detected in more than 200 unaffected individuals. In each case, the normal and the aberrant conformers were cloned and sequenced (Curran et al., 1995).

The one intragenic deletion was a 27 bp deletion beginning at nt 1498 that disrupted the third membrane spanning domain (S3) of *HERG*, the second one was a single base deletion at nt 1261 that resulted in a frameshift in sequences encoding S1 (Curran et al., 1995) (figure 1.11). The three point mutations in the three LQT2 kindreds included a C→T substitution at nt 1692, which resulted in a substitution of valine for a highly conserved alanine at codon 561, altering S5 of the *HERG* protein in the one kindred (figure 1.11). In the second kindred, an A→G

transition resulted in the substitution of aspartic acid for a conserved asparagine at codon 470, located on S2 (figure 1.11). In the third kindred, a G→C substitution was identified, which disrupted the splice-donor sequence of intron III, affecting the cyclic nucleotide-binding domain. The *de novo* mutation identified in the sporadic case resulted from a G→A transition at nt 1882, which caused a substitution of serine for a highly conserved glycine at codon 628, altering the pore-forming domain (Curran et al., 1995) (figure 1.11).

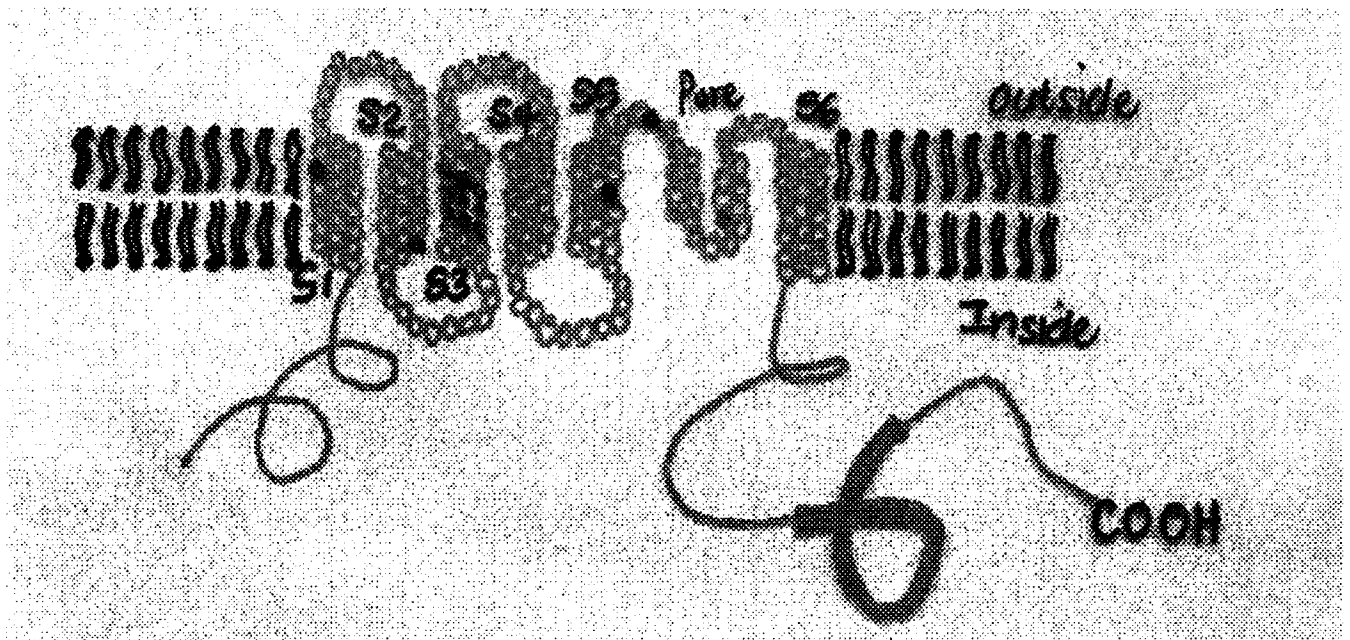


Fig. 1.11 Schematic representation of the predicted topology of the protein encoded by *HERG* and the location of LQTS associated mutations. (figure taken from Curran et al., 1995)

Northern blot analysis showed the strongest hybridization of the *HERG* probes to heart mRNAs, with faint signals in brain, liver and pancreas, and non-specific hybridization in the lung. These data indicated that *HERG* was strongly expressed in the heart, consistent with its involvement in LQTS (Curran et al., 1995). Heterologous expression of *HERG* in *Xenopus* oocytes revealed that the HERG current was similar to a well characterized cardiac delayed rectifier K⁺ current I_{Kr} (Sanguinetti et al., 1995).

In summary, *HERG* became a candidate for *LQT2* based on its chromosomal location and its physiological function, and in their report Curran et al., (1995) provided evidence in favour of this hypothesis. They firstly confirmed the location of *LQT2* to chromosome 7q35-36, and then they mapped *HERG* to chromosome 7q35-36 and demonstrated that *HERG* is strongly expressed in the heart. Finally, Curran and co-workers identified intragenic deletions of *HERG*, associated with LQTS in two families, three point mutations in three LQTS families and a fourth *de novo* point mutation in a sporadic case. Taken together, these data strongly implicated *HERG* as cause of the chromosome 7-linked form of LQTS.

1.7.2.1.2 Identification of the disease-causing LQT gene, *SCN5A*

As mentioned in the previous two sections, cardiac ion channels residing in the refined search area became candidates based on their location. A neuroendocrine calcium channel gene (*CACNL*) (Chin et al., 1991; Seino et al., 1992) and a gene encoding a GTP-binding protein that modulates potassium channels (*GNAI2*) (Weinstein et al., 1988; Magovcevic et al., 1992) became candidates for *LQT3* based on their chromosomal location, however, subsequent linkage analysis excluded these genes (Wang et al., 1995a).

Theoretically, mutations in cardiac Na⁺-channel genes could also cause LQTS, because voltage-gated Na⁺-channels mediate rapid depolarization in ventricular myocytes and also conduct a small current during the plateau phase of the action potential (Wang et al., 1995a). Subtle abnormalities of Na⁺-channel function, e.g. delayed Na⁺-channel inactivation or altered voltage dependence of channel inactivation, could delay cardiac repolarization, leading to QT prolongation and arrhythmias. The cardiac sodium channel gene (*SCN5A*) was cloned and characterized by Gellens et al., (1992) as a large protein of 2016 amino acids, encoded by 28 exons, with a calculated molecular weight of 227kDa (figure 1.12). The human *SCN5A* gene is a member of the human voltage-gated Na⁺-channel gene family. Sodium-channels from different tissues, or even different species, are highly conserved and each of these channels

consists of four homologous domains (DI-DIV) joined by short linking intracellular domains (ID1-2, ID2-3 and ID3-4), each domain containing six putative membrane-spanning segments (S1-S6) (figure 1.12) (Wang et al., 1996b).

In 1995, *SCN5A* was mapped to chromosome 3p21 (George et al., 1995), making it an excellent candidate gene for *LQT3*. Northern blot analyses indicated that *SCN5A* is expressed exclusively in the human heart (Gellens et al., 1992), further contributing to its plausibility as a candidate for *LQT3*. To test the candidacy of *SCN5A* for involvement with *LQT3*, PCR-SSCP analysis was used to identify sequence variants within this gene (Wang et al., 1995a). An aberrant SSCP conformer was identified that was cloned and sequenced, but found not to affect the predicted amino acid sequence of the product of *SCN5A* (Wang et al., 1995a). However, this polymorphism was then used in genotypic analysis in chromosome 3-linked families and no recombination events between *SCN5A* and LQTS were identified. This SSCP anomaly was identified using oligonucleotide primers designed from cDNA sequence because at that time the genomic structure of *SCN5A* was unknown (Wang et al., 1995a).

Two genomic P1 clones, spanning the entire gene, were isolated and characterized in order to determine the genomic structure of *SCN5A* (Wang et al., 1995a). Keating's group hypothesized that LQTS-causing mutations would be subtle and might affect delayed inactivation of encoded Na⁺ channels or alter the voltage dependence of the channel inactivation. Therefore, they focused on regions known for channel inactivation, when they designed primers for SSCP analysis. The cytoplasmic region between DIII and DIV (Fig. 1.13), corresponding to exons 21-23, was analyzed. An identical intragenic deletion of 9bp was identified in two LQTS families, but was absent in 500 control individuals. This deletion disrupts the coding sequence, resulting in a deletion of three conserved amino acids, Lys-1505-Pro1506-Gln-1507 (KPQ) in the cytoplasmic linker between DIII and DIV. This mutation was also present in two more families in a study performed by Wang et al., later that same year (Wang et al., 1995b). The type and the location of the deletion supported the conclusion that *SCN5A* is *LQT3* (Wang et al., 1995a).

In the absence of additional anomalies in the DIII and DIV region corresponding to exons 21-23, the sequences from predicted exons 18-23 were defined (Wang et al., 1995b). Primers were designed to amplify sequences encoding DIV-S3-DIV-S5 (figure 1.13), the linker between DIII-S4 and DIII-S5 (figure 1.12) and DIII-S5 (Fig.1.12) itself. Two point mutations were

identified employing these oligonucleotide primers. The one was a single base substitution, G→A at nt 5081 resulting in a substitution of a highly conserved arginine to histidine at codon 1644 in the S4 segment of DIV (figure 1.12). The second mutation was an A→G substitution at nt 4124, which led to a substitution of an asparagine for serine at codon 1325 in the intracellular domain between S4 and S5 of DIII (figure 1.12) (Wang et al., 1995b).

In summary, *SCN5A* was identified as a highly plausible candidate for *LQT3* based on its chromosomal location, the fact that it is a cardiac Na⁺ channel gene and its exclusive expression in the heart (Wang et al., 1995a). Wang et al., (1995a) provided evidence to strengthen this hypothesis by firstly showing complete linkage between a DNA polymorphism within *SCN5A* and LQTS in families with chromosome 3-linked LQTS. Secondly, they detected an identical intragenic deletion of *SCN5A* in four LQTS families (Wang et al., 1995 a,b), and missense mutations associated with LQTS in two families (Wang et al., 1995b). Taken together, these data strongly implicated *SCN5A* as cause of *LQT3*.

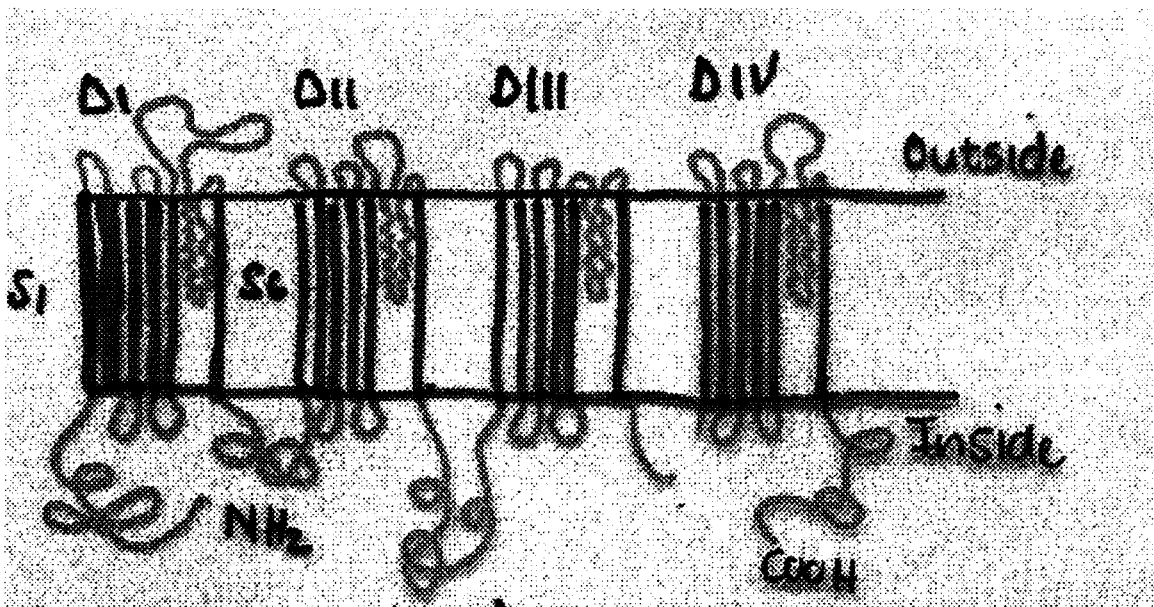


Fig. 1.12 Schematic representation of the predicted topology of the protein encoded by *SCN5A* and the location of an LQTS-associated deletion (figure taken from Wang et al., 1995).

1.7.2.1.3 Identification of the LQTS-causing gene, *KVLQT1*

A candidate gene approach to identify the chromosome 11-linked LQTS-causative gene was unsuccessful. Although two K⁺-channel genes (*KCNA4* and *KCNKI*) were mapped to chromosome 11, both were excluded as candidates for LQT1 by linkage analysis (Russel et al., 1995). Similarly, all other previously characterized cardiac K⁺-, Cl⁻-, Na⁺- and Ca²⁺-channel-encoding genes were excluded based on their chromosomal locations (Wang et al., 1996a).

To determine the precise localization of *LQT1*, Keating's group performed genotypic analysis in a large Utah family of Northern European descent consisting of 217 individuals (Wang et al., 1996a). Preliminary genotypic analyses using markers at *H-ras*, *TH*, *D11S454*, and *D11S12* (figure 1.13) identified informative branches of this family (Russel et al., 1995). Additional genotypic analysis was performed using three highly informative polymorphic markers from chromosome 11p15.5, namely, *D11S922*, *D11S1318* and *D11S860*. These analysis showed that *TH* and *D11S1318* were completely linked to *LQT*, however recombination events were identified with all other markers tested, including *H-ras-1*, but in each case a statistically significant positive LOD score was generated (Wang et al., 1996a).

Haplotype analysis was performed to refine the localization of *LQT1* in this family and nine informative recombination events were identified, which placed *LQT1* in the interval between *D11S922* and *D11S454* (figure 1.13). Together with the studies of Russel et al., (1995), which placed *LQT1* centromeric to *TH*, these data indicated that *LQT1* was located in the interval between *TH* and *D11S454* (figure 1.13) (Wang et al., 1996a). Pulsed-field gel analysis, employing genomic probes from chromosome 11p15.5, was used to estimate the size of the region containing *LQT1*. The probes *TH*, *D11S551* and *D11S454* hybridized to a 700 kb *MluI* restriction fragment, suggesting that the region containing *LQT1* was less than 700kb in size. Physical representation was achieved by screening YAC and P1 libraries with the probes of this region and the order of the markers in these clones was confirmed using fluorescent in situ hybridization (FISH) analysis as: telomere-*TH*-*D11S551*-*D11S679*-*D11S601*-*D11S454*-centromere (Wang et al., 1996a).

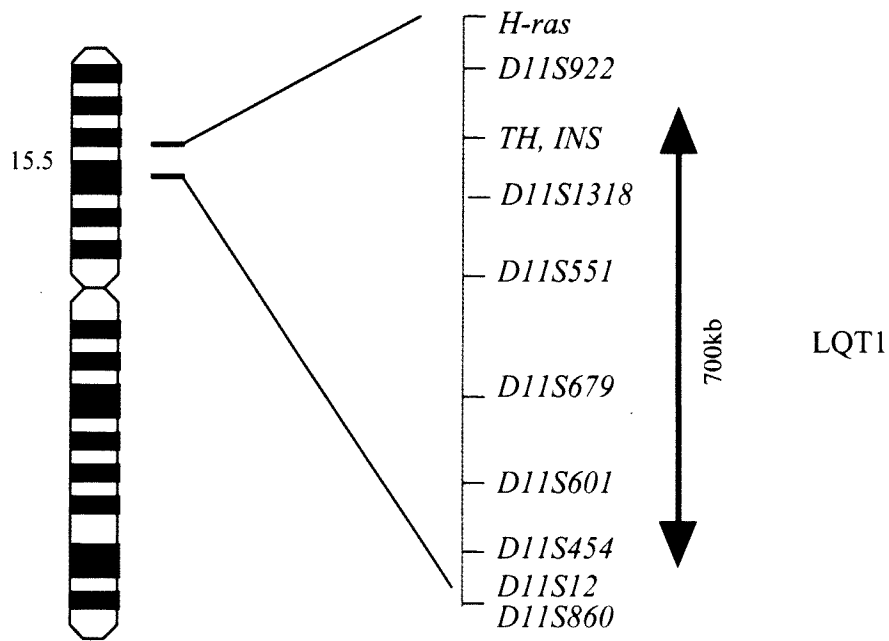


Fig. 1.13 Ideogram and genetic map of chromosome 11 showing the DNA markers in the area of the disease gene. The LQT1 locus was located in an area between *TH* and *D11S454* (Compiled from Russel et al., 1995; Wang et al., 1996a).

Exon amplification was performed with clones identified from the physical map to identify candidate gene DNA sequences and database analysis revealed eight possible trapped exons with predicted amino acid sequence similarity to ion channels (Wang et al., 1996a). Two consensus polyadenylation signals were identified upstream of the poly (A)⁺ tail in the 3' untranslated region, but the identity of the initiation codon was uncertain. The cDNA predicted a protein with structural characteristics of potassium channels, while hydropathy analysis suggested a topology of six major hydrophobic regions that might represent membrane-spanning α -helices. These regions shared sequence similarity with potassium channel transmembrane domains S1-S6 (figure 1.14). Because this gene was similar to voltage-gated potassium channel genes and thus became a strong candidate for *LQT1*, it was named *KVLQT1* (Wang et al., 1996a).

Northern blot analysis showed a 3.2 kb transcript of this gene in human heart, kidney, lung, and placenta, but not in skeletal muscle, liver or brain, with the highest expression in the heart (Wang et al., 1996a). To test the hypothesis that *KVLQT1* is *LQT1*, PCR-SSCP analysis was performed in the affected members of the largest LQTS family that showed linkage to chromosome 11. The focus of the analyses was the region between S2 and S6, since these regions might be important for *KVLQT1* function. The SSCP analyses detected an anomalous conformer in the 70 affected members of this family that was absent in the 147 unaffected members of this kindred and the more than 200 unrelated control individuals. Linkage analysis between this anomaly and LQTS detected a two point LOD score of 14.19 at $\theta = 0$, the absence of recombination between *LQT1* and *KVLQT1* implied that the tested gene and the disease gene are completely linked (Wang et al., 1996a).

To further test the hypothesis that mutations in *KVLQT1* cause LQTS, PCR-SSCP analysis was continued in five large chromosome 11-linked kindreds, as well as smaller families and sporadic cases (Wang et al., 1996a). SSCP anomalies were identified in affected members of the 5 large families, as well as ten smaller families or sporadic cases that were absent in more than 200 unrelated control individuals. The normal and aberrant conformers were cloned and sequenced in each case and it was shown that one of the aberrant conformers resulted from a three base pair deletion, while the rest of the conformers were the result of point mutations (Table 2.3). Two of the 16 families in which *KVLQT1* mutations were detected originated from South Africa (Wang et al., 1996a), and it was in these two families that previous LQTS studies in our laboratory had been performed (De Jager et al., 1996).

The *KVLQT1* gene described by Keating's group early in 1996 (Wang et al., 1996a) as the *LQT1*-causative gene seemed to be lacking the amino terminal domain and was also unable to undergo functional expression. To define the complete sequence of *KVLQT1* a new search was initiated. A new clone, including a putative translational start site and an ATG sequence in-frame with the original *KVLQT1* was isolated after screening several cDNA libraries (Sanguinetti et al., 1996). The new cDNA sequence predicted a 581 amino acid protein with a complete S1 domain and a 27 amino acid N-terminal region. Northern blot analysis with the new *KVLQT1* sequence showed hybridization to a single mRNA of 3.2 kb in human pancreas, heart, kidney, lung and placenta, but not in brain, liver or skeletal muscle (Sanguinetti et al., 1996).

The biophysical properties of KVLQT1 were unlike other known cardiac K^+ channels and it was hypothesized that KVLQT1 might coassemble with another subunit to form a known cardiac channel (Sanguinetti et al., 1996). To test this hypothesis, Chinese hamster ovary (CHO) cells were cotransfected with *KVLQT1* and human minimal potassium (*hminK*) cDNAs. Transfection of CHO cells with *hminK* alone did not induce detectable currents; however, cotransfection of *hminK* with *KVLQT1* induced a slowly activating delayed-rectifier current that was much larger than the current in cells transfected with *KVLQT1* alone. The slow activation of current in cotransfected CHO cells was preceded by a delay that lasted several hundred milliseconds, the current did not saturate during long depolarizing pulses, and required a three exponential function to describe the initial delay and two phases of current activation. Activation of cardiac I_{Ks} is, like coexpressed *KVLQT1* and *hminK* in CHO cells, extremely slow and best described by a three-exponential function. Thus, coexpression of *KVLQT1* and *hminK* in CHO cell induces a current with biophysical properties nearly identical to cardiac I_{Ks} (Sanguinetti et al., 1996). At the same time, the group of Barhanin et al., (1996) also cloned the full length mouse *KVLQT1* cDNA and showed that *KVLQT1* gene product associates with *hminK* gene product to form the channel underlying the I_{Ks} cardiac current.

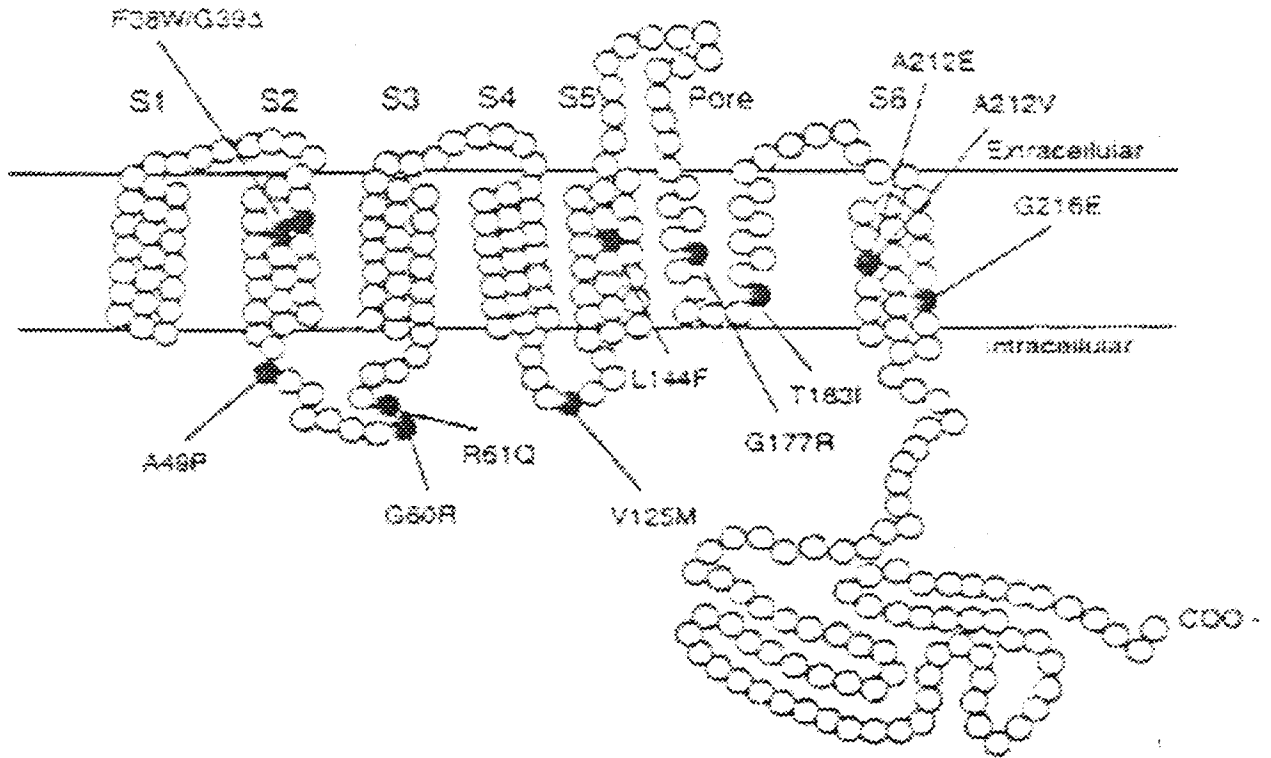


Fig. 1.14 Schematic representation of the predicted topology of the protein encoded by *KVLQT1* and the location of LQTS-associated mutations (figure taken from Wang et al., 1996a).

In summary, *LQT1* was located to a 700kB region in the interval between *TH* and *DIIS454*, exon amplification with clones that map between these flanking markers identified the *KVLQT1* gene as plausible candidate (Wang et al., 1996a). A polymorphism within the *KVLQT1* gene was proven to be completely linked to *LQT1* in a large family and mutations in this gene were shown to cosegregate with the disease in six large families and ten small families or sporadic cases (Wang et al., 1996a). The *KVLQT1* gene encodes the channel subunit forming the important cardiac channel I_{Ks} ; however, this subunit is not sufficient by itself to form the native I_{Ks} but requires *hminK* as an additional subunit (Barhanin et al., 1996; Sanguinetti et al., 1996).

1.7.2.1.4 Identification of a fifth disease-causing locus, *KCNE1*

As described above, it was demonstrated that the product of *KCNE1* (the gene encoding hmin K) coassembles with the product of *KVLQT1* to form the channel underlying the I_{Ks} current. Based on this association, the group of Splawski et al., (1997) hypothesized that, because *KVLQT1* mutations could cause LQTS, mutations in *KCNE1* could also cause this disorder. To test this hypothesis, PCR-SSCP analysis of exons of *KCNE1* was performed in 282 unrelated LQTS affected individuals. Following this mutation screening technique, two conformers was identified in two different individuals, respectively. Both conformers were present in all affected family members of the latter two individuals, however, they were not observed in unaffected family members or in 200 unrelated control individuals. DNA sequencing of these conformers revealed that one was a G to A transition at the first nt of codon 76, causing an Asp→Asn substitution and the second one was a C to T transition in the second nt of codon 74, leading to the substitution of Ser→Leu. The disease gene identified in these families were designated *LQT5* (Splawski et al., 1997).

1.7.2.1.5 Summary of identified LQTS disease-causing genes

A summary of the LQTS disease-causing genes identified to date and their chromosomal positions is shown in Table 1.2.

Table 1.2 Identified LQTS disease genes and their chromosomal positions

Form of LQT	Chromosomal Position	Disease-causing Gene	Reference
LQT1	Chromosome 11	<i>KVLQT1</i>	Wang et al., 1996a
LQT2	Chromosome 7	<i>HERG</i>	Curren et al., 1995
LQT3	Chromosome 3	<i>SCN5A</i>	Wang et al., 1995a
LQT4	Chromosome 4	Not identified	Schott et al., 1995
LQT5	Chromosome 21	<i>KCNE1</i>	Splawski et al., 1997

1.7.3 HYPOTHESIS TO EXPLAIN LQTS

Any hypothesis put forth to explain LQTS must account for all of its features (Jackman et al., 1988; Zipes, 1991). The two most popular hypotheses to explain LQTS are (i) the sympathetic imbalance hypothesis of an altered activity of the autonomic nervous system (Schwartz et al., 1975) and (ii) the myocellular hypothesis of an abnormality of ion channel regulation (Jackman et al., 1988), however definitive proof of either hypothesis has been elusive.

The striking adrenergic dependence of symptoms, and the beneficial effect of antiadrenergic interventions, led to the suggestion that there was an abnormality or imbalance in the sympathetic innervation to the heart. This led to the formulation of the sympathetic imbalance hypothesis that suggested that there is a congenital reduction in right-sided sympathetic activity to the heart that results in dominance of left-sided cardiac sympathetic innervation. (Schwartz, 1975). This hypothesis could explain the abnormal sinus rate, possibly the abnormal repolarization, and adrenergic dependence of arrhythmias and their correction by antiadrenergic drugs (Roden et al., 1996).

The second hypothesis, that of an intrinsic abnormality in myocardial repolarization, assumes that the cause of abnormal repolarization lies within the heart itself, perhaps an abnormal channel protein reducing or blocking an outward repolarizing K^+ current, or increasing an inward depolarizing Ca^{2+} or Na^+ current. This results in early afterdepolarizations, which lengthen repolarization that could cause triggered activity and ventricular tachyarrhythmias such as torsade de pointes (Zipes, 1991). The latter hypothesis can explain the QT prolongation, prominent and peculiar T and U waves, T wave alternans, and ventricular

tachyarrhythmias (Jackson et al., 1988). In addition, it can also serve as the mechanism for acquired LQTS, which the sympathetic concept cannot (Roden et al., 1996). This hypothesis suggested a likely mechanism for the generation of torsade de pointes, and might explain why β -adrenergic blockade is useful in management of some patients with LQTS (Keating, 1996).

Since the “sympathetic imbalance” theory was first proposed by Schwartz et al., (1975), validity of the data supporting the concept has been questioned. Schwartz et al., (1991a) reported that this hypothesis could account for the sinus node abnormalities and the beneficial effects of left-sided cardiac sympathetic denervation, but it inadequately explains the remaining features of this disorder. Rosen asked the following questions: “ If a sympathetic imbalance lies at the root of LQTS, why, then, did successful treatment not result in normalization of the QT interval? Why, too, if Romano-Ward Syndrome is a single syndrome, has there been so much variability in its phenotypic expression? ” (Rosen, 1995). In contrast to the sympathetic imbalance hypothesis, data to support the myocellular hypothesis is accumulating. Three of the LQTS-causing genes identified (*HERG*, *SCN5A* and *KVLQT1*), accounting for almost 90% of known cases of LQTS globally, encoded cardiac ion channels; thus, LQTS is due to an intrinsic abnormality in the vast majority of LQTS patients (Roden et al., 1996).

A delay in cardiac repolarization as manifested by a prolongation of the QT interval may be the result of an increase in action potential duration. As mentioned earlier, Na^+ and K^+ -channels play an important role in the cardiac action potential and it is possible that defects in genes that encode these channels could prolong the action potential. The two delayed-rectifier K^+ currents I_{Kr} and I_{Ks} modulate action potential duration in cardiac myocytes (Brown, 1997). The long QT syndrome is a genetically heterogenous disorder and mutations in one Na^+ - (*SCN5A*) and two K^+ - channels (*HERG* and *KVLQT1*) could cause this disease. The *HERG* gene encodes the major subunit of the cardiac I_{Kr} channel (Sanguinetti et al., 1995) while *KVLQT1* and *hminK* coassemble to form the cardiac I_{Ks} channel (Barhanin et al., 1996); Sanguinetti et al., 1996). It is evident that LQTS represents a common phenotype of a genotypically diverse disorder, and that the underlying mechanism to explain each genetic variant of this disorder could be individualized (Priori, 1997).

A continued depolarizing current during the plateau phase of the cardiac action potential as a result of delayed inactivation of cardiac Na^+ -channels could prolong the action potential

duration and QT interval, providing a possible mechanism for how *SCN5A* mutations could cause LQTS (Wang et al., 1995b). The LQTS-associated deletions identified in *SCN5A* are likely to result in functional cardiac Na⁺-channels with altered properties, such as delayed inactivation or altered voltage dependence of channel inactivation (Wang et al., 1995a). The latter finding provided support for the hypothesis proposed for *LQT3* and suggested new avenues for possible therapeutic endeavors.

The mechanism in which *HERG* might prolong action potential duration and thus cause LQTS is more complicated because K⁺ channels assemble as tetramers (MacKinnon, 1991). Assembly of normal units with mutant *HERG* units might cause a dominant negative effect that may lead to reduced channel function (Benson et al., 1996). Alternatively, channel function could also be decreased by mutations that cause failure of *HERG* assembly, thereby affecting K⁺ channel stoichiometry and thus reducing channel numbers. In either case, the loss of *HERG* function is the pathophysiological basis for prolongation of repolarization (Benson et al., 1996).

The mechanism underlying LQT1 is not clear, however it is postulated that it may also act in a dominant negative fashion, leading to loss of channel function as is the case of *HERG* (Attali, 1996; van den Berg et al., 1997). All the mutations (except for one 3-nucleotide in-frame deletion) known to date in the *KVLQT1* gene are missense mutations (Russel et al., 1996; Tanaka et al., 1997; Wang et al., 1996a; van den Berg et al., 1997). The latter evidence provided support in favour of the dominant negative effect theory, based on the work of Russel et al (1996) who demonstrated that missense mutations resulted in a dominant negative suppression of K⁺-channel activity. The coassembly of *KVLQT1* and *hminK* provide the inward K⁺-current I_{Ks}, the consequence of LQT1 is a reduction in I_{Ks}, thus, the correct function of *KVLQT1* K⁺-channels depends on the co-assembly with the *hminK* protein (Barhanin et al., 1996; Sanguinetti et al., 1996). Therefore, mutations affecting the binding of *hminK* are expected to result in a deregulation of channel function, these mutations could also influence channel function by directly affecting pore activity or the tetrameric configuration leading to channel disfunction. Pore mutations in *KVLQT1* could cause the dominant form of LQTS by partially inactivating the subunits encoded by the normal alleles in heterozygous patients (Wollnik et al., 1996). The reduction in the total current is sufficient to delay the repolarization of cardiac action potentials significantly, causing the prolonged QT intervals on ECGs (Wollnik et al., 1997).

Hence, despite different ion channel abnormalities, the end result is phenotypically similar, providing a unifying explanation of the disorder (Towbin, 1995). This leads to the speculation that the remaining defective genes are also likely to encode ion channels, either other types of K^+ - and Na^+ -channels or Ca^{2+} (and possibly Chloride-channels). This result is reminiscent of the unifying concept described in hypertrophic cardiomyopathy, in which all the defective genes encode various sarcomeric proteins (Towbin, 1995).

1.8 IMPORTANCE OF MAPPING OF LQTS GENES

To avoid sudden cardiac death in LQTS, early diagnosis is crucial (Keating, 1996). Once diagnosed, patients can be treated with anti-arrhythmic drugs and/or implantable defibrillating devices. However, the variables of QT intervals and clinical signs among carriers of mutated LQTS genes makes pre-symptomatic diagnosis difficult (Keating, 1996). Genetic screening using mutational analysis can improve pre-symptomatic diagnosis. The presence of a mutation would unequivocally distinguish affected individuals and identify the gene underlying LQTS even in small families and sporadic cases (Splawski et al., 1998)

If a LQTS-causing mutation is found in a proband, the rest of the family members could be screened and gene carriers identified, this would allow the accuracy of the diagnosis to be confirmed and appropriate actions to be taken. Asymptomatic gene carriers could be advised to avoid stressful conditions and competitive sport, and, depending on the malignancy of the disease in the family, antiadrenergic treatment could be started. Conversely, family members identified as non-carriers could be assured that they could conduct a completely normal life (Priori, 1997).

KVLQT1 mutations account for almost 50% of the reported forms of LQT, and together with *HERG*, *SCN5A* and the chromosome 4 locus it accounts for almost 90% of all reported autosomal dominant forms of LQTS cases (Roden et al., 1996). This implicates a high probability of correct diagnosis, although not 100% by genetic testing. This knowledge also allows the possibility to perform linkage analyses in smaller families, which would normally not be so informative if some of the genes can be excluded.

A complete characterization of LQTS genes may not only benefit all LQTS families at risk for sudden death due to tachyarrhythmias, but may also elucidate a common physiological mechanism of arrhythmias in this and other cardiovascular diseases (Satler et. al., 1996). When

specific mechanisms causing arrhythmias are understood, therapeutic interventions might be tailored to the specific genotypes and specific channel defects (Welsh and Hoshi, 1995). It is hypothesized that Na^+ channel abnormalities, which are caused by the inappropriate action of *SCN5A*, can be treated with Na^+ -channel blockers. Raising the concentration of K^+ in the serum, which should activate the channel, might treat the LQT2 defect caused by mutations in *HERG*. It is proposed that the more common *KVLQT1* defects may respond to drugs that open K^+ -channels (Keating, 1996).

Compton et al., tested the hypothesis that administration of exogenous K^+ would result in an increase in the outward K^+ -current and subsequently shorten the repolarization. The group shown that K^+ -therapy improves repolarization in LQT2, however, this finding requires long term follow up (Compton et al., 1996). Priori et al., (1996) demonstrated that prolonged guinea pig myocyte action potentials are abbreviated by Na^+ -channel blockade in *in vitro* LQT3 models but not LQT2 models.

Identification of LQTS-causing genes also allowed genotype-phenotype studies, to determine if there is a differential phenotypic expression between the varied forms of *LQTS*. In a study performed by Schwartz et al., (1995), the differential responses of *SCN5A* and *HERG* genes to Na^+ channel block and to the increase in heart rate were investigated and it resulted in the first demonstration of differential responses by LQTS patients to interventions targeted to their specific genetic defect. In the same study (Schwartz et al., 1995), it was reported that LQT2 patients had their synocopal episodes under situations of emotional stress, in contrast to LQT3 patients who have episodes either at rest or during sleep. In a study performed by Schwartz's group in 1997 exercise related events were shown to dominate the clinical picture in LQT1 (Schwartz et al., 1997). These findings raised the possibility that the triggers for life-threatening arrhythmias differ among LQTS patients, according to the specific gene mutation involved. This study was performed in a limited population but these implications might become legitimate if these results are confirmed in the larger LQTS population (Schwartz et al., 1995).

In patients with LQTS, the ECG-T-wave repolarization pattern is also found to be influenced by the specific genotype (Moss et al., 1995). Although QT interval is the hallmark for the clinical diagnosis of LQTS, variations in the morphological configuration of prolonged or delayed repolarization that are specific for the different forms of LQT have been recognized by

several investigators. Patients with mutations in the *SCN5A* gene have a distinctive, late appearing T wave that is clearly different from the low-amplitude, moderately delayed T wave observed in affected patients who are carriers of the abnormal *HERG* gene. Both of these repolarization patterns are different from the broad based prolonged T wave pattern found in patients who are carriers of the abnormal gene, *KVLQT1* (Moss et al., 1995).

Many new areas of research are opened up by the exciting new molecular genetic findings in LQTS. Examples include studies of the basic biophysics of the normal and mutant *KVLQT1*, *SCN5A* and *HERG* gene products, studies to identify drug therapies that might correct the defects in these mutations, and studies to determine the relationship between clinical phenotypes and underlying genetic defects.

1.9 THE PRESENT STUDY

As mentioned previously in section 1.3, missed diagnosis and misdiagnosis of LQTS often occur. On account of the resemblance of synocopal attacks displayed by LQTS patients with epilepsy, the misdiagnosis as epilepsy is often made in patients with LQTS. Molecular genetic techniques have been successfully employed in both LQTS and genetic epilepsy syndromes. Subsequently investigations have lead to the identification of four disease-causing genes for LQTS (Curran et al., 1995; Wang et al., 1995; Wang et al., 1996; Splawski et al., 1997) and over one hundred disease-causing loci in the rarer forms of epilepsy which show a simple inheritance pattern (Ryan et al., 1999). The identification of disease-causing genes and their associated mutations would allow an unequivocal diagnosis in both of these disorders, making this avenue of research of vast importance to solve the differential diagnosis in both these conditions.

Given that the establishment of the chromosomal locus is normally the first step in the identification of the defective gene, the aim of this study was to identify the disease-causing locus in a family in whom a form of myoclonic epilepsy segregates, as well as in three LQTS affected families.

The epilepsy study was initiated by Dr Jonathan Carr, who previously saw a case with an interesting form of epilepsy, which was designated FME. This index case was initially part of a study performed on juvenile myoclonic epilepsy at Groote Schuur Hospital (Cape Town). Dr Carr traced and contacted the family and performed clinical examinations on them. In the

absence of obvious candidates for this form of epilepsy, Professor Berkovic in Australia was contacted with the available clinical information to suggest candidate loci in the search for the identification of this disease. In his response (personal communication, Berkovic), he gave some information on a Japanese family with a similar type of disease in which linkage was found with the STRP marker *D8S264*. Two more candidate forms of epilepsy were identified by Dr Carr, namely DRPLA and EPM1. These candidates were chosen because certain clinical features exhibited by these disorders were also present in FME. Consequently, linkage analysis was employed with DNA markers tightly linked to these three candidate loci, viz. chromosome 8 linked epilepsy, DRPLA and EPM1, to determine their involvement in FME.

Previous work in our laboratory in five South African families of Afrikaner descent, in whom LQTS segregates, had demonstrated that, in these families, LQTS was caused by the Ala212Val mutation in *KVLQT1* (Wang et al., 1996a; de Jager et al., 1996). On haplotype construction with markers in the area around the *KVLQT1* gene, the same haplotype was found in all affected members of the five families investigated, suggesting the presence of a founder effect (de Jager et al., 1996). Given this background, all new probands referred to us with the clinical diagnosis of LQTS were first screened for the founder Ala212Val mutation in *KVLQT1*. Globally, mutations in the *KVLQT1* gene account for almost 50% of all reported cases of autosomal dominant LQTS (Roden et al., 1996) and the codon 212 encoded by this gene seems to be a mutational hot spot with the Ala212Val mutation the most common disease-causing mutation (Tanaka et al., 1997). These findings also contributed to the rationale for screening for this specific mutation in all new probands.

In the present study, if the Ala212val mutation was present in the proband, a DNA-based diagnostic test could be delivered to the rest of the family. Families were traced and contacted and pedigrees constructed where possible, using the probands as reference points. In families where the *KVLQT1* Ala212Val mutation was absent in the probands, four of the known LQTS loci, accounting for almost 90% of the known cases of LQTS, were investigated with linkage analysis to determine the disease-causing locus. These loci were *KVLQT1*, *HERG*, *SCN5A* and the chromosome 4 locus. If a particular disease-causing gene was to be implicated by linkage analysis, mutation screening analyses employing PCR-SSCP analysis and ASREA would be initiated to screen for known and novel mutations in the gene. If mobility shifts were to be detected, these would be sequenced to determine the effect on the DNA sequence of the gene.

This information could then be used to design DNA-based diagnostic tests to provide a more effective way of diagnosis in South African families.

CHAPTER 2

MATERIALS AND METHODS

	Page
2.1 CHARACTERIZATION OF FAMILIES	70
2.2 CLINICAL DIAGNOSIS	71
2.2.1 Epilepsy	71
2.2.2 LQTS	71
2.3 MOLECULAR DNA-BASED STUDIES	72
2.3.1 Collection of Blood	72
2.3.2 Preparation of DNA samples	72
2.3.2.1 Isolation of genomic DNA from EDTA blood	72
2.3.2.2 Genomic DNA extraction from nuclei	72
2.3.3 Polymerase Chain Reaction	73
2.3.3.1 Non-radioactive polymerase chain reaction	73
2.3.3.2 Radioactive polymerase chain reaction	75
2.3.3.2.1 Full strand labelling	75
2.3.3.2.2 End-labelling	75
2.3.4 Mutation Screening Techniques	77
2.3.4.1 Allele specific restriction enzyme analysis	77
2.3.4.2 PCR-SSCP analysis	79
2.3.5 Silver Staining	81
2.3.6 Radioactive Gel Electroporesis	81
2.3.6.1 Preparation of gel	81
2.3.6.2 Electrophoresis	82
2.3.7 Autoradiography	82
2.3.8 Genotyping	82
2.3.9 Haplotype Construction	83
2.3.10 Linkage Analysis	83
2.3.11 Direct Sequencing of SSCP-conformers	86
2.3.11.1 Purifying DNA from gel	86
2.3.11.2 Direct sequencing of purified DNA	86

CHAPTER 2

MATERIALS AND METHODS

2.1 Characterization of Families

These investigations followed approval from the ethical committee of the University of Stellenbosch Medical School, and informed verbal consent was obtained from participating adults or parents in the case of minors.

A panel of twelve unrelated LQTS affected probands had been previously established, as part of our group's ongoing investigation of this disease in South Africa. In the epilepsy study, one proband was identified by referral. Through the probands, other members of the families were traced and contacted where possible, the nature of the project explained and pedigrees constructed. Following this route, three LQTS affected families and one epilepsy family were investigated. The three LQTS families were of different South African subpopulation groups, namely, Mixed ancestry, Afrikaner and Indian descent and they were subsequently designated pedigrees 167 (figure 3.10.1), 168 (figure 3.10.2) and 169 (figure 3.10.3) respectively. The pedigree constructed in the epilepsy study was named pedigree 201 (figure 3.1) and was of Mixed ancestry.

The proband in pedigree 201 was initially part of a study performed on juvenile myoclonic epilepsy at the Grootte Schuur hospital, in Cape Town. Dr Jonathan Carr (University of Stellenbosch Medical School, Tygerberg) was particularly interested in this specific case, and learned from the index case that he had family members who were also affected. The rest of the family was traced and contacted and Dr. Carr performed clinical examinations on the family members who were willing to participate in the project.

In pedigree 167, the proband was referred to Tygerberg hospital, where she was diagnosed with LQTS. The proband and one of her maternal aunts provided the information regarding the rest of the family. According to them, the mother of the proband, as well as one of her brothers and one of her sisters, died of a "heart disease". Unfortunately, no information to confirm that these individuals were indeed affected with LQTS was available. A clinical investigation was performed on the rest of the family.

In pedigree 168, the proband was referred by her general practitioner to Dr. Paul Brink (University of Stellenbosch, Cape Town) at Tygerberg hospital to confirm the diagnosis of LQTS. Unfortunately, most members of this family were unwilling to participate in the research project and only a DNA-based diagnostic test was performed in a few individuals who were willing to take part in the study.

In pedigree 169, the proband was referred by Dr Munclinger (University of Natal, Durban) to Dr Paul Brink to confirm the diagnosis of LQTS. After confirmation, Dr Clive Corbett (University of Stellenbosch Medical School, Tygerberg) performed a clinical investigation of family members who were prepared to take part in the study.

2.2 Clinical Diagnosis

2.2.1 Epilepsy

The designation FME was used to describe the clinical entity, which was followed in this study. The diagnosis of epilepsy is a clinical one, thus the diagnosis of FME was made following a clinical examination by a physician (Dr. J. Carr). A detailed clinical description of FME is the subject of a study by Dr. J. Carr (manuscript in preparation). Briefly, FME was classified as a form of myoclonic epilepsy, characterized by generalized tonic-clonic seizures, continuous myoclonic jerks, mostly of the upper arms, distal more than proximal. The jerks were stimulus sensitive, being more apparent when the arms were outstretched. Electroencephalograms showed a generalized polyspike wave discharge, while mild atrophy was seen in a computerized tomography scan.

2.2.2 LQTS

Electrocardiograms were performed on all family members participating in the research project, and the QT values were corrected for heart rate (QTc) using Bazett's formula. The affectedness status was determined by the diagnostic criteria described by Keating et al., (1991). The examining physicians either recorded the actual QTc values or categorized the individuals as affected/unaffected or equivocal according to the diagnostic criteria described by Keating. This was based on a QTc ≥ 0.45 s in symptomatic individuals or a QTc ≥ 0.47 s in asymptomatic individuals. Diagnosis of equivocal clinical status was made if individuals had a QTc value between 0.42s and 0.46s in the absence of symptoms and 0.44s or less in the presence of symptoms. Those for whom ECGs were not available, or in whom complete investigation was not possible, were classified as "disease status unknown".

2.3 Molecular DNA-based Studies

2.3.1 Collection of blood

Blood was drawn from all affected individuals and their immediate family members, into four 5ml EDTA tubes, from which DNA was extracted.

2.3.2 Preparation of DNA samples

2.3.2.1 Isolation of genomic DNA from EDTA-blood

Each sample was processed in duplicate. Blood from two EDTA tubes was transferred to a 50ml plastic centrifuge tube, 20ml of ice cold cell lysis buffer (Appendix I) was added to the blood, and the tubes were inverted a few times. The tubes were left on ice for 5-10 minutes, before centrifuging at 3 000 r.p.m. for 10 minutes in a benchtop centrifuge (Beckman model TJ-6). The supernatant was then discarded and the pellet resuspended in 10ml ice-cold cell lysis buffer. The washing and centrifuging steps were repeated until a pinkish white pellet was obtained. The pellet was resuspended in 90 μ l Na-EDTA (Appendix I) and 100 μ l 10% SDS in a 50ml volume centrifuge tube. DNA could be extracted directly from these nuclei, or they could be frozen at -70°C until required.

2.3.2.2 Genomic DNA extraction from nuclei

The freshly prepared or thawed frozen nuclei were incubated overnight with 100 μ l proteinase K (10mg/ml) at 37°C with gentle agitation. After this incubation, 2ml of sterile dH₂O and 500 μ l 3M NaAc (Appendix I) were added at room temperature. Thereafter, 2.5ml of phenol/chloroform (Appendix I) was added and the mixture was thoroughly mixed for 10 minutes on a rotator (Voss of Maldon, Protea Dento-Medical Services, SA) at 4°C prior to centrifugation at 8 000-10 000 r.p.m. for 10 minutes (Sorvall RC 5B Du Pont, SS34 or HB4 rotor) in glass tubes (Corex). The top aqueous layer was transferred to a fresh centrifuge tube, taking care not to disturb the interface and the bottom layer was discarded. An equal volume of chloroform/octanol (Appendix I) was added to the aqueous layer, which was mixed for 10 minutes on a Voss rotator and centrifuged as described earlier. Again, the top aqueous layer was removed to a fresh tube and the DNA it contained precipitated with 2 volumes of ice-cold 96% ethanol, by gentle mixing until the white strands of DNA appeared. The DNA was transferred with a pipette tip to a clean eppendorf tube and washed by adding 1ml of 70% ethanol and microfuging (Centrifuge 5415C, AMTEC) for 3 minutes, after which the 70% ethanol was carefully decanted. The washing step was repeated before the final pellet was dried either by inverting the Eppendorf tube on carlton paper for an hour or drying under

vacuum (Speed Vac, Savant SVC 100H). The isolated DNA was then resuspended in 300-500 μ l of 1xTris-EDTA (Appendix I) and incubated at 37 $^{\circ}$ C overnight, prior to placing on a Voss rotator for 3 days at 4 $^{\circ}$ C to allow the DNA to resuspend completely. The concentration of the DNA was determined by a spectrophotometric reading (Roy Spectronic 1201, Milton) at 260nm, where an optical density reading (OD) of 1 equaled a concentration of 50 μ g/ml. Subsequently, the DNA concentration was adjusted to 1 μ g/ μ l by either adding 1xTE buffer (Appendix I), if the concentration was too high, or by performing an ethanol precipitation if the concentration was too low, followed by resuspension to give the desired concentration.

2.3.3 Polymerase Chain Reaction

2.3.3.1 Non-radioactive Polymerase Chain Reaction

Non-radioactive PCR amplification of the S1-S6 regions of *KVLQT1* as described by Wang et al., (1996a) (Table 2.1) was used for PCR-SSCP analysis and ASREA. The PCR reaction was performed in a 30 μ l reaction volume using 200ng of template DNA, 120ng of each primer, 100 μ M of deoxyribonucleotides (1.2 μ l of an equimolar solution (2.5mM) of dATP, dTTP, dGTP, dCTP) (Boehringer Mannheim, Germany), 2.5mM MgCl₂ (Promega, USA), 5% formamide (Sigma, USA), 0.5 U Taq polymerase (Promega, USA) and 3 μ l 10 x Taq polymerase buffer supplied by the manufacturer (Promega, USA). Five percent of formamide was included in the PCR reaction mixture to increase the specificity of the primers for the template, in order to eliminate the presence of spurious products. Each sample was overlaid with 40 μ l of mineral oil (BDH Chemicals) prior to the thermocycling step to prevent evaporation. Thermocycling was performed in a Gene E thermal cycler (Techne, UK) and consisted of an initial denaturing step at 94 $^{\circ}$ C for 5 minutes, followed by 5 cycles of denaturation at 94 $^{\circ}$ C for 30s, annealing at 64 $^{\circ}$ C for 30s and elongation at 72 $^{\circ}$ C for 45s. These 5 cycles were linked to 30-cycles, consisting of denaturation at 94 $^{\circ}$ C for 30s, annealing at 62 $^{\circ}$ C for 30s and elongation at 72 $^{\circ}$ C for 45s. A final elongation step at 72 $^{\circ}$ C for 10 minutes was performed.

The success of the PCR amplification was monitored by the electrophoresis of 5 μ l of the PCR product mix with 1 μ l of bromophenol blue tracking dye (Appendix I) on a 1.5 % agarose gel containing ethidium bromide (1 μ g/ml) (Appendix I). The molecular size markers

Table. 2.1 DNA Sequences of the eight regions of the *KVLQT1* gene analyzed

REGION	SEQUENCES
1. S1-S2	gift from M.Keating
2. S2-S3	F- GAGATCGTGCTGGTGGTGTCT R- CTCCTGGTCTGGAAACCTGG
3. S3-S4	F- CTCTCCCTGGGGCCCTGGC R- TGCGGGGGAGCTTGTGGCACAG
4. S4	F- GGGCATCCGCTTCCTGCAGA R- CTGGGCCCTACCCTAACCC
5. S4-S5	gift from M.Keating
6. S5-Pore	F- TCCTGGAGCCCGAACTGTGTGT R- TGTCCTGCCCACTCCTCAGCCT
7. Pore-S6	F- CCCAGGACCCAGCTGTCAA R- AGGCTGACCACTGTCCCTCT
8. S6	F- GCTGGCAGTGGCCTGTGTGGA R- AACAGTGACCAAATGACAGTGAC

All sequences are given in a 5'-3' direction

electrophoresed alongside PCR products were bacteriophage lambda DNA (Promega, USA) digested with *Pst*I (λ *Pst*I) (Boehringer Mannheim, Germany) (Appendix I). The DNA fragments were visualized on a longwave ultraviolet transilluminator (3 UVTM Transilluminator model LMS-26E, UK).

2.3.3.2 Radioactive Polymerase Chain Reaction

In order to genotype individuals at STRP loci prior to linkage analysis, radioactive PCR was performed. Two methods of radioactive labeling were used, namely, full strand labeling by incorporation and end-labeling.

2.3.3.2.1 Full Strand Labelling

Full strand labeling was used to amplify fourteen of the fifteen microsatellite markers which were genotyped. PCR reactions were performed in a 10 μ l reaction volume, using 200ng of template DNA, 50ng of each primer, 200 μ M of each dATP, dTTP, dGTP, (Boehringer Mannheim, Germany) 5 μ M of unlabeled dCTP (Boehringer Mannheim, Germany), 0.5 μ Ci [α -³²P]-dCTP (Amersham, UK), 2.5mM MgCl₂ (Promega, USA) and 0.5 U of Taq polymerase (Promega, USA) in the buffer supplied by the manufacturer. The DNA was amplified in a Gene E thermal cycler (Techne, UK), using the parameters for the different markers listed in table 2.2.

2.3.3.2.2 End-Labeling

One of the microsatellite markers *DIIS1318* was amplified employing end-labelling as this marker repeatedly failed to amplify employing the full strand labelling technique. The forward primer of the marker *DIIS1318* was labeled with [γ -³²P]-ATP (Amersham, UK) prior to performing the PCR reaction. The labeling reaction was performed in a 5 μ l reaction volume using 0.03 μ M forward primer, 3 μ Ci [γ -³²P]-dATP (Amersham, UK), 1.5U of T₄ polynucleotide kinase (Promega, USA) in the buffer supplied by the manufacturer. Labeling was performed at 37⁰C for 6 hours, whereafter the reaction was stopped by placing it at 94⁰C for 5 minutes.

The subsequent PCR reaction was performed in a 10 μ l reaction volume using 200ng of template DNA, 40ng of unlabeled forward primer, 50ng of reverse primer, 200 μ M of each

Table.2.2 Thermocycling parameters used for the STRP markers amplified with radioactive PCR

DNA marker	Number of cycles	Denaturing temp. (°C)	Time (s)	Annealing temp. (°C)	Time (s)	Elongation temp.	Time (s)
<i>D11S1323</i>	1	94°C	5 min	-	-	-	-
	5	94°C	30s	59°C	30s	72°C	45
	25	94°C	30s	55°C	30s	72°C	45
	1	-	-	-	-	72°C	10 min
<i>D7S636</i>	1	94°C	5 min	-	-	-	-
	30	94°C	30s	56°C	30s	72°C	45s
	1	-	-	-	-	72°C	10 min
<i>D11S1331,</i> <i>D11S860,</i> <i>TH,</i> <i>D3S1298,</i> <i>D4S402,</i> <i>D8S264,</i> <i>D8S1781,</i> <i>D8S504,</i> <i>D21S2040,</i> <i>D21S1912</i> & <i>D21S1959</i> <i>DRPLA</i> (trinucleotide repeat)	1	94°C	5 min	-	-	-	-
	30	94°C	30s	55°C	30s	72°C	45s
	1	-	-	-	-	72°C	10 min
	-	-	-	-	-	-	-
<i>D11S1318</i>	1	94°C	5 min	-	-	-	-
	5	94°C	30s	52°C	30s	72°C	45s
	25	94°C	30s	50°C	30s	72°C	45s
	1	-	-	-	-	72°C	10 min

°C = Grade Celsius

s = seconds

min = minutes

temp = temperature

dATP, dCTP, dGTP, dTTP (Boehringer Mannheim, Germany), 0.1 μ l of the labeled forward primer, 2.5mM MgCl₂ (Promega, USA) and 0.5U of Taq polymerase (Promega, USA) in the buffer supplied by the manufacturer. The DNA was amplified in a Gene E thermal cycler (Techne, UK), the thermocycling steps used for this marker are indicated in table 2.2.

2.3.4 Mutation screening

2.3.4.1 Allele specific restriction enzyme analysis

Allele specific restriction enzyme analysis was used to screen for the presence of four of the first ten *KVLQT1* mutations described by Wang et al., (1996), which affect restriction enzyme sites (Table 2.3).

Each amplified PCR product, generated as described in section 2.3.3.1 was dialyzed, against deionised H₂O on a 0.025 μ m millipore VS filter (Millipore), to remove PCR buffer components prior to addition of restriction enzyme buffer. The reaction was performed at room temperature for 10 minutes by dispensing 5 μ l of the amplified PCR product onto the filter that was floating on a dH₂O surface in an ice block tray. Four microlitres of each dialysed sample were subsequently transferred to a 0.5ml Eppendorf tube, taking care not to transfer the mineral oil situated on the periphery of the hydrophilic PCR sample. Five units of the particular restriction enzyme and 1.5 μ l of the appropriate 10 x restriction enzyme buffer provided by the manufacturer were added to the dialyzed sample. Water was added to a final volume of 15 μ l, before the sample was digested at 37⁰C overnight. The restriction enzyme was inactivated by heating the reaction mixture at 65⁰C for 10 minutes.

Fragments generated with restriction enzyme digestion were separated by gel electrophoresis. To this end, a mixture of 5 μ l of each digested sample and 1 μ l of bromophenol blue loading dye was separated by electrophoresis on a 6.5 X 7cm vertical 12% polyacrylamide gel (Appendix I) using 1XTBE running buffer (Appendix I). Electrophoresis was performed at 12V/cm until the bromophenol blue had migrated the length of the gel. To ascertain the presence of a specific mutant allele, as indicated by the restriction fragments generated, an undigested sample was co-electrophoresed as a control, as was a digested wild type control sample and the molecular size marker λ *Pst*I (Appendix I).

Table. 2.3 The first ten *KVLQT1* mutations described by Wang et al., (1996) and the restriction enzyme sites that they affect

MUTATION	REGION	RESTRICTION ENZYME	EFFECT ON ENZYME SITE
DF38W/G39 Δ	S2	/	
A49P	S2-S3	<i>NaeI</i>	loss
G60R	S2-S3	/	
R61Q	S2-S3	<i>PvuII</i>	gain
V125M	S4-S5	<i>StyI</i>	gain
L144F	S5	/	
G177K	Pore	/	
T183I	Pore	/	
A212V	S6	<i>HhaI</i>	loss
G216E	S6	/	

2.3.4.2 PCR-SSCP analysis

After linkage analysis had implicated *KVLQT1* as disease-causing gene in pedigree 167, mutation screening employing PCR-SSCP analysis was performed to screen for known and novel mutations in the S1-S6 regions of this gene as published by Wang et al., (1996). Four different gel conditions were used, namely, 5% polyacrylamide with and without glycerol and 10% polyacrylamide with and without glycerol, made up from a 30 % polyacrylamide stock solution (Appendix I). PCR-SSCP analysis was performed on non-denaturing polyacrylamide gels prepared between two glass plates (400 x 300 x 1mm).

To prepare the gel, glass plates (400 x 300 x 1mm) were washed with soap (Coastal Chemicals), rinsed with H₂O and then wiped with 70% ethanol to remove residual soap. One of the plates was silanised with Wynn'sTM C-thru (Wynn's Oil South Africa (Pty) Ltd) solution to prevent the gel from sticking to the plate when the gel apparatus was dismantled. A sheet of GelbondTM PAG polyester film (FMC Bioproducts, USA) was tightly fixed to the back plate. This was performed by spraying 70% ethanol onto the plate and placing the Gelbond film with the hydrophobic side exposed to the 70% ethanol. Trapped airbubbles were expelled by gently rubbing across the surface of the film with a sheet of Carlton paper. The glass plates were separated by 1mm thick spacers and sealed together with an Easy Boot gel sealing system. (Gibco BRC, UK). The gel was cast carefully on the hydrophilic side of the Gelbond and a 1mm thick square tooth well-forming comb was placed in position and clamped. The gel was left to set for 2-3 hours at room temperature, during the polymerization the gel covalently bonded with the Gelbond, thereby providing a solid support for the gel that made subsequent staining easier. After the gel had set the comb was removed, the wells cleaned under running water and the gel assembled on a vertical electrophoresis apparatus.

The samples were prepared by mixing a 6µl aliquot of the non-radioactively labeled amplified PCR product (section 2.3.3.1) with 6µl of SSCP- loading dye (Appendix I). This mixture was denatured at 94^oC for 10 minutes, after which the total volume was loaded onto the SSCP gel and electrophoresed at 4^oC in 0.5 x TBE running buffer (Appendix I) at a constant power of 30 or 50 Watts, depending on the specific gel condition (Table 2.4). Under all conditions, the bromophenol blue dye was allowed to migrate to the bottom of the glass plates; however, the electrophoresis time varied for the different gel conditions as indicated in table 2.4. The bands were visualized by silver staining as described in section 2.3.5 and either air-dried or dried

Table 2.4 Electrophoreses and gel drying conditions of SSCP gels

GEL CONDITION	ELECTROPHORESED AT:	GEL DRYING CONDITION
5% polyacrylamide (+) Glycerol	50 Watts for 8-10 hours	dried by hanging to drip dry
5% polyacrylamide (-) Glycerol	50 Watts for 3-5 hours	dried by hanging to drip dry
10% polyacrylamide (+) Glycerol	30 Watts for 18-20 hours	vacuum drying
10% polyacrylamide (-) Glycerol	50 Watts for 6-8 hours	dried by hanging to drip dry
0.4XMDE	50Watts for 4hours	dried by hanging to drip dry

under a vacuum on a gel drier (Slab gel drier Hoeffler SE 1160, San Francisco) depending on the gel condition (Table 2.4). If the gel was dried under a vacuum, it was dried for 2 hours with plastic wrap placed on the side of the gel not covered with the Gelbond.

Samples which demonstrated mobility shifts were reamplified and analyzed again under the SSCP condition in which the mobility shift was originally detected and a 0.4XMDE gel (Appendix I) (FMC Bioproducts, USA) to confirm its presence.

2.3.5 Silver Staining

Silver staining was used to visualize the fragments generated with ASREA and PCR-SSCP analysis. Staining was performed while gels were submerged in a suitably sized container agitating on a orbital shaker. First the gel was treated in a 0.1% AgNO₃ solution (Appendix I), for 5 minutes in the case of the smaller gels used in ASREA while the larger SSCP gels were stained for 10 minutes, after which the solution was decanted, and the gel rinsed with dH₂O to remove residual AgNO₃. The gels were then placed in a developing solution (1.5% NaOH, 0.01% NaBH₄, 0.4% formaldehyde) (Appendix I) 10 minutes for the smaller ASREA gels and 15-25 minutes for the SSCP gels. The fragments were visualized on a white light illuminator (EGE LAUDA model), photographed (Sony Video Graphic printer UP-860 CE) for permanent record and the gel sealed in a plastic bag for storage.

2.3.6 Radioactive Gel Electrophoresis

2.3.6.1 Preparation of Gel

Subsequent to radioactive amplification of STRP loci, samples were electrophoresed on a 5% denaturing polyacrylamide gel (Appendix I) to separate alleles containing different numbers of repeat elements. To prepare the gel, glass plates (400 x 300 x 1mm) were washed with soap (Coastal Chemicals), rinsed with H₂O and then wiped with 70% ethanol to remove residual soap. One of the plates was silanised with Wynn'sTM C-thru (Wynn's Oil South Africa (Pty) Ltd) solution to prevent the gel from sticking to the plate when the gel apparatus was dismantled. The plates were separated by 0.4 mm spacers and a Easy Boot gel sealing system (Gibco BRC, UK) was used to seal the plates prior to pouring the gel. The gel was carefully poured while the plates were held at a slight angle and care was taken not to trap any air bubbles between the plates. A shark toothcomb (with the teeth facing up) was placed in position and clamped. The gel was allowed to set at room temperature for 2-3 hours.

2.3.6.2 Electrophoresis

The comb was removed from the gel and excess urea was rinsed from the top surface of the gel and the comb, the gel was mounted on a vertical gel electrophoresis apparatus and the comb was replaced with the teeth just touching the gel. The 0.5 x TBE (Appendix I) running buffer was prepared and 1 litre was preheated in the microwave to 60°C prior to pre-running the gel for 10 minutes at 1800 V. Six microliters sequencing loading dye (Appendix I) was added to the 10µl PCR product and this mixture was denatured in a heating block (Dri Block R Db-3 Techne, UK) at 94°C for 5 minutes, before loading 4µl of this solution. Samples were electrophoresed for 1.5 - 2.5 hours at 1800 V depending on the size of the alleles that were to be separated. The bromophenol blue dye front was allowed to migrate to the bottom of the glass plates for fragments of 100-200 bp in size, while the xylene cyanol dye front was allowed to migrate three quarters of the gel distance for fragments greater than 200 bp in size.

2.3.8 Autoradiography

After dismantling the electrophoresis apparatus, the gel was removed from the plates using a 3MM Whatman paper (Whatman TM 3MM Chromatography, Whatman International Ltd, UK) folded double and cut to the size of the gel, after which the gel was covered with plastic Glad^R wrap (Multi Foil Trading (Pty) Ltd) and dried at 80°C for 1 hour under vacuum (Slab gel drier, Hoeffler SE1160, San Francisco). The dried gel was placed in a cassette (Okomoto) and exposed to X-ray film (Cronex-4, Protea Medical Services, SA) for 6-18 hours, before developing the X-ray film in the dark room. Following exposure, the X-ray film was developed in a Polygon A solution (Champion Photochemistry) (Appendix I) for 1 minute and transferred to a stop solution containing 6% acetic acid (Appendix I) for another minute. Thereafter, the X-ray film was transferred to a fix solution (Appendix I) (M&B Suppliers) for 2 minutes. The autoradiograph was rinsed with water and air-dried. The autoradiographs were then genotyped and independently recorded by two investigators and were only reported after consensus was reached.

2.3.8 Genotyping

The alleles of the STRP markers analyzed at the four LQTS and three FME candidate loci were genotyped as follows. Autoradiographic images of radioactive PCR amplified, electrophoretically separated alleles of each of the STRP markers were numbered in order of decreasing size, based on this numbering system each individual were assigned a genotype. Continuity of allele assignment between different autoradiographs was assured by designating

certain individuals as standards, which were co-electrophoresed on each gel along with samples amplified at that specific locus. Genotypes assigned to individuals were subsequently compared with the family structure to ascertain the mendelian inheritance of alleles and minimize allele labeling error.

Genotyping was performed with DNA markers at the three candidate forms of epilepsy syndromes analyzed in the epilepsy study. The DNA markers used in this analysis were *D21S2040*, *D21S1912* and *D21S1259* at the *EPM1* locus, *D8S264*, *D8S504* and *D8S1781* at the chromosome 8p locus and the triplet repeat in the atrophin gene, which is expanded in DRPLA-affected individuals (Tables 2.5 and 2.6).

Genotyping at the four LQTS loci analyzed was performed by using a set of nine polymorphic microsatellite markers. The *LQT1* locus was genotyped by using DNA markers *TH*, *D11S860*, *D11S1318*, *D11S1323* and *D11S1331*, the *LQT2* locus with marker *D7S636*, the *LQT3* locus with marker *D3S1298* and *LQT4* with marker *D4S402* (Tables 2.5 and 2.6).

2.3.9 Haplotype construction

Haplotypes were constructed across the candidate loci where two or more DNA markers were analyzed. Most likely haplotypes were constructed with reference to gene and marker order on the respective chromosomes and were based on parental genotypes and in a family context, assuming minimal recombination events in each kindred.

2.3.10 Linkage Analysis

Two-point linkage analyses were performed using the *MLINK* program of the Linkage package (Lathrop and Lalouel, 1984). In the case of LQTS, a conservative approach to phenotypic assignment was used, as described by Keating et al., (1991) section 2.2.2. The phenotypic assignment in the epilepsy study was based on the diagnosis made by Dr. Carr as discussed in section 2.2.1. A measure for the support of linkage is the LOD score, which is the log of the probability that the data arose from two linked loci, versus the probability that the data arose from two unlinked loci. Linkage of a marker and the disease gene is indicated by a LOD score of +3.0 or higher, while exclusion of linkage is indicated by a value of -2 or lower. A penetrance of 0.9, a frequency of the disease allele of 0.001 and equal male and female

Table. 2.5 STRP markers analyzed by Radioactive PCR

LOCUS	PRIMERS SUPPLIED BY	REFERENCE
<i>D11S1318</i>	*UCT DNA-LAB	Gyapay, G., 1994
<i>D11S1323</i>	#RESEARCH GENETICS	Gyapay, G., 1994
<i>D11S1331</i>	#RESEARCH GENETICS	Gyapay, G., 1994
<i>D11S860</i>	#RESEARCH GENETICS	Kimberling, W.J., 1992
<i>TH</i>	#RESEARCH GENETICS	n/a
<i>D7S636</i>	#RESEARCH GENETICS	Gyapay, G., 1994
<i>D3S1298</i>	#RESEARCH GENETICS	Weisenbach, J., 1992
<i>D4S402</i>	*UCT DNA-LAB	Weisenbach, J., 1992
<i>D8S264</i>	#RESEARCH GENETICS	[§] Personal communication
<i>D8S504</i>	#RESEARCH GENETICS	[§] Personal communication
<i>D8S1781</i>	#RESEARCH GENETICS	[§] Personal communication
<i>D21S1259</i>	*UCT DNA-LAB	Virtaneva et al., 1996
<i>D21S2040</i>	*UCT DNA LAB	Virtaneva et al., 1996
<i>D21S1912</i>	*UCT DNA LAB	Virtaneva et al., 1996
<i>DRPLA</i> (trinucleotide repeat)	*UCT DNA LAB	

#MapPair™ primers obtained from Research Genetics, Huntsville, Alabama, USA

*Primers designed to published sequences was ordered from the University of Cape Town DNA Lab, South Africa

[§] Berkovic

Table. 2.6 Details on the alleles of the polymorphic markers analyzed by using radioactive PCR.

MARKER	SIZE	HETEROZYGOSITY
<i>D11S1318</i>	123-145 bp	0.78
<i>D11S1323</i>	201-207 bp	0.46
<i>D11S1331</i>	191-205 bp	0.70
<i>D11S860</i>	154-196 bp	0.91
<i>TH</i>	100 bp	n/a
<i>D7S636</i>	130-168 bp	0.90
<i>D3S1298</i>	194-220 bp	0.88
<i>D4S402</i>	287-323 bp	0.92
<i>D8S264</i>	121-145 bp	0.85
<i>D8S504</i>	n/a	0.72
<i>D8S1781</i>	n/a	0.85
<i>D21S1259</i>	222bp	0.67
<i>D21S2040</i>	n/a	n/a
<i>D21S1912</i>	173bp	0.80
<i>DRPLA</i> (trinucleotide repeat)	n/a	n/a

bp - base pair

n/a - not available

Information obtained from <http://www.gdb.org/>

recombination fractions were used for both diseases, while equal allele frequencies were assumed at all the loci in linkage calculations.

2.3.11 Direct Sequencing of SSCP conformers

2.3.11.1 Purification of DNA

In samples in which a mobility shift was confirmed, sequencing was performed to determine the nature of any sequence variations. These samples were first reamplified by PCR in a reaction volume scaled up to 100 μ l. A 1.5% agarose gel containing ethidium bromide (1 μ g/ml) (Appendix I) was prepared and the teeth of the comb used were taped together to form a larger well, that could bear a bigger volume. The total reaction volume was mixed with 10% bromophenol blue dye and loaded on the gel. The samples were allowed to migrate 10cm from the wells, to monitor for the presence of spurious products in the PCR amplified product. After agarose gel electrophoresis, the PCR- amplified DNA fragment was visualized on a UV-light box, and the fluorescent DNA band of the expected size was cut out using a sterile blade. The DNA was purified from the gel slice using the QIAGEN, QIAquick Gel Extraction Kit, following the manufacturers' protocol and resuspended in 30 μ l H₂O.

2.3.11.2 Direct sequencing of purified DNA

The purified DNA prepared as described in section 2.3.11.1 was sequenced by utilizing the fmolTM sequencing kit (Promega, USA) according to the manufacturer's specifications. The forward and reverse primers flanking the S2-S3 region (Table 2.1), which contained a mobility shift were used in separate reactions to sequence 3 μ l of purified amplified DNA. For each sequencing reaction, four 0.5 ml reaction tubes were labeled G, A, T and C, respectively. Two microlitres of each termination mix, ddGTP, ddATP, ddTTP and ddCTP (Appendix I), were aliquoted into the appropriately labeled tube, overlaid with 20 μ l mineral oil and placed on ice. Prior to continuing with the sequencing reaction, a Gene E thermal cycler (Techne, UK) was preheated to 95⁰C and maintained at that temperature. A reaction mixture was prepared which contained 1 μ l of forward or reverse primer (10ng/ μ l), 1 μ l diluted DMSO (30 μ l DMSO and 20 μ l H₂O) (Appendix I), 5 μ l 5X sequencing grade Taq DNA polymerase buffer, 3 μ l purified template DNA, 1 μ l [α^{32} -P] dCTP (3000Ci/mmol) 5 μ l H₂O and 1 μ l of sequencing grade Taq DNA polymerase. Aliquots of 4 μ l of this reaction mixture were added to each termination mix (Appendix I) and the tubes immediately placed into the preheated thermocycler. The same thermocycling parameters as described in section 2.3.3.1 were used, and 4 μ l of stop solution was added to each tube after completion of the thermocycling steps.

The sequences were resolved by electrophoresis through a 5% polyacrylamide sequencing gel, which was prepared as described in section 2.3.6.1. Electrophoresis was performed as described in section 2.3.6.2 but a 3.5 μ l aliquot of the denatured DNA was loaded. The sequencing gel was electrophoresed at 1800 V until the bromophenol blue dye had reached the bottom of the gel. At this point, another denatured 3.5 μ l aliquot was loaded into unused wells and the samples electrophoresed until the latter samples' bromophenol blue dye reached the bottom of the gel. Thereafter, the gel was treated in the same manner as described in section 2.3.7. The dried gel was exposed to X-ray film in a cassette for 3 hours to two weeks depending on the degree of radioactive incorporation and the isotope's activity. The sequences were read and recorded independently on paper by two investigators and were only reported after consensus was reached.

CHAPTER 3

RESULTS

Page

EPILEPSY

3.1 LINKAGE ANALYSIS STUDY	90
3.1.1 Family Study	90
3.1.2 Genotypic Analysis	90
3.1.2.1 Genotypic analysis at the EPM 1 locus	90
3.1.2.2 Genotypic analysis at the chromosome 8 locus	91
3.1.2.3 Genotypic analysis at the DRPLA locus	91
3.1.3 Haplotype Analysis	101
3.1.3.1 Haplotype analysis at the EPM1 locus	101
3.1.3.2 Haplotype analysis at the chromosome 8 locus	101
3.1.4 Two Point LOD scores	101
3.2 NEW AND EXTENDED PEDIGREES	102

LQTS

3.3 FOUNDER MUTATION SCREENING	108
3.4 LINKAGE ANALYSIS STUDY	110
3.4.1 Family Study	110
3.4.2 Genotypic Analysis	110
3.4.2.1 Mutation screening for the <i>KVLQT1</i> Ala212Val mutation	110
3.4.2.2 Genotypic analysis employing DNA markers at four of the known LQTS loci	117
3.4.2.2.1 <i>KVLQT1</i> locus	117
3.4.2.2.2 <i>HERG</i> locus	129
3.4.2.2.3 <i>SCN5A</i> locus	134
3.4.2.2.4 Chromosome 4 locus	134
3.4.3 Haplotype Analysis	143
3.4.3.1 Haplotype analysis at the <i>KVLQT1</i> locus	143
3.4.4 Two point LOD scores	143
3.5 MUTATION SCREENING ANALYSIS	148
3.5.1 PCR-SSCP Analysis in <i>KVLQT1</i>	148
3.5.2 ASREA in <i>KVLQT1</i>	155
3.5.2.1 Ala49Pro mutation in S2-S3 region	155
3.5.2.2 Arg61Glu mutation in S2-S3 region	156
3.5.2.3 Val125Met mutation in the S3-S4 region	156

EPILEPSY

3.1 LINKAGE ANALYSIS STUDY

3.1.1 Family Study

One family in which FME segregates was analyzed in the present study, the pedigree of the three-generation family, designated 201, is shown in figure 3.1. Eleven members of this family were analyzed, six of whom were affected. One individual (III:8) died following a seizure at age 31 years. Post mortem blood was collected from this individual. With consent of the parties involved, the brain of the latter individual was collected to assist in future analysis of this disorder.

3.1.2 Genotypic Analysis of DNA markers

As mentioned earlier, three forms of epilepsies, viz., EPM1, DRPLA and a form of epilepsy that shows linkage to chromosome 8p, have been identified as plausible candidates for FME. To test the candidacy of these loci, linkage analysis, employing microsatellite markers closely linked to these loci, was performed.

3.1.2.1 Genotypic analysis at the *EPM1* locus

At the *EPM1* locus, the DNA markers *D21S2040*, *D21S1959* and *D21S1912* were used, figures 3.2.1-3.2.3 show the autoradiographs with the genotypes generated by amplification and separation of the alleles at each of these markers. Five of the affected members of the family were homozygous for allele 2 at *D21S2040* (figure 3.2.1). The genotype of the sixth individual was 1/2. The genotypes of the affected members at *D21S1259* were: 4/4, 2/5, 3/4, and 4/4 (figure 3.2.2). No genotypes were generated for individuals III:5 and III:7 due to technical difficulties, their DNA repeatedly failed to amplify. At *D21S1912* the genotypes of affected individuals were 2/3, 2/6, 2/6, 6/6, 2/3 and 2/3 (figure 3.2.3). Thus, no specific allele segregating with the disease was detected at any of the three markers analyzed. These observations were statistically confirmed by LOD scores generated, which are reported in section 3.1.4.

3.1.2.2 Genotypic analysis at the chromosome 8 locus

In a Japanese family with similar clinical symptoms to those seen in FME, linkage to the DNA marker *D8S264* was reported (Berkovic, personal communication), therefore, this marker, as well as the closest telomeric marker, *D8S504*, and centromeric marker, *D8S1781*, were analyzed. The representative inheritance patterns of these markers are shown in figures 3.3.1-3.3.3. At marker *D8S504*, the genotypes of the affected family members were 2/3, 3/6, 3/6, 6/6, 3/6 and 1/6 (figure 3.3.1). At marker *D8S264*, the genotypes of the affected family members were 2/3, 3/5, 2/3, 3/5, 2/5 and 2/6, it is clear that there was no unique allele that segregated with the disease at this marker locus (figure 3.3.2). At marker *D8S1781*, the genotypes of five of the affected family members were 2/4, 2/4, 2/4, 1/4 and 2/4, respectively, no genotype was generated for the affected individual, III:8 because its DNA repeatedly failed to amplify (figure 3.3.3). Although allele 4 was present in all affected individuals at *D8S1781*, this allele was also present in one unaffected individual (III-1); thus, it is not segregating with the disease. Thus, at the three DNA markers analyzed at the chromosome 8p-candidate locus, no specific alleles that segregate with the disease were detected.

3.1.2.3 Genotypic analysis at the *DRPLA* locus

The triplet repeat in the atrophin gene was used to analyze the *DRPLA* locus for involvement in FME, figure 3.4.1 shows the autoradiograph of the genotypes derived at this marker. The genotypes identified at the triplet repeat marker are displayed on the pedigree to show the allelic distribution of this marker in pedigree 201 (figure 3.4.2). The genotypes of the affected family members were 5/8, 2/4, 5/5, 5/8, 3/5 and 5/5, allele 5 was present in five of the six affected individuals (figure 3.4.1). However, the latter allele was also present in unaffected individuals, thus suggesting that it is not segregating with the disease. Individuals III:7, III:8 and III:9 the affected children of individual II:7 received allele 5 from their affected father (figure 3.4.2). In individual II:3, the genotype could be deduced as 4/5 based on the genotypes seen in his children and the wife. The affected children of individual II:3 (III:3 and III:5), received the alleles 4 and 5 respectively from their father. The results of this analysis suggest that the tested locus is not involved in FME.

In summary, analyzing the three candidate loci, showed that there was no allele that segregated exclusively with FME at any of the DNA markers tested.

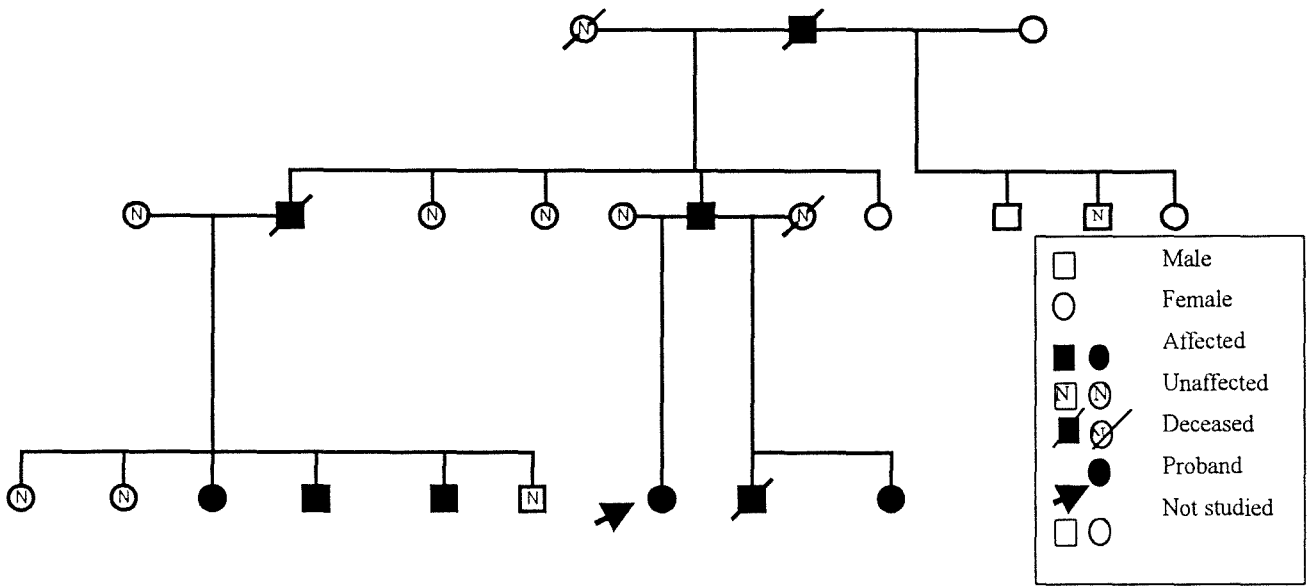


Fig. 3.1a The original pedigree 201 structure showing the family in which FME segregates. Clinically affected individuals were diagnosed according to the criteria stipulated in section 2.2.1.

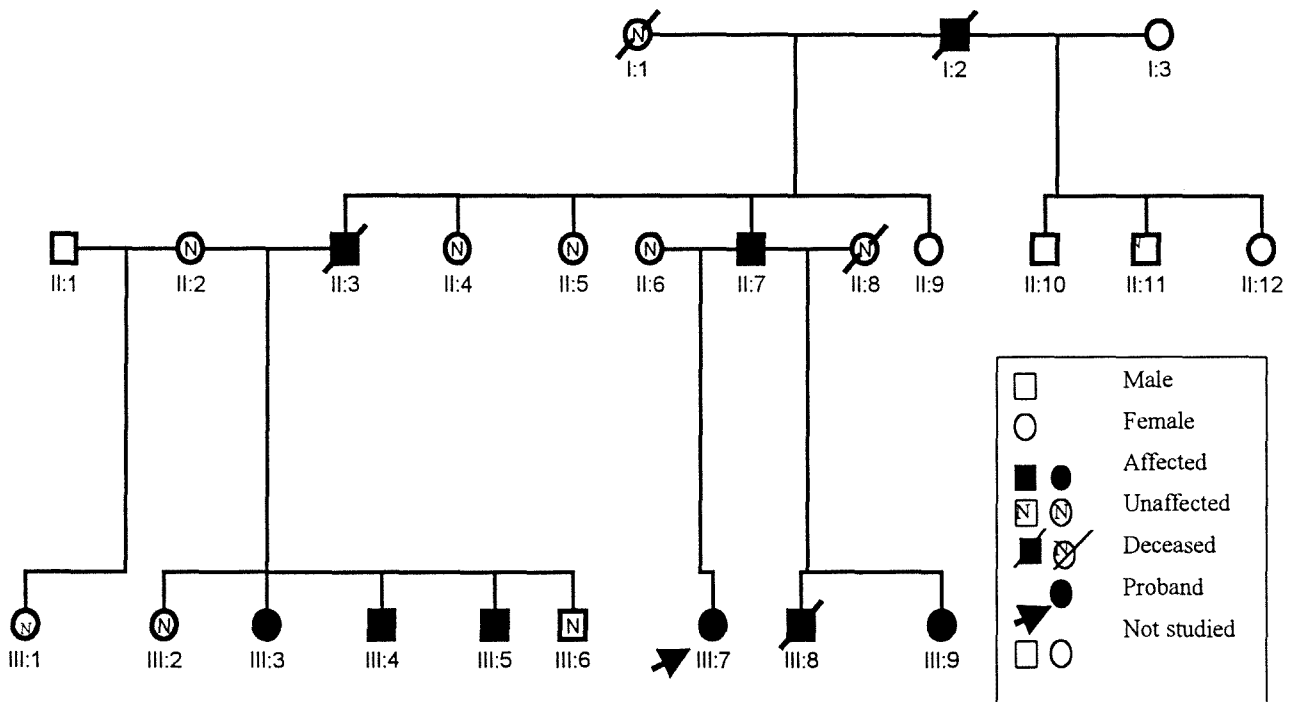


Fig. 3.1b Pedigree 201 structure altered for LOD score analysis. Individual II:1 was not studied but is indicated in the pedigree, as genotyping data was inconsistent with individual II:3 being the father of individual III:1. Individual identity numbers are shown under each individual, these numbers are used to refer to the study subjects in further analyses.

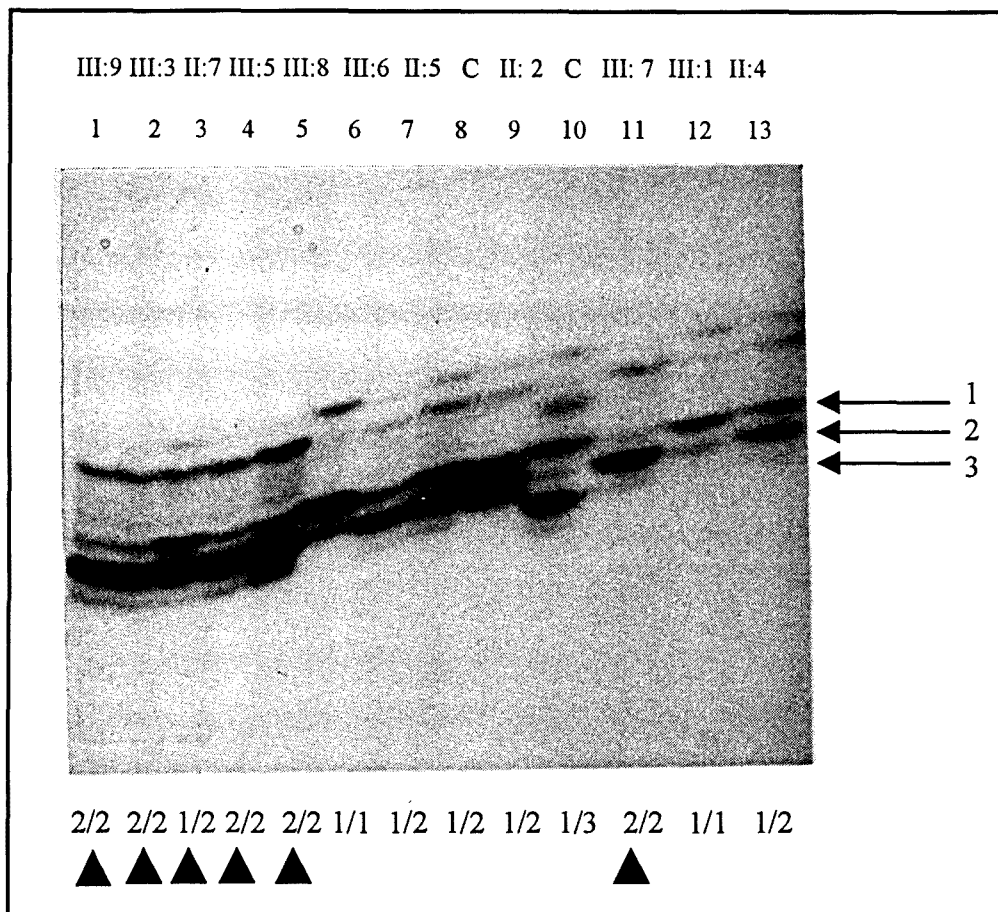


Fig. 3.2.1 Autoradiograph showing alleles at the EPM1 DNA marker *D21S2040* in pedigree 201 in which FME segregates. Assigned genotypes are indicated below each lane, designated allele numbers are indicated on the right. The individual identity numbers are shown above each lane and the lower arrowheads indicate affected individuals represented in the specific lane.

C = standard sample used to ensure continuity of allele assignment

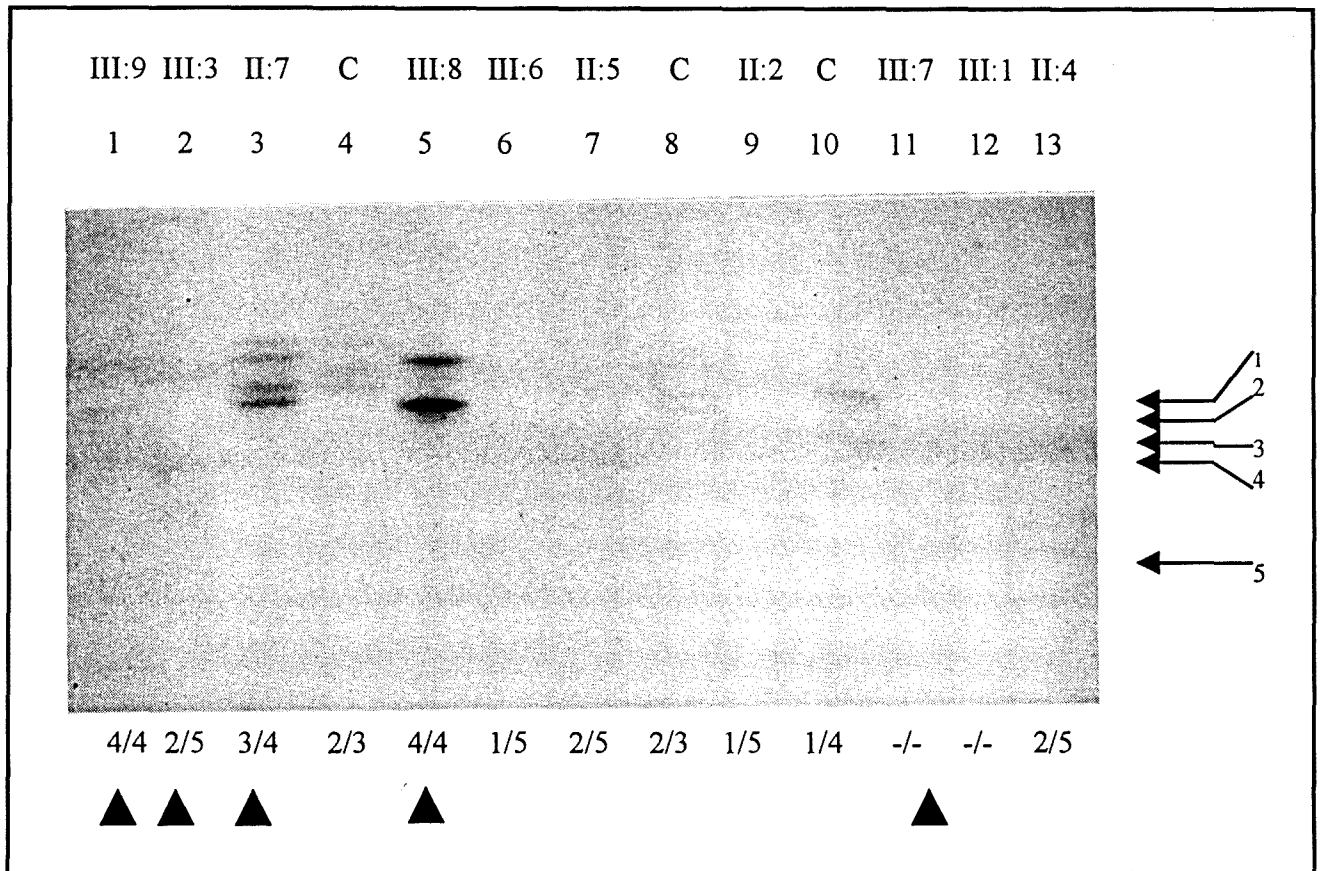


Fig. 3.2.2 Autoradiograph showing alleles at the EPM1 DNA marker *D21S1259* in pedigree 201 in which FME segregates. Assigned genotypes are indicated below each lane, designated allele numbers are indicated on the right. The individual identity numbers are shown above each lane and the lower arrowheads indicate affected individuals represented in the specific lane.

C = standard sample used to ensure continuity of allele assignment

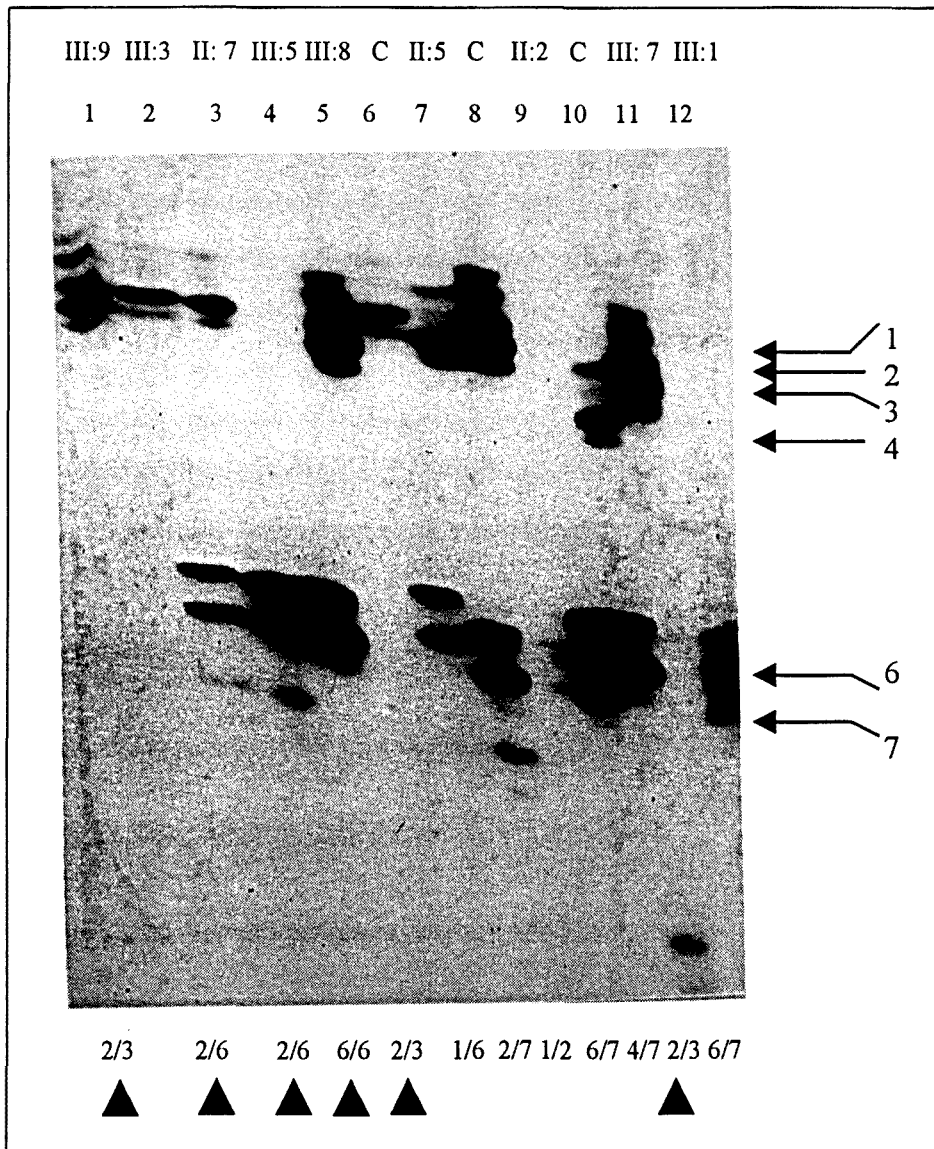


Fig. 3.2.3 Autoradiograph showing alleles at the EPM1 DNA marker *D21S1912* in pedigree 201 in which FME segregates. Assigned genotypes are indicated below each lane, designated allele numbers are indicated on the right. The individual identity numbers are shown above each lane and the lower arrowheads indicate affected individuals represented in the specific lane.

C = standard sample used to ensure continuity of allele assignment

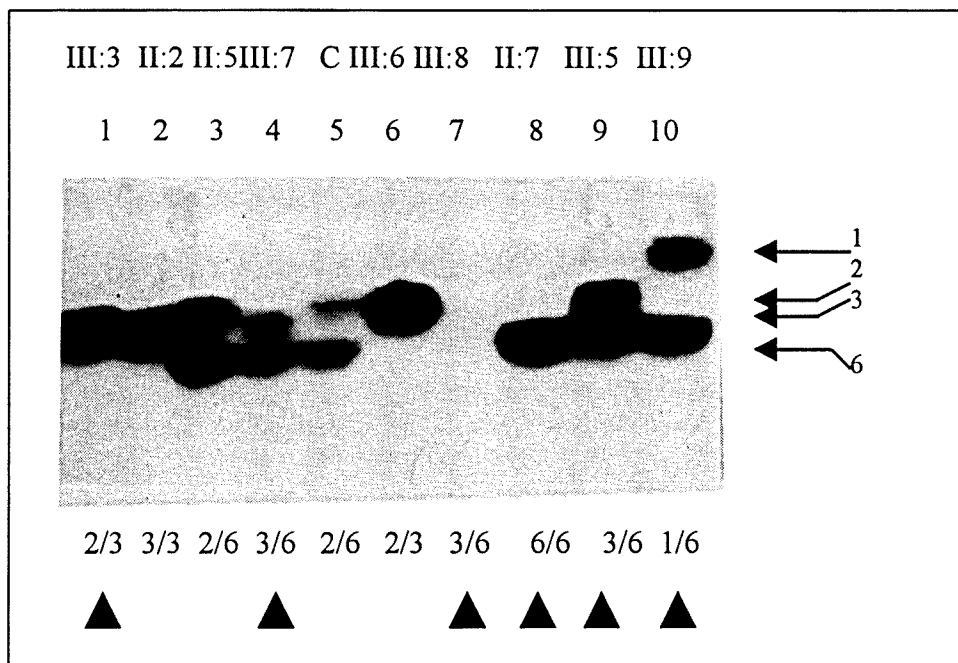


Fig. 3.3.1 Autoradiograph showing alleles at the chromosome 8p DNA marker *D8S504* in pedigree 201 in which FME segregates. Assigned genotypes are indicated below each lane, designated allele numbers are indicated on the right. The individual identity numbers are shown above each lane and the lower arrowheads indicate affected individuals represented in the specific lane.

C = standard sample used to ensure continuity of allele assignment

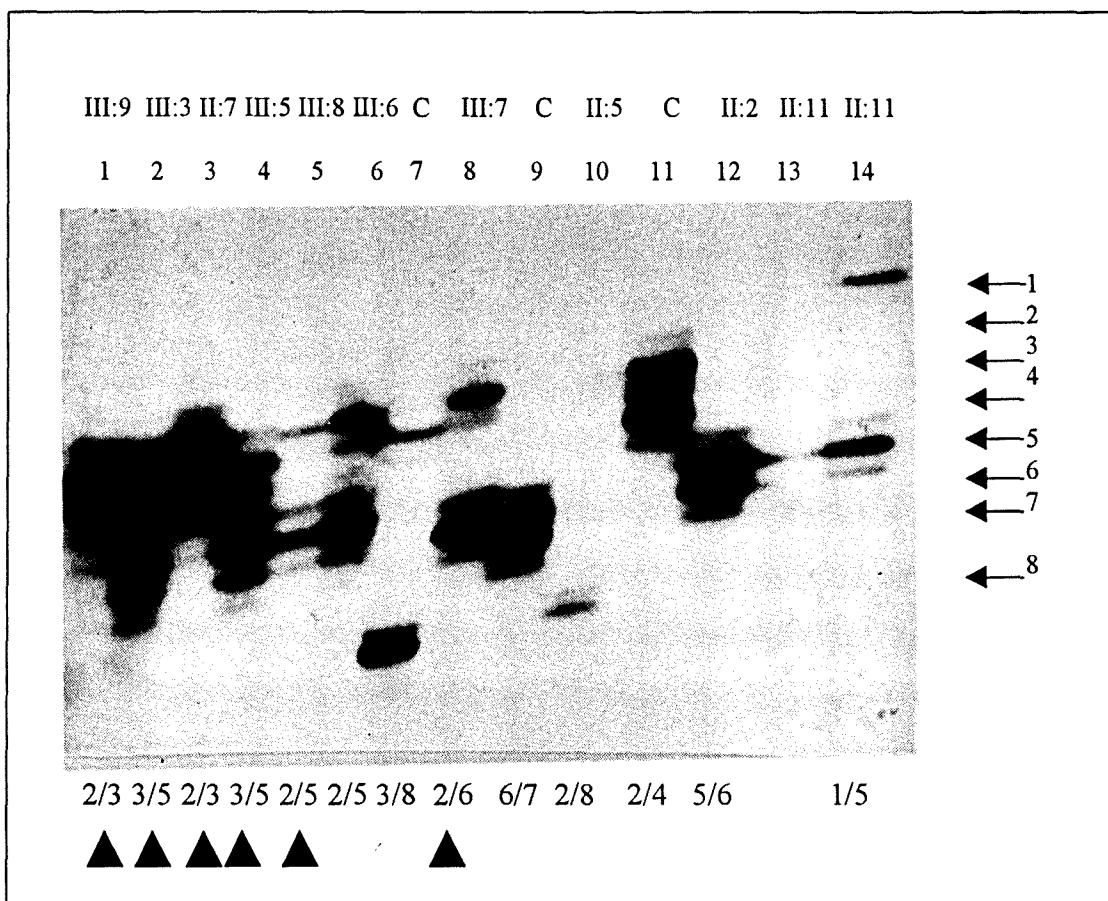


Fig. 3.3.2 Autoradiograph showing alleles of at the chromosome 8p DNA marker *D8S264* in pedigree 201 in which FME segregates. Assigned genotypes are indicated below each lane, designated allele numbers are indicated on the right. The individual identity numbers are shown above each lane and the lower arrowheads indicate affected individuals represented in the specific lane.

C = standard sample used to ensure continuity of allele assignment

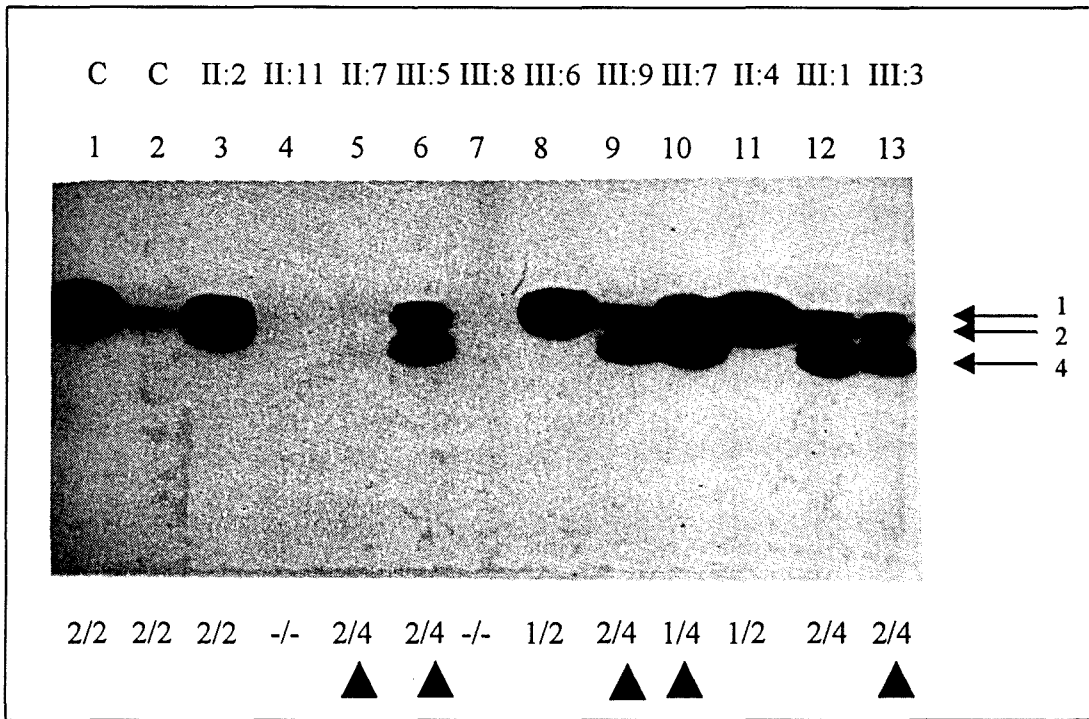


Fig. 3.3.3 Autoradiograph showing alleles of at the chromosome 8p DNA marker *D8S1781* in pedigree 201 in which FME segregates. Assigned genotypes are indicated below each lane, designated allele numbers are indicated on the right. The individual identity numbers are shown above each lane and the lower arrowheads indicate affected individuals represented in the specific lane.

C = standard sample used to ensure continuity of allele assignment

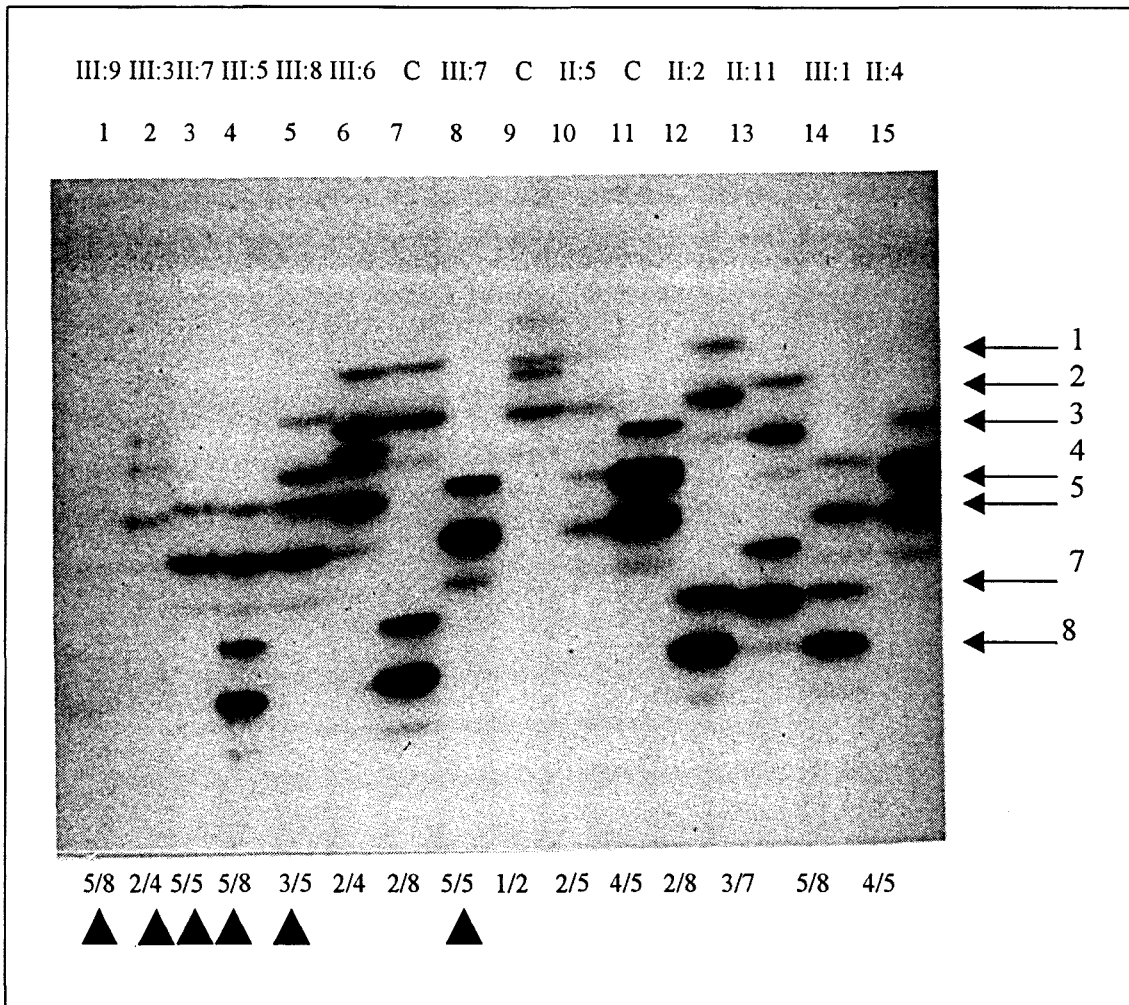


Fig. 3.4.1 Autoradiograph showing alleles of the triplet repeat in atrophin (DRPLA) in pedigree 201 in which FME segregates. Assigned genotypes are indicated below each lane, designated allele numbers are indicated on the right. The individual identity numbers are shown above each lane and the lower arrowheads indicate affected individuals represented in the specific lane.

C = standard sample used to ensure continuity of allele assignment

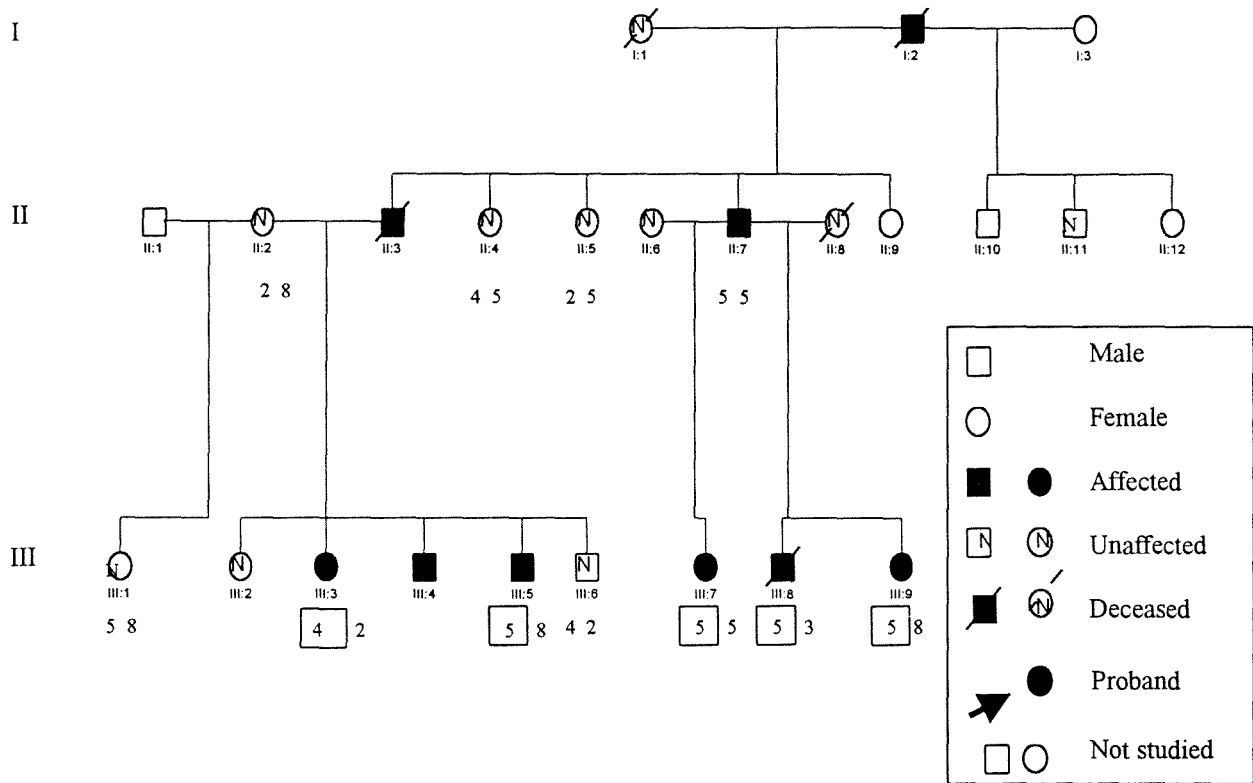


Fig. 3.4.2 Pedigree 201 showing the allelic distribution at the triplet repeat marker in the atrophin gene in those individuals who participated in the linkage study. The individual identity number and assigned genotypes are indicated below each individual. Clinically affected individuals were diagnosed according to the criteria stipulated in section 2.2.1. Where it was possible to deduce, the allele received from the affected parent is boxed.

3.1.3 Haplotype Analysis

Where possible, haplotypes were constructed from the alleles inherited at the *EPM1* and chromosome 8 loci (figures 3.5 and 3.6). The most likely combination of alleles received from each parent was deduced from the available genotypes.

3.1.3.1 Haplotype analysis at the *EPM1* locus

At the *EPM1* locus haplotypes were constructed at *D21S2040/D21S1259/D21S1912* (figure 3.5). The haplotypes of two affected children (III:8 and III:9), of individual II:7 were determined as 2/4/2, no genotype was generated at *D21S1259* for the third affected child (III:7), the haplotype constructed for the latter individual was 2/-/2 (figure 3.5). It is possible that the affected father (II:7), passed the alleles 2/4/2 to his affected children because the phase in the father could also be deduced as 2/4/2. In the other branch of the family, the haplotypes of the affected children of individual II:3 (III:3 and III:5) could be deduced as 2/2/2 and 2/-/6, respectively. The results obtained with the haplotype analysis identified no definitive unique disease-associated haplotype at the *EPM1* locus.

3.1.3.2 Haplotype analysis at the chromosome 8p locus

The construction of haplotypes at the chromosome 8 locus showed that the affected children (III:7, III:8 and III:9) of the affected father (II:7) shared the same haplotype 6/2/4 in the order shown in figure 3.6. This combination of alleles at these three linked markers is also possible in the affected father. In the other branch of the family, the haplotypes of the affected children of individual II:3 were 2/3/4 and 6/3/4 in the order indicated in figure 3.6. Thus, there were no specific disease-associated haplotype shared by all the affected individuals.

3.1.4 Two Point LOD scores

Two point LOD scores were generated using the M-LINK program of the linkage computer package (Lathrop and Lalouel 1984). A LOD score for each marker locus tested was obtained and these are shown in table 3.1; at all three candidate loci tested, significantly negative LOD scores were generated. At the *EPM1* locus, LOD scores of -14.24, -12.83 and -6.82 were generated at the marker loci *D21S2040*, *D21S1259* and *D21S1912*, respectively, at $\theta = 0.00$ (Table 3.1). At the chromosome 8 locus, LOD scores of 0.69, -4.46 and 0.68 were generated at the DNA markers *D8S504*, *D8S264* and *D8S1781*, respectively, at $\theta = 0.00$ (Table 3.1). A LOD score of -14.50 was generated at $\theta = 0.00$, at the DRPLA locus (Table 3.1).

These highly negative LOD scores generated at the tested loci clearly exclude these loci as cause of the disease in pedigree 201.

3.2. NEW AND EXTENDED PEDIGREES

During the course of the study, one new family in whom this form of FME segregates was identified, and was later designated pedigree 202 (figure 3.7). In addition the original family, pedigree 201, was extended (figure 3.8). However, due to time constraints no further analysis was performed in these families during the present study.

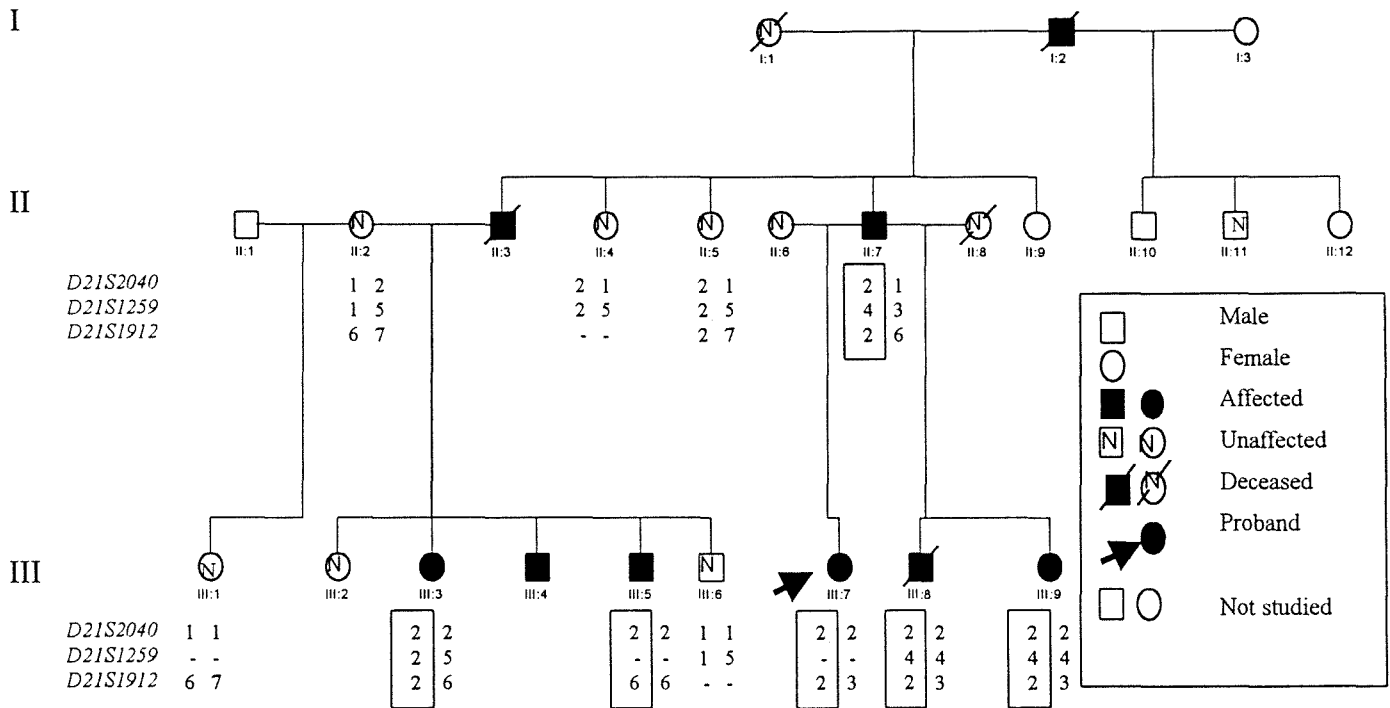


Fig. 3.5 Pedigree 201 showing the haplotypes inherited at the EPM1 locus. Haplotypes are shown below each individual in the order indicated to the left of the pedigree. Clinically affected individuals were diagnosed according to the criteria stipulated in section 2.2.1. The names of the marker loci used in the construction of the haplotype are indicated, to the left of the pedigree, in centromeric-telomeric order, from top to bottom. The most likely haplotypes of the affected individuals are boxed.

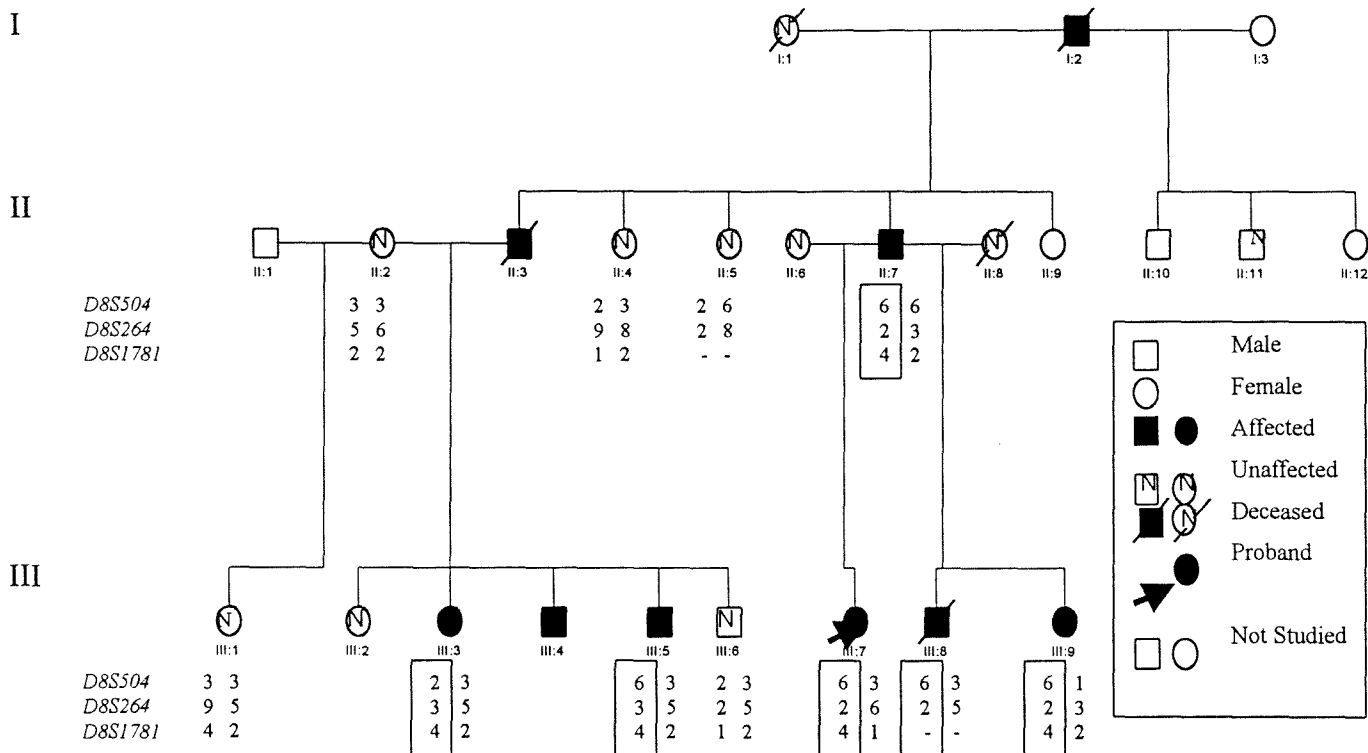


Fig. 3.6 Pedigree 201 showing the haplotypes inherited at the chromosome 8 locus. Haplotypes are shown below each individual in the order indicated to the left of the pedigree. Clinically affected individuals were diagnosed according to the criteria stipulated section 2.2.1. The names of the marker loci used in the construction of the haplotype are indicated, to the left of the pedigree, in telomeric-centromeric order, from top to bottom. The most likely haplotypes of the affected individuals are boxed.

Table 3.1 Pairwise two point LOD scores between FME and the causative loci of the 3 candidate forms of epilepsy, namely EPM1, DRPLA and the chromosome 8p locus.

CANDIDATE LOCI	LOD scores derived at (θ)						
	0.00	0.01	0.05	0.10	0.20	0.30	0.40
<i>Markers</i>	0.00	0.01	0.05	0.10	0.20	0.30	0.40
EPM1							
<i>D21S2040</i>	-14.24	-1.92	-0.65	-0.21	0.06	0.08	0.03
<i>D21S1912</i>	-12.83	-0.94	-0.29	-0.06	0.09	0.09	0.04
<i>D21S1959</i>	-6.82	-0.65	-0.05	0.13	0.18	0.12	0.04
DRPLA							
CAG repeat	-14.50	-4.13	-2.15	-1.32	-0.58	-. 23	-0.05
Chromosome 8p locus							
<i>D8S504</i>	0.69	0.67	0.60	0.51	0.33	0.17	0.04
<i>D8S264</i>	-4.46	-2.02	-0.75	-0.30	-0.01	0.04	0.01
<i>D8S1781</i>	0.68	0.66	0.56	0.45	0.25	0.10	0.02

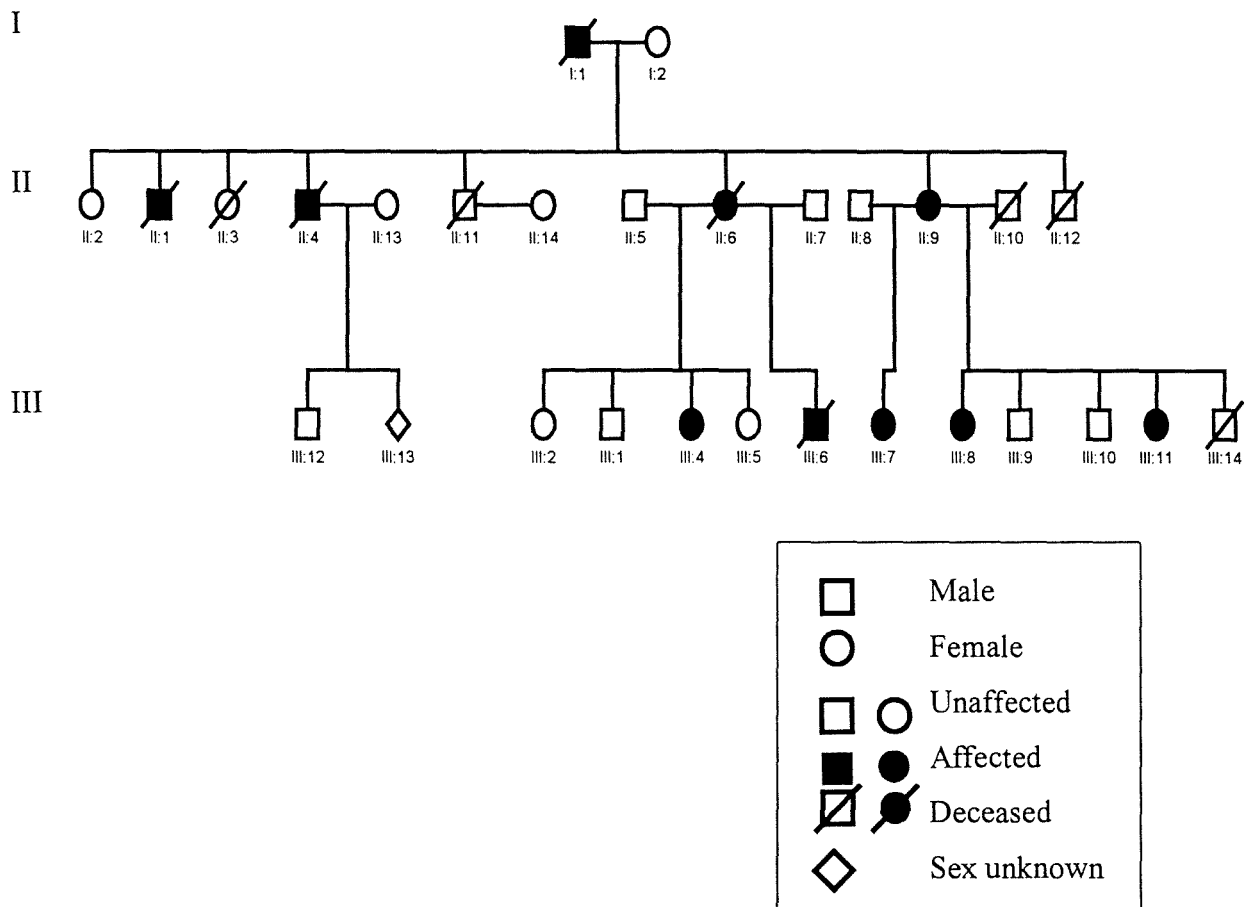


Fig. 3.7 Pedigree 202, the new family identified in whom FME segregates. Clinically affected individuals are diagnosed according to the criteria stipulated in section 2.2.1. Individual identity numbers are shown under each individual.

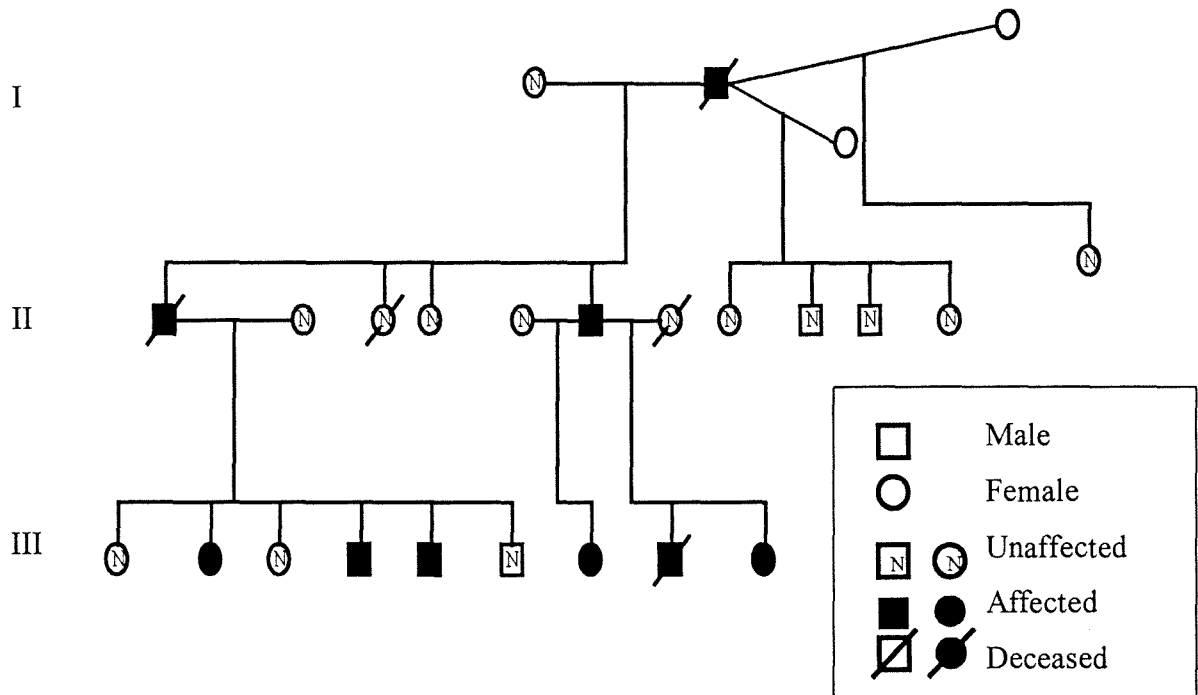


Fig. 3.8 Extended pedigree 201 in whom FME segregates. Clinically affected individuals are diagnosed according to the criteria stipulated in section 2.2.1.

LQTS

3.3. FOUNDER MUTATION SCREENING

As mentioned earlier, all South African families of Afrikaner descent in which LQTS studies were performed previously harboured the same mutation, namely the Ala212Val mutation in the *KVLQT1* gene (de Jager et al., 1996). Consequently, the approach in the present study was to screen for the founder mutation in all new probands referred to our group with the clinical diagnosis of LQTS.

The Ala21Val mutation is situated in the S6-Pore region of the *KVLQT1* gene (figure 1.14), PCR-amplification of this region generated a 160bp product, which was normally cleaved into two fragments of 130bp and 30bp by *HhaI* digestion (figure 3.9a). The presence of a C→A transition at codon 212, in the case of the founder mutation, resulted in the loss of a *HhaI* restriction enzyme site. Consequently, in an individual heterozygous for the founder mutation, three fragments of 160bp, 130bp and 30bp were generated (figure 3.9a).

In a panel of twelve unrelated affected probands tested, the *KVLQT1* Ala212Val mutation was present in four individuals, as is evident by the presence of the three fragments of 160bp, 130bp and 30bp, after *HhaI* digestion of the amplified PCR product (figure 3.9b). In eight of the tested probands, only the 130bp and 30bp fragments were present, indicating the absence of the founder mutation in these individuals (figure 3.9b). A DNA based diagnostic service could be delivered in the four individuals who tested positive for the Ala212Val mutation. Where possible, families were traced using the probands as a reference point, in order to, firstly, deliver a diagnostic service to other family members who choose to have it, if the *KVLQT1* Ala212Val mutation was present in the proband. Secondly, pedigrees were constructed to provide the means to perform linkage analysis at four of the known LQTS loci to determine the disease-causing locus in the remaining probands, in whom the Ala212Val mutation was absent.

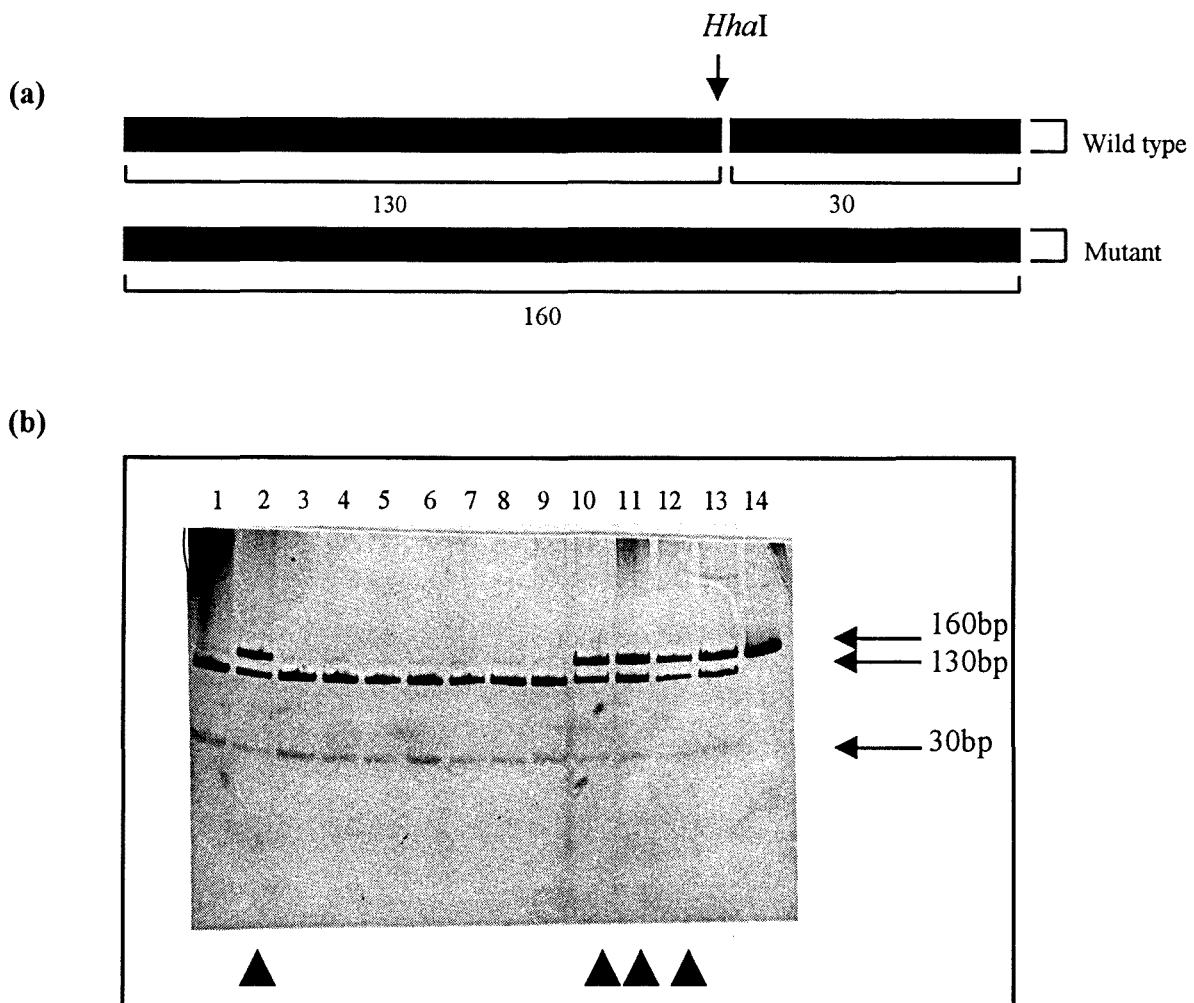


Fig. 3.9 Founder mutation screening by ASREA in a panel of unrelated affected individuals.

- a) Diagrammatic representation of a *HhaI* restriction enzyme map of the S6-Pore region of *KVLQTI* showing the wild type and mutant expected fragment sizes in bp after restriction enzyme digestion.
- b) Panel of 12 probands tested for the *KVLQTI* Ala212val mutation with ASREA. Lanes 1-12 contain the *HhaI* digested amplified S6-Pore region of twelve LQTS-affected probands, lane 13 the positive control, *HhaI* digested S6 region of a LQTS affected individual carrying the *KVLQTI* Ala212Val mutation. Lane 14: an undigested amplified S6 region of *KVLQTI*. Individuals represented in lanes 2, 10, 11 and 12, indicated by the arrows below, carry the Ala212Val mutation, as is evident by the presence of the three fragments of 160bp, 130bp and 30bp indicated by the arrows on the right. In individuals represented in lane 1, and lanes 3-9, the Ala212Val mutation was absent, as indicated by the presence of 2 fragments of 130bp and 30bp.

3.4. LINKAGE ANALYSIS STUDY

3.4.1 Family Study

Three pedigrees were constructed by tracing and contacting family members from the panel of affected probands. The families were of three different population groups residing in South Africa, namely, Mixed ancestry, Afrikaner and Indian descent. The pedigrees that were subsequently constructed were designated pedigrees 167, 168 and 169 respectively (figures 3.10.1-3.10.3). The QTc measurements, an important criterion in the diagnosis of LQTS, are indicated on the family trees in figure 3.10.1-3.10.3. In figure 3.10.1 the exact QTc values of only a few members were available, and the clinical data for the rest of the family only indicated the disease status of the individuals as affected, unaffected or equivocal.

In pedigree 167, 25 individuals were genotyped, of whom four were affected and 21 were unaffected (figure 3.10.1). In pedigree 168, six individuals were genotyped, of whom two were affected and four were unaffected (figure 3.10.2). In pedigree 169, fourteen individuals were genotyped, of whom four were affected and four unaffected, the remaining six were clinically equivocal (figure 3.10.3).

3.4.2 Genotypic Analysis

3.4.2.1 Mutation screening for the *KVLQT1* Ala212Val mutation

In the three LQTS pedigrees constructed, mutation screening employing ASREA was performed to screen for the *KVLQT1* Ala212Val mutation, to deliver a DNA-based diagnostic service in the remaining family members in the case where the Ala212Val was present in the proband. Screening for the Ala212Val mutation was also performed in the families in whom the Ala212Val mutation was absent in the proband, in order to confirm that this mutation was not responsible for the disease in any of the other family members.

In pedigree 167, the *KVLQT1* Ala212Val mutation was absent in all affected members of this family confirming the result obtained with the proband in whom the mutation was also absent (figure 3.11.1). In pedigree 168 of Afrikaner descent, the *KVLQT1* Ala212Val mutation was present in the proband, as well as one other affected member. Three fragments of 160bp, 130 and 30bp were present in clinically affected members of the family after digestion of the amplified S6 region with *HhaI*, however, only the two fragments of 130bp and 30 bp were present in clinically unaffected individuals (figure 3.11.2). In pedigree 169 of Indian descent

the Ala212Val mutation was absent in the proband, as well as the other affected members later screened to confirm the latter result (results not shown).

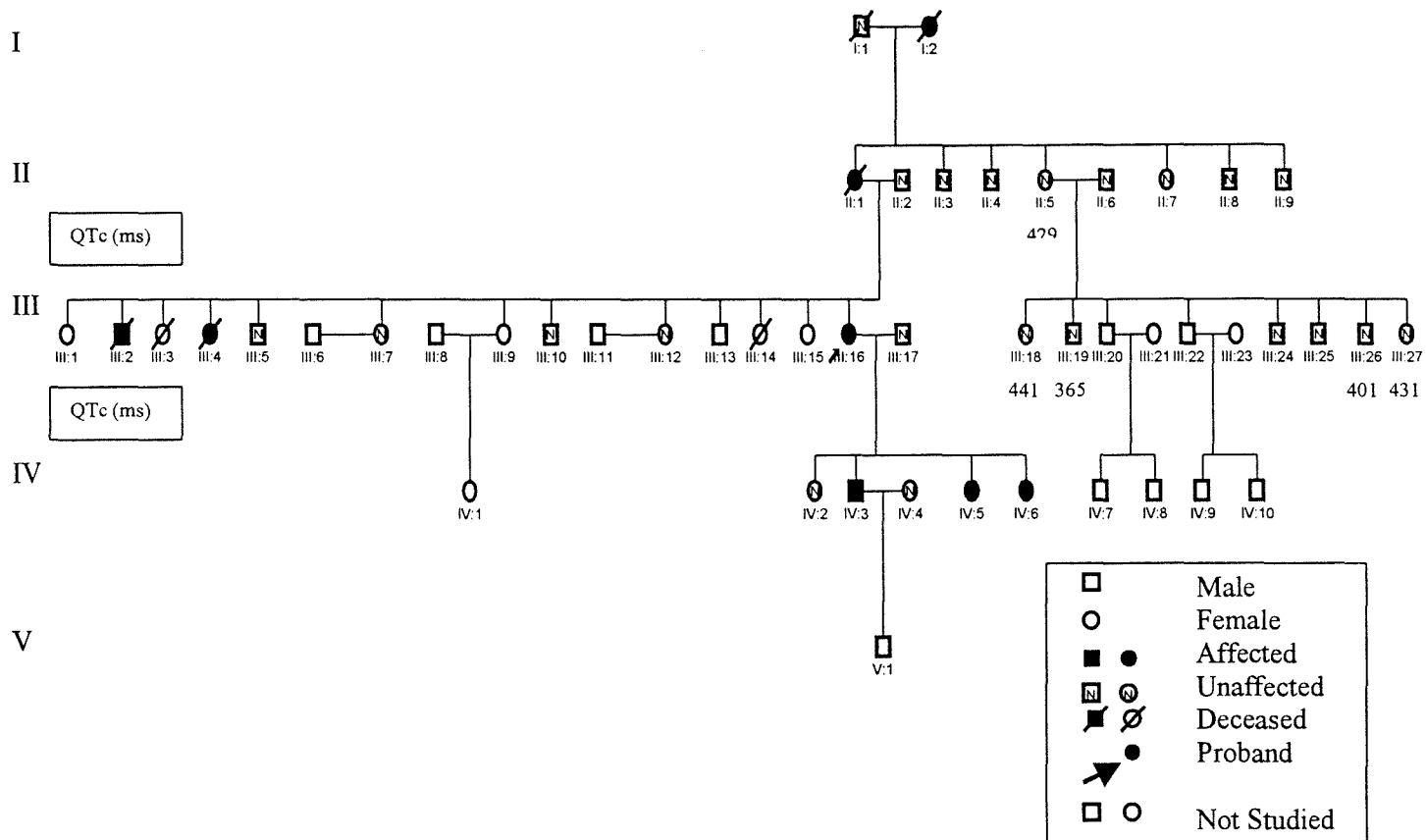


Fig. 3.10.1 Pedigree 167 of Mixed Ancestry in which the autosomal dominant form of LQTS segregates. QTc values in the individuals who participated in the linkage analysis study are indicated below each individual. Clinically affected individuals were diagnosed according to the criteria stipulated in section 2 2.2. Individual identity numbers are shown under each individual, these numbers will be used to refer to the study subjects in further analysis.

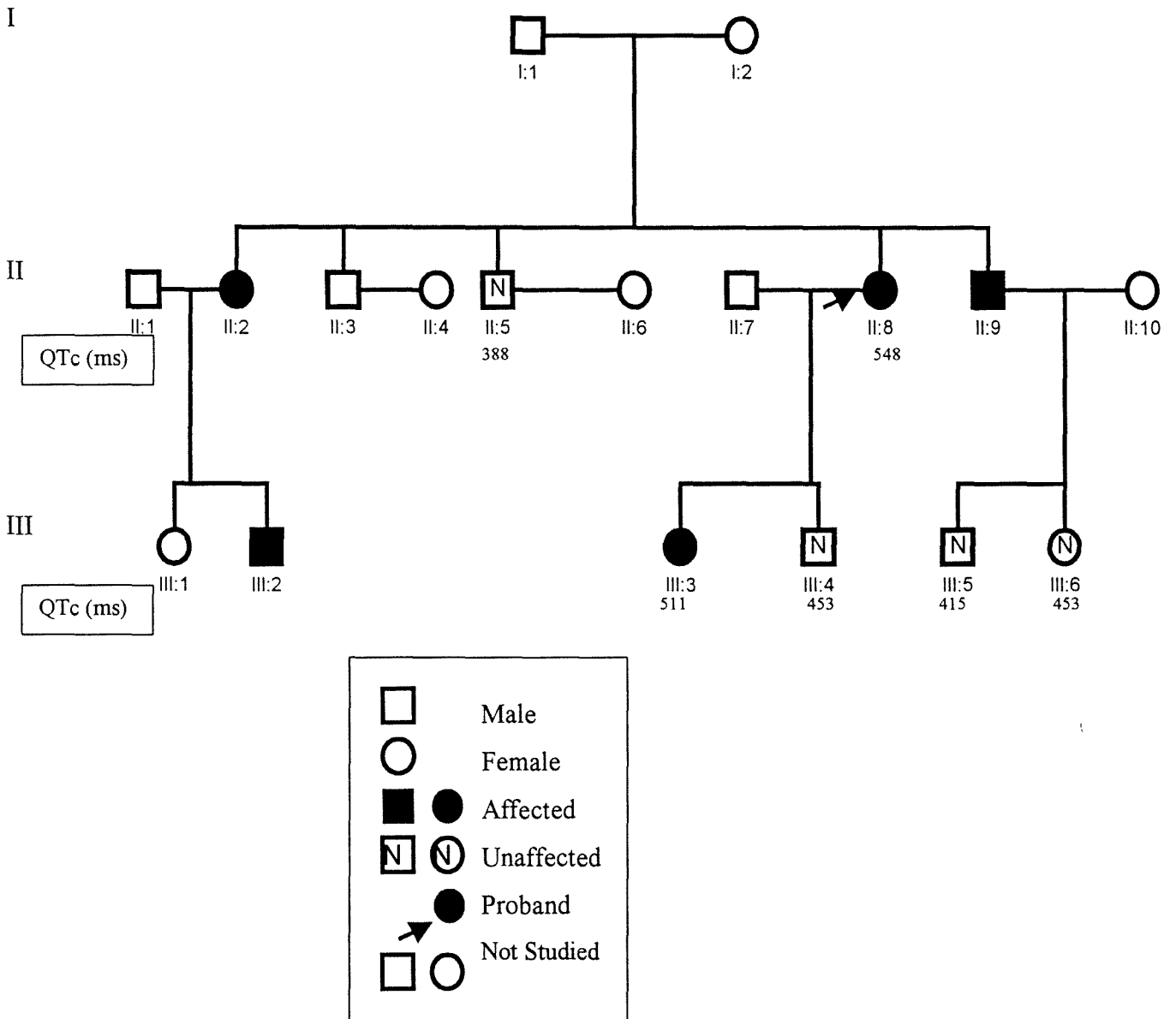


Fig. 3.10.2 Pedigree 168 of Afrikaner descent in which the autosomal dominant form of LQTS segregates. QTc values in the individuals who participated in the linkage analysis study are indicated below each individual. Clinically affected individuals were diagnosed according to the criteria stipulated in section 2 2.2.

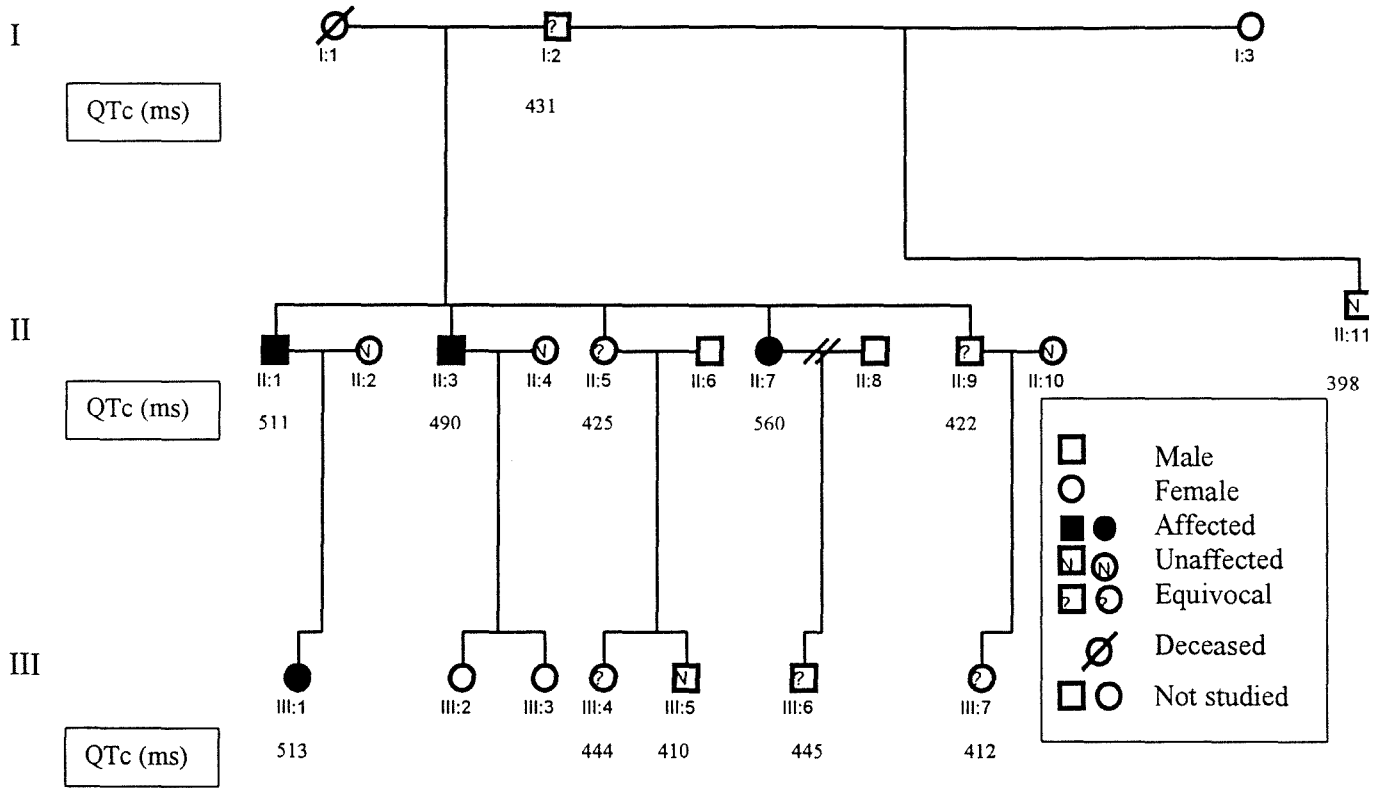


Fig. 3.10.3 Pedigree 169 of Indian descent in which the autosomal dominant form of LQTS segregates. QTc values in the individuals who participated in the linkage analysis study is indicated below each individual. Clinically affected individuals were diagnosed according to the criteria stipulated in section 2 2.2. Individual identity numbers are shown under each individual, these numbers will be used to refer to the study subjects in further analysis.

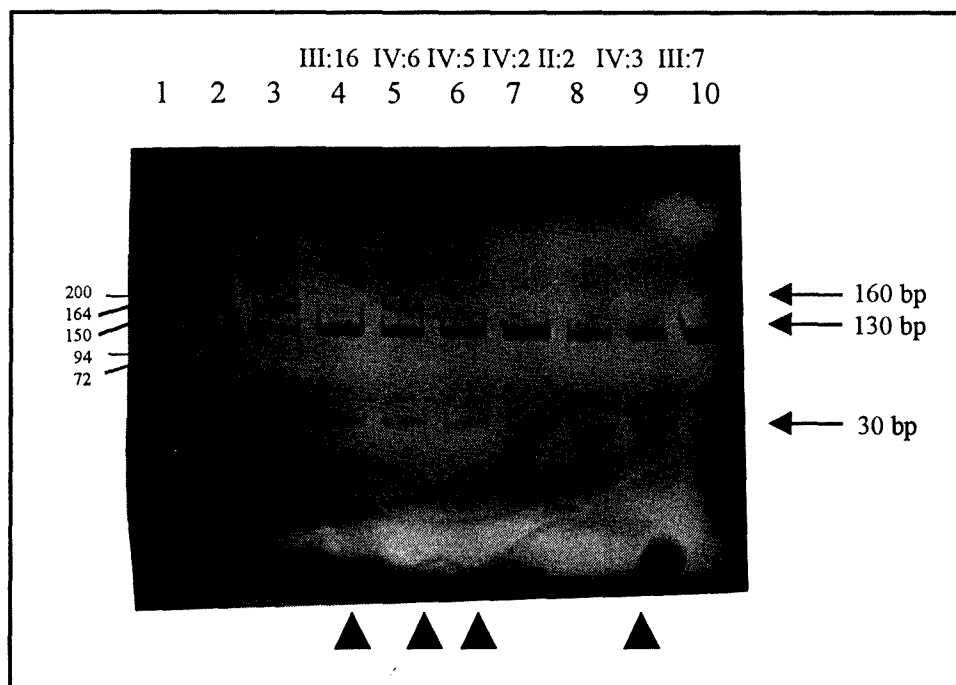


Fig. 3.11.1 Founder mutation screening by ASREA in pedigree 167. Silver stained polyacrylamide gel of the PCR-amplified S6-Pore region of *KVLQT1* digested with *HhaI*. Lane 1 = lambda *PstI* size marker; lane 2 = undigested amplified S6-Pore region of *KVLQT1*; lane 3 = positive control; lane 4-10 = *HhaI* digested amplified S6-Pore region of clinically affected and unaffected members of pedigree 167. Arrows below indicate the clinically affected individuals and arrows on the right indicate the size of the fragments in bp.

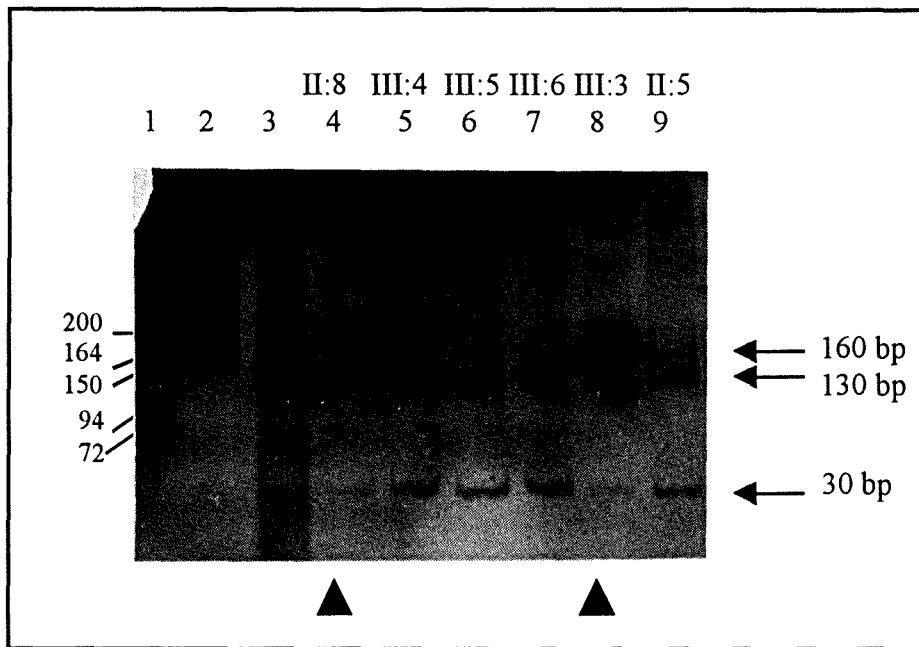


Fig. 3.11.2 Founder mutation screening by ASREA in pedigree 168. Silver stained polyacrylamide gel of the PCR-amplified S6-Pore region of *KVLQT1* digested with *HhaI*. Lane 1 = lambda *PstI* size marker; lane 2 = undigested amplified S6-Pore region of *KVLQT1*; lane 3 = positive control; lane 4-9 = *HhaI* digested amplified S6-Pore region of clinically affected and unaffected members of pedigree 168. Arrows below indicate the clinically affected individuals and arrows on the right indicate the size of the fragments in bp.

3.4.2.2 Genotypic Analysis employing DNA markers at four of the known LQTS loci

The disease-causing locus in pedigree 168 was identified as *KVLQT1* by genotypic analysis for the founder mutation employing ASREA (figure 3.11.2). However, in the other two pedigrees the disease-causing locus remained to be elucidated. Consequently, due to genetic heterogeneity seen in LQTS, four of the known loci, accounting for almost 90% of the known cases of LQTS, were analyzed by linkage analysis.

3.4.2.2.1 *KVLQT1* locus

The fact that the Ala212Val mutation in the *KVLQT1* gene was absent in pedigree 167 and 169 does not exclude this candidate locus from being responsible for causing LQTS in these families, as other mutations in this gene may be present. Thus, linkage analysis was performed, with markers at this locus to determine if further mutation screening of *KVLQT1* was appropriate. To this end, this locus was genotyped employing five polymorphic DNA markers; *TH*, *DIIS1318*, *DIIS860*, *DIIS1323* and *DIIS1331* in both these families (figure 3.12.1-3.12.5 and 3.13.1-3.13.5). Representative inheritance patterns for the alleles at each of these loci are shown in subsets of pedigree 167 (figures 3.12.1-3.12.5) and subsets of pedigree 169 (figures 3.13.1-3.13.5).

Analyzing the genotypes derived at marker locus *TH* in pedigree 167 showed that affected individuals were homozygous for allele 4. However this genotype was also seen in two unaffected individuals, (III:7 and III:12; lanes 7 and 9) (figure 3.12.1). Allele 10 segregated with the disease in the four affected individuals, as well as in two unaffected individuals (III:7 and III:12; lanes 2 and 4) at marker locus *DIIS1318* (figure 3.12.2). At *DIIS860* the genotypes of the affected individuals were 2/5, 2/4, 2/4 and 2/4, the two unaffected individuals (III:7 and III:12 lanes 2 and 4) were homozygous for allele 2 (figure 3.12.3). The genotype of the unaffected father in generation two, was 2/5, but the result was generated on an autoradiograph other than the one shown in figure 3.12.3 (result not shown). Given the genotype of the father and the children in generation three, it is possible to hypothesize that the mother's genotype was 2/2 (figure 3.12.3). Allele 2 was present in all affected individuals, however this allele was also seen in unaffected individuals, consistent with allele being present in both parents. All affected individuals, as well as two unaffected individuals (II:3 and III:10, lanes 1 and 16), were homozygous for allele 3 at *DIIS1323* (figure 3.12.4). Three of the affected individuals were homozygous for allele 2 at the *DIIS1331* DNA marker and the remaining one's genotype was 2/5. Although allele 2 was present in all affected individuals,

this allele was also seen in unaffected individuals who were heterozygous at this locus (IV:2, V:1 and II:8, lanes 8, 9 and 16). Thus, in summary, in pedigree 167 at three of the tested loci (*TH*, *DIIS1318* and *DIIS860*) at the *KVLQT1* locus, alleles were shown to segregate with the disease in all affected members, however, these alleles were also present in the same two unaffected members (II:7 and III:12) in each case. At the remaining two loci (*DIIS1323* and *DIIS1331*) all the affected also showed a specific allele that was present in all affected individuals; however, this alleles was also present in other unaffected individuals.

In pedigree 169 no correlation was seen between the genotypes generated at the five tested loci and the affected status of the study subjects. Analysing the *TH* locus showed that all affected individuals had the genotype 2/3, however, this genotype was also seen in one equivocal individual (II:5, lane 6) and one unaffected individual (III:5, lane 13) (figure 3.13.1). At the *DIIS1318* locus the genotypes of the affected individuals was 3/6, 3/7, 1/7 and 3/6, thus no unique disease-associated allele was present at this locus in this specific family (figure 3.13.2). At the *DIIS860* locus, three affected individuals were homozygous for allele 2, the fourth affected member's genotype was 2/4, however, these genotypes were also present in unaffected members of this family (figure 3.13.3). Three of the affected family members were homozygous for allele 3 at the *DIIS1323* marker locus and the remaining one's genotype was 3/4. Although allele 3 is seen in all affected members, this allele was also present in unaffected family members (figure 3.13.4). The genotypes of the affected family members at DNA marker *DIIS1331* were 4/4, 1/4, 1/4 and 4/4. Allele 4 was present in all affected members, however, it does not segregate with the disease as this allele was also seen in unaffected individuals. It was clear from the results obtained at the tested marker loci that there were no specific allele at these marker loci that was solely present in the affected individuals and thus could be segregating with the disease in this family.

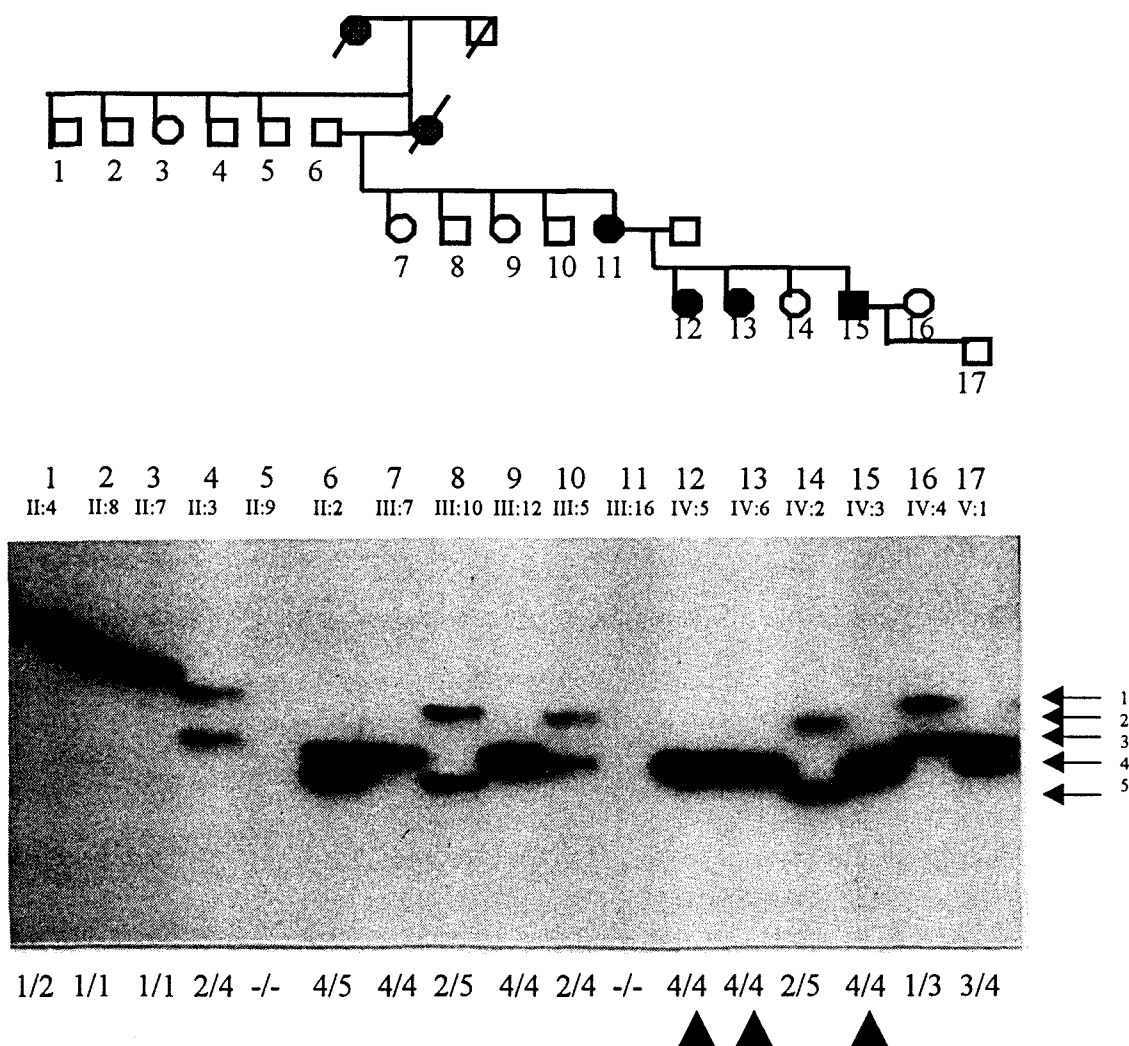


Fig. 3.12.1 Autoradiograph showing alleles at the DNA marker *TH* in pedigree 167. Assigned genotypes are indicated below each lane, designated allele numbers are shown on the right. The number shown below each individual in the pedigree above the autoradiograph corresponds to the lane number in which it is represented. The lower arrowheads indicate affected individuals represented in the specific lane. (Note: representation of pedigree structure has been modified to correspond with lane order).

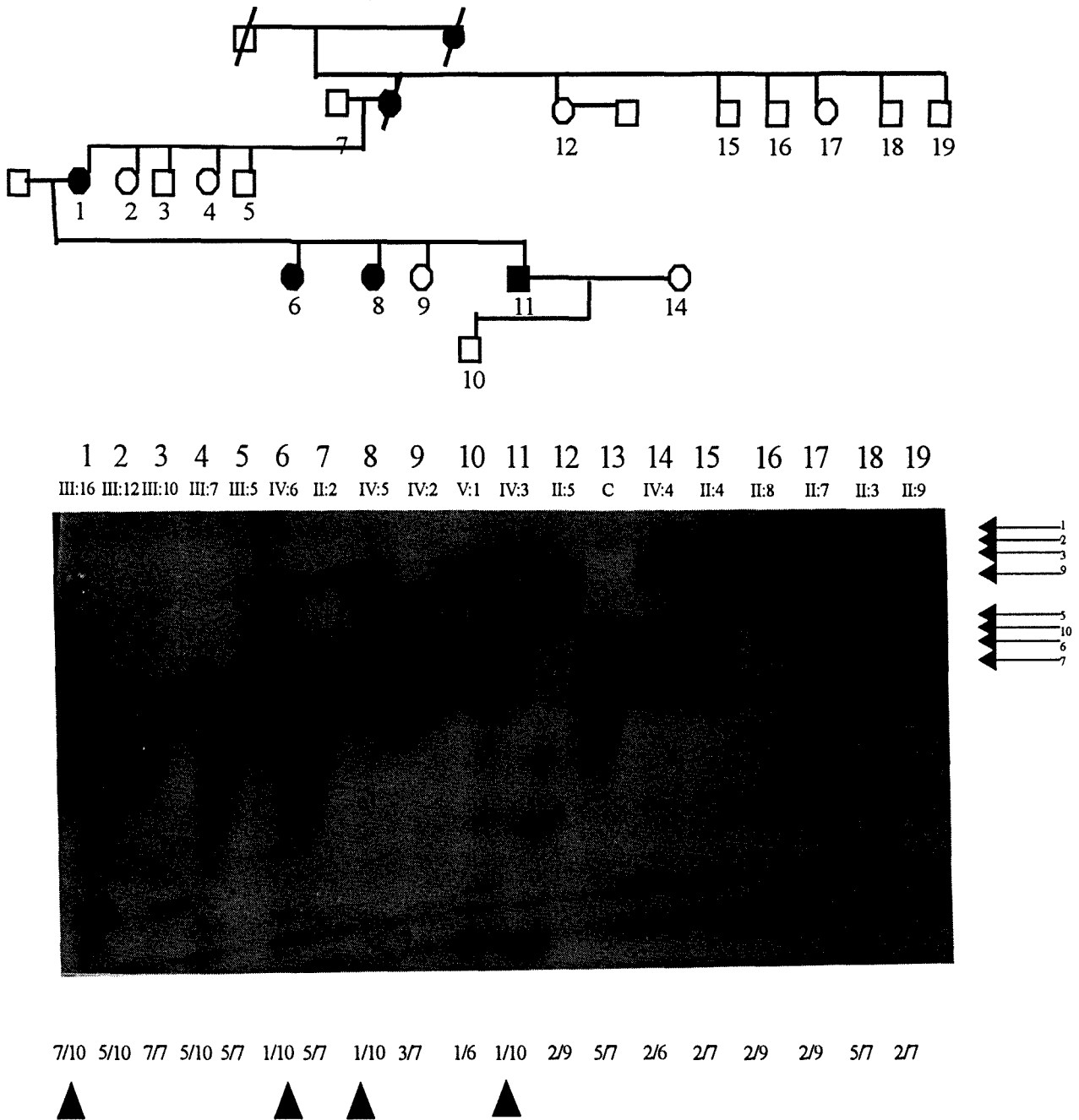


Fig. 3.12.2 Autoradiograph showing alleles at the DNA marker *D11S1318* in pedigree 167. Assigned genotypes are indicated below each lane, designated allele numbers are shown on the right. The number shown below each individual in the pedigree above the autoradiograph corresponds to the lane number in which it is represented. The lower arrowheads indicate affected individuals represented in the specific lane. The allele numbers are not in complete descending order as allele 9 and 10 were identified after assignment of the other alleles. (Note: representation of pedigree structure has been modified to correspond with lane order).

C = standard sample used to ensure continuity of allele assignment

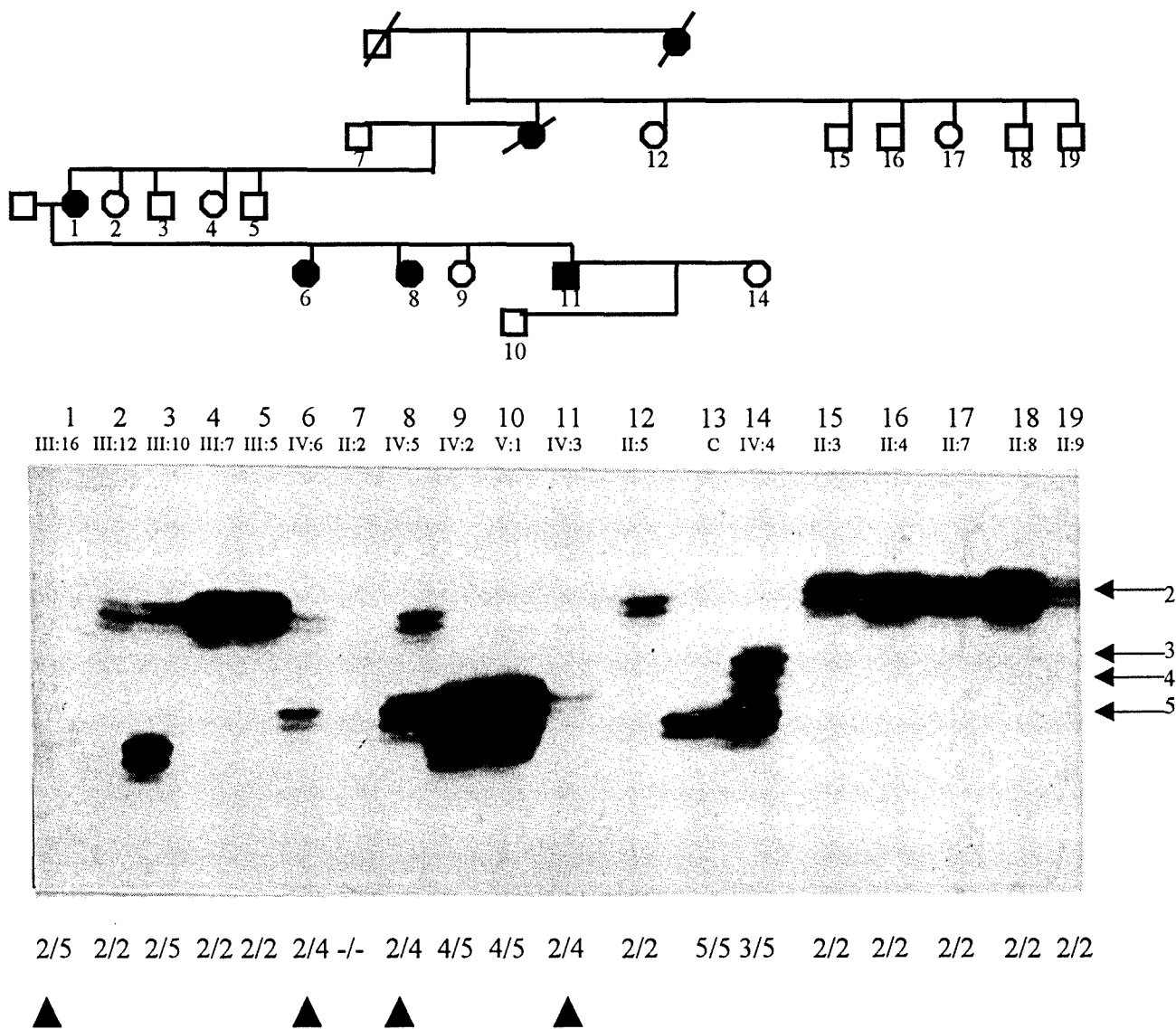


Fig. 3.12.3 Autoradiograph showing alleles at the DNA marker *D11S860* in pedigree 167. Assigned genotypes are indicated below each lane, designated allele numbers are shown on the right. The number shown below each individual in the pedigree above the autoradiograph corresponds to the lane number in which it is represented. The lower arrowheads indicate affected individuals represented in the specific lane. (Note: representation of pedigree structure has been modified to correspond with lane order).

C = standard sample used to ensure continuity of allele assignment

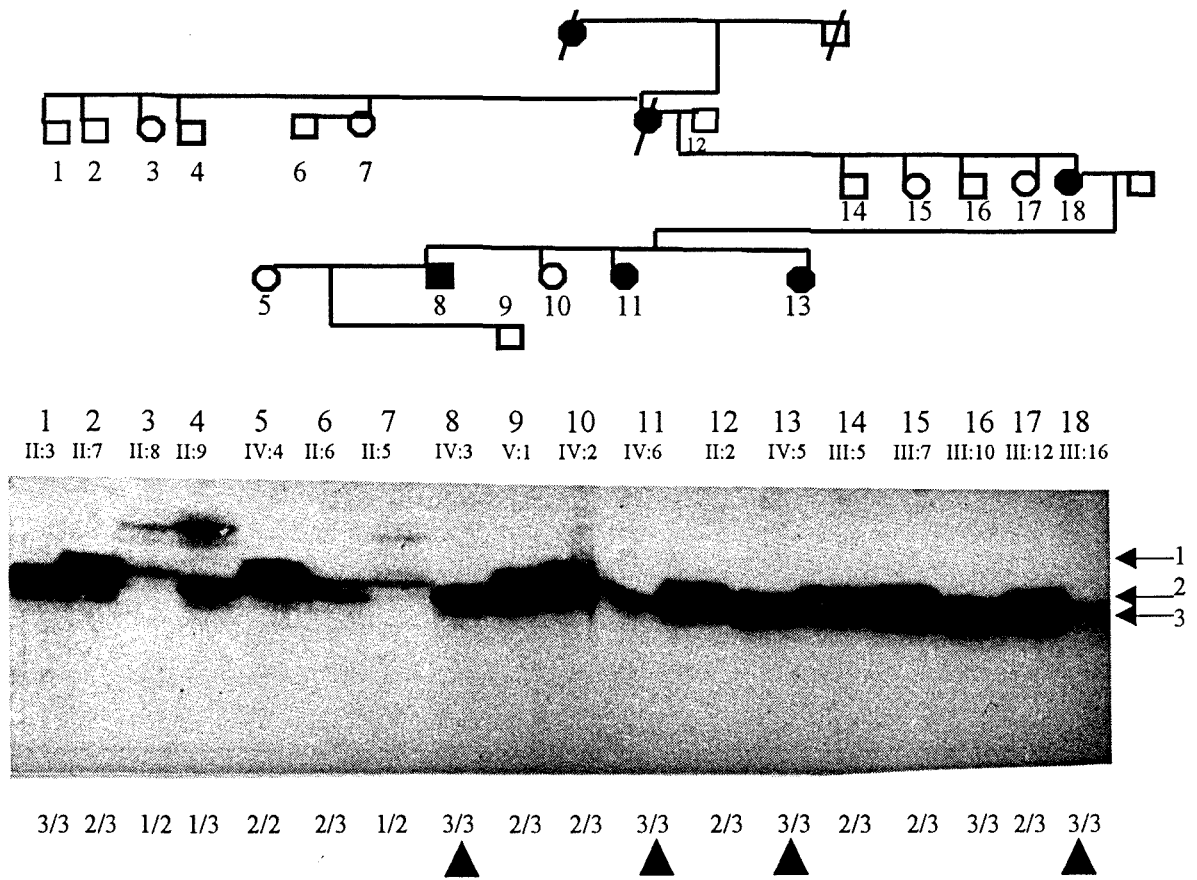


Fig. 3.12.4 Autoradiograph of a polyacrylamide gel showing alleles at the DNA marker *D11S1323* in pedigree 167. Assigned genotypes are indicated below each lane, designated allele numbers are shown on the right. The number shown below each individual in the pedigree above the autoradiograph corresponds to the lane number in which it is represented. The lower arrowheads indicate affected individuals represented in the specific lane. (Note: representation of pedigree structure has been modified to correspond with lane order).

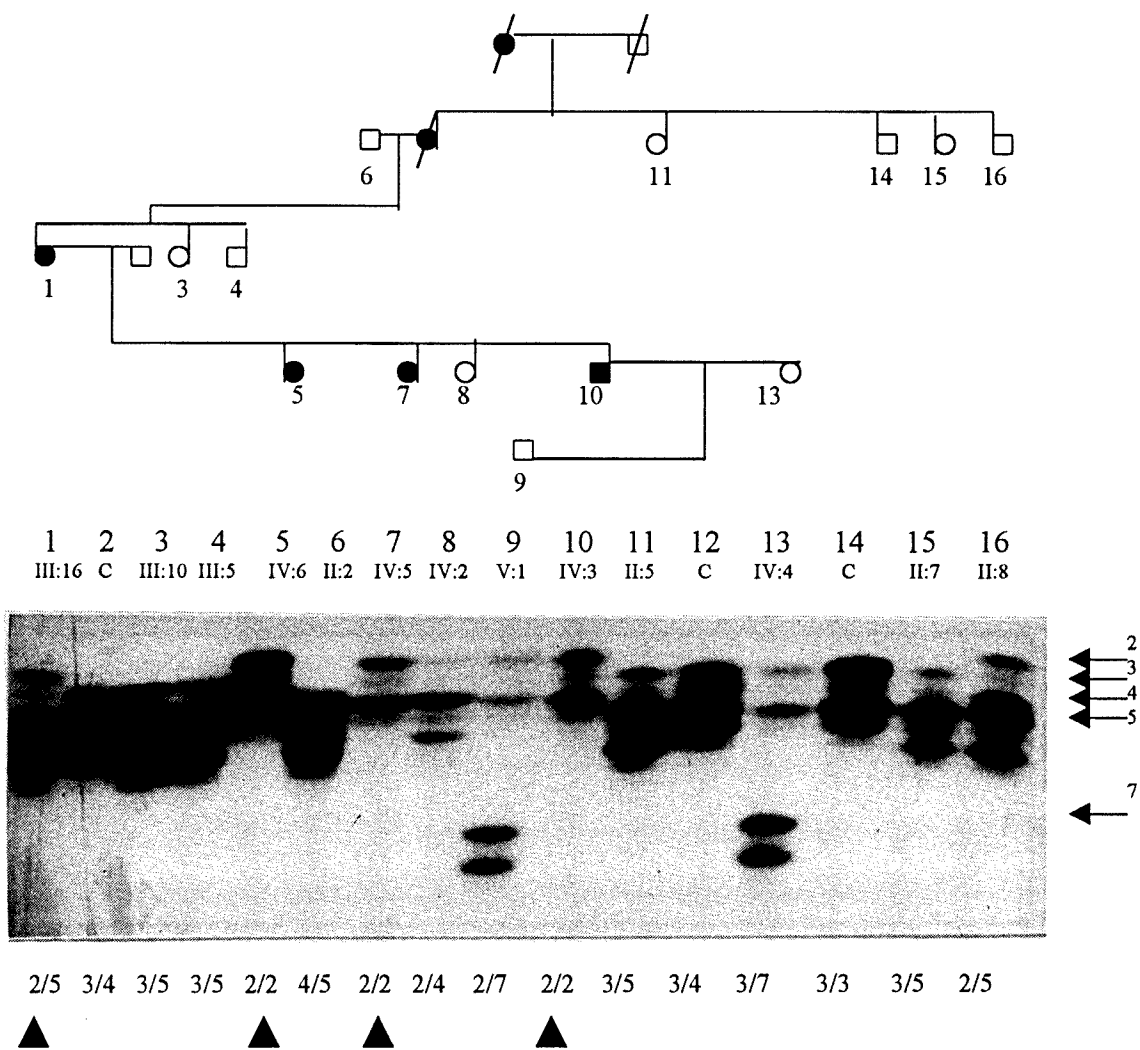


Fig. 3.12.5 Autoradiograph showing alleles at the DNA marker *D11S1331* in pedigree 167. Assigned genotypes are indicated below each lane, designated allele numbers are shown on the right. The number shown below each individual in the pedigree above the autoradiograph corresponds to the lane number in which it is represented. The lower arrowheads indicate affected individuals represented in the specific lane. (Note: representation of pedigree structure has been modified to correspond with lane order).

C = standard sample used to ensure continuity of allele assignment

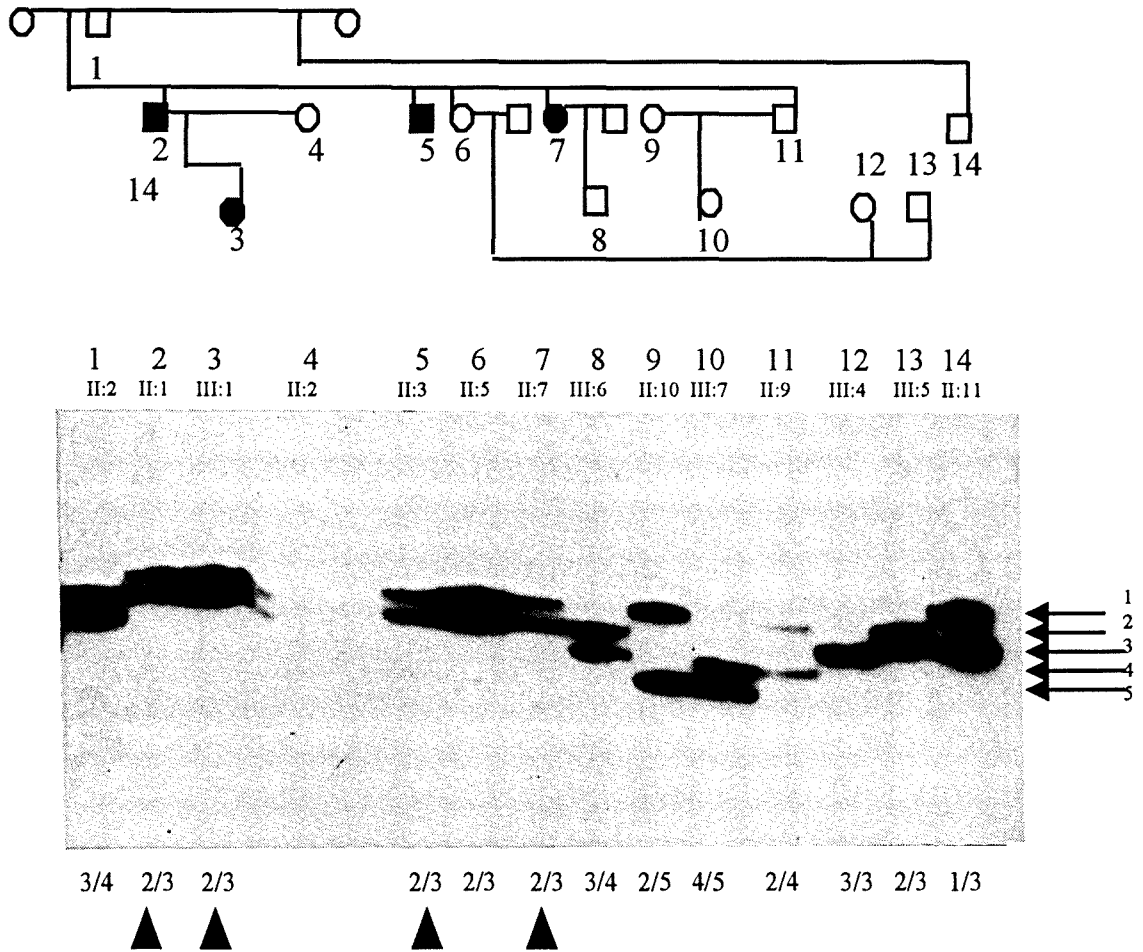


Fig. 3.13.1 Autoradiograph showing alleles at the DNA marker *TH* in pedigree 169. Assigned genotypes are indicated below each lane, designated allele numbers are shown on the right. The number shown below each individual in the pedigree above the autoradiograph corresponds to the lane number in which it is represented. The lower arrowheads indicate affected individuals represented in the specific lane. (Note: representation of pedigree structure has been modified to correspond with lane order).

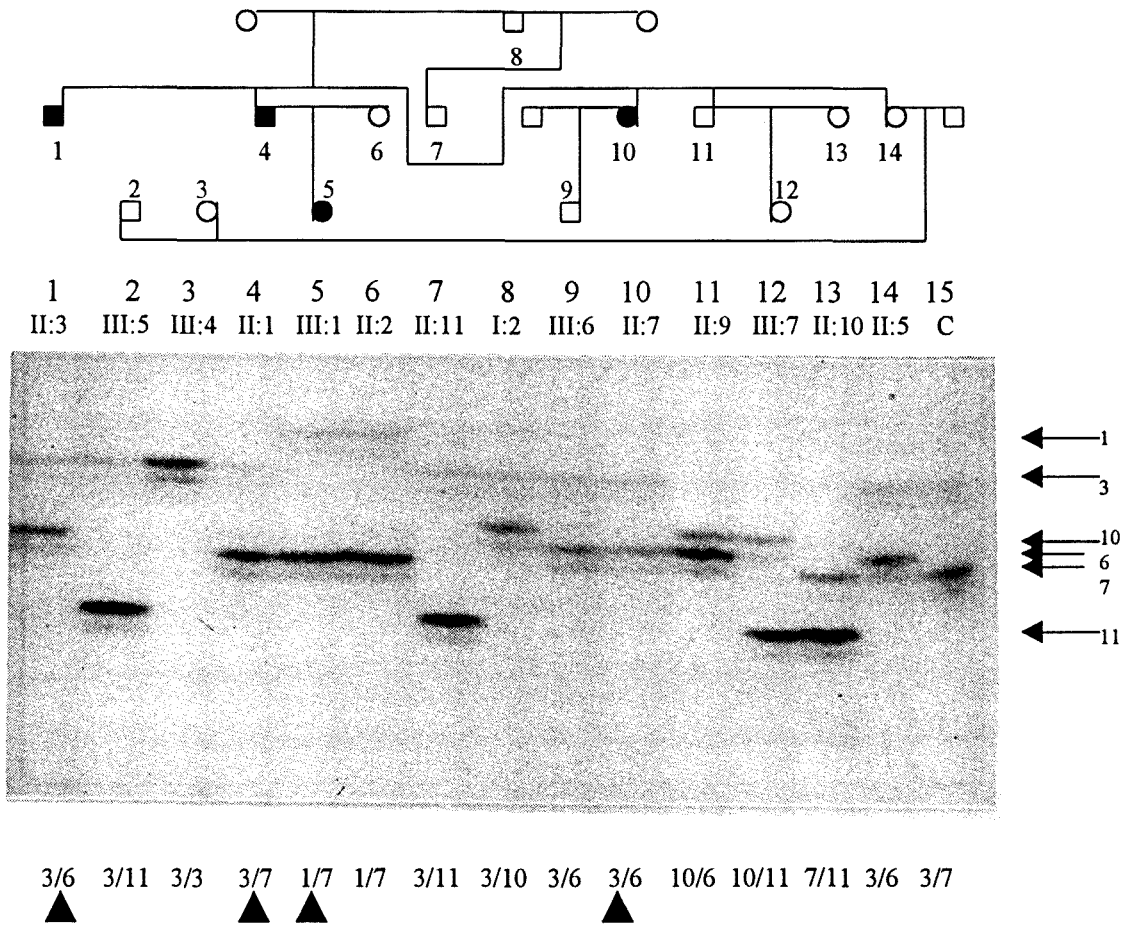


Fig. 3.13.2 Autoradiograph showing alleles at the DNA marker *D11S1318* in pedigree 169. Assigned genotypes are indicated below each lane, designated allele numbers are shown on the right. The number shown below each individual in the pedigree above the autoradiograph corresponds to the lane number in which it is represented. The lower arrowheads indicate affected individuals represented in the specific lane. The allele numbers are not in complete descending order as allele 10 were identified after assignment of the other alleles. (Note: representation of pedigree structure has been modified to correspond with lane order).

C = standard sample used to ensure continuity of allele assignment

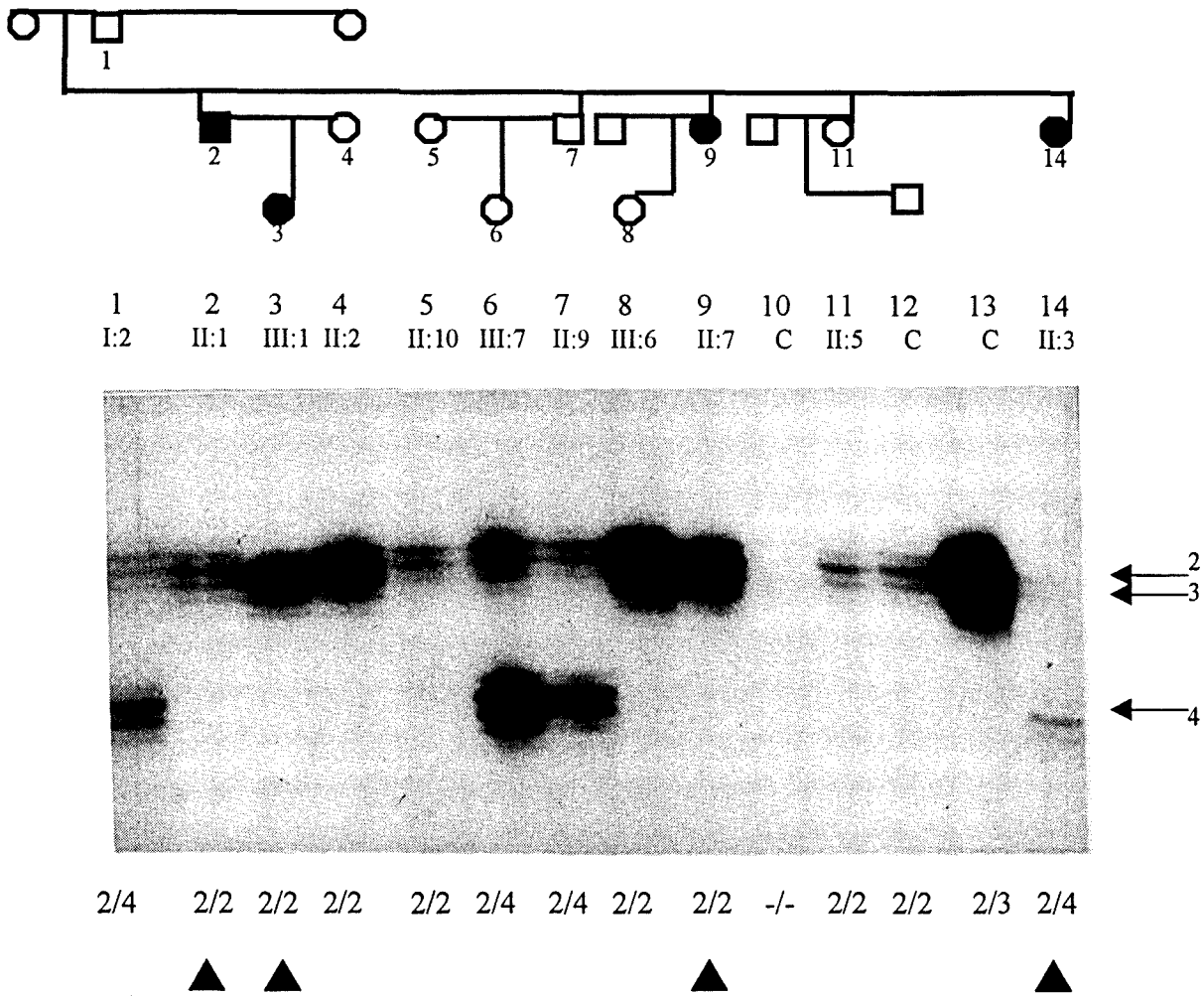


Fig. 3.13.3 Autoradiograph of a polyacrylamide gel showing alleles at the DNA marker *D11S860* in pedigree 169. Assigned genotypes are indicated below each lane, designated allele numbers are shown on the right. The number shown below each individual in the pedigree above the autoradiograph corresponds to the lane number in which it is represented. The lower arrowheads indicate affected individuals represented in the specific lane. (Note: representation of pedigree structure has been modified to correspond with lane order).

C = standard sample used to ensure continuity of allele assignment

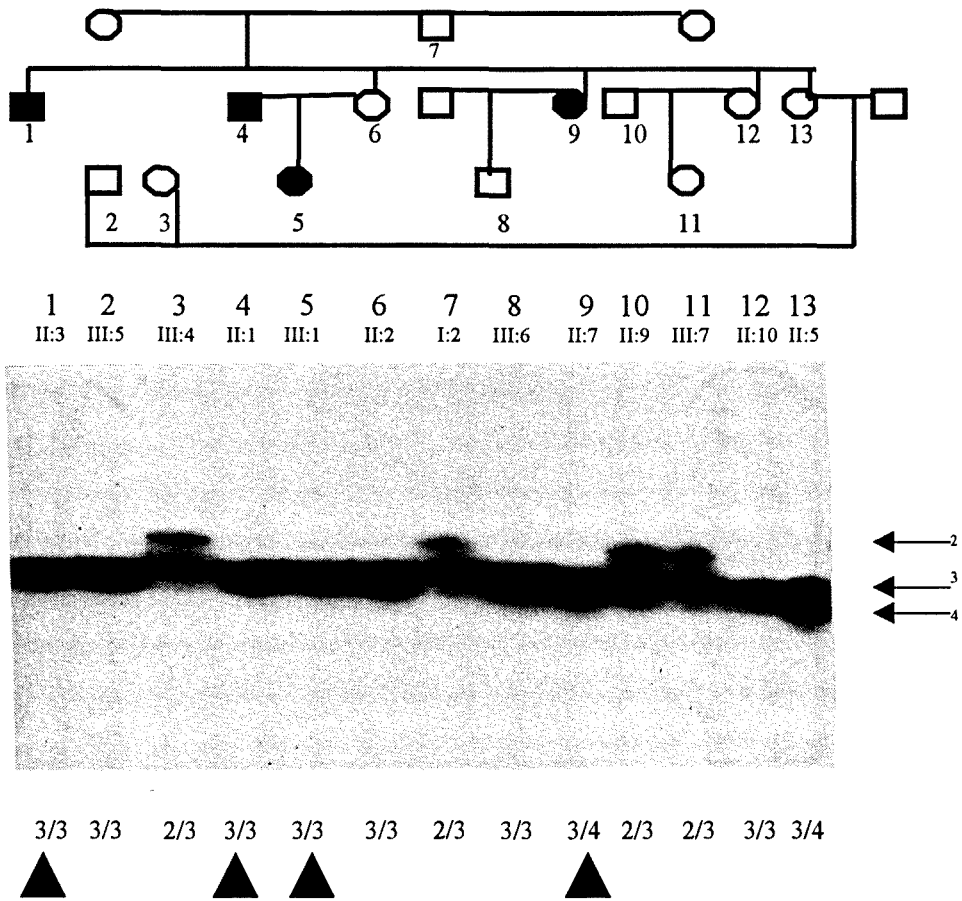


Fig. 3.13.4 Autoradiograph of a polyacrylamide gel showing alleles at the DNA marker *D11S1323* in pedigree 169. Assigned genotypes are indicated below each lane, designated allele numbers are shown on the right. The number shown below each individual in the pedigree above the autoradiograph corresponds to the lane number in which it is represented. The lower arrowheads indicate affected individuals represented in the specific lane. (Note: representation of pedigree structure has been modified to correspond with lane order).

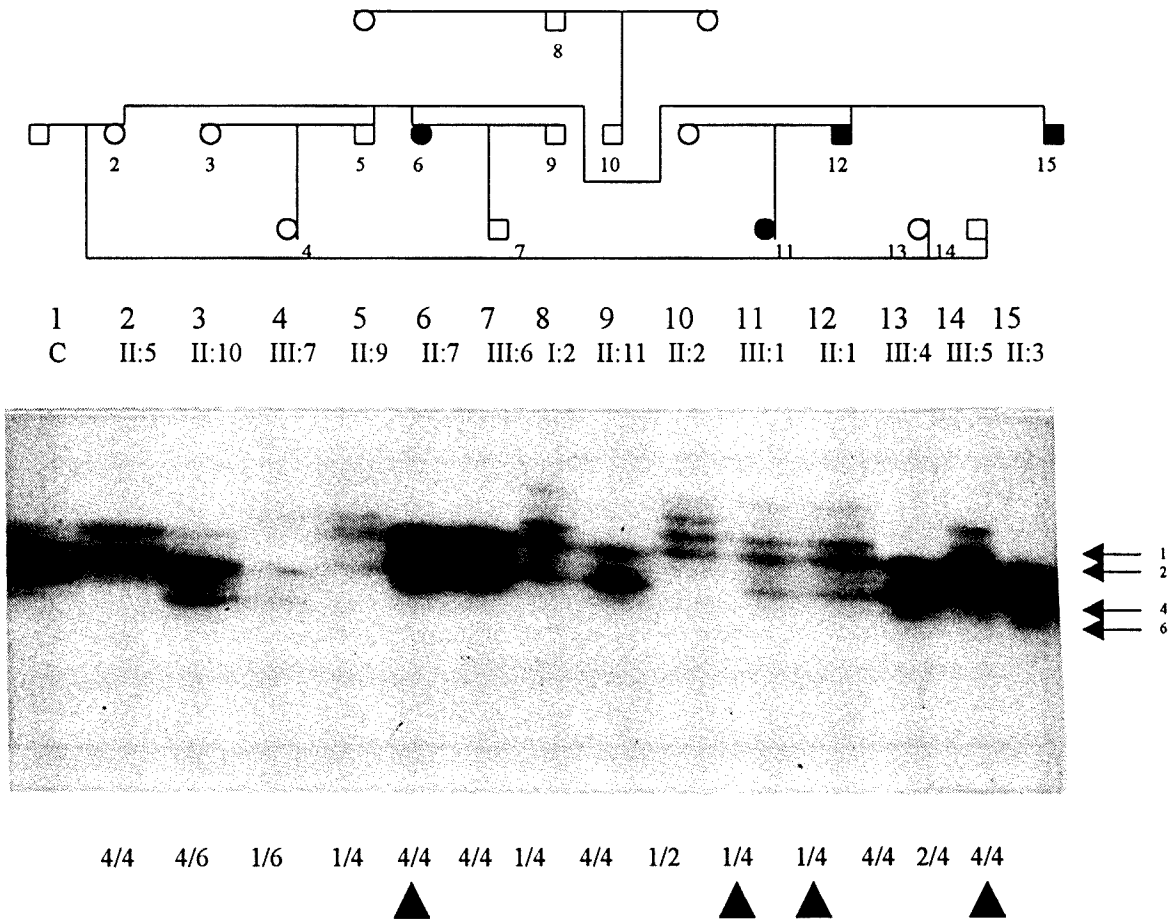


Fig. 3.13.5 Autoradiograph of a polyacrylamide gel showing alleles at the DNA marker *DIIS1331* in pedigree 169. Assigned genotypes are indicated below each lane, designated allele numbers are shown on the right. The number shown below each individual in the pedigree above the autoradiograph corresponds to the lane number in which it is represented. The lower arrowheads indicate affected individuals represented in the specific lane. (Note: representation of pedigree structure has been modified to correspond with lane order).
 C = standard sample used to ensure continuity of allele assignment

3.4.2.2.2 *HERG* locus

The *HERG* locus was genotyped at the single marker locus *D7S636* and the representative inheritance pattern of the alleles at this locus is shown in subsets of pedigree 167 in figure 3.14.1. Individuals III:16, IV:3, IV:5 and IV:6 are the affected individuals in pedigree 167. At *D7S636* the genotypes generated for these individuals are 7/11, 1/11, 7/8 and 8/11. The assigned genotypes are displayed on the pedigree to ascertain Mendelian inheritance; no specific allele segregating with the disease in this family was identified (figure 3.14.2)

The representative inheritance pattern of the alleles at the *D7S636* locus is shown in subsets of pedigree 169 in figure 3.15.1. The affected individuals in pedigree 169 are III:1, II:1, II:7 and II:3, the genotypes generated for these individuals at *D7S636* were 8/9, 4/9, 4/9 and 4/9, respectively (figure 3.15.1). Allele 9 was present in all affected individuals, however, this allele was also present in two equivocal family members (II:5 and III:4). The genotypes generated at *D7S636* in pedigree 169 are displayed on the pedigree to show the allelic distribution of this marker in the family (figure 3.15.2).

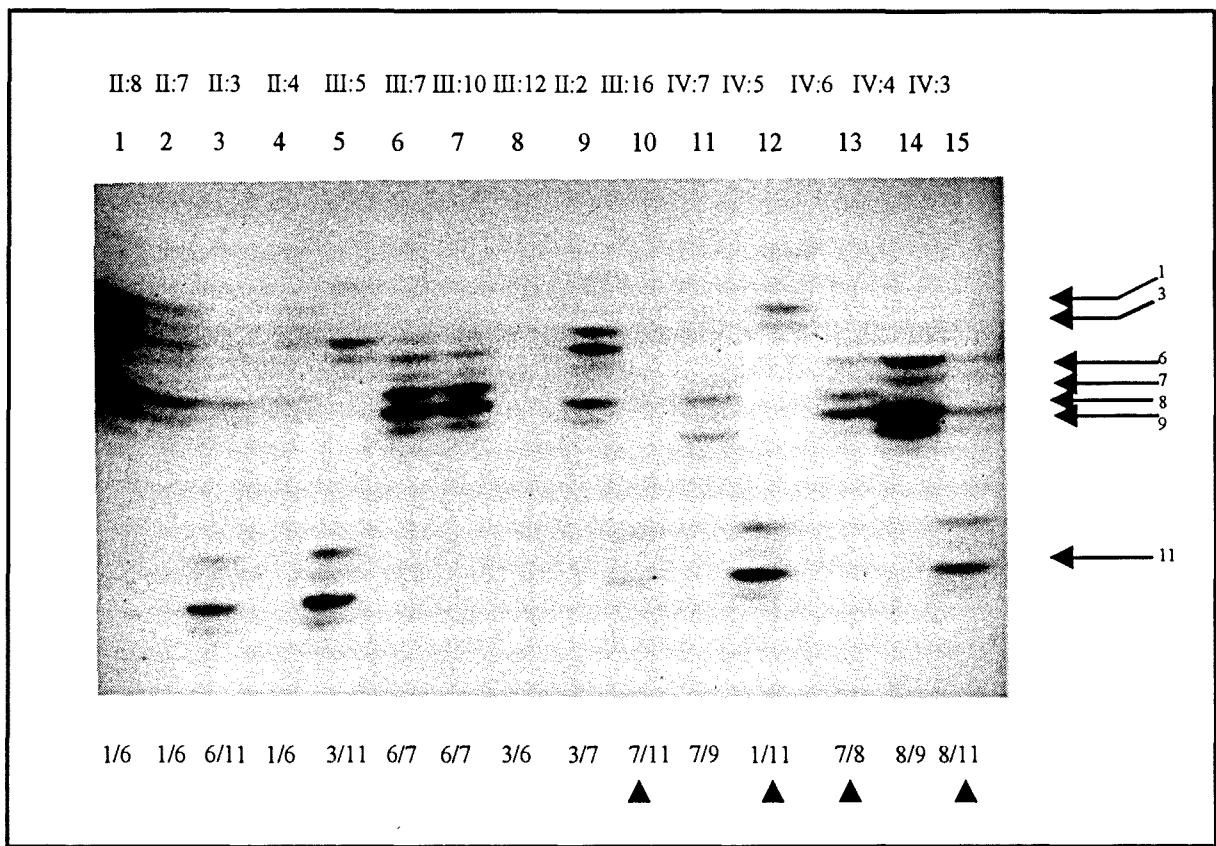


Fig. 3.14.1 Autoradiograph of a polyacrylamide gel showing alleles at the DNA marker *D7S636* in pedigree 167. Assigned genotypes are indicated below each lane, designated allele numbers are shown on the right. The individual identity numbers are indicated above the lane in which it is represented. The lower arrowheads indicate affected individuals represented in the specific lane.

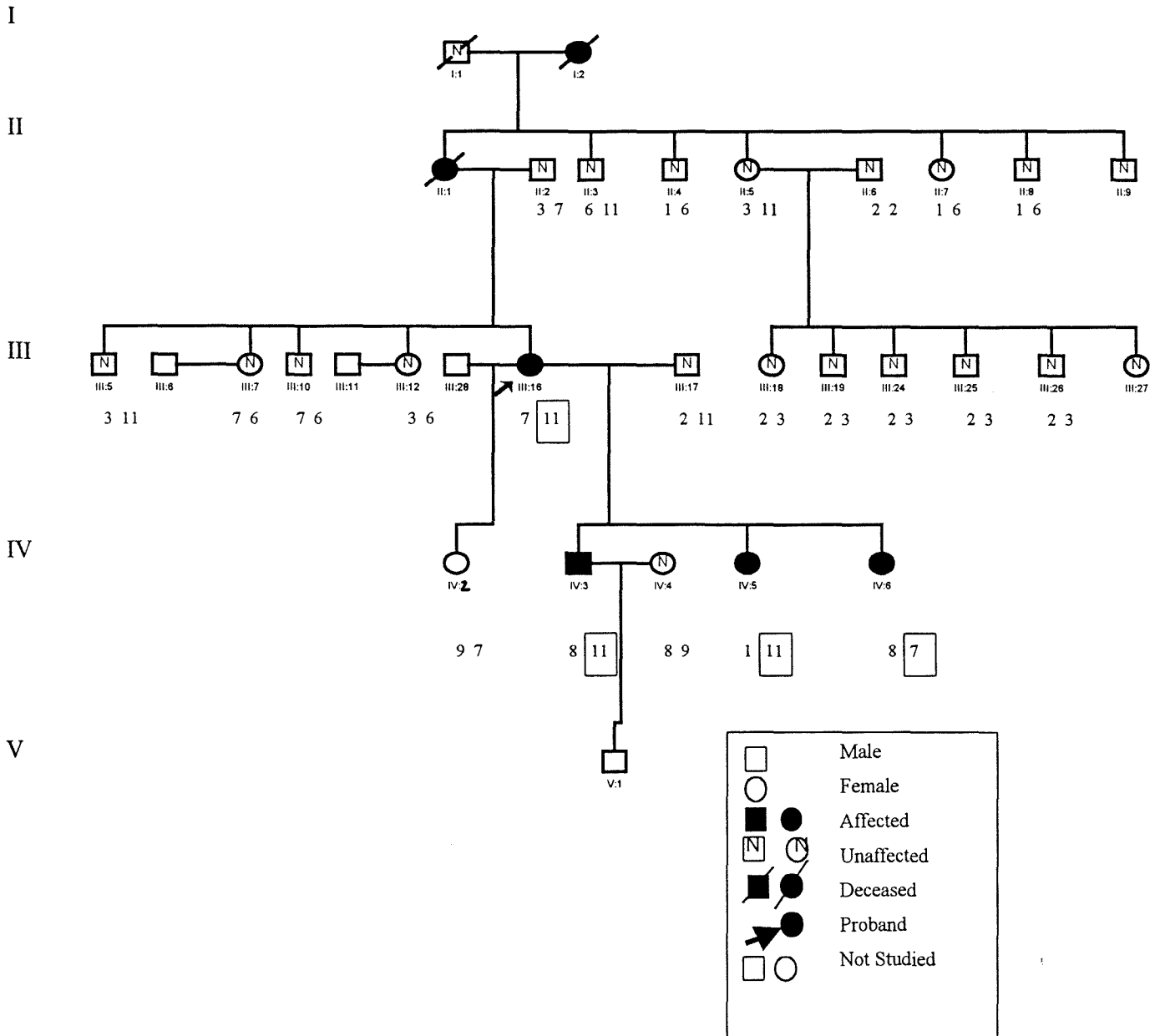


Fig. 3.14.2 Pedigree 167 showing the allelic distribution at the DNA marker *D7S636* in the individuals who participated in the linkage analysis study. The individual identity number and assigned genotypes are indicated below each individual. Where it was possible to deduce, the allele received from the affected parent is boxed. (Note: Pedigree 167 structure was altered for LOD score analysis. Individual III:28 was not studied but is indicated in the pedigree, as genotyping data was inconsistent with individual III:17 being the father of IV:2).

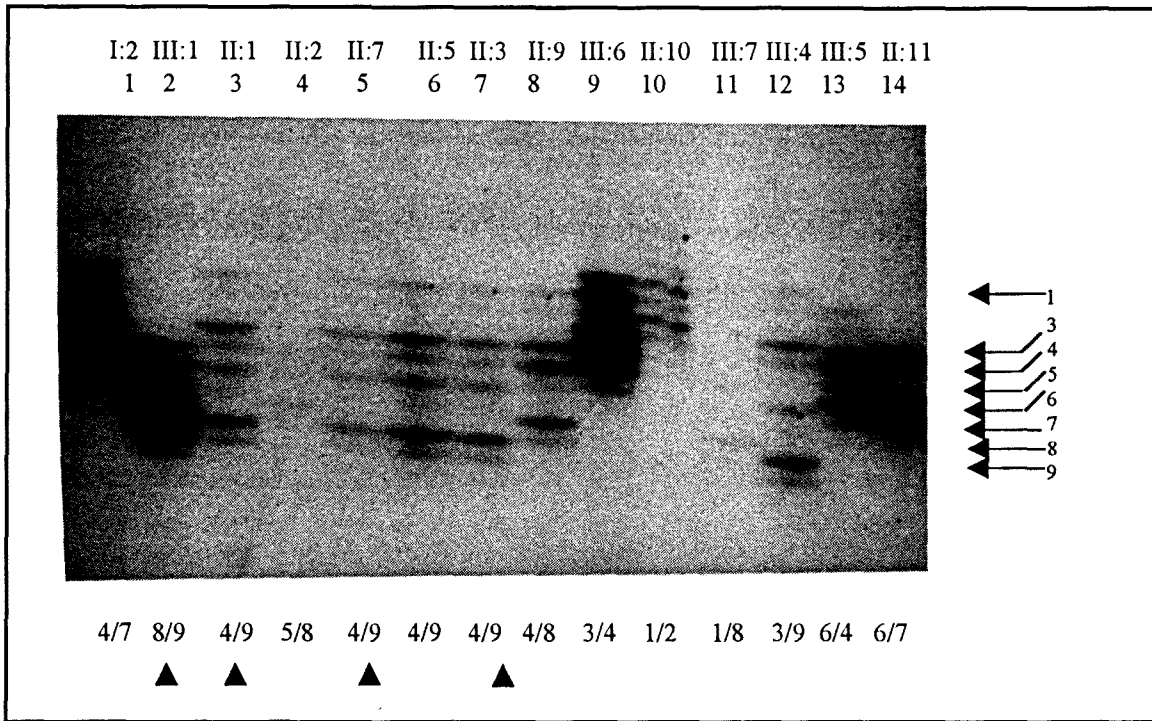


Fig. 3.15.1 Autoradiograph of a polyacrylamide gel showing alleles at the DNA marker *D7S636* in pedigree 169. Assigned genotypes are indicated below each lane, designated allele numbers are shown on the right. The individual identity numbers are indicated above the lane in which it is represented. The lower arrowheads indicate affected individuals represented in the specific lane.

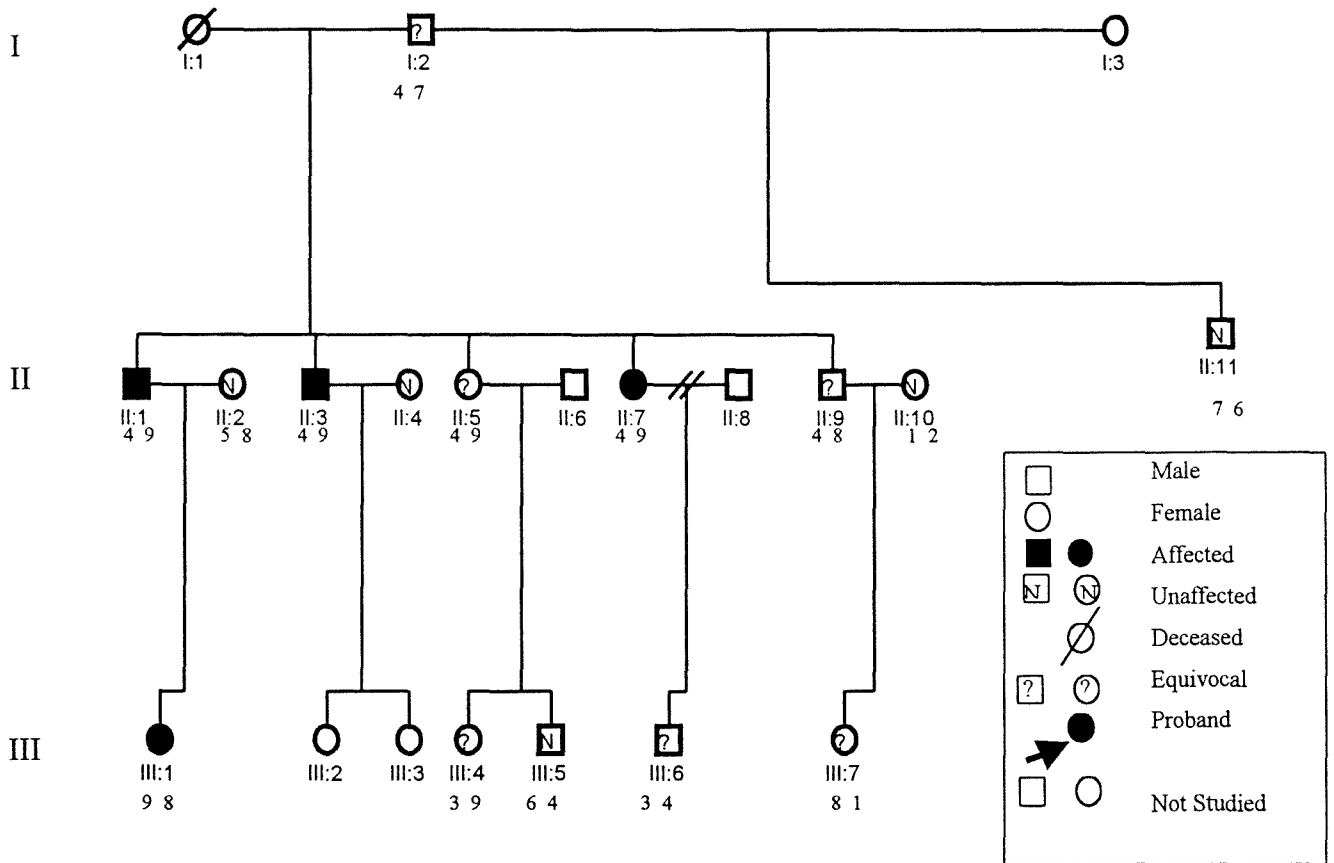


Fig. 3.15.2 Pedigree 169 showing the allelic distribution at the DNA marker *D7S636* in those individuals who participate in the linkage study. The individual identity number and assigned genotypes are indicated below each individual

3.4.2.2.3 *SCN5A* locus

The *SCN5A* locus was genotyped at the marker locus *D3S1298* and representative inheritance patterns of the alleles at this locus are shown in subsets of pedigree 167 in figure 3.16.1. The genotypes of the affected individuals were 2/8, 1/2, 2/3 and 1/8, thus there was no specific allele that segregated with the disease, as can clearly be seen when these genotypes are displayed on the pedigree (figure 3.16.2).

The autoradiograph showing the genotypes generated at *D3S1298* in pedigree 169 is shown in figure 3.17.1, the genotypes of the affected individuals were 6/8, 5/6, 8/9 and 8/9. No specific allele is shown to segregate with the disease in this family at this marker locus, as can be seen when these genotypes are displayed on the pedigree (figure 3.17.2).

3.4.2.2.4 Chromosome 4 locus

The chromosome 4 locus was genotyped at the single marker locus *D4S402* and the representative inheritance pattern of the alleles at this locus is shown in subsets of pedigree 167 in figure 3.18.1. The genotypes generated for the affected individuals at *D4S402* were 5/9, 5/6, 6/9 and 6/9 (figures 3.18.1). The assigned genotypes are displayed on the pedigree, and the fact that no specific allele segregated with the disease in this family at this marker locus is clearly illustrated (figure 3.18.2).

The representative inheritance patterns of the alleles at the *D4S402* locus is shown in subsets of pedigree 169 (figure 3.19.1). The genotypes generated for the affected individuals at *D4S402* were 5/6, 2/5, 6/7 and 6/7 (figure 3.19.1). When these genotypes are displayed on the pedigree, it can be clearly seen that no specific allele segregated with the disease in this family (figure 3.19.2).

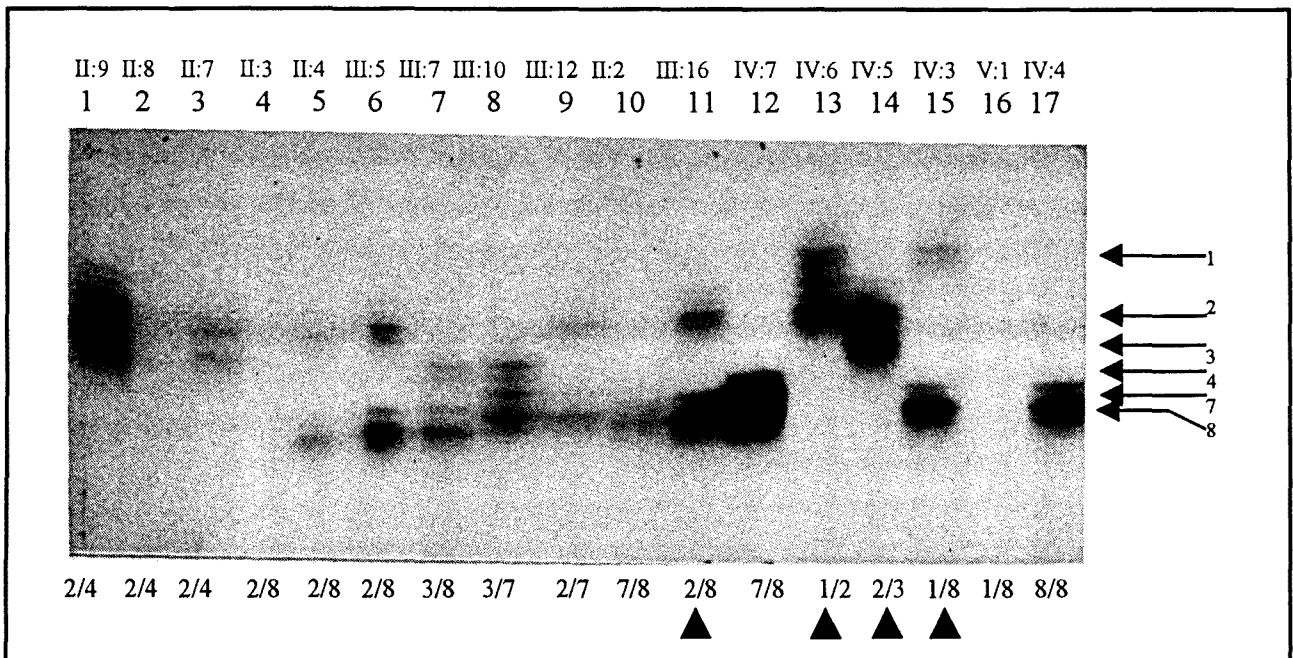


Fig. 3.16.1 Autoradiograph of a polyacrylamide gel showing alleles at the DNA marker *D3S1298* in pedigree 167. Assigned genotypes are indicated below each lane, designated allele numbers are shown on the right. The individual identity numbers are indicated above the lane in which it is represented. The lower arrowheads indicate affected individuals represented in the specific lane.

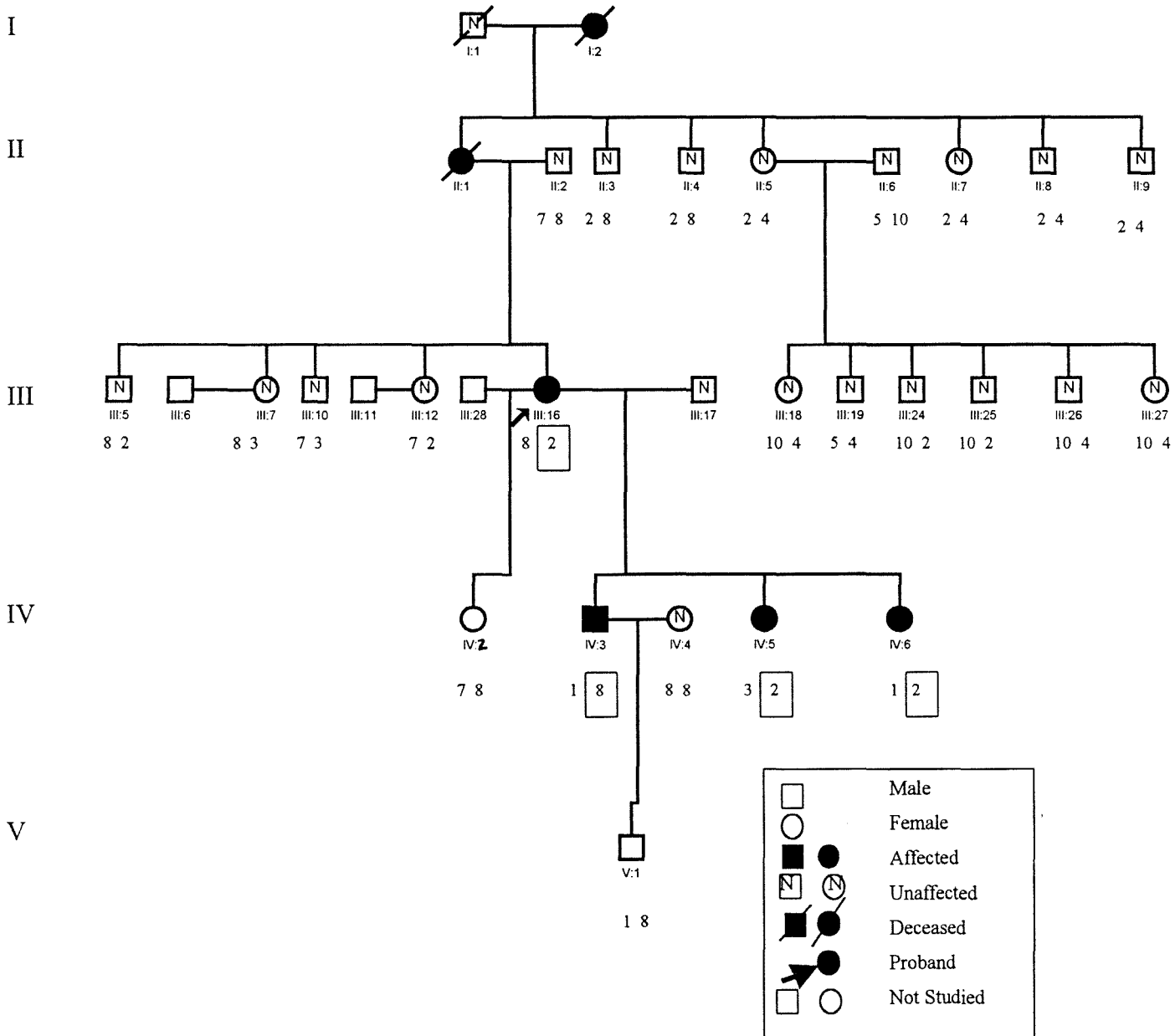


Fig. 3.16.2 Pedigree 167 showing the allelic distribution at the DNA marker *D3S1298* in those individuals who participate in the linkage study. The individual identity numbers and assigned genotypes are indicated below each individual. Where it was possible to deduce, the allele received from the affected parent is boxed. (Note: Pedigree 167 structure was altered for LOD score analysis. Individual III:28 was not studied but is indicated in the pedigree, as genotyping data was inconsistent with individual III:17 being the father of IV:2).

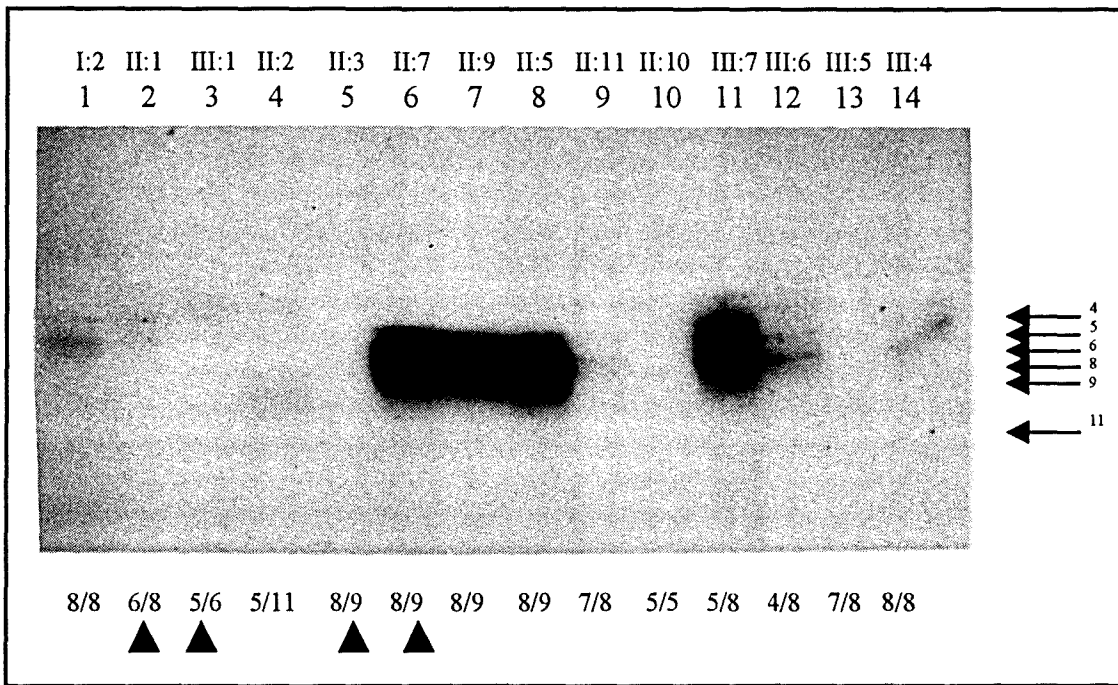


Fig. 3.17.1 Autoradiograph of a polyacrylamide gel showing alleles at the DNA marker *D3S1298* in pedigree 169. Assigned genotypes are indicated below each lane, designated allele numbers are shown on the right. The individual identity numbers are indicated above the lane in which it is represented. The lower arrowheads indicate affected individuals represented in the specific lane.

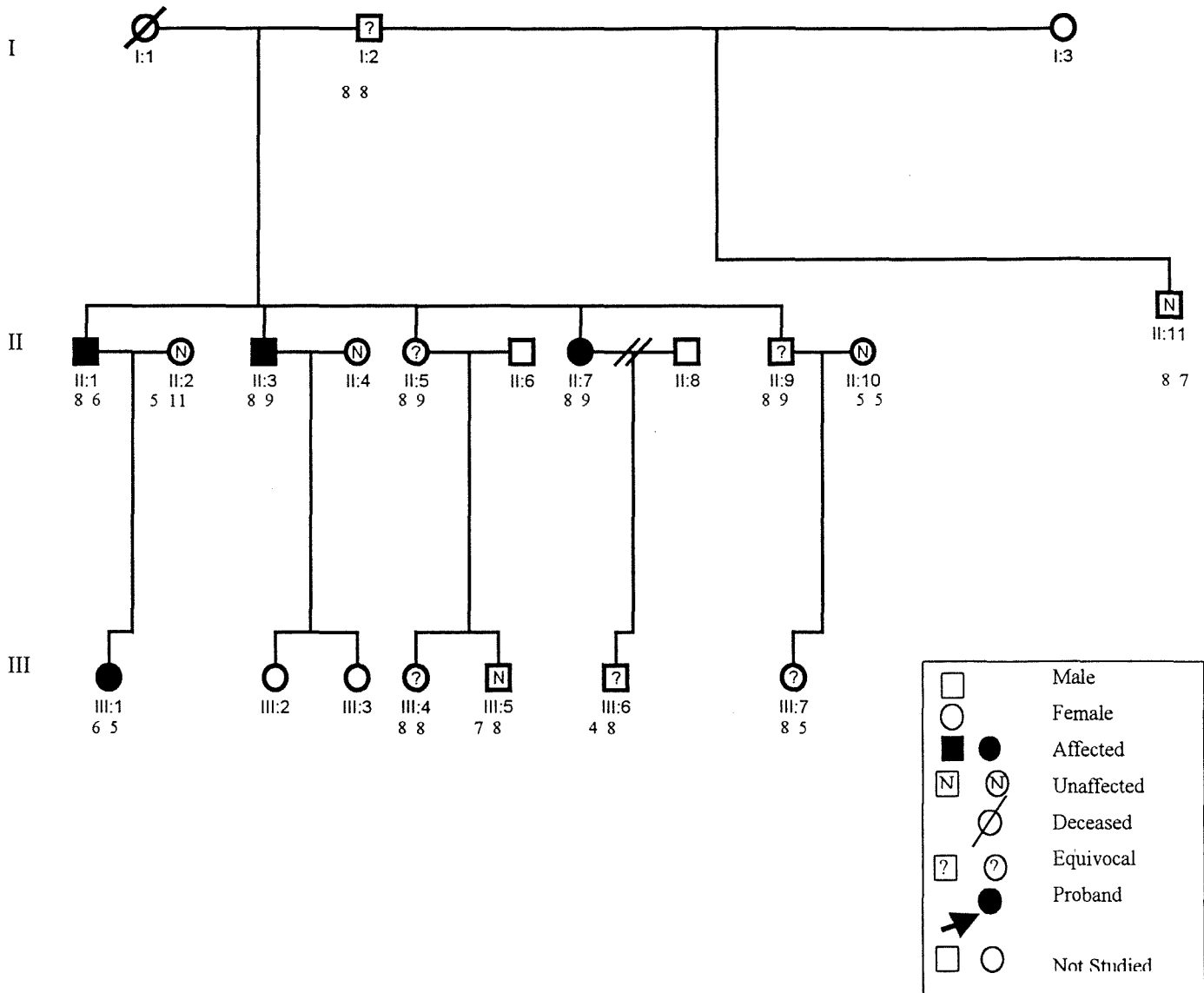


Fig. 3.17.2 Pedigree 169 showing the allelic distribution at the DNA marker *D3S1298* in those individuals who participate in the linkage study. The individual identity number and assigned genotypes are indicated below each individual.

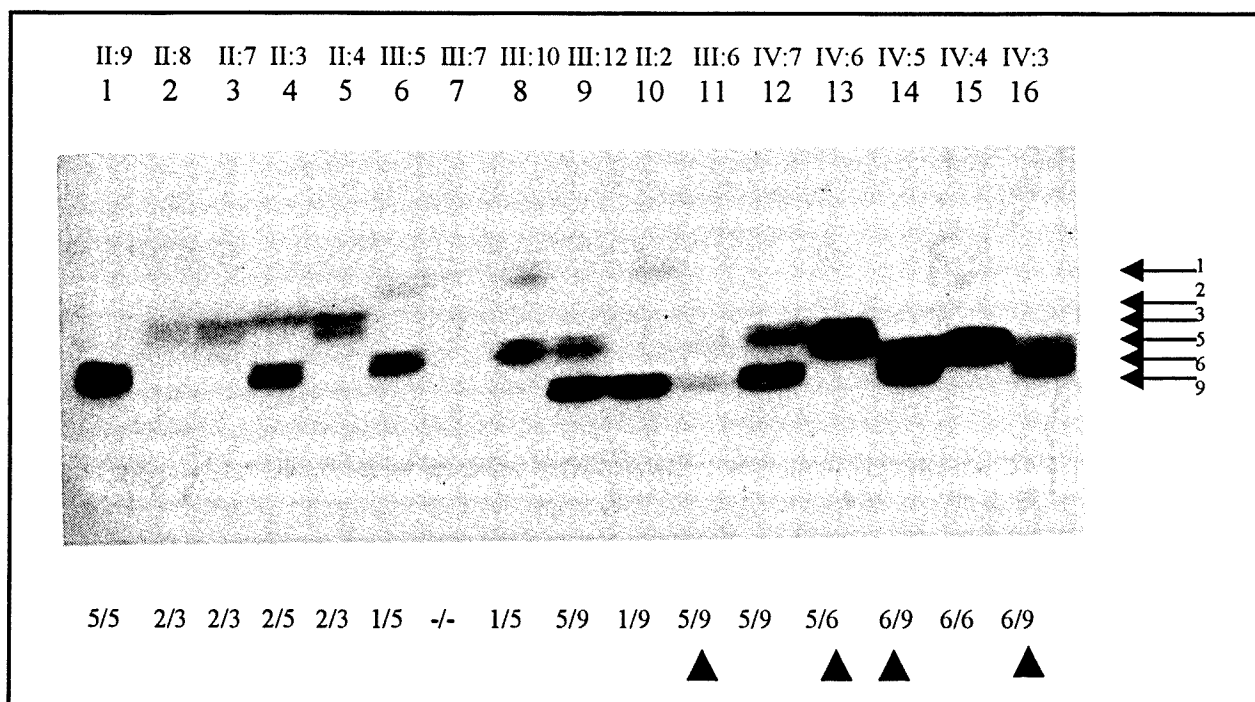


Fig. 3.18.1 Autoradiograph of a polyacrylamide gel showing alleles at the DNA marker *D4S402* in pedigree 167. Assigned genotypes are indicated below each lane, designated allele numbers are shown on the right. The individual identity numbers are indicated above the lane in which it is represented. The lower arrowheads indicate affected individuals represented in the specific lane.

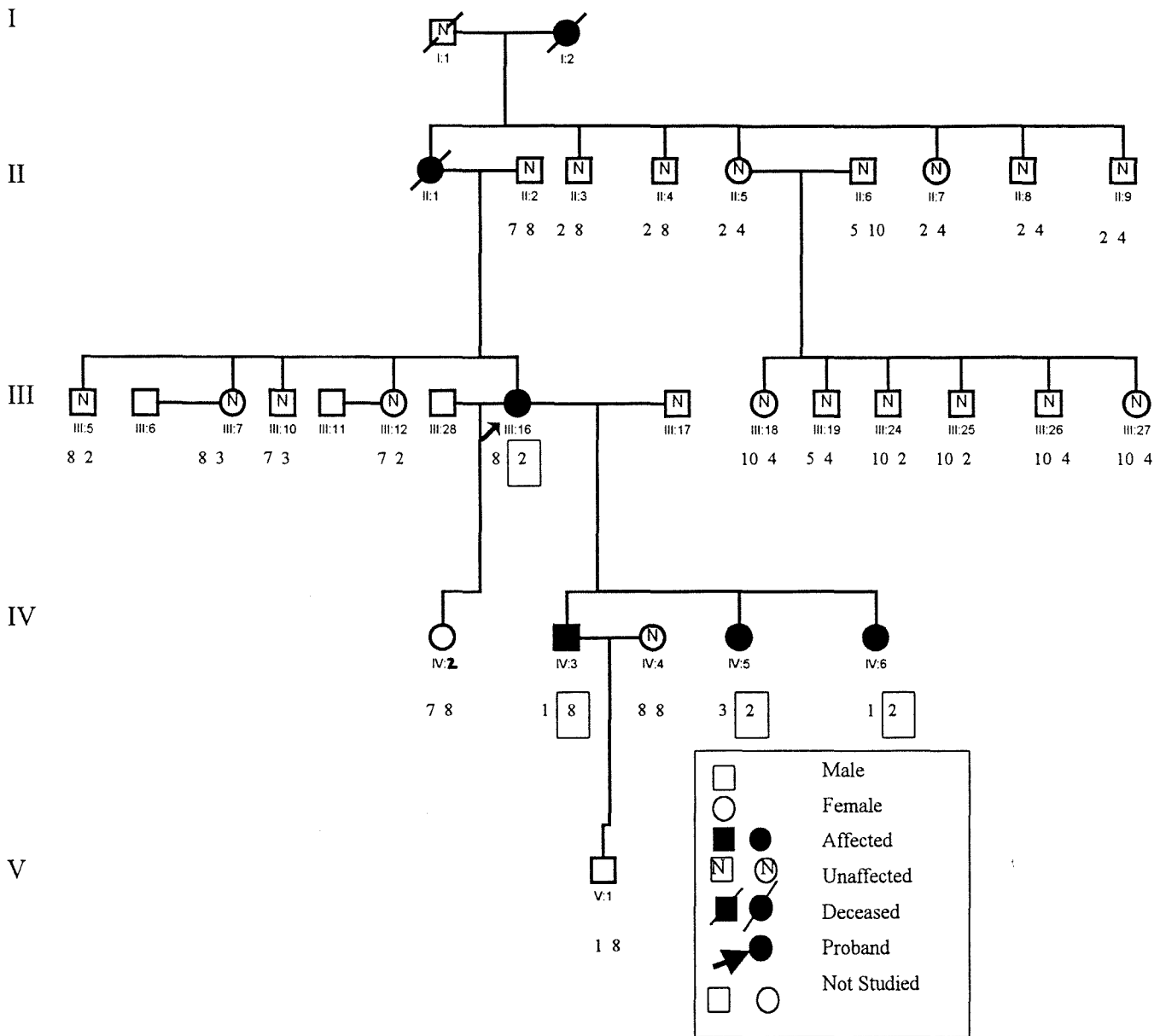


Fig. 3.18.2 Pedigree 167 showing the allelic distribution at the DNA marker *D4S402* in those individuals who participate in the linkage study. The individual identity number and assigned genotypes are indicated below each individual. Were it was possible to deduced the alleles received from the affected parent was boxed. (Note: Pedigree 167 structure was altered for LOD score analysis. Individual III:28 was not studied but is indicated in the pedigree, as genotyping data was inconsistent with individual III:17 being the father of IV:2).

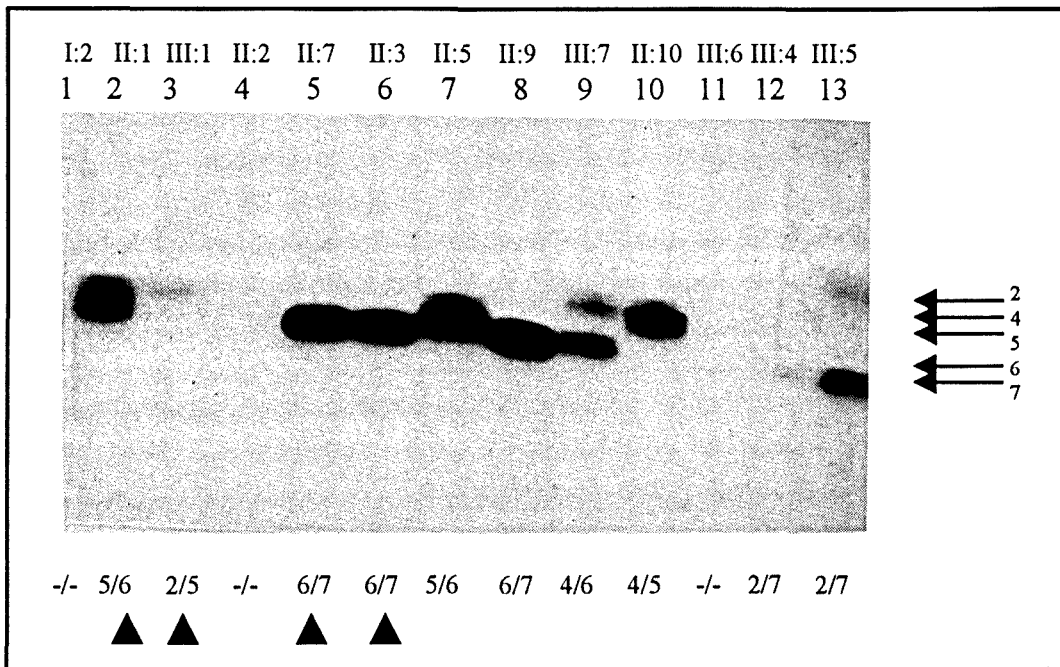


Fig. 3.19.1 Autoradiograph of a polyacrylamide gel showing alleles at the DNA marker *D4S402* in pedigree 169. Assigned genotypes are indicated below each lane, designated allele numbers are shown on the right. The individual identity numbers are indicated above the lane in which it is represented. The lower arrowheads indicate affected individuals represented in the specific lane.

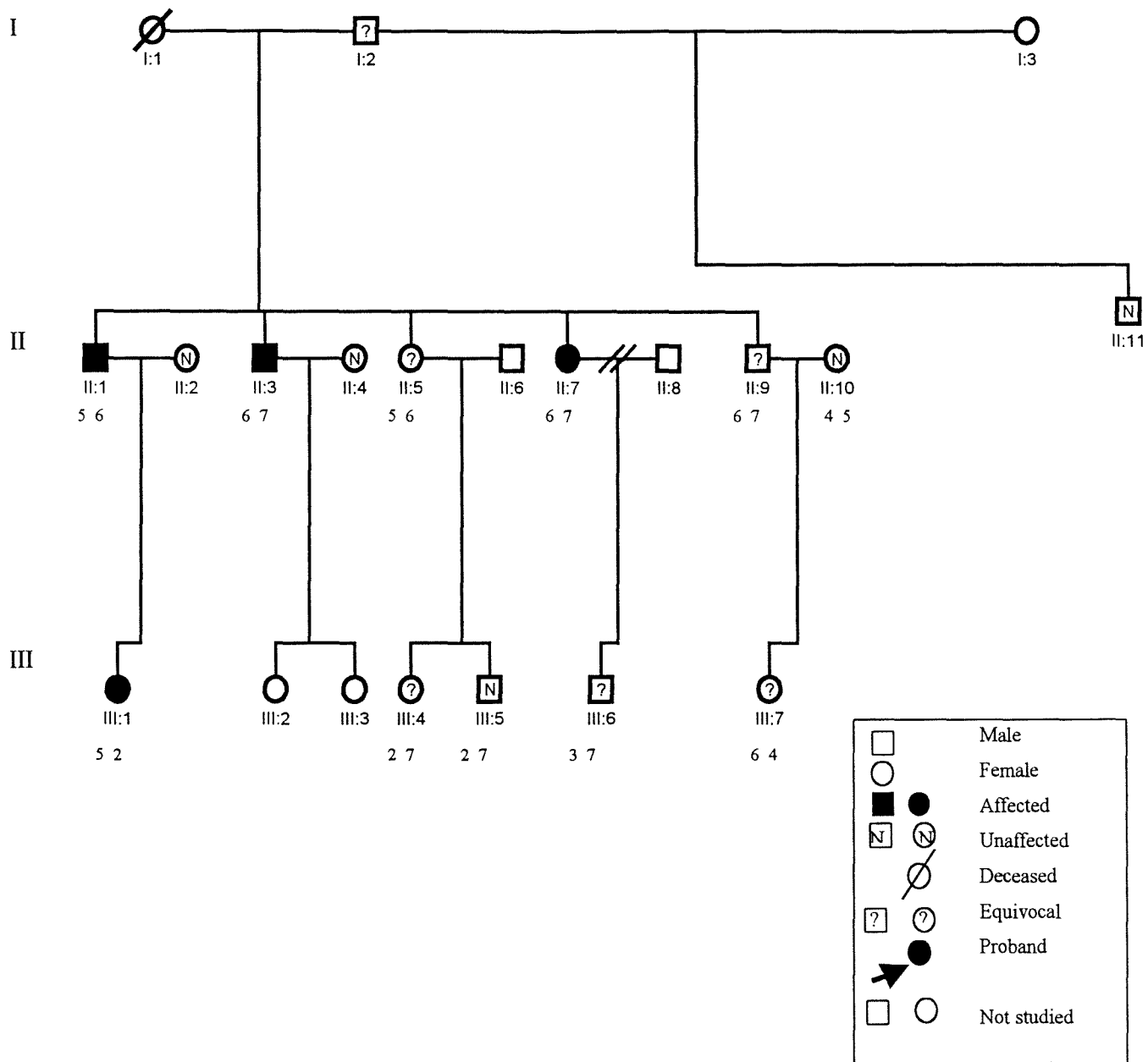


Fig. 3.19.2 Pedigree 169 showing the allelic distribution at the DNA marker *D4S402* in those individuals who participate in the linkage study. The individual identity number and assigned genotypes are indicated below each individual.

3.4.3 Haplotype Analysis

3.4.3.1 Haplotype analysis at the *KVLQT1* locus

Haplotypes were constructed at the *KVLQT1* locus in pedigree 167 and pedigree 169 from the genotypes generated at the five DNA markers analysed at this locus (figures 3.20 and 3.21). Haplotype analysis at the *KVLQT1* locus in pedigree 167 indicated that the four affected individuals III:16, IV:3, IV:5 and IV:6, shared the same haplotype, namely 4-10-2-3-2 at the DNA markers in the order indicated in the figure, suggesting that this might be the disease-associated haplotype (figure 3.20). However, this haplotype is also seen in two unaffected individuals (III:7 and III:12). The distance encompassed by this conserved haplotype is 8cM.

In pedigree 169, the disease status of the first generation is uncertain, this make it difficult to determine from which side the disease is transmitted to the siblings in the second generation. In the third generation, the haplotype of the affected child (III:1) of individual II:1 could clearly be determined as 2/7/2/3/4 (figure 3.21). This haplotype was also seen in individual II:1 (-/7/2/3/4); however, it was absent in the remaining two affected individuals in this family, thus implying that this is not the disease associated haplotype (figure 3.21).

3.4.4 Two Point LOD scores

Two point LOD scores were generated using the M-LINK program of the linkage computer package (Lathrop and Lalouel 1984). A LOD score for each marker locus tested was obtained in pedigree 167 and 169, respectively, and are shown in Table 3.2 and 3.3.

In pedigree 167, significant negative LOD scores of -3.13, -5.01 and -3.23 ($\theta = 0$) were generated at the *HERG*, *SCN5A* and the chromosome 4 loci, respectively (Table 3.2). An equivocal LOD score of 0.92 ($\theta = 0$) was generated at the *KVLQT1* locus with the DNA marker *D11S860* (Table 3.2). In pedigree 169, significant negative LOD scores of -2.62, -2.71 and -2.68 were generated at *KVLQT1*, *SCN5A* and the chromosome 4 loci, respectively at $\theta = 0$ (Table 3.3). An equivocal LOD score of 0.20 was generated at the *HERG* locus with *D7S636* at $\theta = 0$ (Table 3.3).

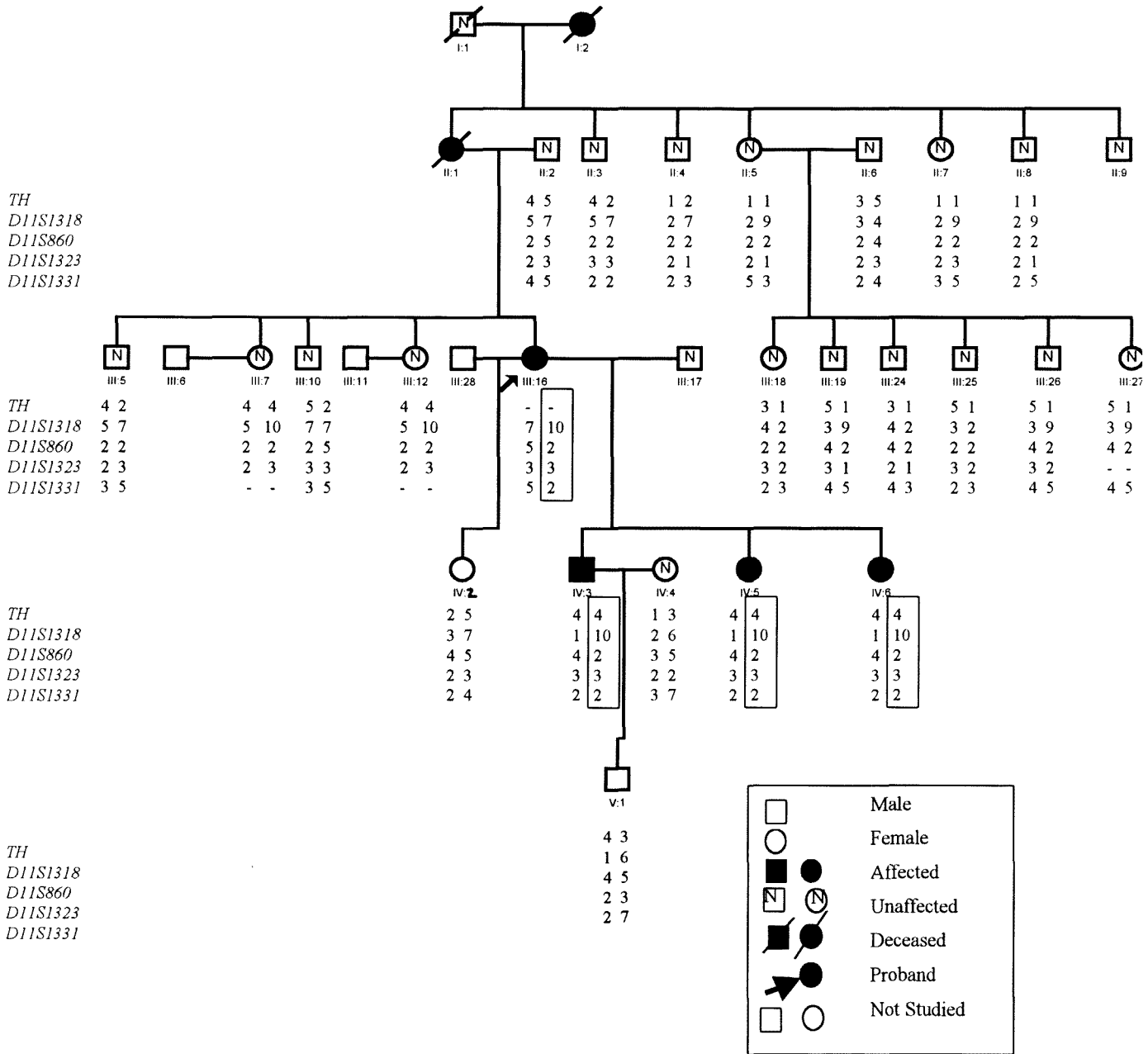


Fig. 3.20 Haplotypes across the *KVLQT1* locus in pedigree 167. Haplotypes are indicated below each individual, and the disease-associated haplotyped is boxed. The names of the marker loci used in the construction of the haplotype are indicated, to the left of the pedigree, in telomeric-centromeric order, from top to bottom. The disease-associated haplotype is boxed with a solid line in the affected individuals and a dotted line in the two unaffected individuals also sharing this disease-associated haplotype. (Note: Pedigree 167 structure was altered for LOD score analysis. Individual III:28 was not studied but is indicated in the pedigree, as genotyping data was inconsistent with individual III:17 being the father of IV:2).

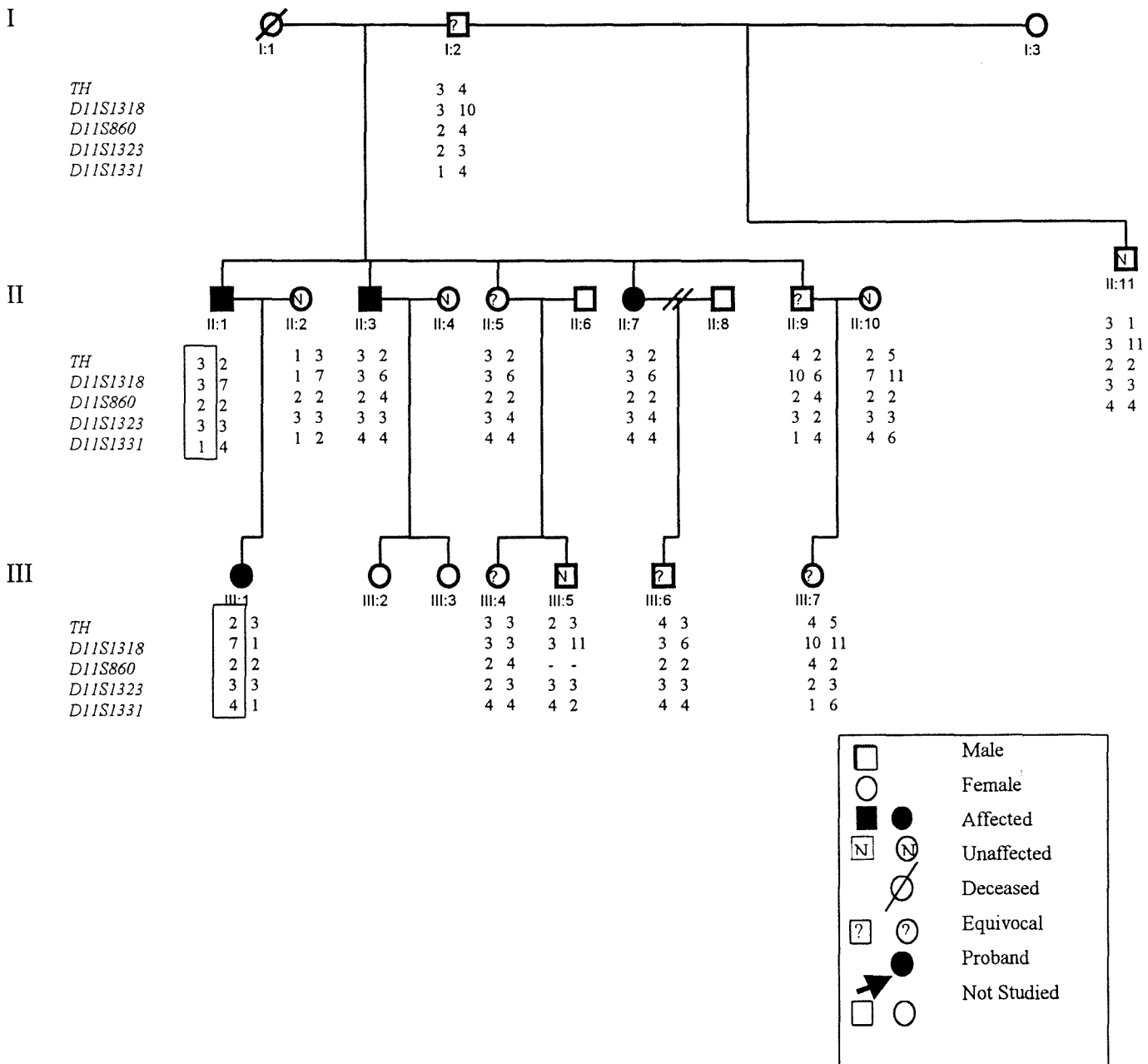


Fig. 3.21 Haplotypes across the *KVLQT1* locus in pedigree 169. Haplotypes are indicated below each individual, and where it was possible the haplotype received from the affected parent was boxed. The names of the marker loci used in the construction of the haplotype are indicated, to the left of the pedigree, in telomeric-centromeric order, from top to bottom. Where possible the haplotype received from the affected parent was boxed.

Table 3.2 Pairwise two point LOD scores between LQTS and polymorphic markers at the *KVLQT1*, *HERG*, *SCN5A* and chromosome 4 loci in pedigree 167.

CANDIDATE LOCUS	LOD scores derived at θ						
	0.00	0.01	0.05	0.10	0.20	0.30	0.40
<i>Marker locus</i>	0.00	0.01	0.05	0.10	0.20	0.30	0.40
<i>KVLQT1</i>							
<i>D11S1318</i>	0.25	0.29	0.40	0.46	0.43	0.29	0.10
<i>TH</i>	-0.27	-0.18	-0.06	0.20	0.27	0.19	0.07
<i>D11S1323</i>	-0.11	-0.09	-0.03	0.02	0.04	0.03	0.01
<i>D11S860</i>	0.92	0.91	0.87	0.79	0.58	0.34	0.11
<i>D11S1331</i>	0.09	0.10	0.10	0.10	0.06	0.02	-0.00
<i>HERG</i>							
<i>D7S636</i>	-3.12	-1.11	-0.38	-0.09	0.11	0.13	0.07
<i>SCN5A</i>							
<i>D3S1298</i>	-5.01	-2.00	-1.14	-0.71	-0.28	-0.08	0.00
Chromosome 4 Locus							
<i>D4S402</i>	-3.23	-1.24	-0.51	-0.20	0.04	0.10	0.05

Figures in bold highlight the weakly positive LOD scores generated at *D11S860* in pedigree167

Table 3.3 Pairwise two point LOD scores between LQTS and polymorphic markers at the *KVLQT1*, *HERG*, *SCN5A* and chromosome 4 loci in pedigree 169.

CANDIDATE LOCI	LOD scores derived at θ						
	0.00	0.01	0.05	0.10	0.20	0.30	0.40
Marker locus	0.00	0.01	0.05	0.10	0.20	0.30	0.40
<i>KVLQT1</i>							
<i>D11S1318</i>	-2.62	-1.73	-0.09	-0.79	-0.46	-0.25	-0.10
<i>TH</i>	-0.57	-0.56	-0.50	-0.43	-0.29	-0.16	-0.07
<i>D11S1323</i>	-0.43	-0.43	-0.42	-0.37	-0.25	-0.14	-0.06
<i>D11S860</i>	-0.62	-0.61	-0.54	-0.44	-0.24	-0.10	-0.02
<i>D11S1331</i>	-0.29	-0.30	-0.31	-0.33	-0.29	-0.18	-0.07
<i>HERG</i>							
<i>D7S636</i>	0.20	0.18	0.13	0.1	0.06	0.02	-0.02
<i>SCN5A</i>							
<i>D3S1298</i>	-2.71	-1.53	-0.88	-0.60	-0.34	-0.19	-0.08
Chromosome 4 locus							
<i>D4S402</i>	-2.68	-1.15	-0.50	-0.25	-0.06	0.00	0.01

Figures in bold highlight the weakly positive LOD scores generated at *D7S636* in pedigree169

3.5. MUTATION SCREENING

The results obtained through linkage analysis and haplotype analysis identified the *KVLQT1* gene as the plausible candidate locus for the disease in pedigree 167. Consequently, PCR-SSCP mutation screening analysis was initiated to search for the disease-causing mutation in this gene in this family.

3.5.1 PCR-SSCP Analysis

In pedigree 167, the partial S1 and the S2-S6 region of the *KVLQT1* gene were screened for known and novel mutations by PCR-SSCP analysis using four different gel conditions namely; 5% and 10% polyacrylamide gels, with and without glycerol. Representative results of PCR-SSCP analysis are shown in figures 3.22.1-3.22.4.

No sequence variations were detected in the regions investigated employing PCR-SSCP analysis, on 10% polyacrylamide gels with and without glycerol and 5% polyacrylamide with glycerol (figure 3.22.1-3.22.3). However, a mobility shift was detected in the S2-S3 region of *KVLQT1* on a 5% polyacrylamide gel without glycerol in the three affected members of pedigree 167, which was absent in the two unaffected members analyzed under this condition (figure 3.22.4). The PCR-SSCP analysis of affected members of this family, as well as appropriate controls, was repeated using the same gel condition, which again revealed the mobility shift, which was also confirmed on an MDE gel (results not shown). After the presence of the mobility shift was confirmed following reamplification and a second PCR-SSCP analysis, the region was sequenced and the result obtained for an affected individual was compared with an unaffected individual and the normal published sequence of the S2-S3 region of *KVLQT1* (figure 3.23). A G→A transition was detected in the intronic sequence in an affected individual (figure 3.23).

To determine the frequency of this G→A transition detected in the affected individuals of pedigree 167, PCR-SSCP analysis was employed in 40 unaffected, unrelated control individuals of Mixed ancestry. Three of the 40 subjects analyzed showed this polymorphism (results not shown). Genotypic analysis was also performed with this polymorphism in pedigree 167. This mobility shift was detected in all affected members of pedigree 167, as well as the two unaffected members who shared the disease-associated haplotype; however, this mobility shift was also seen in an additional unaffected individual (II:7). No other SSCP variants were detected in any of the regions analyzed.

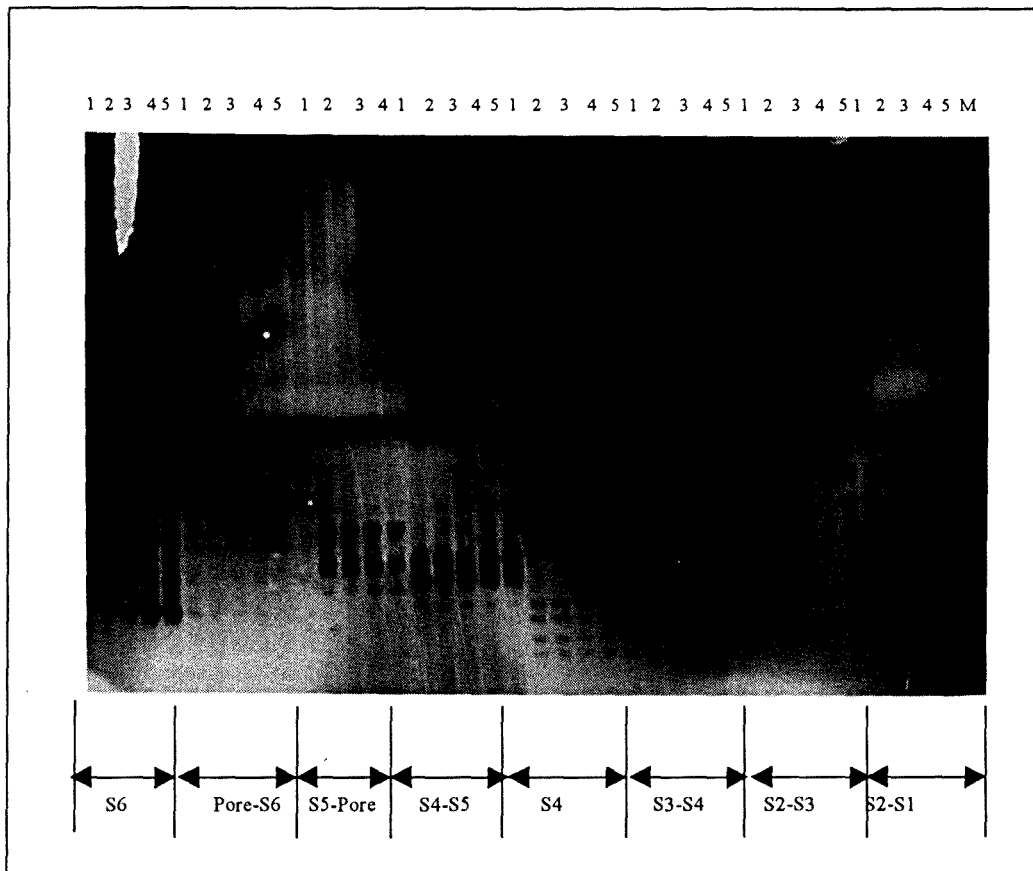


Fig. 3.22.1 PCR-SSCP analysis of the S2-S6 regions of *KVLQT1* in pedigree 167 on a 10% polyacrylamide gel with glycerol. The amplified S2-S6 regions of *KVLQT1* gene were electrophoretically separated on a 10% polyacrylamide gel with glycerol at 4°C and visualized by silver staining. At each region, as indicated by the brackets, 5 individuals were analyzed except for the S5-Pore region where 4 individuals were analyzed. Each region was labeled lane 1-5, representing the 5 individuals analyzed. Lane 1 = unaffected individual, lanes 2-4 = affected individuals and lane = 5 unaffected individual. At the S5-Pore region lanes 1-2 represent unaffected individuals and lanes 3-4 affected individuals.

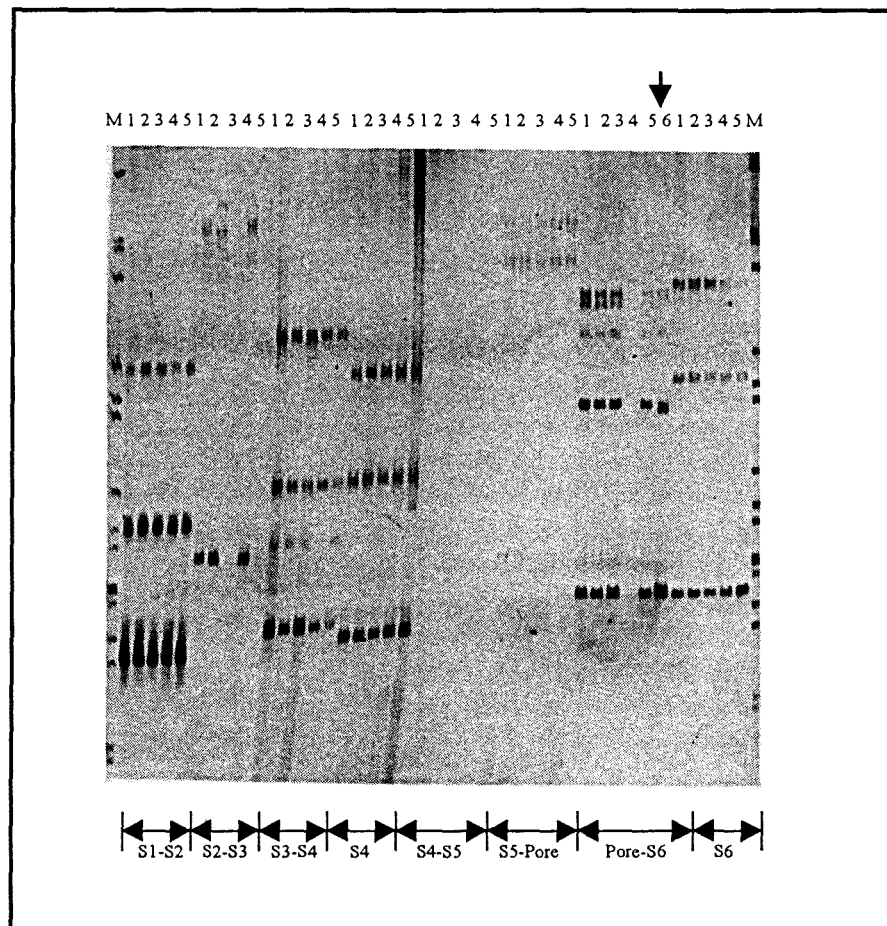


Fig. 3.22.2 PCR-SSCP analysis of the S2-S6 regions of *KVLQT1* in pedigree 167 on a 10% polyacrylamide gel without glycerol. The amplified S2-S6 regions of *KVLQT1* gene were electrophoretically separated on a 10% polyacrylamide gel without glycerol at 4°C and visualized by silver staining. At each region, as indicated by the brackets, 5 individuals were analyzed except for the Pore-S6 region where 6 individuals were analyzed. Each region was labeled lane 1-5, representing the 5 individuals analyzed. Lane 1= unaffected individual, lanes 2-4 = affected individuals and lane 5 = unaffected individual. At the Pore-S6 region, lane 6 = individual where Ala212Val mutation is present. The arrow indicates the mobility shift caused by the C→T transition that resulted in the Ala212Val mutation in *KVLQT1*. At the Pore-S6 region lane 1-2 represent unaffected individuals and lanes 3-5 affected individuals

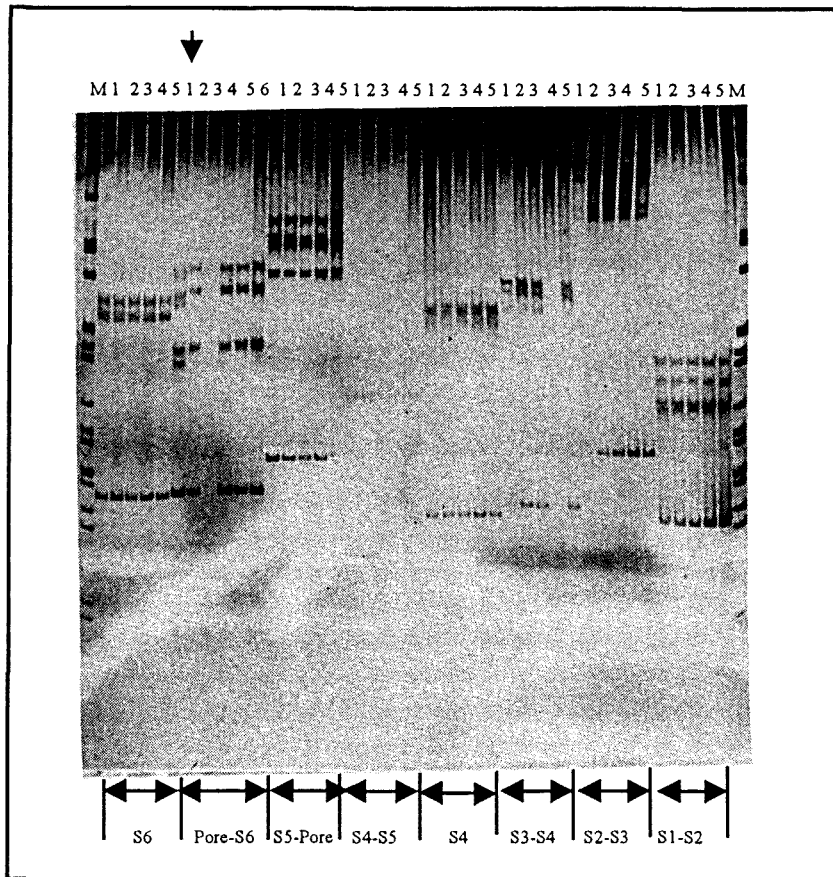


Fig. 3.22.3 PCR-SSCP analysis of the S2-S6 regions of *KVLQT1* in pedigree 167 on a 5% polyacrylamide gel with glycerol. The amplified S2-S6 regions of *KVLQT1* gene were electrophoretically separated on a 5% polyacrylamide gel with glycerol at 4⁰C and visualized by silver staining. At each region, as indicated by the brackets, 5 individuals were analyzed. Each region were labeled lane 1-5, representing the 5 individuals analyzed. Lane 1= unaffected individual, lanes 2-4 = affected individuals and lane 5 = unaffected individual. At the Pore-S6 region lane 1 = individual were Ala212Val mutation is present, lanes 2-3 = unaffected individuals and lanes 4-6 = affected individuals. The arrow indicates the mobility shift caused by the C→T transition that resulted in the Ala212Val mutation in *KVLQT1*.

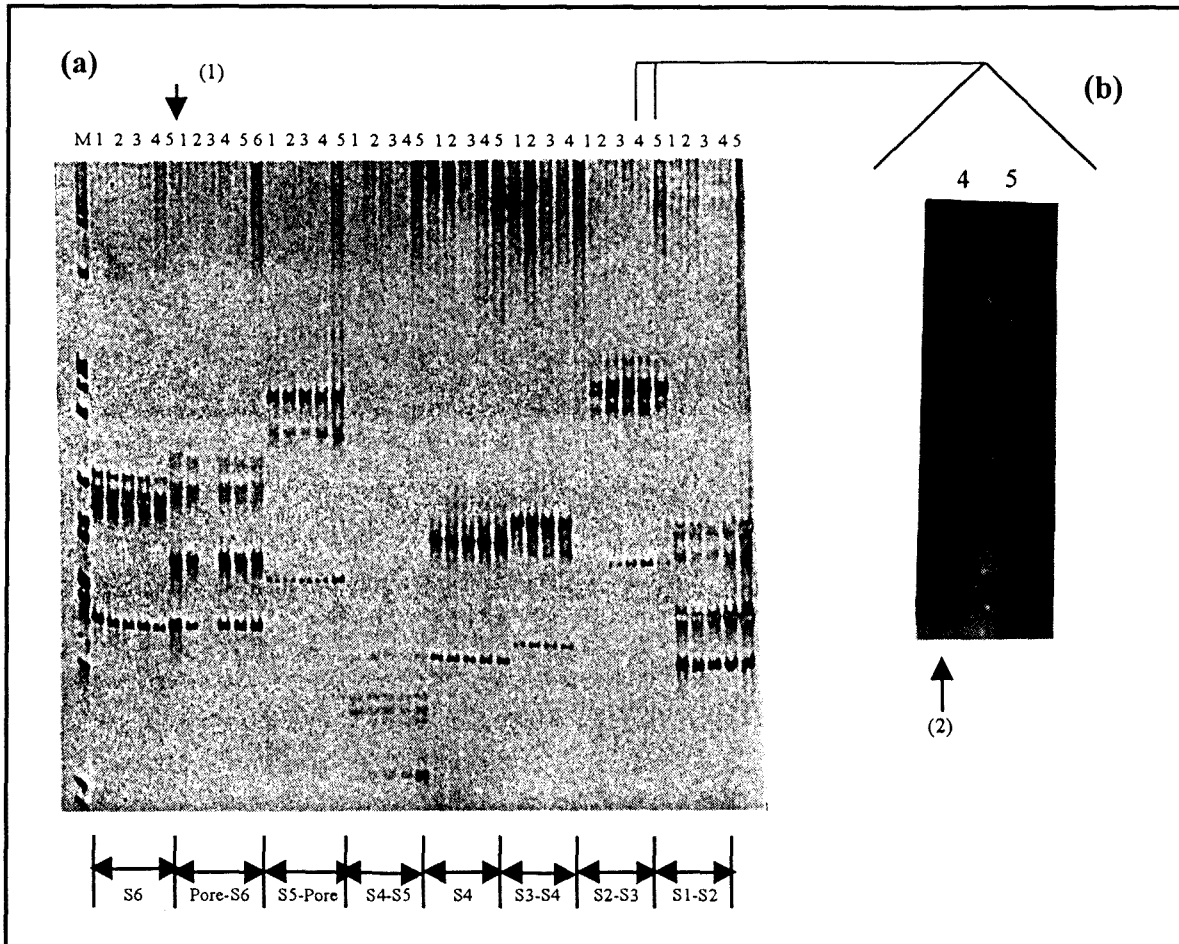


Fig. 3.22.4 PCR-SSCP analysis of the S2-S6 regions of *KVLQT1* in pedigree 167 on a 5% polyacrylamide gel without glycerol.

- a) The amplified S2-S6 regions of *KVLQT1* gene were electrophoretically separated on a 10% polyacrylamide gel with glycerol at 4⁰C and visualized by silver staining. At each region, as indicated by the brackets, 5 individuals were analyzed, except for the S4 region where 4 individuals were analyzed. Each region was labeled lane 1-5, representing the 5 individuals analyzed. Lane 1 = unaffected individual, lanes 2-4 = affected individuals and lane 5 = unaffected individual. At the Pore-S6 and S4 regions the lane order differs, Pore-S6 region lane 1 = individual where Ala212Val mutation is present, lanes 2-3 = unaffected individuals and lanes 4-6 affected individuals. The arrow (1) indicates the mobility shift caused by the C→T transition that resulted in the Ala212Val mutation in *KVLQT1*. In the S4 region, lanes 1-2 represents unaffected individuals and lanes 3-4 affected individuals.
- b) Enlargement of PCR-SSCP analysis of the S2-S3 region of *KVLQT1* in pedigree 167. Lane 1 = affected individual lane 2 = unaffected control. The arrow (2) indicate the mobility shift caused by the G→A transition in the intronic sequence of a heterozygous individual.

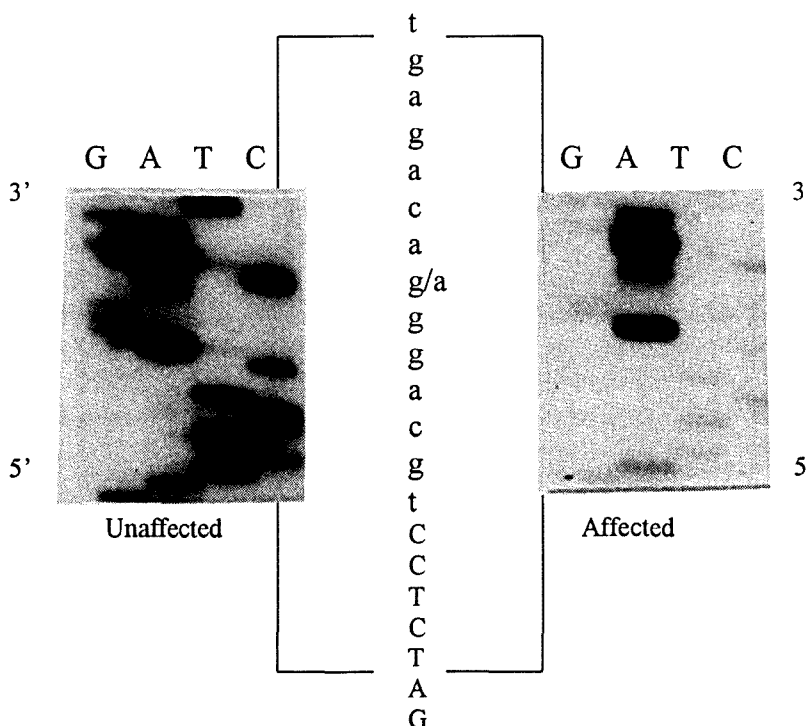
Fig. 3.23 Sequence variation identified in the S2-S3 region of an affected individual of pedigree 167, compared with the sequence of an unaffected individual and the normal published sequence of this region.

(a) Partial sequence of the non-coding strand of the S2-S3 region of *KVLQT1* in an affected and unaffected individual showing the G→A transition in the intronic sequence of the affected heterozygous (G/A) individual compared to the sequence found in an unaffected homozygous (G/G) individual.

(b) Normal published cDNA sequence of the S2-S3 domain of *KVLQT1*. The coding strand is indicated in black and the positions of the introns are shown with solid arrowheads. The non-coding strand is shown in green and red, the red shows the sequence of the exon encoding the S2-S3 region and the S2 and S3 transmembrane segments are underlined.

(c) Sequence of the non-coding region of the S2-S3 domain determined in an affected individual of pedigree 167. Positions of the intron or exon boundaries are indicated with a solid arrowhead, the G→A transition in the intronic sequence is indicated with a clear arrowhead and the S2 and S3 transmembrane segments are underlined. The partial sequence shown in (a) is boxed. The red shows the sequence of the exon and the blue shows the intronic sequence.

(a) Partial sequence of the non-coding strand of the S2-S3 region in an affected and unaffected individual



(b) Normal published cDNA sequence:

5' TATGCCGCCCTGGCCACGGGGACTCTC TTC TGGATGGAGATCGTGCTG
 3' ATACGGCGGGACCGGTGCCCTGAGAGAAGACCTACCTCTAGCACGAC
 S2

GTGGTGTTTTC TTCGGGACGGAGTACGTGGTCCGCCTC TGGTCCGCCGG
CACCACAAGAAGCCCTGCCTCATGCACCAGGCGGAGACCAGGCGGCC

CTGCCGCAGCAAGTACGTGGGCCTCTGGGGGCGGCTGCGCTT TGCCC
 GACGGCGTCGTTTCATGCACCCGGAGACCCCGCCGACGCGAAACGGG

GGAAGCCATTTCCATCATCGACCACATCG TGGTCGTGGCC TCCATGG
CCTTCGGGTAAAGGTAGTAGCTGGAGTAGCACCAGCACCAGGAGGTACC
 S3

TGGTCC TC TGC GTGGGCTCCAAG 3'
ACCAGGAGACGCACCCGAGGTTC 5'

(c) DNA Sequence of non-coding strand determined in affected individual:

5' gacctttggaccgcagggcagcatggactcacCGATGATGGAAATGGGCTTCC
 S3

GGGCAAAGCGCAGCCGCCCCAGAGGCCACGTACTTGCTGCGGCAG

CCGGCGGACCAGAGGCGGACCACGTACTCCGTCCCGAAGAACCAC
 S2

CAGCACGATCTC^gTgcaggaacagagtgggacgctcactgcaggcaggctcg 3'
 S2

3.5.2 ASREA in *KVLQT1*

Four of ten *KVLQT1* mutations described by Wang et al., (1996) which affected restriction enzyme sites (Table 2.3) were screened for by ASREA in pedigree 167. These mutations were the Ala49Pro and Arg61Glu, mutation both situated in the S2-S3 region, and the Val125Met mutation in the S4-S5 region. The fourth mutation was the Ala212Val mutation. The screening for the latter mutation has already been described in section 3.11.1, as this is the South African founder mutation.

For two of these mutations, namely Arg61Glu and Val125Met, the presence of the mutation introduced a *PvuII* and a *StyI* site, respectively. Thus, in the absence of the mutation, after digestion with the respective restriction enzymes, only the undigested PCR fragment would be generated. To ensure that the enzyme was active during the digestion, ideally an internal control should be included in the reaction. For one of these mutations, Arg61Glu it was possible to design an internal control to test the activity of the enzyme. Diluted lambda DNA was included in the reaction mixture prior to digestion. To find a control for the Val125Met mutation proved troublesome, as λ DNA digested with *StyI* generated too many bands, some of which overlap with the expected fragment sizes generated in the presence of Val125Met. Consequently, no control was included for screening the Val125Met mutation.

Negative controls, samples amplified from unaffected LQTS individual, were included on each gel. Ideally, a positive control, a sample amplified from an affected person carrying the mutation in question, would be useful to compare the generated fragment sizes and activity of the enzyme. This type of control was included in the analysis of the Ala212val mutation, however, such samples were not available for the other three mutations. The expected fragment sizes of both the mutant and the wild type alleles were determined with the aid of the computer program Genepro, prior to PCR-based restriction enzyme analysis. This, and the inclusion of a molecular weight marker on each polyacrylamide gel, allowed the investigator to gauge the fragment sizes and the compare them with those predicted.

3.5.2.1 Ala49Pro mutation in S2-S3 region

The PCR amplification of the S2-S3 region of *KVLQT1* resulted in a 240bp product normally cleaved into two fragments of 160bp and 80bp by digestion with *NaeI*. The presence of the G→C mutation causes a Ala→Pro substitution at codon 49, that would result in the loss of a *NaeI*

restriction enzyme site. Therefore, in an individual heterozygous for this mutation an additional undigested 240bp fragment would be generated.

In the affected members of pedigree 167 analyzed, the G→C mutation in codon 49 was not present, as is evident by the complete digestion of the PCR product into two fragments of 160bp and 80bp (figure 3.24).

3.5.2.2 Arg61Glu mutation in the S2-S3 region

The G→A transition causing the Arg→Glu substitution at codon 61 would introduce a *PvuII* restriction enzyme site into the S2-S3 region of *KVLQTI*. Thus, in the absence of the mutation, only the undigested 240bp PCR amplified product would be generated after digestion with *PvuII*, while in an individual heterozygous for this mutation three fragments of 240bp, 150bp and 90bp would be generated. In order to check that the enzyme was active during the digestion, an internal control of λ DNA was included in each sample digested with *PvuII*.

In all the individuals analyzed for the Arg61Glu mutation, only the undigested 240bp fragment was generated indicating the absence of the mutation, the enzyme's activity was indicated by the digested λ DNA fragments (figure 3.25).

3.5.2.3 Val125Met mutation in the S3-S4 region

The G→A transition in codon 125 would introduce a *SlyI* restriction enzyme site into the S3-S4 region of *KVLQTI*. In the absence of the mutation, a single 120bp fragment would be generated after digestion with *SlyI*, while, in an individual heterozygous for the mutation, three fragments of 120bp, 50bp and 70bp would be generated.

However, in all individuals analyzed for the Val125Met mutation in S3-S4 region only the 120bp fragment was generated indicating the absence of this mutation (figure 3.26).

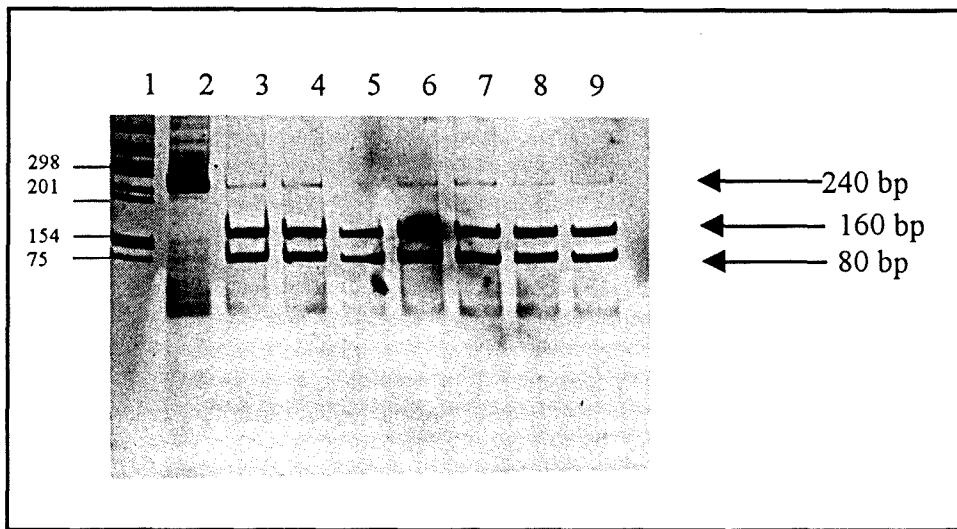


Figure 3.24 Allele specific restriction enzyme analysis (ASREA) of the reported Ala49Pro mutation in the S2-S3 region of *KVLQT1*. A representative 12% polyacrylamide gel of *NaeI* restriction enzyme digestion of the PCR amplified S2-S3 region of affected and unaffected members of pedigree 167. Lane 1: marker, lane 2: undigested S2-S3 PCR amplified fragment, lanes 3-6: affected individuals and lanes 7-10 unaffected individuals

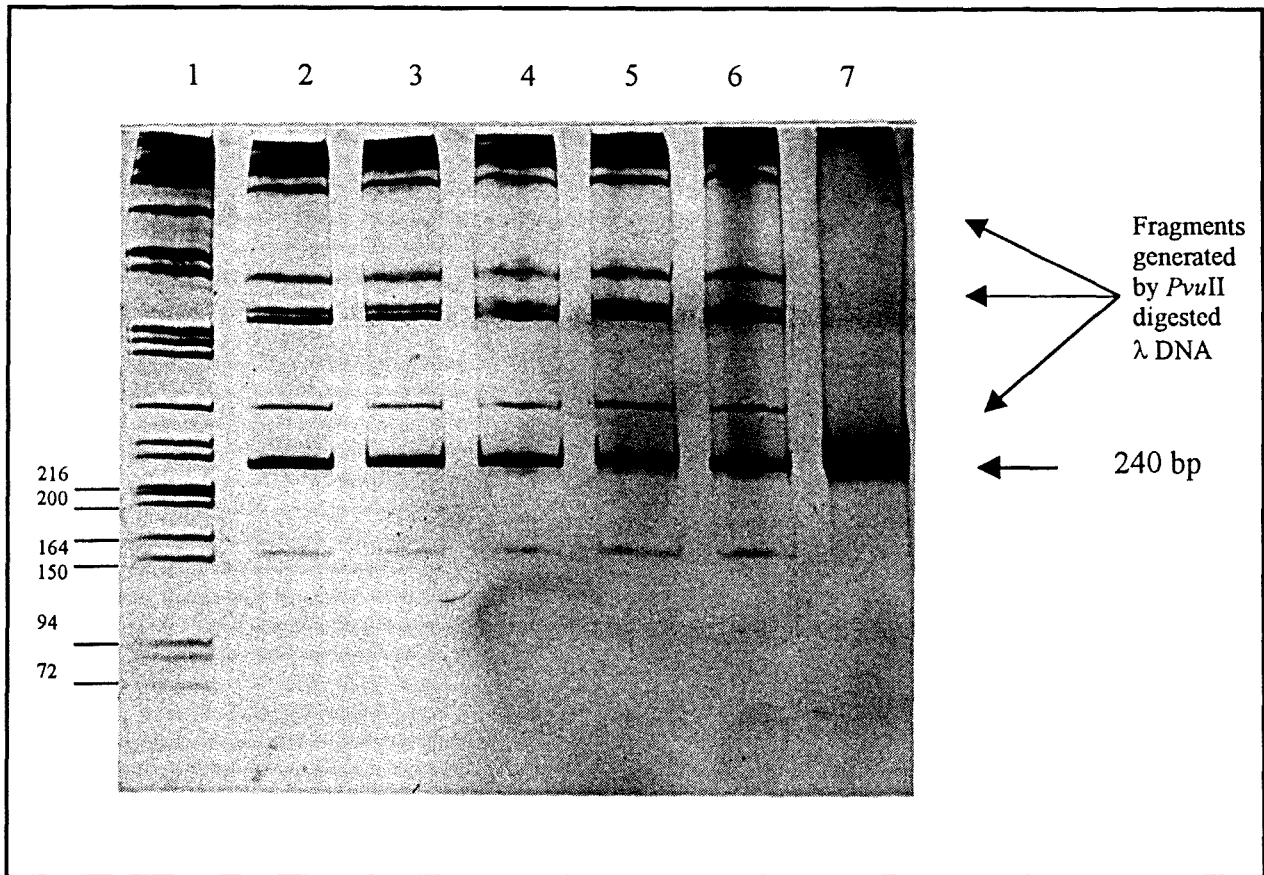


Figure 3.25 Allele specific restriction enzyme analysis (ASREA) of the reported Arg61Glu mutation in the S2-S3 region of *KVLQT1*. A representative 12% polyacrylamide gel of *Pvu*II restriction enzyme digestion of the PCR amplified S2-S3 region of affected and unaffected members of pedigree 167. Lane 1: λ *Pst*I, lanes 2-4: affected individuals, lanes 5-6 unaffected individuals and lane 7: undigested S2-S3 PCR amplified fragment

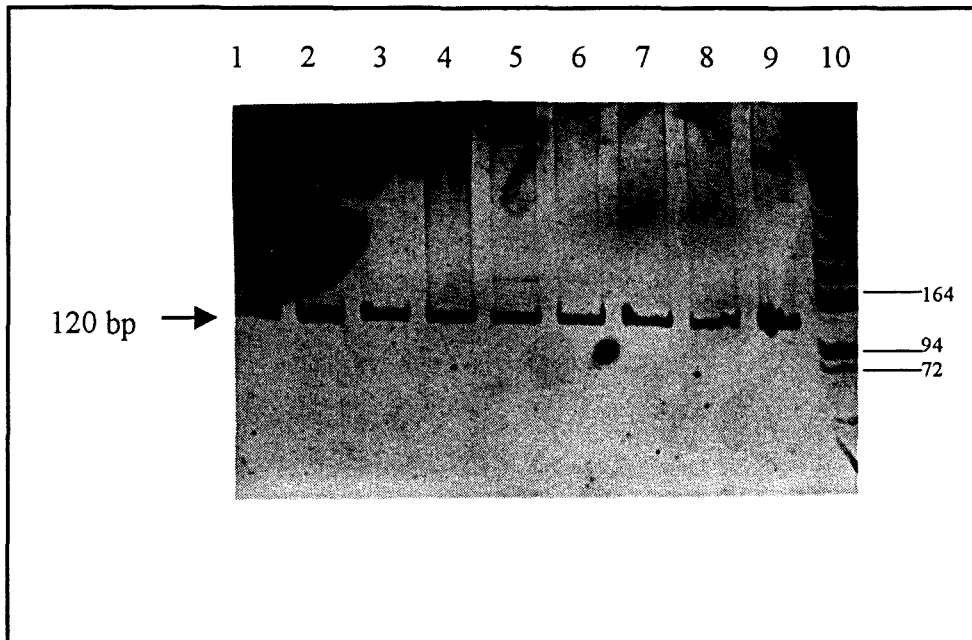


Figure 3.26 Allele specific restriction enzyme analysis (ASREA) of the reported Val125Met mutation in the S4-S5 region of *KVLQT1*. A representative 12% polyacrylamide gel of *SlyI* restriction enzyme digestion of the PCR amplified S4-S5 region of affected and unaffected members of pedigree 167. Lanes 1-4: affected individuals, lanes 5-8: unaffected individuals, lane 9: undigested S3-S4 PCR amplified fragment and lane 10: λ *PstI*.

CHAPTER 4

DISCUSSION

	Page
EPILEPSY	
4.1 Study Design	161
4.2 Linkage Analysis Study	161
4.3 Is FME a new Clinical and Genetic entity?	162
LQTS	
4.4 Study Design	164
4.5 Founder Mutation Screening	164
4.6 Advantages and Disadvantages of Genetic Testing	165
4.7 Linkage Analysis Study	167
4.8 Haplotype Analysis	169
4.9 Mutation Screening	169
4.9.1 ASREA	169
4.9.2 PCR-SSCP analysis	170
4.9.3 Why were no mutations detected?	171
4.10 Future Studies	172
4.11 Conclusion	173

EPILEPSY

4.1 Study Design

In this study, the molecular genetic technique of linkage analysis was used to test if a rare form of myoclonic epilepsy (FME) was the same as any one of three candidate types of the disease, for which the causative genes or locus had been determined. These candidate loci were assessed for their possible involvement in the development of FME by the generation of two point LOD scores between the disease phenotype and DNA markers at these three test loci.

The candidate forms of epilepsy were chosen based on their clinical similarities with that exhibited by FME. The clinical features were used as a criterion for candidate selection, because the diagnosis of epilepsy is clinical and the classification of individual epileptic syndromes into different entities is based on defining similarities in the type of seizure, age of onset, associated neurologic and other clinical signs, family history, EEG findings and prognosis (Scheuer and Pedley, 1990). A form of epilepsy linked to chromosome 8p (Berkovic, personal communication), DRPLA (Smith, 1958) and EPM1 (Berkovic, 1986) were identified as plausible candidates. Genetic markers closely linked to these candidate loci were employed, to determine if the abnormal gene in FME is the same, or in the same chromosomal location, as in the candidate forms of epilepsy.

4.2 Linkage Analysis Study

The statistical evidence provided by the linkage analysis results indicated that the plausible candidates tested are not the disease-associated loci in the family investigated.

At the *EPM1* locus, two point LOD scores of -14.24, -12.83 and -6.82 were generated at the DNA markers *D21S2040*, *D21S1912* and *D21S1959*, respectively (Table 3.1). These three markers were completely linked to the *EPM1* locus in the study performed by Virtaneva et al., (1996). However, the highly negative LOD scores generated at these markers in pedigree 201 definitely excluded this candidate locus from being involved in FME. At DNA marker *D21S2040*, a LOD score of -1.92 was generated at $\theta = 0.01$ (Table 3.1), this exclusion covers a range of approximately 1% recombination on either side of *D21S2040*, which corresponds to an excluded genetic distance of 1cM telomeric and centromeric to the latter marker.

The triplet repeat in the atrophin gene was used to analyze the DRPLA locus. The choice of this marker in the analysis was twofold, firstly, to determine if this triplet was expanded in FME patients, as is the case in DRPLA (Koide et al., 1994; Nagafuchi et al., 1994) and, secondly, to act as a genotypic marker for use in linkage analysis. The latter approach would allow the investigation of the possible involvement of mutations other than the triplet repeat expansion in the atrophin gene in the development of FME. However, this triplet repeat was not expanded in FME patients as no single larger band was seen in affected individuals that was not present in unaffected individuals. In fact, only two alleles, in the normal size range were seen in all affected individuals (figure 3.4.1). The two point LOD score derived at the *DRPLA* locus was -14.50 at $\theta = 0.00$, thus excluding DRPLA as the causative locus; furthermore, at $\theta = 0.05$, a LOD score of -2.15 was generated (Table 3.1), based on this, approximately 5cM telomeric and centromeric to this marker could be excluded from involvement in FME.

The two point LOD score generated at the DNA marker *D8S264*, to which linkage was found in the Japanese family (Berkovic, personal communication), was -4.46 at $\theta = 0.00$, excluding linkage of this marker locus to FME (Table 3.1). A LOD score of -2.02 was generated at $\theta = 0.01$ at *D8S264* (Table 3.1), this corresponds to exclusion of 1% recombination on both sides of the marker and thus an exclusion of approximately 1cM telomeric and centromeric to *D8S264*. The two other markers analyzed at this locus, *D8S504* 1cM telomeric to *D8S264* and *D8S1781* 2cM centromeric to *D8S264*, generated equivocal LOD scores of 0.69 and 0.68, respectively (Table 3.1). The latter result could possibly be because the alleles of these markers were not very informative in this pedigree.

4.3 Is FME a new clinical and genetic entity?

The three candidate epilepsy syndromes investigated were selected because they were the most closely related to FME with respect to their clinical presentation. The mode of inheritance and the age of onset of the disease made DRPLA a plausible candidate for FME. A form of epilepsy linked to chromosome 8p was considered as candidate based on personal communication with Professor Berkovic.

The form of epilepsy investigated in the present study was considered to be a form of PME (Carr, personal communication). At least five disease groups account for most cases of PME (Berkovic,

1986). However, based on characteristic features, four of the five disease groups could definitively be excluded from being candidates for FME. Sialidosis type 1 was excluded based on the fact that the characteristic clinical feature of macular cherry-red spots in fundus and painful burning hands and feet associated with this disease were absent in FME patients. The age of onset of neuronal ceroid-lipofuscinoses, 2-5 years in the late infantile form and 4-10 years in the juvenile type also led to its exclusion as candidate for FME. The mode of inheritance, autosomal recessive, and the fatality, death within 5-10 years after the first symptom, ruled out Lafora's disease as candidate. In MERRF the inheritance is consistent with mitochondrial (maternal) transmission, thus cancelling out this candidate, as this mode of transmission is not seen in FME. Unlike the preceding forms of PME, the candidature of EPM1 could not be completely ruled out based on any characteristic clinical feature. The age of onset of the disease, 6-18 years, and the fact that it is not a fatal form of PME compared with the other forms of PME, placed it in an equivocal area where its candidacy could not definitively be ruled out or confirmed. Superficially, its involvement as cause of FME is unlikely, as EPM1 is a recessive disorder and the mode of inheritance of FME is autosomal dominant. However, recent findings have shown that mutations in the same genes could be responsible for both the autosomal recessive and the autosomal dominant form of the LQTS (Wang et al., 1996a; Neyroud et al., 1997; Splawski et al., 1997 ; Schulze-Bahr et al., 1997). As described in the present review, the RWS and JLNS forms of LQTS share many of the same clinical features (section 1.2.1 and 1.2.2); however, they differ with respect to mode of inheritance, RWS being autosomal dominant and JLNS autosomal recessive and in their involvement with deafness (Jervell and Lange-Nielsen, 1957; Ward, 1964). The RWS patients have normal hearing while JLNS patients present with deaf mutism. Despite the differences between RWS and JLNS, mutations in the same two genes, *KVLQT1* and *KCNE1*, have been implicated as cause of the disease in both disorders (Wang et al., 1996a; Neyroud et al., 1997; Splawski et al., 1997 ; Schulze-Bahr et al., 1997). Therefore, despite the differences between EPM1 and FME, EPM1 was still considered as candidate for the reasons discussed above.

In the present study, evidence was provided to definitively prove that the three candidate epilepsy syndromes investigated were not responsible for the disease in FME. The fact that these three highly plausible candidates were excluded from being involved in FME does not prove that this is a new genetic entity; however, it does not exclude this hypothesis either. The definitive answer to this question could only be provided after the disease-causing locus is identified.

LQTS

4.4 Study Design

All South African Afrikaner families, in which previous LQTS studies were performed, harboured the same *KVLQT1* Ala212Val mutation (de Jager et al., 1996). All affected members of these families also shared the same haplotype, suggesting the presence of a founder effect. Given this background, the strategy of this study was to first screen for the founder mutation in all probands referred to our group, with the clinical diagnosis of LQTS. If the founder mutation was present in the individual tested, a DNA-based diagnostic test could be offered to the rest of the family, on request. Where possible, family members of the probands were traced and contacted and pedigrees constructed. In the pedigrees constructed, linkage analysis was performed at four of the known causative loci to identify the disease-causing gene. The four loci analyzed were, *HERG*, *KVLQT1*, *SCN5A* and the chromosome 4 locus, which together account for >90% of the known cases of LQTS (Roden et al., 1996). If linkage analysis implicated a specific gene as being the causative gene, intensive mutation screening would be performed in that gene to find the disease-causing mutation(s).

4.5 Founder Mutation Screening

A panel of 12 clinically-affected LQTS individuals newly entered in our group's program was screened for the presence of the Ala212Val mutation in *KVLQT1* and in four individuals this mutation was identified (figure 3.9). Using the probands from the panel as reference point, it was possible to construct three LQTS pedigrees, which were of three different South African sub-population groups, namely persons of Mixed ancestry, Afrikaner and Indian descent.

In the family of Afrikaner descent, named pedigree 168, the Ala212Val mutation was present in the proband, thus a DNA-based diagnostic service could be provided to members of the family who chose to have it. This finding provided further support for the founder gene effect reported by de Jager et al., (1996) in this sub-population group. The Afrikaners are the descendants of a small number of European settlers who arrived in South Africa in the seventeenth and eighteenth centuries and then underwent a rapid expansion in size, largely due to natural population increase (Jenkins, 1990). The "Great Treks", a series of migrations of these Europeans away from the coastal areas, to establish farming communities in the interior of South Africa, took place in the first half of the nineteenth century. The small number of European founders of the Afrikaner population in Cape

Town, the lack of large amounts of immigration from Europe, the Great Treks and the rapid increase in the Afrikaner population all have contributed to the genetic isolation and relative homogeneity of this sub-population group (Jenkins, 1990). The historical background of the Afrikaners in South Africa favoured the presence of founder effects and these have previously been reported in several heritable disorders in this group, including familial hypercholesterolaemia, porphyria variegata, keratolytic winter erythema and hypertrophic cardiomyopathy (Brink et al., 1987; Meissner et al., 1996; Starfield et al., 1997; Moolman-Smook et al., 1999).

The fact that the other two pedigrees investigated in the present study belonged to sub-population groups other than the Afrikaners added a new dimension to the project, because previous LQTS studies in South Africa did not include any other sub-population groups (de Jager et al., 1996). The family of Mixed ancestry, named pedigree 167, tested negative for the *KVLQTI* Ala212Val mutation. Members of this sub-population group originated 150-300 years ago, as a result of admixture of Black African, San, Khoi-Khoi, European and Asian groups (Moolman-Smook et al., 1999). It is not possible to predict from which ancestral group the mutation in pedigree 167 originated because LQTS in this family is not caused by any of the reported *KVLQTI* mutations in the regions investigated with PCR-SSCP analysis and ASREA. To date, LQTS has not been reported in Khoisan or Black Africans, it is not known if this is because of the absence of the disease in this sub-population or because clinical studies have not identified it. The other possibility is that this is a mutation that arose *de novo* since the establishment of this group.

In the family of Indian descent, named pedigree 169, the *KVLQTI* Ala212Val mutation was also not the cause of LQTS. Most Indians in South Africa are descended from people who came from India to South Africa between 1860 and 1911 to work in the sugar plantations of what is now called Kwa-Zulu Natal (Bhana and Bain, 1990). The LQTS has been reported in India (el Mauhoud et al., 1988; MerChant et al., 1988; Behera, 1989), however, as far as could be determined, no disease-causing mutations in any of the known LQTS causative genes have been identified. Thus, it is not possible to predict the origin of the potential mutation, as it could have arisen in India; conversely it could have arisen *de novo* in this sub-population after its establishment in South Africa.

4.6 Advantages and disadvantages of genetic testing

Genetic testing for the *KVLQTI* founder mutation is a diagnostic service offered by our group. The goal of our group is to establish a genetic testing service for all the known forms of LQTS. Unlike

other disorders, where early diagnosis is of limited clinical value because no treatment is available, molecular diagnosis in LQTS, if extended to the treatment of gene carriers, could prevent the occurrence of sudden death (Priori, 1997). However, the impact of genetic information within a family is enormous; those identified as being in the line of transmission of the disease may feel guilty for having passed the “bad” genes. Individuals who were considered to be clinically unaffected may be profoundly upset by the knowledge that they are gene carriers. Immediate relatives of affected individuals will experience emotional and mental anguish, even if they are not screened. Screening has an obvious advantage to the 50% in whom the test result is negative. In addition knowledge that not all their children are affected can be extremely positive and reassuring for affected parents (Priori, 1997).

The alternative to genetic testing is regular clinical monitoring in immediate relatives of affected individuals for signs of the disease (Ryan et al., 1995). However, it is because of the limitations manifested by the clinical diagnostic criteria, that the need for genetic testing arose. Genetic testing is not absolutely necessary in patients who have a definitive diagnosis based on established clinical diagnostic criteria, as all the elements necessary to decide about initiation of therapy are present (Priori et al., 1999). However, genetic testing could prove useful in these individuals, because, depending on the gene identified as responsible for the disease, the precipitating factors, management and treatment varies. Alternatively, when the diagnosis of LQTS is suspected or the patient has an equivocal diagnosis based on clinical criteria, genetic testing could be very useful in establishing the presence of the mutated LQTS genes thereby providing a definitive diagnosis. However, the failure to identify a mutation does not rule out the diagnosis. Genetic testing could also prove worthwhile in a family setting where the disease-causing mutation has been identified in the proband (Priori et al., 1999).

Genetic testing has the potential to define with 100% sensitivity and 100% specificity the genetic status of any member of an affected family. However for this potential to be fully expressed, all the disease-causing genes and associated mutations must be identified (Priori et al., 1999). This has not yet been achieved in LQTS, and therefore, clinical criteria to establish diagnosis are still very important. However, genetic testing could provide knowledge of the gene carrier status of the tested individuals if one of the known LQTS disease-associated mutations is present. This could provide peace of mind in non-gene carriers, and knowledge for gene carriers that could allow them to adopt a preventative lifestyle, as this disease could be fatal and sudden death could occur in individuals

who have no idea that they had the condition. However, gene carriers identified through genetic testing could be disadvantaged in their opportunities for employment, life insurance and loans, which is unfortunate especially in asymptomatic gene carriers who may never express the condition (Ryan et al., 1995).

The decision to undergo genetic testing remains with the patient, or the parents in the case of minors. As sudden death, the most devastating consequence of this disease, could strike without warning, it is of utmost importance to inform not only the public, but especially sufferers and their relatives, about genetic testing, so that they can make an informed decision (Goodwin et al., 1995).

In the present study, the *KVLQT1* Ala212Val mutation was identified in the proband of pedigree 168 of Afrikaner descent. It would have been useful to determine if this family also shares the founder haplotype, as was identified in the previous LQTS studies in South African Afrikaner families (de Jager et al., 1996). However, this was not possible as this family was unwilling to take part in the study and genetic testing was performed in only a few individuals, and most of these individuals were children from which only a small amount of blood was collected (section 3.4.2.1; figure 3.10.2). This emphasizes that the choice of receiving genetic testing remains with the patients, and their wishes must be respected.

4.7 Linkage Analysis Study

In pedigree 167, four of the known LQTS loci were studied by linkage analysis. The results of these analyses led to the definitive exclusion of three of these loci, namely *HERG*, *SCN5A* and the chromosome 4 locus, with LOD scores of -3.12 , -5.01 and -3.23 , respectively (Table 3.2). The five DNA markers used to analyze the *KVLQT1* locus all generated equivocal LOD scores, with the highest LOD score of 0.92 at *DIIS860* (Table 3.2). These five markers spanned a region of 8cM, with the closest linked markers to *KVLQT1* being *TH*, *DIIS1318* and *DIIS860*. The equivocal LOD scores could be explained by the small number of family members who were genotyped and the specific genotypes generated at each of the five marker loci (fig 3.12.1-3.12.5). At each of the five loci analyzed, a specific allele was identified that was present in all affected individuals, however, in each case, the specific allele was also present in 2 other unaffected individuals (section 3.4.2.2.1 and 4.8; figure 3.12.1-3.12.5). The disease status of these two unaffected individuals will be discussed in section 4.8.

Given that the four loci analyzed account for 90% of the known cases of LQTS, the definitive exclusion found at three of the four loci enhances the chance of the fourth locus being the causative locus. Thus, the weakly positive LOD scores generated at the *KVLQT1* locus became relevant, and *KVLQT1* is strongly implicated as the disease-causing gene in pedigree 167. However, an alternative possibility is that this is not the disease gene and furthermore the *KCNE1* locus was not analyzed at the time of this study.

In pedigree 169, three of the four tested loci could again be definitively excluded, these loci were *SCN5A*, the chromosome 4 locus and *KVLQT1* (Table 3.3). At the *KVLQT1* locus, DNA markers which were located further away from *KVLQT1* generated equivocal LOD scores; however, at *DIISI318*, a DNA marker that was shown to be completely linked to *KVLQT1* in a previous study (Wang et al., 1996a), a LOD score of -2.62 was generated. At the *HERG* locus, an equivocal LOD score of 0.2 was generated with *D7S636*. The genotype analysis at this marker showed that allele 9 was present in all affected individuals, as well as two equivocal individuals (section 3.4.2.2.2 figure 3.15.1-3.15.2.). The latter result could explain why an equivocal LOD score was generated at *D7S636*. The definitive exclusion found at three of the 4 loci made the weakly positive LOD score generated at the *HERG* locus relevant and strongly suggests that this is the disease-causing locus in pedigree 169. However, an alternative possibility is that this is not the disease gene and furthermore the *KCNE1* locus was not analyzed at the time of this study. It can be speculated that the two equivocal individuals, II:5 and III:4, carry the disease-causing mutation and are at risk of developing LQTS and sudden cardiac death. A haplotype diagnosis, employing more DNA markers closely linked to the *HERG* locus, could be offered to family members who require it. However, with the caveat that until the actual disease-causing mutation has been identified no molecular diagnosis can be given with absolute certainty.

Linkage analysis requires a single large family or multiple small families from a single genetic isolate to be successful (Berkovic, 1997). In the present study, a relatively small family was analyzed, thus, the equivocal LOD scores generated could be attributed to the small sample size of the study.

4.8 Haplotype Analysis

Haplotype analysis in pedigree 167 showed that all the affected members of this family shared the same combination of alleles at the five DNA markers tested at the *KVLQTI* locus, suggesting that this is the disease-associated haplotype (figure 3.20). However, two unaffected individuals whose QTc fell within the normal range also shared this haplotype, suggesting that they also carried the defective gene (figure 3.20). As mentioned earlier, the diagnosis of LQTS is difficult and often missed by clinicians, resulting in individuals at risk of syncope and sudden death not receiving appropriate treatment (Moss et al., 1991; Vincent et al., 1992). Thus, although definite proof of their carrier status can only be provided after the disease-causing mutation has been found, the two individuals sharing the disease-associated haplotype, should be treated as at risk of LQTS in the mean time. Taken together, the haplotype analysis provided further evidence in favour for linkage to *KVLQTI* in pedigree 167.

4.9 Mutation Screening

The linkage analysis results, as well as the haplotype analysis, implicated the *KVLQTI* gene as disease-causing gene in pedigree 167. Given this evidence, the six transmembrane domains of *KVLQTI*, as published by Wang et al., (1996a), were screened for known and novel mutations employing ASREA and PCR-SSCP analysis.

4.9.1 ASREA

To date, 35 different mutations have been reported in the *KVLQTI* gene and the search for the identification of more disease-causing mutations continues (Wang et al., 1996a; Russel et al., 1996; Donger et al., 1997; van den Berg et al., 1997; Itoh et al., 1998; Saarinen et al., 1998; Splawski et al., 1998; Neyroud et al., 1999). The *KVLQTI* has recently been renamed *KCNQ1* (Neyroud et al., 1999), however, in this report it is still referred to as *KVLQTI*. At the time the study was initiated, the first ten *KVLQTI* mutations described by Wang et al., (1996a) were known and three of these mutations, which affected restriction enzyme sites, were screened for. These mutations were the Ala49Pro mutation situated in S2-S3 region, Arg61Glu also in the S2-S3 region and the Val125Met mutation in the S4-S5 region. However, none of these mutations was detected in the affected individuals of pedigree 167. No other described mutations were screened for by ASREA, as extensive SSCP analysis was performed in the partial S1 and S2-S6 region of *KVLQTI*. It was argued that if any mutation, known or novel were present in these regions it would be picked up

with the SSCP analysis. The absence of the three mutations tested for by ASREA was also confirmed in the results obtained with the SSCP analysis.

In two of three mutations screened with ASREA, namely Arg61Glu and Val125Met, the presence of the mutation introduce a *PvuII* a *StyI* site, respectively. Thus, in the absence of the mutation, after digestion with the respective restriction enzymes, only the undigested PCR fragment would be generated. To ensure that the enzyme was active during the digestion, ideally an internal control should be included in the reaction. For one of these mutations, Arg61Glu it was possible to design an internal control to test the activity of the enzyme. Diluted lambda DNA was included in the reaction mixture prior to digestion. To find a control for the Val125Met mutation proved troublesome, as λ DNA digested with *StyI* generated too many bands, some of which overlapped with the expected fragment sizes generated in the presence of Val125Met. Subsequently, no control was included for screening the Val125Met mutation.

Negative controls, samples amplified from unaffected LQTS individual, were included on each ASREA gel. Ideally, a positive control, a sample amplified from an affected person carrying the mutation in question, would be useful to compare the generated fragment sizes and activity of the enzyme. This type of control was included in the analysis of the Ala212Val mutation; however, such samples were not available for the other three mutations. The expected fragment sizes of both the mutant and the wild type alleles were determined with the aid of the computer program Genepro, prior to PCR-based restriction enzyme analysis. This, and the inclusion of a molecular weight marker on each polyacrylamide gel, allowed the investigator to gauge the fragment sizes and the compare them with those predicted.

4.9.2 PCR-SSCP analysis

The main mutation screening technique used in the present study was PCR-SSCP analysis, because of its simplicity and potential for high output of up to 100% mutation detection efficiency using multiple conditions (Michaud et al., 1992). Four different electrophoresis conditions were used to perform PCR-SSCP analysis, as variable conditions improve the resolution power and also increase mutation detection sensitivity. On each gel, the PCR amplified S6-Pore region of a person harbouring the *KVLQTI* Ala212Val mutation was included, this sequence variation was detected under all four conditions, attesting to the sensitivity of the SSCP analysis. No abnormally migrating

bands were identified in the partial S1-S2, S3-S4, S4, S4-S5, Pore-S5, S6-Pore and S6 regions under any of the electrophoretic conditions (figure 3.22.1-3.22.4). However, a mobility shift was detected in all affected members of pedigree 167 in the PCR fragment derived from the S2-S3 region of the *KVLQT1* gene and also the two unaffected individuals that shared the disease-associated haplotype. However, this mobility shift was also detected in a third unaffected individual, of pedigree 167, indicating that this is not the disease-associated mutation. This mobility shift was repeatedly detected by PCR-SSCP under two different gel conditions. DNA sequence analysis of the S2-S3 region revealed a G→A transition in the intronic sequence.

A panel of 40 unaffected control individuals of Mixed ancestry was screened for this sequence variation and three heterozygous G/A individuals were detected. Thus, the ratio of the G:A alleles was 0.96:0.037, indicating that this sequence variation is a non-pathological polymorphism. A polymorphism is defined as “a Mendelian trait that exists in the population in at least two phenotypes, neither of which occurs at a frequency less than 1%” (Cotton and Scriver, 1998).

4.9.3 Why were no mutations detected?

As discussed above, no novel or known mutations were detected employing ASREA or PCR-SSCP analysis in *KVLQT1* in pedigree 167. This is in conflict with the hypothesis that *KVLQT1* is the disease-causing gene in pedigree 167. However, the fact that no disease-associated mutation was detected could be attributed to the fact that not the entire *KVLQT1* gene was screened in the present study, as the complete sequence was unavailable at the time the study was initiated. Thus, although the disease-causing mutation was not present in the regions investigated, it may be located in the regions not analyzed. Another possible explanation why no disease-associated mutation was detected could be because it is situated within the regulatory regions or intronic sequences important for splicing or transcription, which were not investigated

Incomplete mutation scanning, compounded by use of only one PCR-SSCP condition, which is reported to detect less than 80% of mutations, can thus generate a low mutation detection rate (Cotton, 1996). However, in the present study, multiple different SSCP conditions were used, thus the absence of mobility shifts detected most probably indicates the absence of mutations in the regions investigated.

4.10 Future Studies

The aim of the present study was to identify the disease-causing locus in four families with episodic loss of consciousness, in three of these families the clinical diagnosis of LQTS was made and the remaining family showed a form of epilepsy, termed FME.

In the epilepsy study, three highly plausible candidate forms of epilepsy were analyzed, to test if they are responsible for the disease in FME. The results obtained through this analysis provided irrefutable evidence that none of these three candidate epilepsy syndromes is involved in FME. This was not unexpected, as our group's hypothesis is that this is a new clinical and genetic entity and, as these candidates were the most closely clinically related epilepsies to FME, this result provided evidence in favour of our hypothesis. In the absence on any other obvious candidates for this disease, a random genome search would be the next logical step; however, this will require the presence of a single large or multiplex small, families. To this end, the focus of the study is currently to extend the present family and also to seek new families in whom this form of epilepsy segregates. A second family, pedigree 202, was identified; this family lived in a small town close to where the first family was identified. Although a common ancestor could not be identified, the rarity of the disorder and the geographical proximity of the families make it highly likely that they are related. A high mortality rate in of the older generation, due to homicide and other causes, and the lack of birth records have made the task of linking the two families more difficult (J. Carr, manuscript in preparation). However, it is possible that together the two pedigrees may strengthen the power of future studies.

In the LQTS study, the results obtained are the first report of genetic heterogeneity in South African LQTS families. This is also the first report of LQTS in ethnic groups other than the Afrikaners in South Africa. In pedigree 168 of Afrikaner descent, the founder mutation, the *KVLQT1* Ala212Val mutation, was identified as cause of the disease, providing further support for the founder effect previously reported in this sub-population group (de Jager et al., 1996). A mutation, other than this founder mutation, in *KVLQT1* was implicated as the cause of the disease in the family of Mixed ancestry. In the family of Indian descent, *HERG* was implicated as the defective gene.

Although the *KVLQT1* gene was implicated as the disease-causing gene in pedigree 167, the disease-associated mutation was not identified; thus, future studies should focus on finding the

disease-associated mutation. At the time of the study, the complete sequence of *KVLQTI* was not available, therefore, only part of this gene was screened for mutations. Thus, future work on this project could include screening the regions of *KVLQTI* not analyzed in the present study. In pedigree 169, *HERG* was implicated as the causative gene; however, no mutation screening was performed in this gene due to time constraints.

Three pedigrees were constructed from a panel of twelve probands and new probands are continuously added to the panel. Thus, future work could also focus on constructing more pedigrees from this panel of affected individuals to perform linkage analysis at the other known LQTS loci. The fifth disease-causing locus, *KCNE1* was not investigated because it was identified close to the completion of the present study. Thus, future studies should also focus on analyzing its involvement in pedigree 167 and 169 to confirm the evidence implicating *KVLQTI* and *HERG* in pedigree 167 and 169, respectively.

Currently, an easy and cost-effective DNA-based diagnostic test and an unequivocal diagnosis can only be made if one of the reported mutations which affects restriction enzyme sites is present in the tested individual. However, it is important to identify and characterize the disease-causing genes and mutations found in South African LQTS families, firstly, because it could help to improve the current DNA-based diagnostic service. In addition, although preliminarily, data are accumulating that therapy for LQTS should be individualized for each disease-causing gene and its associated mutation, also the precipitating factors of the different forms of the disease are diverse (Schwartz et al., 1999 (submitted)). Thus, if the disease-causing locus and mutation is identified in a pedigree, it could have important implications for therapy and avoidance of precipitating factors.

4.12 Conclusion

In conclusion, the results obtained in the present study paved the way for further studies to describe and characterize precisely the two diseases studied, a task that is important because of genetic heterogeneity seen in both these group of disorders.

The long term goal of this project is to identify the disease-causing gene(s) and associated mutation(s) in the families investigated. The importance of such studies has clearly been explained, namely, that it could facilitate early identification of susceptible individuals and early treatment of

the disease. A presymptomatic molecular diagnosis in both LQTS and epilepsy could prove fruitful, because in both cases treatment is available, unlike disorders where no successful treatment is available, in which case knowing that the disease is present is of limited clinical value and may cause distress for the patient. Molecular diagnosis would also allow for the avoidance of misdiagnosis of LQTS as epilepsy.

A lack of an adequate and systematic classification system has been a major stumbling block in the clarification of the aetiology of epilepsy. Identification and characterizing of epilepsy susceptibility genes, as was the objective in the present study, could play an important role in the development of a more clinically useful classification of seizure disorders.

In the present study, the molecular basis of two clinical causes of loss of consciousness was investigated, namely LQTS and FME. In the LQTS families, the application of genetic markers allowed the differentiation between three molecular causes of LQTS. The latter finding is useful as the precipitating factors for the life threatening arrhythmias of LQTS differ according to the specific gene involved (Schwartz et al., 1995). Also data are accumulating to indicate that the abnormalities caused by the different causative genes of LQTS could be corrected by gene specific therapies (Compton et al., 1996; Keating et al., 1996; Priori et al., 1996). In the epilepsy family, the cause of loss of consciousness could not be determined, however, three highly plausible candidate loci were ruled out.

APPENDIX I

BUFFERS, SOLUTIONS AND MARKERS

1. BUFFERS

1.1 Cell Lysis Buffer

Sucrose	0.32M
Triton-X-100	1%
MgCl ₂	5mM
Tris-HCl (pH7.6)	10mM
Make up to 1L with dH ₂ O	

1.2 50 X TAE-Buffer

Tris-OH	40mM
Glacial acetic acid	20mM
Na ₂ EDTA	2mM
pH to 8.1 with glacial acetic acid	

1.3 10 X TBE-Buffer

Tris-OH (pH 8.0)	89mM
Boric Acid	89mM
Na ₂ EDTA (pH 8.0)	2mM

1.4 1 X TE-Buffer

Tris-HCl (pH 8.0)	10mM
EDTA (pH 8.0)	1mM

2. SOLUTIONS

2.1 SOLUTIONS FOR DNA EXTRACTION

2.1.1 Phenol:/Chloroform

Mix phenol saturated with 1 X TE, chloroform and 8 hydroxyquinoline in a ratio of 25:24:1. Store at 4⁰C.

2.1.2 Chloroform:/Octanol

Mix chloroform and octanol in a ratio 24:1. Store at 4⁰C.

2.1.3 NaAc

NaAc.3 H₂O 40.81g

H₂O 50ml

pH to 5.2 with glacial acetic acid

H₂O to 100ml

2.1.4 Na-EDTA

NaCl 75mM

EDTA 25mM

2.2 ACRYLAMIDE GEL STOCK SOLUTIONS

2.2.1 30% Acrylamide stock solution (2.7%) cross linking for PCR-SSCP and other polyacrylamide gels

Acrylamide		30g
Bis-acrylamide		0.8g
H ₂ O	to	100ml

First add 50ml of dH₂O and mix solution on magnetic stirrer for 2 hours. Make up to 100ml with dH₂O and store at 4⁰C.

2.2.2 10% Ammonium persulphate (APS)

APS		1g
H ₂ O	to	10ml

Mix well and store at 4⁰C. Make fresh weekly.

2.3 GELS

2.3.1 1.5% Agarose Gels For Monitoring PCR Products

Agarose		1.5g
10 X TBE		10ml
H ₂ O		100ml
Ethidium bromide (10mg/ml)		10µl

2.3.2 Gels For PCR-SSCP Analysis Under Non-Denaturing Conditions**2.3.2.1 5% Polyacrylamide gel without glycerol**

30% acrylamide/0.8%

Bis-acrylamide	33ml
H ₂ O	156ml
10 X TBE	10ml
10% APS	1ml
TEMED	100µl

2.3.2.2 5% Polyacrylamide gel with 10% glycerol

30% acrylamide/0.8%

Bis-acrylamide	33ml
H ₂ O	136ml
10 X TBE	10ml
Glycerol	20ml
10% APS	1ml
TEMED	100µl

2.3.2.3 10% Polyacrylamide gel without glycerol

30% acrylamide/0.8%

Bis-acrylamide	66ml
H ₂ O	123ml
10 X TBE	10ml
10% APS	1ml
TEMED	100µl

2.3.2.4 10% Polyacrylamide gel with glycerol

30% acrylamide/0.8%

Bis-acrylamide	66ml
H ₂ O	103ml
Glycerol	20ml
10 X TBE	10ml
10% APS	1ml
TEMED	100µl

2.3.2.5 0.35 X MDE gel

2 X MDE TM Stock solution	28ml
10 X TBE	9.7ml
H ₂ O	122ml
10% APS	1.6ml
TEMED	160µl

2.3.3 12% Polyacrylamide Gel For Restriction Enzyme Mutation Analyses

30% acrylamide/0.8%

Bis-acrylamide	4ml
H ₂ O	5ml
10 X TBE	1ml
10% APS	80µl
TEMED	20µl

2.3.4 5% Denaturing Polyacrylamide Gel

Urea	33.3g
H ₂ O	30ml
30% acrylamide/0.8%	
Bis-acrylamide	12.75ml
10 X TBE	7.5ml
10% APS	375µl
TEMED	37.5µl

2.4 SOLUTIONS FOR ETHIDIUM BROMIDE STAINING (10mg/ml)

Ethidium bromide	500mg
H ₂ O	to 50ml

Stir well on magnetic stirrer for 4 hours, store in a dark container at 4⁰C.

2.5 SOLUTIONS FOR SILVER STAINING

2.5.1 0.1% AgNO₃

AgNO ₃	1g
H ₂ O	to 1L

Prepare fresh solution before use

2.5.2 Developing Solution

NaOH	15g
NaBH ₄	0.1g
Formaldehyde	4ml
H ₂ O	to 1L

Mix well using magnetic stirrer. Prepare fresh solution before use.

2.6 SOLUTION FOR SEQUENCING-DMSO

DMSO 30 μ l

H₂O 20 μ l

2.7 SOLUTIONS FOR AUTORADIOGRAPHY**2.7.1 Developer Solution (Polygon A) (Champion Photochemistry)**

Solution 1 (Champion Photochemistry) 1.98ml

Solution 2 (Champion Photochemistry) 18.1ml

H₂O to 9900ml

Mix well.

2.7.2 Stop Solution

6% acetic acid (BDH) 540ml

H₂O to 9000ml

Mix well.

2.7.3 Fixer Solution

Perfix 1800ml

Hardener-S 225ml

H₂O to 9000ml

Mix well.

2.8 LOADING DYES**2.8.1 Bromophenol Blue Loading Dye For Agarose And Polyacrylamide Gels**

Bromophenol Blue	0.2%
Glycerol	50%
Tris-HCl (pH 8)	10mM
Mix by vortexing solution	

2.8.2 SSCP Loading Dye

Formamide	95ml
NaOH	10mM
EDTA	20mM
Bromophenol blue	0.05g
Xylene cyanol	0.05g
Mix well. Aliquot into 2ml eppendorf tubes. Store at 4 ⁰ C.	

2.8.3 Sequencing Stop Buffer

Formamide	95%
Bromophenol blue	0.01%
Xylene Cyanol	0.01%

2.9 SEQUENCING TERMINATION MIX**2.9.1 ddGTP**

ddGTP	30μm
7-Deaza dGTP	20μm
dATP	20μm
dTTP	20μm
dCTP	20μm

2.9.2 ddATP

ddATP	350µm
7-Deaza dGTP	20µm
dATP	20µm
dTTP	20µm
dCTP	20µm

2.9.3 ddTTP

ddGTP	600µm
7-Deaza dGTP	20µm
dATP	20µm
dTTP	20µm
dCTP	20µm

2.9.4 ddCTP

ddGTP	200µm
7-Deaza dGTP	20µm
dATP	20µm
dTTP	20µm
dCTP	20µm

3. MOLECULAR SIZE MARKER**3.1 BACTERIOPHAGE LAMBDA *Pst* I**

Lambda DNA (10µg)	10µl
Buffer H	2µl
<i>Pst</i> I (Promega)	20U
H ₂ O	to 20µl

Incubate at 37⁰C for 2 hours, heat inactivate at 65⁰C for 5 minutes. Load 1µl onto silver stained polyacrylamide gels 3µl on an ethidium bromide stained agarose gel.

APPENDIX II

LIST OF SUPPLIERS

$[\alpha\text{-}^{32}\text{P}]\text{dCTP}$	Amersham
Agarose	Seakem
Ammonium Persulphate	Merck
Acetic acid	BDH chemicals
AgNO ₃	Merck
Acrylamide	BDH Chemicals
Bisacrylamide	Merck
Boric acid	Merck
Bromophenol blue	BDH Chemicals
Chloroform	BDH Chemicals
dATP	Boehringer Mannheim
dCTP	Boehringer Mannheim
dGTP	Boehringer Mannheim
dTTP	Boehringer Mannheim
DMSO	Sigma
Ethanol	Boehringer Mannheim
Ethidium bromide	Sigma
EDTA	Boehringer Mannheim
λ mol TM sequencing kit	Promega
FIX solution	M&B Suppliers
Formamide	Merck
Formaldehyde	Merck
Gel sealing tape	Sigma
Gelbond TM PAG polymer	FMC
GLAD ^R WRAP	Multifoil Trading (Pty) Ltd
Glycerol	BDH Chemicals
Hha1	Amersham

Iso-amyl alcohol	Merck
Lambda DNA	Promega
Lysozyme	Boehringer Mannheim
MgCl ₂	Sigma
Mineral oil	BDH Chemicals
3MM Whatman paper	Merck
NaBH ₄	Merck
NaCl	BDH Chemicals
NaOH	Merck
NaAc	Merck
Octanol	Merck
Proteinase K	Sigma
Phenol	Merck
Polycon A	Champion photochemistry
PstI	Promega
Qiagen kit	Stratagen
Taq polymerase	Promega
Temed	Promega
Tris	Merck
Triton X100	BDH Chemicals
Urea	BDH Chemicals
X-ray film	Protea
Xylene cyanol	M&B laboratory chemicals

REFERENCES

- Attali B. (1996). **A new wave for heart rhythms.** *Nature* **384**: 24-25.
- Ballardie F. W., Murphy R. P. and Davis J. (1983). **Epilepsy: a presentation of the Romano-Ward syndrome.** *Br. Med. J.* **287**: 896-897.
- Barhanin J., Lesage F., Guillemare E., Fink M., Lazdunski M. and Romey G. (1996). **KVLQT1 and Isk (minK) proteins associate to form the IKs cardiac potassium current.** *Nature* **384**: 78-80.
- Barinaga M. (1998). **Tracking down mutations that can stop the heart.** *Science* **281**: 32-34.
- Behera M. (1987). **Jervell and Lange-Nielsen syndrome in a middle-aged patient.** *Postgrad. Med. J.* **63**: 395-396.
- Benhorin J., Kalman Y.M., Medinna A., Towbin J., Rave-Harel N., Dyer T.D., Blangero J., MacCluer J.W. and Kerem B. (1993). **Evidence of genetic heterogeneity in the long QT syndrome.** *Science* **260**: 1960-1962.
- Benson D.W., MacRae C.A., Vesely M.R., Walsh E.P., Seidman J.G., Seidman C.E. and Satler C.A. (1996). **Missense mutation in the pore region of HERG causes familial long QT syndrome.** *Circulation* **93**: 1791-1795.
- Berkovic S.F., Andermann F., Carpenter S. and Wolfe L.S. (1986). **Progressive myoclonus epilepsy: specific causes and diagnosis.** *New Engl. J. Med.* **315**: 296-305.
- Berkovic S.F., Cochius J., Andermann E. and Andermann F (1993). **Progressive myoclonus epilepsies: clinical and genetic aspects.** *Epilepsia* **34** (suppl 3): S19-S30.
- Berkovic S. F. (1997). **Epilepsy genes and the genetics of epilepsy syndromes: The promise of new therapies based on genetic knowledge.** *Epilepsia* **38** (Suppl. 9): S32-S36.

- Berkovic S.F., Howell R.A., Hay D.A. and Hopper J.L (1998). **Epilepsies in twins: Genetics of the major epilepsies syndromes.** *Ann. Neurol.* **43**: 435-445.
- Bhana S. and Bain J. (1990). **Setting down roots: Indian migrants in South Africa.** Johannesburg, South Africa: Witwatersrand University Press, 1990:15-43.
- Bhandari A., Scheinman M.M., Morady F., Svinarich J., Mason J. and Winkle R. (1984). **Efficacy of left sympathectomy in the treatment of patients with the long QT syndrome.** *Circulation* **70**: 1018-1023.
- Bird A.P. (1986). **CpG-rich islands and the function of DNA methylation.** *Nature* **321**: 209-213.
- Bonner T.I., Buckley N.J., Young C. and Brann M.R. (1987). **Identification of a family of muscarinic acetylcholine receptor genes.** *Science* **237**: 527-532.
- Brink P.A., Steyn L.T., Coetzee G.A. and van der Westhuyzen D.R. (1987). **Familial hypercholesterolaemia in South African Afrikaners. PvuII and StuI polymorphisms in the LDL-receptor gene consistent with a predominating founder gene effect.** *Hum Genet.* **77**:32-35.
- Brook J.D., McCurrach M.E., Harley H.G., Buckler A. J., Church D., Aburatani H., Hunter K., Stanton V.P., Thirion J.P., Hudson T., Sohn R., Zemelman B., Snell R.G., Rundle S.A., Crow S., Davies J., Shelbourne P., Buxton ., Jones C., Juvonen V., Johnson K., Harper P.S., Shaw D.J. and Housman D.E. (1992). **Molecular basis of myotonic dystrophy: Expansion of a trinucleotide (CTG) repeat at the 3' end of a transcript encoding a protein kinase family member.** *Cell* **68**: 799-808.
- Brown A.M. (1997). **Cardiac potassium channels in health and disease.** *Trends Cardiovasc. Med.* **7**: 118-124.
- Bruggeman A., Pardo L.A., Struhmer W. and Pongs O. (1993). **Ether-a-go-go encodes a voltage-gated channel permeable to K⁺ and Ca²⁺ and modulated by cAMP.** *Nature* **365**: 445-448.

Buxton J., Shelbourne P., Davies J., Jones C., Van Tongeren T., Aslanidis C., de Jong P., Jansen G., Anvret M., Riley B., Williamson R. and Johnson K. (1992). **Detection of an unstable fragment of DNA specific to individuals with myotonic dystrophy.** *Nature* **355**: 547-548.

Charlier C., Singh N.A., Ryan S.G., Lewis T.B., Reus B.E., Leach R.J. and Leppert M. (1998) **A pore mutation in a novel KQT-like potassium channel gene in an idiopathic epilepsy family.** *Nat. Genet.* **18**: 53-55.

Chin H., Kozak C., Kim H.L., Mock B. and McBride O.W. (1991). **A brain L-type calcium channel α 1 subunit gene (CCHL1A2) maps to mouse chromosome 14 and human chromosome 3.** *Genomics* **11**: 914-919.

Collins F.S. (1992). **Positional cloning: Lets not call it reverse anymore.** *Nat. Genet.* **1**: 3-6.

Collins F. and Galas D. (1993). **A new five-year plan for the U.S. Human Genome Project.** *Science* **262**: 43-47.

Commission of Classification and Terminology of the Internasional League Against Epilepsy (1981). **Proposal for revised clinical and electroencephalographic classification of epileptic seizures.** *Epilepsia* **22**: 489-501.

Commission of Classification and Terminology of the International League Against Epilepsy (1989). **Proposal for revised classification of epilepsies and epileptic syndromes.** *Epilepsia* **30**: 389-399.

Compton S.J., Lux R.L., Ramsey M.R., Strellich K.R., Sanguinetti M.C., Green L.S.M., Keating M.T. and Mason J.W. (1996). **Genetically defined therapy of inherited long QT syndrome: Correction of abnormal repolarization by potassium.** *Circulation* **94**: 1018-1022.

Cotton R.G. (1996). **Detection of unknown mutations in DNA: catch-22.** *Am. J. Hum. Genet.* **59**: 289-291.

Cotton R.G.H. and Scriver C.R. (1998). **Proof of "disease causing" mutation.** *Hum. Mut.* **12**:1-3.

Curran M., Atkinson D., Timothy K., Vincent G.M., Moss A.J., Leppert M. and Keating M. (1993). **Locus Heterogeneity of Autosomal Dominant Long QT Syndrome.** *J. Clin. Invest.* **92**: 799-803.

Curren M.E., Splawski I., Timothy K.W., Vincent G.M., Green E.D. and Keating M.T. (1995). **A molecular basis for cardiac arrhythmia: *HERG* mutations cause long QT syndrome.** *Cell* **80**: 795-803.

De Jager T., Corbett C.H., Badenhorst J.C.W., Brink P.A. and Corfield V.A. (1996). **Evidence of a long QT founder gene with varying phenotypic expression in South African families.** *J. Med. Genet.* **33**: 567-573.

Delgado-Escueta A.V., Serratosa J.M., Liu A., Weissbecker K., Medina M.T., Gee M., Treiman L.J. and Sparkes R. S. (1994). **Progress in mapping epilepsy genes.** *Epilepsia* **35 (Suppl.1)**: S29-S40.

De Martinville B. and Francke U. (1983). **The c-H-ras1, insulin and β -globin loci map outside the deletion associated with aniridia –Wilms' tumour.** *Nature* **305**: 641-643.

Dichter M.A. (1997). **Basic mechanisms of epilepsy: Targets for therapeutic intervention.** *Epilepsia* **38 (Suppl. 9)**: S2-S6.

Donger C., Denjoy I., Berthet M., Neyroud N., Cruaud C., Bennaceur M., Chivoret G., Schwartz K., Coumel P. and Guicheney P. (1997). ***KVLQT1* C-terminal missense mutation causes a forme fruste long QT syndrome.** *Circulation* **96**: 2778-2781.

Dorney P. Langer F. and Panozzo D. (1990). **Cardiac anatomy and physiology.** *In*: Eckman M., Falk D., Law K., Namy C. and Price M.E. (Eds.) ECG interpretation. Springhouse corporation pp. 1-15.

Duchowny M. and Harvey A. S. (1996). **Pediatric Epilepsy Syndromes: An update and critical review.** *Epilepsia* **37(Suppl.1)**: S26-S40.

Duggal P., Vesely M.R., Wattanasirichaigoon D., Villafane J., Kaushik V. and Beggs A.H. (1998). **Mutation of the gene for IsK associated with both Jervell and Lange-Nielsen and Romano-Ward forms of long QT syndrome.** *Circulation* **97**: 142-146.

Dumaine R., Wang Q., Keating M.T., Hartmann H.A., Schwartz P.J., Brown A.M. and Kirsch G.E. (1996). **Multiple mechanisms of Na⁺ channel-linked long QT syndrome.** *Circ. Res.* **78**: 916-924.

Duyk G.M., Kim S., Myers R.M. and Cox D.R. (1990). **Exon trapping: a genetic screen to identify candidate transcribed sequences in cloned mammalian genomic DNA.** *Proc. Nat. Acad. Sci. USA* **87**: 8995-8999.

Engel J.Jr. 1989. **Perspectives In: Seizures and Epilepsy.** F.A Davis Company. Philadelphia, pp22-37.

Eldar M., Griffin J.Y., Abbott J.A., Benditt D., Bhandari A., Herre J.M., Benson D.W. and Scheinman M.M. (1987). **Permanent cardiac pacing in patients with the long QT syndrome.** *J. Am. Coll. Cardiol.* **10**: 600-607.

El Mauhoud M., Sabharwal H.S., Aggarwal V.P., Ben-Musa A.A. and Shembesch A.A. (1988). **Idiopathic long QT syndrome masquerading as epilepsy.** *India Pediatr.* **25**: 94-96.

Fraser G.R., Froggatt P. and James T.N. (1964). **Congenital deafness associated with electrocardiographic abnormalities, fainting attacks and sudden death.** *Quart. J. Med.* **33**: 361-385.

Fu Y.H., Kuhl D.P., Pizzuti A., Pieretti M., Sutcliffe J.S., Richards S., Verkerk A.J.M.H., Holden J.J.A., Fanwick R.G.Jr., Warren S.T., Oostra B.A., Nelson D.L. and Caskey C.T. (1991). **Variation of the CGG repeat at the fragile X site results in genetic instability: resolution of the Sherman paradox.** *Cell* **67**: 1047-1058.

Fu Y.H., Pizzuti A., Fenwick G., King Jr. J., Rajnarayan S., Dunne P.W., Dubel J., Nasser T., Ashizawa P., De Jong P., Wieringa B., Korneluk R., Perryman M.B., Epstein H.F. and Caskey C.T.

(1992). **An unstable triplet repeat in a gene related to myotonic muscular dystrophy.** *Science* **255**: 1256-1258.

Gejman P.V and Gelernter J. (1993). **Mutational analysis of candidate genes in psychiatric disorders.** *Am. J. Med. Genet.* **48**: 184-191.

Goldensohn E. S., Porter R.J. and Schwartzkroin P.A. (1997). **The American Epilepsy Society: An historic perspective on 50 years of advances in research.** *Epilepsia* **38**: 124-150.

Gellens M., George A., Chen L., Chahine M., Horn R., Barchi R. and Kallen R. (1992). **Primary structure and functional expression of the human cardiac tetrodotoxin-insensitive voltage-dependent sodium channel.** *Proc. Natl. Acad. Sci. USA* **89**: 554-558.

George A.L., Varkony T.A., Drabkin H.A., Han J., Knops J.F., Finley W.H., Brown G.B., Ward D.C. and Hass M. (1995). **Assignment of the human heart tetrodotoxin-resistant voltage-gated Na⁺ channel α -subunit gene (SCN5A) to band 3p21.** *Cytogenet. Cell. Genet.* **68**: 67-70.

Goodwin J.F. (1995) **Genetic testing for familial hypertrophic cardiomyopathy in newborn infants. Hypertrophic cardiomyopathy can be treated but not cured.** *BMJ* **311**: 58.

Green E.D., Idol J.R., Mohr-Tidwell R.M., Branden V.V., Peluso D.C., Fulton R.S., Massa H.F., Magness C.L., Wilson A.M., Kimura J., Weissenbach J. and Trask B.J. (1994). **Integration of physical, genetic and cytogenic maps of human chromosome 7: isolation and analysis of yeast artificial chromosomes for 117 mapped genetic markers.** *Hum. Mol. Genet.* **3**: 489-501.

Green E.D. and Maynard V.O. (1990). **Systematic screening of yeast artificial-chromosome libraries by use of the polymerase chain reaction.** *Proc. Natl. Acad. Sci. USA* **87**: 1213-1217.

Gusella J.F., Wexler N.S. and Conneally P.M. (1983). **A polymorphic DNA marker genetically linked to Huntington's disease.** *Nature* **305**: 234-238.

Hamada H., Petrino M.G. and Kakunaga T. (1984). **Characterization of genomic poly (dT-dG). poly (dC-dA) sequences: Structure, organization and conformation.** *Mol. Cell. Biol.* **4**: 2610-2621.

Hästbacka J., de la Chapelle A., Mahtani M.M., Clines G., Reeve-Daly M.P., Daly M., Hamilton B.A., Kusumi K., Trivedi B., Weaver A., Coloma A., Lovett M., Buckler A., Kaitila I. and Lander E.S. (1994). **The diastrophic dysplasia gene encodes a novel sulfate transporter: Positional cloning by fine-structure Linkage disequilibrium mapping.** *Cell* **78**: 1073-1087.

Hästbacka J., de la Chapelle A., Kaitila I., Sistonen P., Weaver A and Lander E.S (1992). **Linkage disequilibrium mapping in isolated founder populations: diastrophic dysplasia in Finland.** *Nat. Genet.* **2**: 204-211.

Hochgeschwender U., Sutcliffe J.G. and Brennan M.B. (1989). **Construction and screening of a genomic library specific for mouse chromosome 16.** *Proc. Natl. Acad. Sci. USA.* **86**: 8482-8486

Itoh T., Tanaka T., Nagai R., Kikuchi K., Ogawa S., Okada S., Yamagata S., Yano K., Yazaki Y. and Nakamura Y. (1998). **Genomic organization and mutational analysis of KVLQT1, a gene responsible for familial long QT syndrome.** *Hum. Genet.* **103**: 290-294.

Jackman W.M., Friday K.J., Anderson J.L., Aliot E.M., Clark M. and Lazzara R. (1988). **The long QT syndromes: A critical review, new clinical observations and a unifying hypothesis.** *Prog. Cardiovasc. Dis.* **31**: 115-172.

Jain S., Padma M.V., Puri A., Jyoti and Maheshwari M.A. (1997). **Occurrence of epilepsies in family members of Indian probands with different epileptic syndromes.** *Epilepsia* **38**: 237-244.

Jeffery S., Jamiesonn R., Patton M. and Till J. (1992). **Long QT and Harvey-ras.** *Lancet* **339**: 255.

Jenkins T. (1990). **Medical genetics in South Africa.** *J. Med. Genet.* **27**: 760-779.

Jervell A. and Lange-Nielsen F. (1957). **Congenital deaf-mutism, functional heart disease with prolongation of the Q-T interval and sudden death.** *Am. Heart J.* **54**: 59-68.

Jhanwar S.C., Neel B.C., Hayward W.S. and Chaganti R.S.K. (1983). **Localization of c-ras oncogene family on human germ-line chromosomes.** *Proc. Natl. Acad. Sci. USA* **80**: 4794-4797.

Jiang C., Atkinson D., Towbin J., Splawski I., Lehmann M.H., Li H., Timothy K., Taggart R.T., Schwartz P.J., Vincent G.M., Moss A.J. and Keating M.T. (1994). **Two long QT syndrome loci map to chromosome 3 and chromosome 7 with evidence for further heterogeneity.** *Nat. Genet.* **8**: 141-147.

Jorde L.B. (1995). **Linkage disequilibrium as a gene mapping tool.** *Am. J. Hum. Genet.* **56**: 11-14.

Kamb A., Wang C. Thomas A., DeHoff B.S., Norris F.H., Richardson K., Rine J., Skolnick M.H. and Rostek P.R. Jr (1995). **Software trapping: a strategy for finding genes in large genomic regions.** *Comput. Biomed. Res.* **28**: 140-153.

Keating M., Atkinson D., Dunn C., Timothy K., Vincent G.M. and Leppert M. (1991). **Linkage of cardiac arrhythmia, the long QT syndrome, and the Harvey *ras-1* gene.** *Science* **252**: 704-706.

Keating M. (1992). **Linkage analysis and long QT syndrome: Using genetics to study cardiovascular disease.** *Circulation* **85**: 1973-1986.

Keating M. (1993). **Evidence of Genetic Heterogeneity in the Long QT Syndrome.** *Science* **260**: 1960-1962.

Keating M. (1996). **The long QT Syndrome: A review of recent molecular genetic and physiologic discoveries.** *Medicine* **75** (1): 1-5.

Kidd K.K., Bowcock A.M., Schmidtke J., Track R.K., Ricciuti F., Hutchings G., bale A., Pearson P. and Willard H.F, with help from Gelerner J., Giuffra L. and Kubzaela K. (1989). **Report of the**

DNA committee and catalogs of cloned and mapped genes and DNA polymorphisms. *Cytogenet. Cell Genet.* **51**: 622-947.

Koch M.C., Steinmeyer K., Lorenz C., Ricker K., Wolf F., Otto M., Zoll B., Lehmann-Horn F., Grzeschik K.H. and Jentsch T.J. (1992). **The skeletal muscle chloride channel in dominant and recessive human myotonia.** *Science* **257**: 797-800.

Koide R., Ikeuchi T., Onodera O., Tanaka H., Igarashi S., Endo K., Takahashi H., Kondo R., Ishikawa A., Hayashi T., Saito M., Tomoda A., Miike T., Naito H., Ikuta F. and Tsuji S. (1994). **Unstable expansion of CAG repeat in hereditary dentatorubral-pallidolusian atrophy (DRPLA).** *Nat. Genet.* **6**: 9-13.

Komure O., Sano A., Nishino N., Yamauchi N., Ueno S., Kondoh K., Sano N., Takahasi M., Murayama N., Kondo I., Nagafuchi S., Yamada M. and Kanazawa I. (1995). **DNA analysis in hereditary dentatorubral-pallidolusian atrophy: Correlation between CAG repeat length and phenotypic variation and the molecular basis of anticipation.** *Neurology.* **45**: 143-149.

Kondo I., Ohta H., Yazaki M., Ikeda J.E., Gusella J.F. and Kanazawa I. (1990). **Exclusion mapping of the hereditary dentatorubropallidolusian atrophy gene from the Huntington's disease locus.** *J. Med. Genet.* **27**: 105-108.

Koskiniemi M., Donner M., Majuri H., Haltia M. and Norio R. (1974). **Progressive myoclonus epilepsy: a clinical and histopathological study.** *Acta Neurol. Scand.* **50**: 307-332.

Lafreniere R.G. de Jong P.J. and Rouleau G. A. (1995). **A 405-kb cosmid contig and HindIII restriction map of the progressive myoclonus epilepsy type 1 (EPM1) candidate region in 21q22.3.** *Genomics.* **29**: 288-290.

Lafrenière R.G., Rochefort D.L., Chrétien N., Rommens J.M., Cocuis J.I., Kälviäinen R., Nousiainen U., Patry G., Farrell K., Söderfeldt B., Federico A., Hale B.R., Cossio O.H., Sorensen T., Pouliot M.A., Kmiek T., Uldall P., Janszky J., Pranzatelli M.R., Andermann E. and Rouleau

G.A. (1997). **Unstable insertion in the 5' flanking region of the cystatin B gene is the most common mutation in progressive myoclonus epilepsy type 1, EPM1.** *Nat. Genet.* **15:** 298-302.

La Spada A.R., Wilson E.M., Lubahn D.B., Harding A.E. and Fischbeck K.H. (1991) **Androgen receptor gene mutations in X-linked spinal and bulbar muscular atrophy.** *Nature* **352:** 77-79.

Lathrop G.M. and Lalouel J.M. (1984). **Easy calculations of LOD scores and genetic risks on small computers.** *Am. J. Hum. Genet.* **36:** 460-465.

Lehesjoki A., Koskiniemi M., Sistonen P., Miao J., Hästbacka J., Norio R. and De La Chapelle A. (1991). **Localization of a gene for progressive myoclonus epilepsy to chromosome 21q22.** *Proc Natl. Acad. Sci. USA* **88:** 3696-3699.

Lehesjoki A.E., Koskiniemi M., Pandolfo M., Antonelli A., Kyllerman M., Wahlström J., Nergårdh A., Burmeister M., Sistonen P., Norio R. and de la Chapelle A. (1992). **Linkage studies in progressive myoclonus epilepsy: Unverricht-Lundborg and Lafora's diseases.** *Neurology* **42:** 1545-1550.

Lehesjoki A.E., Koskiniemi M., Norio R., Tirrito S., Sistonen P., Lander E. and de la Chapelle A. (1993). **Localization of the EPM1 gene for progressive myoclonus epilepsy on chromosome 21: linkage disequilibrium allows high resolution mapping.** *Hum. Mol. Genet.* **2:** 1229-1234.

Li S.H., McInnis M.G., Margolis R.L., Antonarakis S.E. and Ross C.A. (1993). **Novel triplet repeat containing genes in human brain: cloning, expression and length polymorphisms.** *Genomics* **16:** 572-579.

MacKinnon R. (1991). **Determination of the subunit stoichiometry of a voltage-activated potassium channel.** *Nature* **350:** 232-235.

Magovcevic I., Ang S. L., Seidman J.G., Tolman C., Neer E. and Mortons C. (1992). **Regional localization of the human G protein α_{12} (GNA12) gene: assignment to 3021 and a related sequence (GNA12L) to 12p12-p13.** *Genomics* **12:** 125-129.

- Marseille Consensus Group (1990). **Classification of progressive myoclonus epilepsies and related disorders.** *Ann. Neurol.* **28**: 113-116.
- Marx J. (1991). **Rare Heart Disease Linked to Oncogene.** *Science* **251**: 647.
- Meissner P.N., Dailey T.A., Hift R.J., Ziman M., Corrigan A.V., Roberts A.G. and Meissner (1996). **A R59W mutation in human protoporphyrinogen oxidase results in decreased enzyme activity and is prevalent in South Africans with variegate porphyria.** *Nat Genet.* **13**: 95-97.
- Merchant K.H., Dirckar K. and Singu K. (1989). **Long QT syndrome.** *India Pediatr.* **25**: 96-99.
- Michaud J., Brody L.C., Steel G., Fontaine G., Martin L.S., Valle D. and Mitchell G. (1992). **Strand-separating conformational polymorphism analysis: Efficacy of detection of point mutations in the human ornithine δ -aminotransferase gene.** *Genomics.* **13**: 389-394.
- Miwa S. (1994). **Triplet repeats strike again.** *Nat. Genet.* **6**: 3-4.
- Monaco A.P., Neve R.L., Colletti-Feener C., Bertelson C.J., Kurnit D.M. and Kunkel L.M. (1986). **Isolation of candidate cDNAs for portions of the Duchenne muscular dystrophy gene.** *Nature* **323**: 646-650.
- Moolman-Smook J.C., De Lange W.J., Bruwer E.C.D., Brink P.A. and Corfield V.A. (1999). **The origins of Hypertrophic Cardiomyopathy-causing mutations in two South African subpopulations: A unique profile of both independent and founder events.** *Am. J. Hum. Gen.* **65**:1308-1320.
- Moss A.J. and McDonald J. (1971). **Unilateral cervicothoracic sympathetic ganglionectomy for the treatment of long QT interval syndrome.** *New Engl. J. Med.* **285(16)**: 903-904.
- Moss A.J., Schwartz P.J., Crampton R.S., Locati E. and Carleen E. (1985). **The long QT syndrome: a prospective international study.** *Circulation* **71 (1)**: 17-21.

Moss A.J. (1986). **Prolonged QT interval syndrome.** *JAMA* **256**: 2985-2987.

Moss A.J., Lui J.E., Gottlieb S., Locati E.H., Schwartz P.J. and Robinson J.L. (1991). **Efficacy of permanent pacing in the management of high-risk patient with long QT syndrome.** *Circulation* **84**: 1524-1529.

Moss A.J. and Robinson J. (1992). **Clinical features of the idiopathic long QT syndrome.** *Circulation (suppl 85)* : I-140-I-144.

Moss A.J., Zareba W., Benhorin J., Locati E., Hall W.J., Robinson J.L., Schwartz P.J., Towbin J.A., Vincent G.M., Lehmann M.H., Keating M.T., MacCluer J.W. and Timothy K.W. (1995). **ECG T-Wave patterns in genetically distinct forms of the hereditary long QT syndrome.** *Circulation* **92**: 2929-2934.

Nagafuchi S., Yanagisawa H., Sato K., Shirayama T., Ohsaki E., Bundo M., Takeda T., Tadokoro K., Kondo I., Murayama N., Tanaka Y., Kikushima H., Umino K., Kurosawa T., Furukawa T., Nihei K., Inoue T., Sano A., Komure O., Takahashi M., Yosizawa T., Kanazawa I. and Yamada M. (1994). **Dentatorubral and pallidolusian atrophy expansion of an unstable CAG trinucleotide on chromosome 12p.** *Nat. Genet.* **6**: 14-18.

Naito H. and Oyanagi S. (1982). **Familial myoclonus epilepsy and choreoathetosis: hereditary dentatorubral-pallidolusian atrophy.** *Neurology.* **32**: 798-807.

Neyroud N., Richard P., Vignier N., Donger C., Denjoy I., Demay L., Shkolnikova M., Pesce R., Chevalier P., Hainque B., Coumel P., Schwartz K. and Guicheney P. (1999). **Genomic organization of the KCNQ1 K⁺ channel gene and identification of C-terminal mutations in the long QT syndrome.** *Circ. Res.* **84**: 290-297.

Neyroud N., Tesson F., Denjoy I., Leibovici M., Donger C., Barhanin J., Faure S., Gary F., Coumel P., Petit C., Schwartz K. and Guicheney P. (1997). **A novel mutation in the potassium channel**

- gene *KVLQT1* causes the Jervell and Lange-Nielsen cardioauditory syndrome. *Nat. Genet.* **15**: 186-189.
- Nørremølle A., Nielsen J.E., Sørensen S.A. and Hasholt L. (1995). **Enlongated CAG repeats of the B37 gene in a Danish family with dentato-rubro-pallido-luysian atrophy.** *Hum. Genet.* **95**: 313-318.
- O'Callaghan C.A. and Trump D. (1993). **Prolonged QT syndrome presenting as epilepsy.** *Lancet* **341**: 759-760.
- Onodera O., Oyake M., Takano H., Ikeuchi T., Igarashi S. and Tsuji S. (1995). **Molecular cloning of a full-length cDNA for dentatorubral-pallidoluysian atrophy and regional expressions of the expanded alleles in the CNS.** *Am. J. Hum. Genet.* **57**: 1050-1060.
- Orita M., Iwahana H., Kanazawa H., Hayashi K. and Sekiya T. (1989a). **Detection of polymorphisms of human DNA by gel electrophoresis as single strand conformation polymorphisms.** *Pro. Natl. Acad. Sci. USA.* **86**: 2766-2770.
- Orita M., Suzuki Y., Sekiya T. and Hayashi K., (1989b). **Rapid and sensitive detection of point mutations and DNA polymorphisms using the polymerase chain reaction.** *Genomics* **5**: 874-879.
- Orr H.J., Chung M.Y., Banfi S., Kwiatkowski Jr J., Servadio A., Beaudet A.L., McCall A.E., Duvick L.A., Ranum L.P.W. and Zoghbi H.Y. (1993). **Expansion of an unstable trinucleotide CAG repeat in spinocerebellar ataxia type 1.** *Nat. Genet.* **4**: 221-226.
- Ottman R., Annegers J.F., Risch N., Hauser W.A. and Susser M (1996). **Relations of genetic and environmental factors in the etiology of epilepsy.** *Ann. Neurol.* **39**: 442-449.
- Ottman R. (1997). **Genetic epidemiology of epilepsy.** *Epidemiol. Rev.* **19**: 120-128.

Pacia S.V., Devinsky O., Luciano D.J. and Vazquez B. (1994). **The prolonged QT syndrome presenting as epilepsy.** *Neurology* **44**: 1408-1410.

Pennacchio L.A., Lehesjoki A., Stone N.E., Willour V.L., Virtaneva K., Miao J., D'Amato E., Ramirez L., Faam M., Koskiniemi M., Warrington J.A., Norio R., de la Chapelle A., Cox D.R. and Myers R.M. (1996). **Mutations in the Gene Encoding Cystatin B in Progressive Myoclonus Epilepsy (EPM1).** *Science* **271**: 1731-1734.

Plaster N.M., Uyama E., Uchino M., Ikeda T., Flanigan K.M., Kondo I. and Ptacek L.J. (1999). **Genetic localization of the familial adult myoclonic epilepsy (FAME) gene to chromosome 8q24.** *Neurology* **53**: 1180-1183

Priori S.G., Napolitano C., Cantù F., Brown A. M. and Schwartz P.J. (1996). **Differential response to Na⁺ channel blockade, β -adrenergic stimulation, and rapid pacing in a cellular model mimicking the SCN5A and HERG defects present in the long QT syndrome.** *Circ. Res.* **78**: 1009-1015.

Priori S.G. (1997). **Is long QT entering the area of molecular diagnosis?** *Heart* **71**: 5-6

Priori S.G., Barhanin J., Hauer R.N.W., Haverkamp W., Jongsma H.J., Kleber A.G., McKenna W.J., Roden D.M., Rudy Y., Schwartz K., Schwartz P.J., Towbin J.A. and Wilde A. (1999). **Genetic and molecular basis of cardiac arrhythmias: Impact on clinical management Part I and II.** *Circulation* **99**: 518-528.

Roden D.M., Lazzara R., Rosen M., Schwartz P.J., Towbin J. and Vincent M. (1996). **Multiple Mechanisms in the Long-QT Syndrome: Current Knowledge, Gaps and Future Directions.** *Circulation* **94**: 1996-2012.

Romano C., Gemme G. and Pongiglione R. (1963). **Aritmie cardiache rare dell'eta pediatrica. arrhythmia.** *Clin. Pediatr.* **45**: 658-683.

Rosen M.R. (1995). **Long QT Syndrome Patients with Gene Mutations.** *Circulation* **92**: 3373-3375.

Rouyer F., de la Chapelle A. and Weissenbach J. (1990). **A polymorphic DNA sequence from the terminal part of chromosome 21q [D21S154].** *Nucleic Acids Res.* **18:** 1663.

Russel M.W., MacDonald D., Campbell R.M., Hulse J.E., Munroe D.J., Bric E., Housman D.E., Collins F.S. and Brody L.C. (1995). **Localization of Romano-Ward Long QT Syndrome Gene, LQT1, to the Interval between Tyrosine Hydroxylase (TH) and D11S1349.** *Am. J. Hum. Genet.* **57:** 503-507.

Russel M.W., Dick II M., Collins F.S. and Brody L.C. (1996). **KVLQT1 mutations in three families with familial or sporadic long QT syndrome.** *Hum. Mol. Genet.* **5:** 1319-1324.

Ryan S.G (1995) **Partial epilepsy: chinks in the armour.** *Nat. Genet.* **10:** 4-6.

Ryan M.P., French J., Al-Mahdavi S., Nihoyannopoulos P., Cleveland J.G.F. and Oakley C.M., (1995). **Genetic testing for familial hypertrophic cardiomyopathy in newborn infants.** Comments by Harper P.S., Clarke A., Davis J., Grigg I.J. *BMJ* **310:** 856-859.

Ryan S.G (1999). **Ion channels and the genetic contribution to epilepsy.** *J. Child Neurol.* **14:** 58-66.

Saarinen K., Swan H., Kainulainen K., Toivonen L., Viitasalo M. and Kontula K. (1998). **Molecular genetics of the long QT syndrome : Two novel mutations of the KVLQT1 gene and phenotypic expression o the mutant gene in a large kindred.** *Hum. Mut.* **11:** 158-165.

Sanguinetti M.C., Jiang C., Curran M.E. and Keating M.T. (1995). **A mechanistic link between an inherited and a acquired cardiac arrhythmia: *HERG* encodes the I_{Kr} potassium channel.** *Cell* **81:** 299-307.

Sanguinetti M.C., Curran M.E., Zou A., Shen J., Spector P.S., Atkinson D.L. and Keating M.T. (1996). **Coassembly of KVLQT1 and minK (*IsK*) proteins to form cardiac I_{Ks} potassium channel.** *Nature* **384 :** 80-83.

- Sano A., Yamauchi N., Kakimoto Y., Komure O., Kawai J., Hazama F., Kuzume K., Sano N. and Kondo I. (1994). **Anticipation in hereditary dentatorubral-pallidolusian atrophy.** *Hum. Genet.* **93**: 699-702.
- Satler C.A., Walsh E.P., Vesely M.R., Plummer M.H., Ginsburg G.S. and Jacob H.J. (1996). **Novel missense mutations in the cyclic nucleotide-binding domain of HERG causes long QT syndrome.** *Am. J. Med. Genet.* **65**: 27-35.
- Scheuer M.L and Pedley T.A (1990). **The evaluation and treatment of seizures.** *New Eng. J. Med.* **323**: 1468-1474.
- Schott G.D., McLeod A.A. and Jewitt D.E. (1977). **Cardiac arrhythmias that masquerade as epilepsy.** *Br. Med. J.* **1**: 1454-1457.
- Schott J.J., Charpentier F., Peltier S., Foley P., Drouin E., Bouhour J.B., Donnelly P., Vergnaud G., Bachner L., Moisan J.P., Le Marec H. and Pascal O. (1995). **Mapping of a Gene for Long QT Syndrome to Chromosome 4q25-27.** *Am. J. Hum. Genet.* **57**: 1114-1122.
- Schulze-Bahr E., Haverkamp W., Wedekind H., Rubie C., Hordt M., Borggrefe M., Assmann G., Breithardt G. and Funke H. (1997) **Autosomal recessive long QT syndrome (Jervell Lange-Nielsen syndrome) is genetically heterogeneous.** *Hum Genet.* **100**: 573-576.
- Schwartz P.J., Periti M. and Malliani A. (1975). **The long Q-T syndrome.** *Am. Heart J.* **89**: 378-390.
- Schwartz P.J. (1985). **Idiopathic long QT syndrome: Progress and questions.** *Am. Heart J.* **109**: 399-411.
- Schwartz P.J., Locati E.H., Moss A.J., Crampton R.S., Trazzi R. and Roberti U. (1991a). **Left cardiac sympathetic denervation in the therapy of congenital long QT syndrome.** *Circulation* **84**: 503-511.

Schwartz P.J., Zaza A., Locati E and Moss A.J. (1991b) **Stress and sudden death: The case of the long QT syndrome.** *Circulation* **83 (suppl II):** II-71-II-80.

Schwartz P.J., Moss A.J., Vincent G.M., Richard M.D. and Crampton M.D. (1993). **Diagnostic criteria for the long QT syndrome: an update.** *Circulation* **88:** 782-784.

Schwartz P.J., Priori S.G., Locati E.H., Napolitano C., Cantù F., Towbin J.A., Keating M.T., Hammoude H., Brown A.M., Chen L.S.K. and Colatsky T.J. (1995). **Long QT syndrome patients with mutations of the *SCN5A* and *HERG* genes have differential responses to Na⁺ channel blockade and to increases in heart rate: Implications for gene-specific therapy.** *Circulation* **92:** 3381-3386.

Schwartz P.J., Moss A.L., Priori S.G., Wang Q., Lehmann M.H., Timothy K., Denjoy I.F., Haverkamp W., Guicheney P., Paganini V., Scheinmam M.M. and Karnes P.S. (1997). **Gene-specific influence on the triggers for cardiac arrest in the long QT syndrome.** *Circulation* **96 (suppl I):** I-212.

Schwartz P.J., Priori S.G., Spazzolini C., Moss A.J., Vincent G.M., Schwartz K., Coumel P., Breithardt G., Kating M.T., Towbin J.A., Beggs A.H., Brink P., Wilde A.A.M., Toivonen L., Zareba W., Robinson J.L., Timothy K.W., Wattanasirichaigoon D., Corfield V., Corbett C., Haverkamp W., Schulze-Bahr E., Lehmann M.H., Denjoy I., Guicheney P., Napolitano C., Bloise R. and Terreni L. (1999). **Gene-specific triggers for life threatening arrhythmias in the long QT syndrome.** (submitted).

Seino S., Yamada Y., Espinosa R., LeBeeau M. and Bell G. (1992) **Assignment of the gene encoding the α_1 subunit of the neuroendocrine/brain-type calcium channel (*CACNL1A2*) to human chromosome 3 bands p14.3.** *Genomics* **13:** 1375-1377.

Singh B., Al Shawan S.A. and Habbap M.A. Al Deeb S.M. and Bairy N. (1993). **Idiopathic long QT syndrome: asking the right question.** *Lancet* **341:** 741-742.

Singh N.A., Charlier C., Stauffer D., DuPont B.R., Leach R.J., Melis R., Ronen G.M., Bjerre I., Quattlebaum T., Murphy J.V., McHarg M.L., Gangnon D., Rosales T.O., Peiffer A., Anderson V.E. and Leppert M. (1998). **A novel potassium channel gene, KCNQ2 is mutated in an inherited epilepsy of new-borns.** *Nat. Genet.* **18**: 25-29.

Slightom J.L., Blechl A.E. and Smithies O. (1980). **Human fetal $G\gamma$ - and $A\gamma$ -globin genes: complete nucleotide sequences suggest that DNA can be exchange between these duplicated genes.** *Cell* **21**: 627-638.

Smith J. K., Gonda V. E. and Malamud N. (1958). **Unusual form of cerebellar ataxia: Combined dentato-rubral and pallido-luysian degeneration.** *Neurology* **8**: 205-209.

Smith R.P. and Wilder B.J. (eds) 1968. **Classification of Epilepsy** *In: Epilepsy.* Blackwell Scientific Publications. Oxford, pp 2-7.

Splawski I., Tristani-Firouzi M., Lehmann M.H., Sanguinetti M.C. and Keating M.T. (1997). **Mutations in the hminK gene cause long QT syndrome and suppress I_{Ks} function.** *Nat. Genet.* **17**: 338-340.

Splawski I., Shen J., Timothy K.W., Vincent G.M., Lehmann M.H. and Keating M.T. (1998). **Genomic Structure of three long QT syndrome genes: *KVLQT1*, *HERG* and *KCNE1*.** *Genomics* **51**: 86-97.

Starfield M., Hennies H.C., Jung M., Jenkins T., Wienker T., Hull P., Spurdle A., Wolfgang K., Ramsay M. and Reis A. (1997). **Localization of the gene causing keratolytic winter erythema to chromosome 8p22-p23, and evidence for a founder effect in South African Afrikaans speakers.** *Am. J. Hum. Genet.* **61**: 370-378.

Steinlein O.K (1998). **New insights into the molecular and genetic mechanisms underlying idiopathic epilepsies.** *Clin. Genet.* **54**: 169-175.

Steinlein O., Mulley J.C., Propping P., Wallace R.H., Phillips H.A., Sutherland G.R., Scheffer I.E. and Berkovic S.F. (1995). **A missense mutation in the neuronal nicotinic acetylcholine receptor $\alpha 4$ subunit is associated with autosomal dominant nocturnal frontal lobe epilepsy.** *Nat. Genet.* **11**: 201-203.

Sternberg N. (1990). **Bacteriophage P1 cloning system for the isolation, amplification and recovery of DNA fragments as large as 100 kilobase pairs.** *Proc Natl. Acad. Sci. USA* **87**: 103-107.

Takahasi H., Ohama E., Naito H., Takeda S., Nakashima S., Makifuchi T. and Ikuta F. (1988). **Hereditary dentatorubral-pallidoluysian atrophy: clinical and pathological variants in a family.** *Neurology.* **38**: 1065-1070.

Takahata N., Ito K., Yoshimura Y., Nishihori K. and Suzuki H. (1978). **Familial chorea and myoclonus epilepsy.** *Neurology.* **28**: 913-919.

Tanaka T., Nagai R., Tomoike H., Takata S., Yano K., Yabuta K., Haneda N., Nakano O., Shibata A., Sawayama T., Kasai H., Yazaki Y. and Nakamura Y. (1997). **Four novel *KVLQT1* and four novel *HERG* mutations in familial long QT syndrome.** *Circulation* **95**: 565-567.

The Huntington's Disease Collaborative Research Group (1993). **A novel gene containing a trinucleotide repeat that is expanded and unstable on Huntington's disease chromosomes.** *Cell* **72**: 971-983.

Towbin J.A. (1995). **Clinical implication of basic research, new revelations about the long- QT syndrome.** *New Eng. J. Med.* **333**: 384-385.

Trudeau M.C., Warmke J.W., Ganetzky B. and Robertson G.A. (1995). **HERG a human inward rectifier in the voltage-gated potassium channel family.** *Science* **269**: 92-95.

Tyson J., Tranebjaerg L., Bellman S., Wren C., Taylor J.F.N., Bathen J., Aslaksen B., Sørland S.J., Lund O., Malcolm S., Pembrey M., Bhattacharya S. and Bitner-Glindzicz M. (1997). **IsK and**

KVLQT1: mutation in either of the two subunits of the slow component of the delayed rectifier potassium channel can cause Jervell and Lange-Nielsen syndrome. *Hum. Mol. Genet.* **6:** 2179-2185.

Van den Berg M.H., Wilde A.A.M., Robles de Medina E.O., Meyer H., Geelen J.L.M.C., Jongbloed R.J.E., Wellens H.J.J. and Geraedts J.P.M. (1997). **The long QT syndrome: a novel missense mutation in the S6 region of the KVLQT1 gene.** *Hum. Genet.* **100:** 356-361.

Vincent G.M., Timothy K.W., Leppert M. and Keating M. (1992). **The Spectrum of Symptoms and QT intervals in Carriers of the Gene for the Long-QT Syndrome.** *N. Engl. J. Med.* **327:** 846-852.

Virtaneva K., Miao J., Träskelin A., Stone N., Warrington J.A., Weissenbach J., Myers R.M., Cox D.R., Sistonen P., de la Chapelle A. and Lehesjoki A. (1996). **Progressive Myoclonus Epilepsy EPM1 Locus Maps to a 175-kb Interval in Distal 21q.** *Am. J. Hum. Genet.* **58:** 1247-1253.

Virtaneva K., D'Amato E., Miao J., Koskiniemi M., Norio R., Avanzini G., Franceschetti S., Michelucci R., Tassinari C.A., Omer S., Pennacchio L.A., Myers R.M., Dieguez-Lucena J.L., Krahe R., de la Chapelle A. and Lehesjoki A.E. (1997). **Unstable minisatellite expansion causing recessively inherited myoclonus epilepsy, EPM1.** *Nat. Genet.* **15:** 393-396.

Wang Q., Shen J., Splawski I., Atkinson D., Li Z., Robinson J.L., Moss A.J., Towbin J.A. and Keating M. (1995a). **SCN5A mutations associated with an inherited cardiac arrhythmia, long QT syndrome.** *Cell* **80:** 805-811.

Wang Q., Shen J., Li Z., Timothy K., Vincent G.M., Priori S.G., Schwartz P.J. and Keating M.T. (1995b). **Cardiac sodium channel mutations in patients with long QT syndrome, an inherited cardiac arrhythmia.** *Hum. Mol. Genet.* **4 (9):** 1603-1607.

Wang Q., Curran M.E., Splawski I., Burn T.C., Millolland J.M., VanRaay T.J., Shen J., Timothy K.W., Vincent G.M., de Jager T., Schwartz P.J., Towbin J.A., Moss A.J., Atkinson D.L., Landes

- G.M., Connors T.D. and Keating M.T. (1996a). **Positional cloning of a novel potassium channel gene: *KVLQT1* mutations cause cardiac arrhythmias.** *Nat. Genet.* **12**: 17-23.
- Wang Q., Li Z., Shen J. and Keating M.T. (1996b). **Genomic organization of the human *SCN5A* gene encoding the cardiac sodium channel.** *Genomics* **34**: 9-16.
- Ward O.C. (1964). **A New Familial Cardiac Syndrome in Children.** *J.Ir. Med. Assoc.* **54**: 103-106.
- Warmke J.E. and Ganetzky B. (1994). **A family of potassium channel genes related to *eag* in *Drosophila* and mammals.** *Proc. Natl. Acad. Sci.* **91**: 3438-3442.
- Weber J.L. and May P.E. (1989). **Abundant class of human DNA polymorphisms which can be typed using the polymerase chain reaction.** *Am. J. Hum. Genet.* **44**: 388-396.
- Weber J.L. (1990). **Informativeness of human (dC-dA)_n . (dG-dT)_n polymorphisms.** *Genomics* **7**: 524-530.
- Weinstein L.S., Spiegel A.M. and Carter A.D. (1988). **Cloning and characterization of the human gene for the α -subunit of G₁₂, a GTP-binding signal transduction protein.** *FEBS Lett.* **232**: 333-340.
- Welsh M.J. and Hoshi T. (1995). **Ion channels lose the rhythm.** *Mol. Cardio.* **376**: 640-641.
- White R. and Lalouel J.M. (1988). **Chromosome mapping with DNA markers.** *Scientific American* **258**: 20-28.
- Wicking C. and Williamson B. (1991). **From linked marker to gene.** *TIG* **7**: 288-293.
- Williams D. (1988). Foreword *In*: Laidlaw J., Richens A. and Oxley J. (eds). **A Textbook of Epilepsy.** Churchill Livingstone Edinburgh London Melbourne and New York. ppv-vi.

Willets N. and Skurray R. (1987). In Neidhardt F.C. (Eds). *Escherichia coli and Salmonella typhimurium: Cellular and Molecular Biology*, (American Society of Microbiology). **2**: 1134-1137.

Wollnik B., Schroeder B.C., Kubisch C., Esperer H.D., Wieacker P. and Jentsch T.J. (1997). **Pathophysiological mechanisms of dominant and recessive *KVLQT1* K⁺ channel mutations found in inherited cardiac arrhythmias.** *Hum. Mol. Genet.* **6**: 1943-1949.

Xiong M. and Guo S.W. (1997). **Fine-scale genetic mapping based on linkage disequilibrium mapping: Theory and applications.** *Am. J. Hum. Genet.* **60**: 1513-1531.

Zareba W., Moss A.J., Schwartz P.J., Vincent G.M., Robinson J.L., Priori S.G., Benhorin J., Locati E.H., Towbin J.A., Keating M.T., Lehmann M.H. and Hall W.J. for the International Long QT Syndrome Registry Research Group. (1998). **Influence of the genotype on the clinical course of the long QT syndrome.** *New Eng. J. Med.* **339**: 960-965.

Zipes D.P. (1991). **The long QT interval syndrome: A Rosetta stone for sympathetic related ventricular tachyarrhythmias.** *Circulation* **84**: 1414-1418.